Hudson River PCBs Site

Phase 1
Intermediate Design Report
Attachment E - Dredge Resuspension Modeling

Prepared by:

Quantitative Environmental Analysis, LLC

Montvale, NJ

Prepared for:

General Electric Company

Albany, NY

August 22, 2005

Hudson River PCBs Site

Phase 1
Intermediate Design Report
Attachment E - Dredge Resuspension Modeling

Prepared by:

Quantitative Environmental Analysis, LLC

Montvale, NJ

Prepared for:

General Electric Company

Albany, NY

Job Number:

GENdes:232

August 22, 2005

Table of Contents

List of Tables

List of Figures

List of Acronyms

ADCP	acoustic Doppler current profiler
BMP	Baseline Monitoring Program
EFDC	Environmental Fluid Dynamics Code
EGIA	East Griffin Island Area
EPS	Engineering Performance Standards
HRM	Hudson River Monitoring
NTIP	Northern Thompson Island Pool
PCB	polychlorinated biphenyls
RM	River Mile
ROD	Record of Decision
RPS	Resuspension Performance Standard
SSAP	Sediment Sampling and Analysis Program

TID	Thompson Island Dam
TIP	Thompson Island Pool
TSS	total suspended solids
USEPA	United States Environmental Protection Agency
USGS	United States Geological Survey

E.1 INTRODUCTION

E.1.1 Background

In the Record of Decision for the Hudson River (ROD; USEPA 2002), the United States Environmental Protection Agency (USEPA) required establishment of performance standards for, among other things, resuspension during dredging. USEPA undertook responsibility for development of the standards and issued the standards in 2004 (Malcolm Pirnie and TAMS 2004). The Performance Standard for resuspension, hereafter referred to as the Resuspension Performance Standard or RPS, establishes limits for concentrations of polychlorinated biphenyls (PCBs) in river water and downstream transport of PCBs.

The RPS includes a primary standard of a not-to-exceed river water PCB concentration of 500 ng/L and two action levels (Evaluation and Control) meant to trigger efforts to identify and correct remediation-related problems that might result in an exceedence of the standard. The action levels are defined by far-field (more than 1 mile downstream of dredging activities) and near-field (within 300 m of the dredging activities) criteria. The far-field criteria include PCB and total suspended solids (TSS) concentrations and PCB mass flux. The near-field criteria consist of TSS concentrations at specified distances from the dredging activities. These action level criteria as they apply to Phase 1 dredging in River Section 1 are listed in Tables E-1-1 and E-1-2.

Table E-1-1. Resuspension standard criteria for far-field stations[3].

Parameter	Evaluation Level	Control Level
7-d Running Average Total PCB Concentration		350 ng/L
7-d Running Average Total PCB Load	300 g/d	600 g/d
7-d Running Average Tri+ PCB Load	100 g/d	200 g/d
Dredging Season Cumulative Total PCB Load		65 kg
Dredging Season Cumulative Tri+ PCB Load		22 kg
TSS (6 hr average or average of day's dredging period if less)	12 mg/L[1]	24 mg/L[2]

Notes: [1]*6-hour running average or average of day's dredging period if less.*
[2]*24-hour running average or average of day's dredging period if less.*
[3]*PCB load and TSS are net above baseline conditions.*

Table E-1-2. Resuspension standard criteria for near-field stations[4].

Parameter	Evaluation Level	Control Level
TSS @ 100 m (or channel side of dredging)	700 mg/L[1]	
TSS @ 300 m	100 mg/L[2]	100 mg/L[3]

Notes: [1]*3-hour running average.*
[2]*6-hour running average or average of day's dredging period if less.*
[3]*24-hour running average or average of day's dredging period if less.*
[4]*TSS values are net above baseline conditions.*

E.1.2 Technical Approach

Evaluation of the effects of sediment and PCB releases during dredging operations on water column concentrations at near-field and far-field locations is accomplished through application of a mathematical model. This modeling framework is used to simulate the transport and fate of resuspended sediment and PCBs in River Section 1 (i.e., Thompson Island Pool or TIP) during the five-month dredging season, which extends from May through November. Predicted TSS at the near-field stations (100 and 300 m downstream of the dredging operation) and TSS and PCB concentrations (and PCB loads) at the far-field station (Thompson Island Dam or TID) are compared to the Evaluation, Control, and Standard Levels of the RPS. The approach makes it possible to quantitatively analyze the effects of various dredging plans on TSS and PCB concentrations, and associated PCB loads, at the far-field station. Thus, the potential for a specific dredging plan to exceed the RPS criteria can be estimated prior to implementing that plan. As part of the design of the dredging project it is necessary to determine where engineered resuspension control or containment systems (i.e., silt curtains, silt barriers, sheet piling, or other physical barriers) may be needed during dredging to maintain resuspension levels at or below the Control Level of the RPS. The modeling provides a means to evaluate the ability of various control options to reduce downstream transport and water column concentrations to levels at or below the Control Level of the RPS.

E.1.3 Overview of Modeling Framework

This analysis involves use of a mathematical model, which consists of three sub-models that are linked together: 1) hydrodynamics; 2) sediment transport; and 3) PCB fate and transport (see Figure E-1-1). The hydrodynamic model predicts depth-averaged current velocity, water depth (or stage height), and bottom shear stress, which is the frictional force that moving water exerts on the sediment bed. The sediment transport model predicts water column concentrations of suspended sediment, and deposition onto the sediment bed. The PCB fate and transport model predicts water column concentrations of dissolved and particle-associated PCBs, and deposition of particle-associated PCBs to the bed. For this application, erosion of sediment and particle-associated PCBs from the bed are not considered.

Figure E-1-2 shows a generalized conceptual diagram of the modeling framework. The primary fate and transport mechanisms considered are:

- resuspension of sediment and particulate-bound PCBs due to dredging;
- hydrodynamic advection and dispersion of suspended sediment and PCBs;
- deposition of suspended sediment and associated sorbed PCBs;
- sorption and desorption of PCBs; and
- volatilization of dissolved phase PCBs.

This model is only concerned with the fate and transport of resuspended material as a result of dredging activity. Moreover, the dredge resuspension simulated is only that sediment released to the water column from direct dredge operation and does not include other dredge-related sources such as debris removal and barge movement. High-flow event resuspension (erosion) is not considered as dredging activities will not be taking place during such river conditions. Other non-dredging related sources of sediment and PCBs known to be present in the river (e.g. upstream and tributary inputs) are also not considered as the focus is material resulting from dredge activity. This approach is in accordance with the RPS standards because most standards are based on net increase of suspended sediment and PCBs as a result of dredging. For the far-field absolute PCB concentration standard, a baseline concentration resulting from the Baseline Monitoring Program (BMP) data and added to the dredge resuspension PCBs predicted by modeling.

E.2 SEDIMENT RESUSPENSION DURING DREDGING

E.2.1 Summary of USEPA Findings

The Feasibility Study (USEPA 2000), the Responsiveness Summary released with the ROD (USEPA 2002), and the Engineering Performance Standards (EPS; Malcolm Pirnie and TAMS 2004) present evaluations of dredging-induced resuspension. In these evaluations resuspension is normalized to the rate of dredging to yield a fractional resuspension rate (i.e., kg resuspended/kg dredged) expressed as a percentage.

The Feasibility Study reviews field and modeling studies of resuspension and concludes that resuspension rates at the dredge head of 0.35% (hydraulic - cutterhead) and 0.30% (mechanical - environmental bucket) represent conservative estimates of the resuspension likely to occur during the dredging of the Upper Hudson River. The value of 0.35% was derived from field studies of resuspension during cutterhead dredging of fine sediments in Calumet Harbor and Lavaca Bay. The value of 0.30% was derived from a field study of an enclosed bucket dredge operating in Boston Harbor. The sediments at all of these sites are dominated by small particles capable of being resuspended, thus the release rate essentially represents percentage of resuspendable sediment dredged that is released to the water column.

The Responsiveness Summary presents additional reviews of field and modeling studies and affirms the use of the values of 0.30% and 0.35% at the dredge head. In addition, it presents the results of calculations to estimate the dredging release rate at a distance of 10 meters from the dredge head. Mass-weighted average release rates were reported to be 0.13% for and environmental bucket dredge and 0.065% for a conventional hydraulic cutterhead dredge[1]. The report concludes that these values "... represent conservative estimates of the potential releases due to dredging and are consistent with direct observations made on several sites." (USEPA 2002).

[1] These percentages were presented as kg of fine sediment transported downstream per kg of total sediment dredged. Given that the rates at the dredge head were based on the dredging of fine sediments, kg of fine sediment dredged and kg of total sediment dredged are roughly equivalent.

The EPS provides further affirmation of the Feasibility Study release rates, using a dredge head release rate of 0.3% as the starting point for near-field and far-field resuspension modeling (Malcolm Pirnie and TAMS 2004). However, it appears that this rate was applied incorrectly for purposes of modeling. First, it is adjusted upward to 0.5% based on the incorrect assumption that the fine sediment fraction of Upper Hudson River sediments should be used to convert the rate from bulk sediment based resuspension to fine sediment based resuspension. In fact, the fine sediment fraction of the sediments from which the estimate was derived (i.e., Boston Harbor, Calumet Harbor, or Lavaca Bay) should be used for such a conversion. Since the fine sediment fractions of the field study sites were all close to one, the Feasibility Study values essentially represent kg fine sediment released/kg fine sediment dredged and the conversion does not alter the rate. Second, the dredge head release rate is applied 10 m downstream of the dredge without downward adjustment to account, as was done in the Responsiveness Summary, for the solids losses that occur in the first 10 m.

E.2.2 Assumptions Used in Predictive Modeling

On the basis of the USEPA findings, a value of 0.35% was used as the dredging-induced sediment resuspension rate at the dredge head. This rate was interpreted to represent the kg of resuspendable sediment resuspended/kg of resuspendable sediment dredged.

Given the uncertainty inherent in reliance on extrapolation from other sites as a means to determine the need for resuspension controls, a resuspension release rate of 0.70% was evaluated to identify those areas for which controls would be necessary if the release rate was twice that used for design. This 0.70% release rate was used to evaluate the need for resuspension control measures to be included in design as a contingency measure.

E.3 HYDRODYNAMIC MODELING

E.3.1 Model Description

The hydrodynamic model used in this study is the Environmental Fluid Dynamics Code (EFDC), which was originally developed by Dr. John Hamrick (Hamrick 1992). EFDC is a general purpose hydrodynamic model capable of simulating flow in rivers, lakes, reservoirs, estuaries and coastal oceans. This model solves the conservation of mass and momentum equations, which are the fundamental equations governing the movement of water in a river. A complete description of the model is given in Hamrick (1992).

The Upper Hudson River is relatively shallow and its flow is unstratified. These conditions make it reasonable to assume that the water column is vertically well-mixed. Thus, the two-dimensional, vertically-averaged equations are an accurate approximation to the general three-dimensional equations of motion for an incompressible fluid. The conservation of mass and momentum equations applied to TIP are (Ziegler et al. 2000):

$$\frac{\partial \eta}{\partial t}+\frac{\partial (uh)}{\partial x}+\frac{\partial (vh)}{\partial y}=0 \tag{E-3-1}$$

$$\frac{\partial (uh)}{\partial t}+\frac{\partial (u^2h)}{\partial x}+\frac{\partial (uvh)}{\partial y}=-gh\frac{\partial \eta}{\partial x}-C_f qu+\frac{\partial}{\partial x}\left(hB_H\frac{\partial u}{\partial x}\right)+\frac{\partial}{\partial y}\left(hB_H\frac{\partial u}{\partial y}\right) \tag{E-3-2}$$

$$\frac{\partial (vh)}{\partial t}+\frac{\partial (uvh)}{\partial x}+\frac{\partial (v^2h)}{\partial y}=-gh\frac{\partial \eta}{\partial y}-C_f qv+\frac{\partial}{\partial x}\left(hB_H\frac{\partial v}{\partial x}\right)+\frac{\partial}{\partial y}\left(hB_H\frac{\partial v}{\partial y}\right) \tag{E-3-3}$$

where: h is total water depth ($h_o+\eta$); h_o is reference water depth; η is water surface displacement with respect to reference depth; u, v are velocities along the x- and y-axes, respectively; $q = (u^2 + v^2)^{1/2}$; C_f is bottom friction factor; and B_H is horizontal eddy viscosity.

Note that the x-axis is oriented in the longitudinal (along-channel) direction and the y-axis is oriented in the lateral (cross-channel) direction. Equations E-3-1 to E-3-3 were transformed from Cartesian coordinates to orthogonal, curvilinear coordinates (see Hamrick (1992) for detailed discussion) in order to resolve the complex geometry and bathymetry of TIP more accurately.

An important variable in the hydrodynamic and sediment transport models is bottom shear stress (τ_b), which represents the frictional force exerted on the sediment bed by moving water in the river. The bottom shear stress is related to depth-averaged current velocity by the quadratic stress law:

$$\tau_b = \rho \, C_f \, q^2 \tag{E-3-4}$$

where: ρ is water density.

The bottom friction factor in Equation (E-3-4) is dependent on the local water depth and effective bottom roughness (Ziegler et al. 2000).

$$C_f = MAX\left[\frac{\kappa^2}{\left(\ln\dfrac{h}{2z_o}\right)^2} \quad , \quad C_{f,\min}\right] \tag{E-3-5}$$

where: κ is von Karman's constant (0.4); z_o is the effective bottom roughness; and $C_{f,min}$ is the minimum bottom friction factor (typically, set at 0.0025).

E.3.2 Model Development

Development of the hydrodynamic model of the TIP involved four main tasks: 1) specification of the geometry of the study area; 2) generation of a numerical grid; 3) projection of river bathymetry onto the numerical grid; and 4) specification of boundary conditions.

The region of the Upper Hudson River considered in this modeling evaluation extends from a location approximately 1,300 feet upstream of Rogers Island to TID. The location of the river shoreline within this region was determined using aerial photography information obtained during Spring 2002. The approximate flow rate at the time the aerial photographs were taken was 5,000 cfs at the United States Geological Survey (USGS) gauging station at Fort Edward).

A curvilinear, boundary-fitting numerical grid was generated to represent the study area, which is approximately six miles long. The river channel within the TIP is discretized using 230 longitudinal (i.e., along channel) and 22 lateral (i.e., cross channel) grid cells (Figure E-3-1). Average longitudinal cell size is 160 ft. and typical lateral cell size is about 30 ft. The grid resolution was chosen such that a plume resulting from resuspension of sediment and PCBs during dredging operations can be adequately simulated. Note that all three sub-models (i.e., hydrodynamic, sediment transport, and PCB fate and transport) use the same numerical grid.

Bathymetry data used to specify model inputs were obtained during two studies: 1) single-beam bathymetry data collected during a 2001 survey; and 2) supplemental water depth data obtained during the Sediment Sampling and Analysis Program (SSAP) in 2002 and 2003. The 2001 bathymetry data were collected along cross-channel transects, with a typical distance between transects of 125 ft. Bathymetry data from this survey were reprocessed during Spring 2003 and contoured at 1-ft. intervals to support the remedial design. The reprocessed data form the 2001 survey was included in the Hudson River GIS database. The reprocessed bathymetry data were projected onto the numerical grid, with the water depth (or bed elevation) in a specific grid cell representing the average water depth (bed elevation) within the area encompassed by that grid cell. A graphical representation of the TIP bathymetry is shown on Figure E-3-2 (a through e).

Two boundary conditions are needed for the hydrodynamic model: 1) incoming flow rate at the upstream boundary; and 2) water surface elevation (stage height) at the downstream boundary, which is location at TID. Flow rate collected at the USGS gauging station at Fort Edward is used to specify incoming flow at the upstream boundary of the model. Discharge from the TIP tributaries (e.g., Snook Kill, Moses Kill) is not included in these simulations because the tributary flow is small compared to the river discharge (i.e., about 4% of the total flow rate at TID, on average). Neglecting tributary flows has negligible effect on model results.

Water surface elevation (or stage height) at TID is specified as a function of river flow rate. Stage heights measured by Champlain Canal personnel at Crockers Reef, which is located at the entrance to the canal near River Mile (RM) 189, were used to develop this relationship between flow rate and stage height at TID (QEA 1999).

$$\eta_{dam} = 117.2 + 3.57\left(\frac{Q}{10000}\right)^{0.44} \quad \text{(E-3-6)}$$

where: η_{dam} is stage height [ft. with respect to NAVD 88] and Q is flow rate [cfs].

E.3.3 Calibration and Validation

Assessment of the predictive capability of the hydrodynamic model is achieved through comparisons of predicted and measured stage height (water surface elevation) and current velocity. The model parameter that is adjusted to achieve the optimum agreement between model predictions and observed values is the effective bottom roughness (z_o). The model calibration exercise indicated that an effective bottom roughness of 1 cm is appropriate for the study area. Horizontal eddy viscosity was set at a value of 0.06 m^2/s, which is the minimum value that ensures numerical stability. No adjustment of horizontal eddy viscosity was made during model calibration and validation.

Model calibration was conducted using stage height data obtained during the 1983 spring flood at Gauge 119, which is located near the entrance to the Champlain Canal lock at Fort

Edward. This flood had a maximum daily-average flow rate at Fort Edward of 34,100 cfs, which represents a return period of approximately 10 years. An effective bottom roughness of 1 cm produced the best agreement between observed and predicted stage heights during the 1983 flood (Figure E-3-3). These results indicate that the model adequately predicts stage height in the study area.

Model validation was accomplished using acoustic Doppler current profiler (ADCP) data collected during June 2004 (QEA 2004). Sampling locations are shown on Figures E-3-4 through E-3-7. No model parameters were adjusted during the validation exercise. Comparisons between predicted and measured current velocities at stations BMP1 and SEDC1 to SEDC5 are shown on Figures E-3-8 through E-3-13. These results indicate that the model is able to adequately reproduce observed current velocities in the TIP.

E.3.4 Application

Simulation of suspended sediment and PCB transport in the river due to resuspension during dredging operations requires specification of a hydrograph during the six-month dredging season. An analysis of historical flow rate data was conducted to develop hydrographs that are representative of a range of discharge conditions during the dredging season. Developing representative hydrographs requires that seasonal variations in flow conditions are incorporated into the analysis. For example, discharge during May is typically higher than discharge during August.

Representative hydrographs were developed by analyzing historical flow rate data at the Fort Edward gauging station that were collected during the six-month period from May through October. The 6-month dredging season is divided into 18 sub-periods, with each sub-period being 10 or 11 days long. A statistical analysis of the flow data, which were analyzed for each of the 18 sub-periods, produced estimates of median (50 percentile) flow rates, as well as 10 and 90 percentile flows, for each sub-period during the dredging season. The 10 and 90 percentile flows are assumed to represent lower- and upper-bound estimates, respectively.

The bounding flows, together with the median flow, are used to develop three hydrographs for the dredge season: 1) low-flow (i.e., 10 percentile); 2) typical flow (i.e., 50 percentile); and 3) high-flow (i.e., 90 percentile). For a specific hydrograph associated with a hydrodynamic simulation, flow rate is assumed to be constant during each sub-period. The hydrographs for the six-month dredging season are listed in Table E-3-1. These hydrographs are designed to approximate seasonal variations in discharge, as well as represent the range of flow rates that may be reasonably expected to occur during the dredging season.

Table E-3-1. Inflow hydrographs for six-month dredging season.

Month	Sub-Period Dates	10 Percentile Flow Rate (cfs)	50 Percentile Flow Rate (cfs)	90 Percentile Flow Rate (cfs)
May	1-10	3,000	6,800	16,700
	11-20	2,400	5,600	16,700
	21-31	2,400	4,600	11,400
June	1-10	2,200	3,800	8,800
	11-20	2,200	3,600	7,700
	21-30	1,900	3,200	6,000
July	1-10	1,500	2,400	4,600
	11-20	1,700	2,800	4,100
	21-31	1,900	2,800	4,100
August	1-10	1,900	2,800	4,100
	11-20	1,700	2,800	4,600
	21-31	1,700	2,800	4,400
September	1-10	1,900	2,600	4,100
	11-20	1,900	2,800	3,800
	21-30	2,200	2,800	4,900
October	1-10	2,200	3,000	5,300
	11-20	2,200	3,400	5,600

The hydrodynamic model was used to estimate average velocity in the TIP for a range of flow conditions. Simulations were conducted with inflows corresponding to high-flow events with these return periods: 2, 5, 10, 20, 50, and 100 years (see Table E-3-2). Results of these simulations were used to determine the area-weighted average velocities for the TIP for each high-flow event (see Table E-3-2 and Figure E-3-14).

Table E-3-2. Average TIP velocity for various high-flow conditions.

High-Flow Event Return Period (years)	Flow Rate (cfs)	Average Velocity (m/s)
2	23,000	0.71
5	30,000	0.86
10	34,500	0.95
20	38,000	1.01
50	44,000	1.11
100	47,300	1.17

E.4 SEDIMENT TRANSPORT MODELING

E.4.1 Overview of Sediment Transport Processes

Sediment released to the water column during dredging operations is composed of a mixture of clay, silt, sand and gravel, with the relative amounts of each sediment type depending on local bed conditions. The amount of released sediment that is transported away from the dredge-head is dependent on the sediment type. Coarser sediment, i.e., coarse sand and gravel (which are typically transported as bed load), will be redeposited within the immediate vicinity of the dredge-head because of the high settling speed of this type of sediment. Fine and medium sands, which are transported as suspended and bed load in rivers, may have the following fates after being released during dredging: 1) redeposition within the immediate vicinity dredge-head; and/or 2) carried downstream of the dredge-head as suspended load and redeposited on the bed. Clay and silt that are released during dredging will tend to behave as flocculating cohesive sediment that is transported as suspended load. Typically, this fine sediment type will be transported significantly further downstream from the dredge-head than fine/medium sand.

E.4.2 Model Description

The sediment transport model used in this study is based on the SEDZL algorithm (Ziegler et al. 2000). This model is capable of simulating the transport, resuspension and deposition of cohesive (muddy) and non-cohesive (sandy) sediments. A description of the model is provided in Ziegler et al. (2000). This model has been applied to approximately 20 sediment transport studies in rivers, including: Upper Hudson River (New York), Lower Fox River (Wisconsin), Tennessee River, Grasse River (New York), Saginaw River (Michigan), and Upper Mississippi River (Minnesota). Water-column transport of suspended sediment is governed by a conservation of mass equation. For this analysis, erosion from the sediment bed is not considered because it does not affect simulation of sediment released during dredging operations, and dredging will not take place during high flow events.

Suspended sediment particles in a river have a large range of sizes, from less than 1 µm clays to medium sands on the order of 400 µm. Simulation of the entire particle size spectrum is impractical. Therefore, particles were broadly segregated into two groups: silt and clay that may interact and form flocs and sand that is transported as discrete particles. The model uses this approach to approximate the particle size spectrum. Class 1 particles include all flocculating particles, i.e., clays and silts, with disaggregated particle diameters of less than 62 µm. Suspended sands are separated into two size classes. Class 2 particles correspond to very fine sand, which ranges in size from 75 to 150 µm. Class 3 particles represent fine and medium sands, with a size range of 150 to 425 µm.

A two-dimensional, vertically-averaged sediment transport equation for size-class k is used (Ziegler et al. 2000).

$$\frac{\partial(hC_k)}{\partial t}+\frac{\partial(uhC_k)}{\partial x}+\frac{\partial(vhC_k)}{\partial y}=\frac{\partial}{\partial x}\left(hE_x\frac{\partial C_k}{\partial x}\right)+\frac{\partial}{\partial y}\left(hE_y\frac{\partial C_k}{\partial y}\right)+R_k-D_k \qquad \text{(E-4-1)}$$

where: C_k is concentration of suspended sediment of size-class k; E_x, E_y are horizontal eddy diffusivities along the x- and y-axes, respectively; R_k is resuspension (erosion) flux of size-class k; and D_k is deposition flux of size-class k.

Results from the hydrodynamic model provide information about the transport field in Equation E-4-1, i.e., u, v, and h. Similar to the hydrodynamic equations, Equation E-4-1 has been transformed into an orthogonal, curvilinear coordinate system and solved numerically. The hydrodynamic and sediment transport models use the same numerical grids.

Deposition Processes

Flocculating sediments in the water column range from clay particles smaller than 1 µm up to ~62 µm silts. The discrete particles aggregate and form flocs that can vary greatly in size and effective density. Variations in concentration and shear stress affect both floc diameter and settling speed (Burban et al. 1990). Previous modeling studies (Ziegler and Nisbet 1994, 1995; Gailani et al. 1996; Ziegler et al. 2000) indicate that an effective approximation is to treat suspended flocculating sediments as a single class. This approach assumes that the settling and depositional characteristics of flocculating sediments can be represented by average values of a distribution of properties. Using this approximation, the deposition flux of flocculating (Class 1) sediments to the sediment bed is expressed as (Ziegler et al. 2000).

$$D_1 = P_1 \; W_{s,1} \; C_1 \tag{E-4-2}$$

where: $W_{s,1}$ is flocculating sediment settling speed and P1 is probability of deposition for flocculating sediments.

Settling speeds of cohesive flocs have been measured over a large range of concentrations and shear stresses in freshwater (Burban et al. 1990). The Burban settling speed data for cohesive flocs in freshwater were analyzed to develop a formulation to approximate the effects of flocculation on settling speed (Ziegler et al. 2000). This analysis indicates that the settling speed is dependent on the product of the concentration (C_1) and the water column shear stress (G) at which the flocs are formed, resulting in the following relationship:

$$W_{s,1} = 2.5 \left(C_1 G\right)^{0.12} \tag{E-4-3}$$

where: the units of $W_{s,1}$, C_1, and G are m/day, mg/l and Pa, respectively (Figure E-4-1). For a depth-averaged model, as used in this study, the relevant shear stress for use in Equation (E-4-3) is the bottom shear stress (i.e., $G = \tau_b$, see Equation E-3-4).

Modeling suspended flocculating sediments as a single class, with an effective $W_{s,1}$ given by Equation E-4-3 makes it necessary to use a probability of deposition (P_1) to parameterize the effects of particle/floc size heterogeneity and near-bed turbulence on the deposition rate. The complex interactions occurring in the vicinity of the sediment-water interface cause only a certain fraction of the settling flocculating sediments, represented by P_1, to become incorporated into the bed (Krone 1962, Partheniades 1992). An experimentally-based formulation that represents the effects of variable floc size on probability of deposition was developed by Partheniades (1992) (Figure E-4-2).

$$P_1 = 1 - (2\pi)^{-1/2} \int_{-\infty}^{Y} e^{-\frac{w^2}{2}} dw \qquad \text{(E-4-4)}$$

where:

$$Y = 2.04 \ln\left[0.25\left(\frac{\tau_b}{\tau_{b,\min}} - 1\right)e^{1.27\tau_{b,\min}}\right] \qquad \text{(E-4-5)}$$

and: $\tau_{b,min}$ is bottom shear stress below which P_1=1.

A value of 0.01 Pa is used for $\tau_{b,min}$ (Ziegler et al. 2000). This value is consistent with $\tau_{b,min}$. values reported by Partheniades (1992).

Class 2 and 3 particles, i.e., fine and medium sand, suspended in the water column have an effective settling speed ($W_{s,k}$) that depends on the effective particle diameter (d_k). The relationship between $W_{s,k}$ and d_k was developed by Cheng (1997). The depositional flux for this sediment class is estimated as:

$$D_2 = P_2 W_{s,2} \Gamma C_2 \qquad \text{(E-4-6)}$$

where: P_k is probability of deposition for non-cohesive sediment class k and Γ_k is stratification correction factor for class k.

Significant vertical stratification can occur in the water column due to the high settling speeds of fine and medium sand. This characteristic means that accurate calculation of sand deposition flux requires use of the near-bed concentration ($C_{a,k}$), where $C_{a,k} = \Gamma_k C_k$ and $\Gamma_k > 1$. Note that Γ_k is dependent upon $W_{s,k}$, τ_b, bottom roughness, and local depth.

The settling speed of a sand particle is related to the particle diameter, representing class k sediment, as follows (Cheng 1997):

$$W_{s,k} = \frac{\nu}{D_k}\left[\left(25 + 1.2D_*^2\right)^{1/2} - 5\right]^{1.5} \qquad \text{(E-4-7)}$$

where: D* = non-dimensional particle parameter.

$$D_* = D_k\left[\frac{(s-1)g}{\nu^2}\right]^{1/3} \qquad \text{(E-4-8)}$$

where: s is specific density of particle (assumed to be 2.65 for sand particles) and v is kinematic viscosity of water.

The settling speeds of suspended sand particles (i.e., 62< Dk < 500 μm) range from about 200 to 5,000 m/day (Figure E-4-3).

Most sediment transport models applied to riverine systems have used a vertically-averaged approximation of the vertical distribution of sediment in the water column (e.g., Ziegler et al. 2000). This approach assumes that particles are uniformly distributed throughout the water column, which is a good approximation for cohesive sediments due to their lower settling velocities (~1 to 10 m/day). The high settling speeds of suspended sands cause significant stratification to occur, with order of magnitude increases in concentration typically occurring between the top and bottom of the water column. Thus, simulation of suspended sand transport with a vertically-averaged model necessitates the use of a correction factor (Γ_k) to account for effects of concentration stratification.

This correction factor will relate the vertically-averaged sediment concentration of class k sediment (C_k), which is calculated by the sediment transport model, to the near-bed concentration ($C_{a,k}$). The vertical distribution of non-cohesive sediment in the water column can be calculated using (van Rijn 1984):

$$C_2(z) = \begin{cases} C_{a,2}\left[\left(\dfrac{a}{h-a}\right)\left(\dfrac{h}{z}-1\right)\right] & , \quad \dfrac{z}{h} < 0.5 \\ C_{a,2}\left(\dfrac{a}{h-a}\right)^{\zeta} e^{-4\zeta\left(\frac{z}{h}-0.5\right)}, & \dfrac{z}{h} \geq 0.5 \end{cases} \tag{E-4-9}$$

where: a is the near-bed reference height (where a = MAX[$11z_o$, 0.01 h]); z is vertical coordinate (z = 0 at sediment-water interface and z = h at water surface); and ζ is the suspension parameter defined by (van Rijn 1984):

$$\zeta = \frac{W_{s,2}}{\beta \kappa u_*} \tag{E-4-10}$$

where: κ is von Karman constant (assumed to be 0.4) and the β-factor, which is related to the vertical diffusion of particles, is given by (van Rijn 1984):

$$\beta = 1 + 2\left(\frac{W_{s,2}}{u_*}\right)^2 \quad , \quad 0.1 < \frac{W_{s,2}}{u_*} < 1 \tag{E-4-11}$$

The vertically-averaged concentration, C_k, is defined as:

$$C_2 = \frac{1}{h}\int_a^h C_2(z)\, dz \tag{E-4-12}$$

Using Equation E-4-9 in the above integral yields:

$$C_2 = \frac{C_{a,2}}{h}\left(\frac{a}{h-a}\right)^{\zeta}\left\{\int_a^{0.5h}\left(\frac{h}{z}-1\right)^{\zeta}dz + \int_{0.5h}^{h} e^{-4\zeta\left(\frac{z}{h}-05\right)}dz\right\} \qquad \text{(E-4-13)}$$

The integrals in this equation will be evaluated separately. The first integral does not have a closed form solution. Approximating the solution using the trapezoidal rule and three segments between z = a and z = 0.5 h, i.e., $\delta z = (0.5\ h - a)/3$, yields:

$$\int_a^{0.5h}\left(\frac{h}{z}-1\right)^{\zeta}dz = \frac{1}{3}\left[0.5\left(\frac{h}{a}-1\right)^{\zeta} + \left(\frac{h}{a+2\delta z}-1\right)^{\zeta} + 0.5\right] \qquad \text{(E-4-14)}$$

The second integral has the following solution:

$$\int_{0.5h}^{h} e^{-4\zeta\left(\frac{z}{h}-0.5\right)}dz = \frac{h}{4\zeta}\left(1-e^{-2\zeta}\right) \qquad \text{(E-4-15)}$$

Inserting Equations E-4-14 and E-4-15 into Equation E-4-13 and solving for $C_{a,k}$ produces:

$$C_{a,2} = \Gamma C_2 \qquad \text{(E-4-16)}$$

where:

$$\Gamma = \left(\frac{h}{a}-1\right)^{\zeta}\left\{\frac{1}{4\zeta}\left(1-e^{-2\zeta}\right) + \frac{1}{3}\left(0.5-\frac{a}{h}\right)\left[0.5\left(\frac{h}{a}-1\right)^{\zeta} + \left(\frac{h}{a+\delta z}-1\right)^{\zeta} + \left(\frac{h}{a+2\delta z}-1\right)^{\zeta} + 0.5\right]\right\}^{-1}$$

(E-4-17)

The dependence of Γ_k on h, a, $W_{s,k}$ and Γ_b is shown on Figure E-4-4.

The probability of deposition parameter (P_k) in Equation E-4-6 accounts for the effects of near-bed turbulence and particle size variations on deposition of fine sand. In quiescent water, the bottom shear stress will be zero and P_k will equal one. As the bottom shear stress increases, the probability of deposition decreases. The dependence of P_k on bottom shear stress was investigated by Gessler (1967), who determined that P_k could be described by a Gaussian distribution:

$$P_2 = \frac{1}{(2\pi)^{1/2}} \int_{-\infty}^{Y} e^{-\frac{1}{2}x^2}\, dx \qquad \text{(E-4-18)}$$

where:

$$Y = \frac{1}{\sigma}\left(\frac{\tau_{c,2}}{\tau_b} - 1\right) \qquad \text{(E-4-19)}$$

and: $\tau_{c,k}$ is critical shear stress for class k sand and σ is standard deviation of the Gaussian distribution for incipient motion. Based upon experimental results, Gessler (1967) determined that σ was equal to 0.57. The relationship between P_k, particle diameter and bottom shear stress is illustrated on Figure E-4-5.

Lateral Dispersion Coefficient

Suspended sediment and PCBs in the water column will be transported downstream by river currents. In addition, these solids and chemicals will be dispersed laterally across the river channel by turbulent diffusion and dispersion processes in the river. The rate at which the sediment and chemical transport models disperse suspended or dissolved material across the channel is determined by the lateral diffusion coefficient ($E_{lateral}$); this coefficient determines the rate and extent of cross-channel spreading of a plume. Based on data collected in various rivers, the following relationship is valid (Rutherford 1994):

$$E_{lateral} = \alpha \, U^* \, h \qquad \text{(E-4-20)}$$

where: α is an empirical constant and U^* is bed shear velocity.

For slightly meandering rivers, such as the Upper Hudson River, the value of α ranges between about 0.1 and 1.1, with an average value of 0.45 (Figure E-4-6). For this study, α was set at 0.45 for all simulations. This approach provides an objective, data-based method for estimating lateral dispersion in the Upper Hudson River.

E.4.3 Model Development

Development of the sediment transport model required specification of these model inputs: 1) bed map, which delineates areas of cohesive and non-cohesive sediment; 2) effective particle diameter for the two sand classes (i.e., Classes 2 and 3); and 3) magnitude and composition of dredge resuspension loads.

Side-scan sonar data were obtained for the TIP during 2002. These data were analyzed and used to broadly separate sediment bed types into three classes: 1) cohesive; 2) non-cohesive; and 3) hard bottom. The bed map for TIP resulting from this analysis is presented on Figure E-4-7.

The effective diameters for Classes 2 and 3 (i.e., fine and medium sand) were estimated using grain size distribution data collected from the TIP. This analysis suggests that representative effective diameters for Classes 2 and 3 are 113 and 267 μm, respectively. The settling speeds corresponding to these effective diameters are about 600 and 2,400 m/day, respectively. Note that the settling speed of flocculating cohesive sediment (i.e., Class 1) ranges between 1 and 10 m/day. An effective diameter of 26 μm is used for Class 1 sediment.

Magnitude and Composition of Dredge Releases

The composition of sediment to be dredged in each grid cell was estimated based on the primary visual texture description of the SSAP core segments. Each sediment core was associated with a volume of sediment that was defined by overlaying Thiessen polygons developed from the locations of the cores on the areal dredge delineation. The volume associated with each core was the product of its Thiessen polygon area (truncated at the dredge area boundaries) and a dredging depth equal to the volume-weighted average dredge depth for the dredge area under the Thiessen polygon. Each texture description in a core was assigned a fraction of the core's associated dredge volume based on it relative length over the dredging depth. If the dredge depth was deeper than the last core section, then it was assumed that the texture description for the last core section extends down to the average dredge depth. The Thiessen polygon-based sediment composition was mapped onto the model grid using an area-weighted approach.

In order to translate the qualitative visual sediment classifications into quantitative estimates of the volume fractions of the three sediment classes used in the model, correlations were developed between primary visual texture description and measured grain size. These correlations were based on a subset of approximately 5% of the SSAP data that were analyzed for grain size distribution. The average grain size distribution of each of the primary visual textures is shown on Figure E-4-8. The estimated grain size distribution is aggregated into the three sediment classes. Class 1 is composed of clay and silt. Class 2 represents very fine sand. Class 3 consists of fine and medium sand. Transport of very coarse material (i.e., coarse sand and gravel) is not simulated because this type of sediment is only transported as bed load. Figures E-4-9 through E-4-11 show the average sediment composition of dredged areas for the three sediment classes.

The mass of sediment released during dredging operations is based on the dredging plan. For a particular grid cell, the mass of dredged sediment and the duration of dredging are specified. These two quantities are used to calculate the sediment mass removal rate during dredging in a grid cell:

$$W_{ij,k} = M_{ij} \, f_{ij,k} \, / \, T_{ij} \qquad \text{(E-4-21)}$$

where: $W_{ij,k}$ is the mass loading rate for sediment class k in grid cell (i,j); M_{ij} is total mass of dredged sediment in grid cell (i,j); $f_{ij,k}$ is fraction of sediment class k in the bed in grid cell (i,j); and T_{ij} is the duration of dredging grid cell (i,j).

E.4.4 Application

Effects of Grid Resolution on Near-Field Transport

The numerical grid used in this study has a relatively high spatial resolution for a far-field model. Typical grid cell dimensions are about 160 ft. in the longitudinal (along channel) direction and about 30 ft. in the lateral (cross-channel) direction. This grid resolution is adequate for simulating plume structure and transport outside the immediate vicinity of the dredge-head (i.e., the far-field).

Sediment released during dredging is input as a water column load to the grid cell in which the dredge is operating. Deposition and transport of sediment within that grid cell are simulated using the far-field model. The immediate vicinity of the dredge-head corresponds to the near-field region, which has a spatial extent of approximately 30 ft. (10 m). The near-field region is smaller than a typical grid cell. Thus, the far-field model cannot resolve sediment transport processes within the near-field region. The far-field model, however, does provide an approximate simulation of transport processes within the near-field region.

An investigation was conducted to determine the extent that approximating near-field transport processes, through specification of the dredge release load as described above, affects sediment transported away from the immediate vicinity of the dredge-head. A typical far-field grid cell has dimensions of about 30 ft. in the lateral direction by about 160 ft. in the longitudinal direction, with the water column represented by one vertical layer because of the use of a vertically-averaged model. This far-field grid cell is assumed to encompass the near-field region.

To investigate the effects of grid resolution on near-field transport processes, a single two-dimensional (2-D), far-field grid cell was represented as a three-dimensional (3-D), high-resolution grid with approximately 6-ft. square grid cells and 10 layers in the vertical (Figure E-4-12). The 3-D grid was used to evaluate whether the 2-D model provides a reasonable approximation of the near-field sediment transport processes. The effects of the following model input parameters on sediment transport within the 2-D (far-field) and 3-D (near-field) grids were evaluated: 1) river flow rate; 2) longitudinal location within 3-D grid of sediment load release; and 3) location of far-field grid cell (i.e., sediment load release location) in TIP channel. In addition, the effect of vertical location in the water column of load release was evaluated for all three input parameters; sediment loads were released at bottom, mid-depth and surface points.

For these simulations, only two classes of sediment were used: flocculating cohesive sediment (Class 1) and very fine sand with an effective diameter of 113 μm (Class 2). Model simulations were set up such that the total inflow rate along the upstream boundary of the 3-D grid matched the inflow rate to the 2-D grid cell; the total inflow rate was uniformly distributed along the 3-D inflow boundary. In the vertical, the velocity distribution at the 3-D inflow boundary was assumed to be uniform.

A 2-D grid cell located near RM 193 was chosen to investigate the effects of flow rate and longitudinal location within the 3-D grid (Figure E-4-12). Water depth at this grid cell is approximately 3 m. The impact of flow rate on the flux of suspended sediment transported across the downstream boundary of the near-field region (which is located at the downstream face of the 2-D grid cell) is shown on Figure E-4-13, which presents the ratio of the 3-D flux to the 2-D flux. These results indicate that more sediment is transported out of the near-field region by the 2-D model than the 3-D model, with the 3-D:2-D flux ratio increasing as flow increases. The 3-D model predicts that more sediment is deposited within the near-field region (Figure E-4-14). Additional insights from these results are: 1) deposition decreases with increasing flow rate due to probability of deposition effects; 2) more sediment is deposited when the load release is at the bottom than at the surface location; and 3) sand deposition is more sensitive to flow rate than deposition of fine (Class 1) sediment 1.

For the 2-D far-field model, sediment loading from releases during dredging is input to a single grid cell, such that the load is uniformly distributed over the entire cell. In contrast, the 3-D near-field model has 70 grid cells in the longitudinal (along channel) direction, such that the sediment load can be specified at any of those 70 grid cells. For the 3-D simulation results discussed above (see Figures E-4-13 and E-4-14), the sediment load was specified in the center of the 3-D grid (i.e., halfway between the upstream and downstream boundaries of the grid). The longitudinal location of the sediment release affects the transport of sediment out of the near-field region and the impacts of this location were evaluated (see Figures E-4-15 and E-4-16). Generally, the amount of sediment transported out of the near-field region increases as the release location gets closer to the downstream boundary.

The relative location of the far-field grid cell where the sediment release occurs in the channel may also affect the transport of solids within the near-field region of the dredge-head. Variation of solids release location within the channel was investigated at two general areas in the TIP: 1) in the northern TIP near RM 193; and 2) near Griffin Island. At each of these two areas, model sensitivity to channel location was evaluated by specifying the solids release point at three locations: 1) near-shore; 2) approximate mid-point between the shore and edge of navigation channel; and 3) edge of navigation channel. Results of the analysis in the northern TIP near RM 193 are presented on Figures E-4-17 and E-4-18. Similarly, results for the area near Griffin Island are shown on Figures E-4-19 and E-4-20. At both locations, differences between the 2-D far-field and 3-D near-field predictions of the downstream transport of released sediment tend to decrease as the release point moves from the near-shore area to the navigation channel.

The results of this analysis suggest that the 2-D far-field model tends to overpredict the transport of released sediment from the immediate vicinity of the dredge-head, i.e., the 2-D grid cell in which sediment loading is specified. Increasing the grid resolution within the immediate vicinity of the dredge-head through use of a 3-D model results in redeposition of more sediment, particularly coarser sediment (sand), than is predicted by the 2-D far-field model. The effects of increased grid resolution on model predictions are complex, as indicated on Figures E-4-13 through E-4-20. This complexity makes it difficult to generalize the results and develop an algorithm that might be used to adjust the 2-D model in the grid cell where dredge releases are specified such that better agreement is achieved between the 2-D and 3-D models within the immediate vicinity of the dredge-head. Additional work may make it possible to develop an adjustment algorithm for the 2-D far-field model at the location of dredge releases.

While these results indicate that the 2-D far-field model tends to overpredict transport of sediment within the immediate vicinity of the dredgehead, examination of the comparisons of the 2-D and 3-D model results shows that the overprediction is primarily related to coarse sediment (i.e., sands). Differences in cohesive (Class 1) sediment transport between the 2-D and 3-D models are generally minor. Thus, simulation of the transport of particle-associated PCBs within the immediate vicinity of the dredgehead may be minimally affected because the PCBs tend to be concentrated in the cohesive sediment fraction. Additionally, the 2-D model predicts that most of the PCBs associated with the coarse sediments do not desorb before redeposition, thus any overprediction of sand transport does not impact PCB levels predicted at far-field locations.

Linking of Sediment Transport and PCB Fate Models

Sediment transport model results are used in the PCB fate model as follows. The two models are run in parallel within the model framework. Predicted water column concentrations and deposition fluxes for all three sediment classes are calculated in each grid cell. This sediment transport information is then used to calculate PCB partitioning and deposition fluxes.

E.5 PCB FATE AND TRANSPORT MODELING

E.5.1 PCB Metric

The RPS specifies criteria for Total PCB concentration and Total and Tri+ PCB flux. The Tri+ PCB flux criterion was "… derived from the Total PCB criterion and the observation that the Total PCB to Tri+ PCB ratio in the sediments is approximately 3:1. Since sediments are the main form of release of PCBs, it is expected that the net addition of Tri+ PCBs will be one-third that of Total PCBs …" (Malcolm Pirnie and TAMS 2004). Given the derivative nature of the Tri+ PCB flux and the desire to keep the resuspension modeling effort tractable, modeling was conducted for Total PCBs. Compliance with the Total PCB flux criteria was presumed to ensure compliance with the Tri+ PCB flux criteria.

E.5.2 Overview of PCB Fate and Transport Processes

The purpose of the PCB modeling is to assess the fate and transport of resuspended material as a result of dredging activity. For this reason, the only sources of PCBs considered are those caused by resuspension during dredging. Other sources, such as resuspension due to other dredging-related activities (e.g., barge movement, debris removal, control structure placement), upstream loadings, flow-induced resuspension (i.e., bed erosion), and diffusional loads from the sediment bed are not included in the simulations. As shown in Figure E-1-2, the relevant PCB kinetic processes are sorption/desorption and volatilization. The PCB desorption process is integral to predicting the fate of resuspended PCBs as a result of dredging because sorbed PCBs will be transported with sediment particles while dissolved PCBs will be transported with the water. Volatilization from the river, while not expected to be a major loss mechanism of PCBs, is also included in order to assess the amount of PCBs released to the atmosphere as a result of dredging.

E.5.3 Model Description

Desorption Kinetics Sub-Model

In the analyses of organic compounds in natural waters, it is common practice to assume equilibrium partitioning between the aqueous and sediment-sorbed chemical phases. This implies that the kinetics of adsorption and desorption are much faster than the processes affecting PCBs. Sorption has fast and slow stages (Pignatello and Xing 1996). The fast stage has a time scale of minutes to hours, whereas the slow stage's time scale is weeks to months. The conventional conceptual model of biphasic sorption includes a reversibly sorbing component with fast stage kinetics and a resistantly bound component with slow stage kinetics.

It appears that sediments have a limited capacity for resistant sorption. Studies with field contaminated Hudson River sediments (Carroll et al. 1994) and laboratory-contaminated sediments (Kan et al. 1997) indicate a saturation of the resistant compartment at environmentally relevant concentrations of sorbed contaminant. Carroll et al. (1994) found that about 1000 ug Total PCB/g organic carbon was resistantly bound in Hudson River sediments with total sorbed PCB concentrations ranging from 2500 to 8700 ug Total PCB/g organic carbon. Kan et al. (1997) found that the resistant component on a river sediment saturated at about 2400 ug naphthalene/g organic carbon and about 70 ug 2,2',5,5' tetrachlorobiphenyl/g organic carbon.

Ignoring biphasic sorption by assuming instantaneous equilibrium introduces error in the PCB fate model. The equilibrium model over-estimates desorption of PCBs from resuspended sediment depending on the time scales of slow desorption. This will result in over-estimation of PCB flux from sediments and downstream transport of PCBs. The significance of this over-estimation depends on the magnitude of resuspension and the fraction of the sediment PCB that is resistantly sorbed.

In dredging analyses, the transport of contaminated sediments occurs on relatively short time scales (i.e., minutes to hours). For environmental analyses that occur on such short scales, comparable to that of labile desorption, the kinetics of desorption cannot be ignored. Equilibrium partitioning is not a good approximation. Any accurate modeling analysis of the fate and transport of sediment-sorbed organic contaminants introduced into the water column as a result of dredging must consider the dynamics of chemical desorption.

It has been proposed that the differential rates of organic compound desorption arise from the disparate diffusional rates of adsorbed chemical from swollen and condensed phases of organic matter (Pignatello 1990). Another common conceptual model is the radial diffusion model proposed by Wu and Gschwend (1986). A conceptual model that considers both disparate phases and radial diffusion was proposed by Famularo et al. (1980). This model assumes that the particle consists of two compartments, an outer shell and an inner core. Instantaneous equilibrium is assumed between the bulk aqueous phase chemical and the immediate surface of the outer shell. Diffusional processes are responsible for the transport from the surface of the shell to the interior of the shell as well as the transport from the shell interior to the inner core. Figure E-5-1 shows the conceptual model. Desorption from the outer shell is responsible for the fast labile phase of PCB desorption, while diffusion from the inner core to the outer shell controls the slow refractory phase desorption. This model was successfully applied to the desorption of the pesticide Kepone from resuspended sediments (Connolly et al. 1983).

Using this model and assuming constant particulate density and organic carbon content, the transfer rate of labile to dissolved PCB is given by:

$$\frac{dC_d}{dt} = -\left(\frac{3 * K_f * m}{1000 * R * \rho}\right) * \left(C_d - \frac{r_s * 1000}{f_{oc} * K_{ow}}\right) \qquad \text{(E-5-1)}$$

The transfer rate of the refractory to labile phase of PCB is given by:

$$\frac{dC_c}{dt} = \left(\frac{3 * K_c * ratio_R * m}{R}\right) * (r_s - r_c) \qquad \text{(E-5-2)}$$

where: C_d = dissolved chemical concentration (mg/L)

C_c = core (refractory) chemical concentration (mg/L)

r_c = core (refractory) chemical concentration on a mass basis (mg/g)

r_s = shell (labile) chemical concentration (mg/g)

m = solids concentration (g/L)

K_f = diffusion rate constant for the shell (cm/s)

K_c = diffusion rate constant for the core (cm/s)

f_{oc} = fraction organic carbon

K_{ow} = octanol-water partition coefficient (L/kg)

ρ = particle density (g/cc)

R = radius of shell (particle radius) (cm)

$ratio_R$ = ratio of core/shell radius (<1)

With this model, most parameters depend on properties of the sediment particles; the only chemical-dependent property is the octanol-water partition coefficient.

Volatilization

Volatilization is the process by which PCBs are transported across the air-water interface. A chemical's tendency to volatilize is determined by the ratio of its equilibrium activities in air and water (Henry's Constant). This ratio is a fundamental property of the chemical that is defined by Henry's Law. The value of Henry's Constant may be calculated from the vapor pressure of the chemical and its solubility in water (i.e., Henry's Constant equals the vapor pressure divided by the solubility) or it may be calculated from the equilibrium ratio of gas phase and water phase concentrations in a laboratory experiment. A high Henry's Constant is indicative of a volatile chemical that preferentially accumulates in the air phase. A low Henry's Constant is indicative of a non-volatile chemical that preferentially accumulates in the water phase. Values of Henry's Constant are presented either in units of partial pressure per unit aqueous concentration (e.g., atm-m^3/mol) or as a dimensionless ratio of concentrations (e.g., $(mol/m^3)/(mol/m^3)$). The dimensionless ratio is derived from the dimensioned ratio by dividing by the product of the universal gas constant and absolute temperature, i.e., RT, thus converting pressure into concentration using the ideal gas law.

Volatile chemicals have dimensionless Henry's Constants greater than about 0.1 (0.0025 atm-m^3/mol). As points of reference, the highly volatile chemicals vinyl chloride and oxygen have Henry's Constants at 20°C of about 4 and 21 (0.1 and 0.5 atm-m^3/mol), respectively. Numerous experimental determinations of Henry's Constants for PCBs have been published (e.g., Bopp 1983, Burkhard et al. 1985, Murphy et al. 1987, Dunnivant and Elzerman 1988, Brunner et al. 1990). These studies have used various methodologies that have yielded differing estimates. Values range from about 0.05 to 0.0005. They are highest for the lowest chlorinated congeners and decrease as chlorination increases. Values for Aroclors 1242 and 1254, as reported by Murphy et al. (1987) are about 0.1 and 0.008, respectively. While all of the reported PCB Henry's Constants are below the level of volatile chemicals, they are of sufficient magnitude to make volatilization a significant process, particularly in systems with large surface areas and long residence times.

The PCB Henry's Constants have a positive dependency on temperature. Laboratory data indicate an approximate doubling of the Henry's Constant for every 10°C temperature increase (Tateya et al. 1988, ten Hulscher et al. 1992), however, for this modeling application, the Henry's Constant was held constant at the 25°C value

The rate at which volatilization occurs is dependent on the mass transfer coefficient at the air-water interface and the concentration of PCBs in the water column. Only freely-dissolved PCB can be transported across the interface and sorption to particulate or dissolved organic carbon reduces volatilization. The equation used to describe PCB flux due to volatilization is as follows:

$$S_v = \frac{k_L}{h}\left(c - \frac{c_{air}}{H}\right) \tag{E-5-3}$$

where: S_v is the PCB volatilization flux; k_L is volatilization mass transfer coefficient; h is the water depth; c is the dissolved phase PCB concentration in water; c_{air} is vapor-phase PCB concentration in air; and H is dimensionless Henry's Constant.

The mass transfer coefficient (k_L) is dependent on the rates of mass transfer through relatively thin layers of water and air at the interface, which are in turn dependent on the concentration gradients in the layers, and the diffusivity of PCBs in the layers (O'Connor 1983, 1984).

$$k_L = \frac{k_g k_l}{k_g + \frac{k_l}{H}} \qquad \text{(E-5-4)}$$

where: k_g is vapor-phase mass transfer coefficient and k_l is water-phase mass transfer constant.

E.5.4 Model Development

Development of the PCB fate model required specification of model inputs associated with the dredge resuspension loads, desorption, and volatilization.

Resuspension PCB Loads

Total PCB concentrations in the sediment bed are calculated in the following manner. Sediment volumes, based on primary texture description, are calculated for Thiessen polygons and grid cells as described in Section E.4.3. Using core data, a volume-weighted average concentration by primary texture description is calculated down to the average dredge depth for each Thiessen polygon. Both measured Total PCB concentrations and extrapolated Total PCB concentrations are used for CL 1A, 2A, 2B, 2E, 2F, and 2G. Only measured concentrations are used for CL 2C, 2R, 2D, and 2H. Abandoned locations are not included. The average Total PCB concentrations for each primary texture description in a Thiessen polygon are used to calculate a volume-weighted average Total PCB concentration for each grid cell by texture description.

In order to estimate PCB concentrations for the three sediment classes used in the model, the correlations developed in Section E.4.3 (Figure E-4-8) are used to calculate the average PCB concentration for each of the sediment classes. These estimated concentrations are weight-averaged for the three sediment classes. Figures E-5-2 through E-5-4 show the average PCB concentrations for the three sediment classes used in the modeling.

Desorption

The experiments performed by Carroll et al. (1994) was used to calibrate the PCB desorption parameters. These experiments were considered to be the most appropriate source of published data as it used field contaminated Hudson River sediments. Recent experiments performed by Schneider et al. at the University of Maryland also have used field contaminated Hudson River sediments. Some results of these experiments have been presented (Schneider 2004); however, the results have yet to be published.

Carroll's experiments observed both short-term (days) and long-term (months) desorption of PCBs from Hudson River sediments for a range of contaminant levels from 25 to 205 mg/kg. The short-term portion of the desorption curve was chosen as the main calibration target. This was chosen since the relevant time scales of transport between dredging locations and monitoring stations (near and far-field) are on the order of minutes to hours. Moreover, the desorption of 25 mg/kg contaminated sediment was used as it was felt that that level was representative of the average levels found in the TIP. Figure E-5-5 shows the portion of this data set that was used for calibration.

Inspection of Equations E-5-1 and E-5-2 shows a number of parameters are needed for calibration. The organic carbon content was measured at 0.96%. The average particle radius was estimated to be 220 μm. Particle density was assumed at 2.65 g/cc based on typical values for sand. The octanol/water partition coefficient, $K_{ow,}$ has been shown to be approximately linearly related to laboratory determined K_{oc} values (Karickhoff 1981, 1984; Baker et al. 1997) and it is common to assume that K_{oc} is equal to K_{ow}. Since K_{ow} values of PCBs range over 3 orders of magnitude, increasing with increasing chlorination, the appropriate K_{oc} value to describe partitioning of PCBs as a group (Total PCB in the model) will depend on congener composition. Paired dissolved and particulate water data collected in the Upper Hudson River at Thompson Island and Schuylerville in 2004 and 2005 (BMP, QEA and ESI 2004) yield an average total PCB K_{oc} of $10^{5.4}$. Using the data shown in Figure E-5-5, the model was calibrated (also shown) with a very high degree of agreement between model and data. The calibrated parameters are given in Table E-5-1.

Table E-5-1. Desorption sub-model calibration parameters.

Parameter	Value	Units
K_f	0.25	cm/min
K_c	1.0×10^{-7}	cm/min
$ratio_R$	0.75	
f_{ref}	0.47	

To assess the validity of the desorption sub-model, the model was compared to the results of the Treatability Studies (DRET) performed by General Electric Company as described in the main body of the Intermediate Design Report. These experiments investigated the settling and PCB desorption of sediment by adding water to sediments, thoroughly agitating for one hour, and then allowing to sit for one hour. After this, the overlying water was analyzed for sediment and PCB. Although the intense and prolonged agitation of the sediments is not representative of field conditions during dredging, these data were used a semi-quantitative validation of the desorption model. Figure E-5-6 shows the dissolved PCB concentration predicted by the model compared to the DRET results. Generally, the model fell within the range of the observed data. There seems to be a slight underprediction of desorption of the model, however, this may be a result of increased desorption due to the intense agitation of these sediments.

The desorption sub-model also agrees with the results (as yet unpublished) of experiments conducted by Schneider et al. (2004). During these experiments, contaminated Hudson River sediments were resuspended with very low turbulence in large tanks. The resuspension 'event' lasted for three days. This was repeated three times with a one-day quiescent phase in between each resuspension phase. The sediment and PCB concentrations were monitored during each simulated event. For the purposes of predicting desorption due to dredging, only the first simulated resuspension event is appropriate. During this event 20% of total PCBs desorbed during the first hour and 40% desorbed during the first six hours. The six hour desorption is most representative of the labile portion of the PCB desorption. Assuming this value represents the entire labile phase desorption, it can be compared to the desorption sub-model calibration parameter, f_{ref}, from Table E-5-1. The initial fraction labile in the model is therefore 53% (1-f_{ref}), and is generally comparable to the 40% found by Schneider et al.

Volatilization

The overall volatilization mass transfer coefficient was calculated from water phase and vapor phase mass transfer coefficients and from Henry's Constant as indicated in Equation E-5-4 The Henry's Constant for Total PCBs used in the model calculations was estimated as the average of the values for the di-chlorinated congeners reported by Brunner et al. (1990) at 25ºC. Both experimentally determined and calculated Henry's Constants were included in the average to yield a Henry's Constant of 23.7 Pa-m3/mol (0.0136 unitless). Brunner's predictive equation calculates Henry's Constants based on the number of chlorine atoms and number of chlorine atoms in the ortho position:

$$\text{Log } H' = -1.38-0.32(\text{no. of Cl}) + 0.18(\text{no. of o-Cl}) \qquad \text{(E-5-5)}$$

Using an average Henry's Constant for di-chlorinated PCBs is a conservative estimate for Total PCBs which allows for the evaluation of the importance of volatilization losses during dredging.

E.6 SIMULATION OF DREDGING OPERATIONS

E.6.1 Development of a Dredge Plan

The details of the development of the dredging plan are given in the main body of the Intermediate Design Report. The dredging schedule was based on same the numerical grid that was used for the resuspension modeling. The sediment volumes to be dredged were divided into discrete volumes that reside below each corresponding river grid element. The total sediment mass removed, dredge ID number, dredge start time, and dredge end time were specified for each of these grid cells A base dredging plan was developed assuming no structural resuspension controls. The planned dredging utilizes four dredges and covers the period from May 21, 2007 to October 2, 2007. Table E-6-1 presents the schedule used for the dredging simulations. Figures E-6-1a and E-6-1b show graphical representations of the dredging schedule.

Table E-6-1. Dredging schedule for May 21 to October 2, 2007.

Grid ID		Dredge Area	Dredge ID (1,2,3,4)	Eng. Consideration Dredge Weight (tons)	Design Factored Time (hr)	Start Time	Finish Time
I	J						
20	20	NTIP01	1	22.5	0.7	05/21/07 00:00	05/21/07 00:43
20	21	NTIP01	1	421.8	11.7	05/21/07 00:43	05/21/07 12:24
20	22	NTIP01	1	536.2	17.3	05/21/07 12:24	05/22/07 05:45
20	23	NTIP01	1	63.8	2.1	05/22/07 05:45	05/22/07 07:48
21	19	NTIP01	1	130.9	4.2	05/22/07 07:48	05/22/07 12:02
21	20	NTIP01	1	1380.7	44.6	05/22/07 12:02	05/24/07 08:41
21	21	NTIP01	1	2096.3	117.8	05/24/07 08:41	05/31/07 06:30
21	22	NTIP01	1	1603.3	105.1	05/31/07 06:30	06/05/07 15:39
22	19	NTIP01	1	6.9	0.2	06/05/07 15:39	06/05/07 15:52
22	20	NTIP01	1	928.3	60.9	06/05/07 15:52	06/08/07 04:45
22	21	NTIP01	1	1207.1	67.9	06/08/07 04:45	06/12/07 00:36
22	22	NTIP01/NTIP02A	1	1051.4	68.9	06/12/07 00:36	06/14/07 21:33
22	23	NTIP01/NTIP02A	1	423.2	20.5	06/14/07 21:33	06/15/07 18:05
23	22	NTIP02A	1	3.4	0.3	06/16/07 00:00	06/16/07 00:16
23	23	NTIP02A	1	0.3	0.0	06/16/07 00:16	06/16/07 00:17
24	21	NTIP02A	1	0.5	0.0	06/16/07 00:17	06/16/07 00:18
24	22	NTIP02A	1	2.3	0.2	06/16/07 00:18	06/16/07 00:32
24	23	NTIP02A	1	0.0	0.0	06/16/07 00:32	06/16/07 00:32
25	21	NTIP02A	1	29.7	1.6	06/16/07 00:32	06/16/07 02:05
25	22	NTIP02A	1	101.0	9.9	06/16/07 02:05	06/16/07 12:01
25	23	NTIP02A	1	3.8	0.1	06/16/07 12:01	06/16/07 12:09
26	21	NTIP02A	1	126.9	3.5	06/16/07 12:09	06/16/07 15:40
26	22	NTIP02A	1	314.8	20.6	06/16/07 15:40	06/18/07 12:18

Grid ID I	Grid ID J	Dredge Area	Dredge ID (1,2,3,4)	Eng. Consideration Dredge Weight (tons)	Design Factored Time (hr)	Start Time	Finish Time
26	23	NTIP02A	1	38.2	1.9	06/18/07 12:18	06/18/07 14:09
27	20	NTIP02A	1	44.4	1.4	06/18/07 14:09	06/18/07 15:36
27	21	NTIP02A	1	257.0	14.4	06/18/07 15:36	06/19/07 06:02
27	22	NTIP02A/NTIP02B	1	402.3	39.6	06/19/07 06:02	06/20/07 21:37
27	23	NTIP02A	1	18.4	0.9	06/20/07 21:37	06/20/07 22:30
28	19	NTIP02B	1	14.0	0.3	06/21/07 00:00	06/21/07 00:20
28	20	NTIP02B	1	474.6	15.3	06/21/07 00:20	06/21/07 15:40
28	21	NTIP02B	1	560.1	15.5	06/21/07 15:40	06/22/07 07:12
28	22	NTIP02B	1	621.0	20.1	06/22/07 07:12	06/23/07 03:16
28	23	NTIP02B	1	58.9	1.4	06/23/07 03:16	06/23/07 04:42
29	19	NTIP02B	1	138.1	3.4	06/23/07 04:42	06/23/07 08:03
29	20	NTIP02B	1	572.4	28.2	06/23/07 08:03	06/25/07 12:12
29	21	NTIP02B	1	906.5	18.8	06/25/07 12:12	06/26/07 07:02
29	22	NTIP02B	1	737.0	17.9	06/26/07 07:02	06/27/07 00:54
29	23	NTIP02B	1	783.6	19.0	06/27/07 00:54	06/27/07 19:55
30	19	NTIP02B	1	563.7	13.7	06/27/07 19:55	06/28/07 09:35
30	20	NTIP02B	1	906.2	44.6	06/28/07 09:35	06/30/07 06:10
30	21	NTIP02B	1	791.9	16.5	06/30/07 06:10	06/30/07 22:37
30	22	NTIP02B	1	41.5	1.7	06/30/07 22:37	07/02/07 00:22
30	23	NTIP02B	1	64.2	1.6	07/02/07 00:22	07/02/07 01:55
31	19	NTIP02B	1	838.2	41.2	07/02/07 01:55	07/03/07 19:09
31	20	NTIP02B	1	1174.9	24.4	07/03/07 19:09	07/05/07 19:34
31	21	NTIP02B	1	963.0	20.0	07/05/07 19:34	07/06/07 15:35
31	22	NTIP02B	1	824.6	30.0	07/06/07 15:35	07/07/07 21:34
31	23	NTIP02B	1	44.0	1.1	07/07/07 21:34	07/07/07 22:38
32	18	NTIP02B	1	221.9	5.4	07/07/07 22:38	07/09/07 04:01
32	19	NTIP02B	1	3893.0	94.4	07/09/07 04:01	07/13/07 02:24
32	20	NTIP02B	1	2971.2	61.7	07/13/07 02:24	07/16/07 16:09
32	21	NTIP02B	1	1532.8	31.9	07/16/07 16:09	07/18/07 00:00
32	22	NTIP02B	1	1295.3	47.1	07/18/07 00:00	07/19/07 23:07
32	23	NTIP02B	1	227.1	8.3	07/19/07 23:07	07/20/07 07:22
33	18	NTIP02B	1	67.3	2.4	07/20/07 07:22	07/20/07 09:49
33	19	NTIP02B	1	1320.3	48.0	07/20/07 09:49	07/23/07 09:50
33	20	NTIP02B	1	2109.1	76.7	07/23/07 09:50	07/26/07 14:32
33	21	NTIP02B	1	1555.1	56.6	07/26/07 14:32	07/28/07 23:06
33	22	NTIP02B	1	1389.8	50.6	07/28/07 23:06	08/01/07 01:41
33	23	NTIP02B	1	27.7	1.0	08/01/07 01:41	08/01/07 02:41
34	19	NTIP02B	1	1196.3	29.0	08/01/07 02:41	08/02/07 07:41
34	20	NTIP02B	1	1839.4	38.2	08/02/07 07:41	08/03/07 21:55
35	19	NTIP02B	1	905.8	22.0	08/03/07 21:55	08/04/07 19:52
35	20	NTIP02B	1	2155.4	44.8	08/04/07 19:52	08/07/07 16:40
36	19	NTIP02B	1	1581.7	38.3	08/07/07 16:40	08/09/07 07:01
36	20	NTIP02B	1	3125.2	64.9	08/09/07 07:01	08/12/07 23:58
37	18	NTIP02B	1	9.5	0.2	08/12/07 23:58	08/13/07 00:12
37	19	NTIP02B	1	713.1	17.3	08/13/07 00:12	08/13/07 17:29
37	20	NTIP02B	1	1168.7	24.3	08/13/07 17:29	08/14/07 17:46
38	17	NTIP02B	1	169.5	4.1	08/14/07 17:46	08/14/07 21:53
38	18	NTIP02B	1	651.0	15.8	08/14/07 21:53	08/15/07 13:40
38	19	NTIP02B	1	735.0	17.8	08/15/07 13:40	08/16/07 07:29

Grid ID		Dredge Area	Dredge ID (1,2,3,4)	Eng. Consideration Dredge Weight (tons)	Design Factored Time (hr)	Start Time	Finish Time
I	J						
39	16	NTIP02B	1	67.3	1.6	08/16/07 07:29	08/16/07 09:07
39	17	NTIP02B	1	704.6	17.1	08/16/07 09:07	08/17/07 02:12
39	18	NTIP02B	1	610.1	14.8	08/17/07 02:12	08/17/07 17:00
40	15	NTIP02B/NTIP02F	1	260.8	9.5	08/17/07 17:00	08/18/07 02:29
14	8	NTIP02C	2	31.5	1.3	06/18/07 00:00	06/18/07 01:18
15	2	NTIP02C	2	92.0	3.8	06/18/07 01:18	06/18/07 05:08
15	3	NTIP02C	2	186.3	7.7	06/18/07 05:08	06/18/07 12:52
15	4	NTIP02C	2	170.4	7.1	06/18/07 12:52	06/18/07 19:57
15	5	NTIP02C	2	210.7	17.8	06/18/07 19:57	06/19/07 13:43
15	6	NTIP02C	2	203.7	8.5	06/19/07 13:43	06/19/07 22:11
16	1	NTIP02C	2	167.3	8.1	06/19/07 22:11	06/20/07 06:18
16	2	NTIP02C	2	355.7	35.0	06/20/07 06:18	06/21/07 17:18
16	3	NTIP02C	2	251.1	10.4	06/21/07 17:18	06/22/07 03:44
16	4	NTIP02C	2	149.1	6.2	06/22/07 03:44	06/22/07 09:56
16	5	NTIP02C	2	148.9	6.2	06/22/07 09:56	06/22/07 16:07
16	6	NTIP02C	2	258.3	10.7	06/22/07 16:07	06/23/07 02:51
17	0	NTIP02C	2	25.8	1.3	06/23/07 02:51	06/23/07 04:06
17	1	NTIP02C	2	148.9	7.2	06/23/07 04:06	06/23/07 11:20
17	2	NTIP02C	2	162.1	6.7	06/23/07 11:20	06/23/07 18:04
17	3	NTIP02C	2	70.5	2.9	06/23/07 18:04	06/23/07 21:00
17	4	NTIP02C	2	60.3	2.5	06/23/07 21:00	06/23/07 23:30
17	5	NTIP02C	2	347.5	29.3	06/23/07 23:30	06/26/07 04:48
17	6	NTIP02C	2	300.6	12.5	06/26/07 04:48	06/26/07 17:17
18	3	NTIP02C	2	77.4	3.2	06/26/07 17:17	06/26/07 20:30
18	4	NTIP02C	2	293.8	12.2	06/26/07 20:30	06/27/07 08:43
18	5	NTIP02C	2	314.0	13.0	06/27/07 08:43	06/27/07 21:46
19	0	NTIP02C	2	30.5	1.5	06/27/07 21:46	06/27/07 23:15
19	1	NTIP02C	2	101.9	4.9	06/27/07 23:15	06/28/07 04:11
19	2	NTIP02C	2	161.7	6.7	06/28/07 04:11	06/28/07 10:55
19	3	NTIP02C	2	319.3	26.9	06/28/07 10:55	06/29/07 13:50
19	4	NTIP02C	2	347.2	14.4	06/29/07 13:50	06/30/07 04:16
20	0	NTIP02C	2	26.8	1.3	06/30/07 04:16	06/30/07 05:34
20	1	NTIP02C	2	227.9	11.1	06/30/07 05:34	06/30/07 16:37
20	2	NTIP02C	2	310.9	26.2	06/30/07 16:37	07/02/07 18:50
20	3	NTIP02C	2	353.5	14.7	07/02/07 18:50	07/03/07 09:31
20	4	NTIP02C	2	371.6	15.4	07/03/07 09:31	07/05/07 00:58
21	0	NTIP02C	2	0.0	0.0	07/05/07 00:58	07/05/07 00:58
21	1	NTIP02C	2	192.2	18.9	07/05/07 00:58	07/05/07 19:52
21	2	NTIP02C	2	346.5	29.2	07/05/07 19:52	07/07/07 01:05
21	3	NTIP02C	2	399.9	33.7	07/07/07 01:05	07/09/07 10:49
21	4	NTIP02C	2	415.7	35.0	07/09/07 10:49	07/10/07 21:51
21	5	NTIP02C	2	413.9	34.9	07/10/07 21:51	07/12/07 08:45
22	0	NTIP02C	2	2.3	0.2	07/12/07 08:45	07/12/07 08:55
22	1	NTIP02C	2	291.2	21.2	07/12/07 08:55	07/13/07 06:06
22	2	NTIP02C	2	627.3	45.6	07/13/07 06:06	07/16/07 03:44
22	3	NTIP02C	2	410.5	60.6	07/16/07 03:44	07/18/07 16:18
22	4	NTIP02C	2	442.0	32.1	07/18/07 16:18	07/20/07 00:27
22	5	NTIP02C	2	457.5	33.3	07/20/07 00:27	07/21/07 09:43
23	0	NTIP02C	2	59.3	2.2	07/21/07 09:43	07/21/07 11:53

Grid ID I	Grid ID J	Dredge Area	Dredge ID (1,2,3,4)	Eng. Consideration Dredge Weight (tons)	Design Factored Time (hr)	Start Time	Finish Time
23	1	NTIP02C	2	488.3	17.8	07/21/07 11:53	07/23/07 05:39
23	2	NTIP02C	2	462.2	19.5	07/23/07 05:39	07/24/07 01:08
23	3	NTIP02C	2	380.7	7.9	07/24/07 01:08	07/24/07 09:03
23	4	NTIP02C	2	537.0	11.2	07/24/07 09:03	07/24/07 20:13
23	5	NTIP02C	2	547.1	11.4	07/24/07 20:13	07/25/07 07:35
24	0	NTIP02C	2	20.9	0.5	07/25/07 07:35	07/25/07 08:05
24	1	NTIP02C	2	444.7	10.8	07/25/07 08:05	07/25/07 18:53
24	2	NTIP02C	2	544.2	11.3	07/25/07 18:53	07/26/07 06:11
24	3	NTIP02C	2	684.1	14.2	07/26/07 06:11	07/26/07 20:24
24	4	NTIP02C	2	364.4	15.4	07/26/07 20:24	07/27/07 11:46
24	5	NTIP02C	2	430.1	8.9	07/27/07 11:46	07/27/07 20:42
25	0	NTIP02C	2	31.2	1.1	07/27/07 20:42	07/27/07 21:50
25	1	NTIP02C	2	371.7	13.5	07/27/07 21:50	07/28/07 11:21
25	2	NTIP02C	2	684.8	50.5	07/28/07 11:21	07/31/07 13:53
25	3	NTIP02C	2	1084.9	39.5	07/31/07 13:53	08/02/07 05:20
25	4	NTIP02C	2	523.6	19.0	08/02/07 05:20	08/03/07 00:22
25	5	NTIP02C	2	102.2	6.0	08/03/07 00:22	08/03/07 06:24
26	0	NTIP02C	2	12.8	0.3	08/03/07 06:24	08/03/07 06:43
26	1	NTIP02C	2	257.8	6.3	08/03/07 06:43	08/03/07 12:58
26	2	NTIP02C	2	466.4	11.3	08/03/07 12:58	08/04/07 00:17
26	3	NTIP02C	2	179.1	3.7	08/04/07 00:17	08/04/07 04:00
26	4	NTIP02C	2	269.2	5.6	08/04/07 04:00	08/04/07 09:36
26	5	NTIP02C	2	434.3	9.0	08/04/07 09:36	08/04/07 18:37
27	0	NTIP02C	2	78.6	1.9	08/04/07 18:37	08/04/07 20:32
27	1	NTIP02C	2	312.3	7.6	08/04/07 20:32	08/06/07 04:06
27	2	NTIP02C	2	507.2	10.5	08/06/07 04:06	08/06/07 14:38
27	3	NTIP02C	2	140.8	2.9	08/06/07 14:38	08/06/07 17:34
27	4	NTIP02C	2	12.3	0.3	08/06/07 17:34	08/06/07 17:49
27	5	NTIP02C	2	182.8	4.4	08/06/07 17:49	08/06/07 22:15
28	0	NTIP02C/NTIP02E	2	150.3	3.6	08/06/07 22:15	08/07/07 01:54
28	1	NTIP02C/NTIP02E	2	492.6	11.9	08/07/07 01:54	08/07/07 13:51
28	2	NTIP02C/NTIP02E	2	140.0	2.9	08/07/07 13:51	08/07/07 16:45
28	4	NTIP02E	2	10.4	0.3	08/08/07 00:00	08/08/07 00:15
28	5	NTIP02E	2	8.7	0.2	08/08/07 00:15	08/08/07 00:27
29	0	NTIP02E	2	237.5	8.6	08/08/07 00:27	08/08/07 09:06
29	1	NTIP02E	2	304.2	7.4	08/08/07 09:06	08/08/07 16:29
29	2	NTIP02E	2	315.5	6.6	08/08/07 16:29	08/08/07 23:02
29	3	NTIP02E	2	79.4	1.6	08/08/07 23:02	08/09/07 00:41
29	4	NTIP02E	2	226.2	5.5	08/09/07 00:41	08/09/07 06:10
29	5	NTIP02E	2	210.0	10.3	08/09/07 06:10	08/09/07 16:30
30	1	NTIP02E	2	350.6	8.5	08/09/07 16:30	08/10/07 01:00
30	2	NTIP02E	2	458.1	22.5	08/10/07 01:00	08/10/07 23:32
30	3	NTIP02E	2	200.3	4.2	08/10/07 23:32	08/11/07 03:42
30	4	NTIP02E	2	336.5	8.2	08/11/07 03:42	08/11/07 11:51
30	5	NTIP02E	2	458.6	11.1	08/11/07 11:51	08/11/07 22:59
31	1	NTIP02E	2	194.2	4.7	08/11/07 22:59	08/13/07 03:41
31	2	NTIP02E	2	348.5	8.5	08/13/07 03:41	08/13/07 12:08
31	3	NTIP02E	2	27.0	0.9	08/13/07 12:08	08/13/07 13:03
31	4	NTIP02E	2	330.2	13.9	08/13/07 13:03	08/14/07 02:58

Grid ID		Dredge Area	Dredge ID (1,2,3,4)	Eng. Consideration Dredge Weight (tons)	Design Factored Time (hr)	Start Time	Finish Time
I	J						
31	5	NTIP02E	2	666.1	16.1	08/14/07 02:58	08/14/07 19:07
32	1	NTIP02E	2	269.0	6.5	08/14/07 19:07	08/15/07 01:39
32	2	NTIP02E	2	460.0	11.2	08/15/07 01:39	08/15/07 12:48
32	3	NTIP02E	2	370.0	7.7	08/15/07 12:48	08/15/07 20:29
32	4	NTIP02E	2	534.9	11.1	08/15/07 20:29	08/16/07 07:36
32	5	NTIP02E	2	556.5	11.6	08/16/07 07:36	08/16/07 19:10
33	1	NTIP02E	2	326.4	7.9	08/16/07 19:10	08/17/07 03:05
33	2	NTIP02E	2	607.4	14.7	08/17/07 03:05	08/17/07 17:49
33	3	NTIP02E	2	572.9	11.9	08/17/07 17:49	08/18/07 05:43
33	4	NTIP02E	2	476.9	9.9	08/18/07 05:43	08/18/07 15:38
33	5	NTIP02E	2	385.7	8.0	08/18/07 15:38	08/18/07 23:39
33	6	NTIP02E	2	1636.0	34.0	08/18/07 23:39	08/21/07 09:39
34	0	NTIP02E	2	25.6	0.6	08/21/07 09:39	08/21/07 10:16
34	1	NTIP02E	2	320.9	7.8	08/21/07 10:16	08/21/07 18:03
34	2	NTIP02E	2	541.1	13.1	08/21/07 18:03	08/22/07 07:10
34	3	NTIP02E	2	597.1	25.2	08/22/07 07:10	08/23/07 08:21
34	4	NTIP02E	2	252.3	5.2	08/23/07 08:21	08/23/07 13:35
34	5	NTIP02E	2	166.0	3.5	08/23/07 13:35	08/23/07 17:02
34	6	NTIP02E	2	1939.3	40.3	08/23/07 17:02	08/25/07 09:20
35	1	NTIP02E	2	216.2	5.2	08/25/07 09:20	08/25/07 14:35
35	2	NTIP02E	2	451.7	22.2	08/25/07 14:35	08/27/07 12:48
35	3	NTIP02E	2	524.7	10.9	08/27/07 12:48	08/27/07 23:42
35	4	NTIP02E	2	474.2	9.9	08/27/07 23:42	08/28/07 09:34
35	5	NTIP02E	2	26.0	0.5	08/28/07 09:34	08/28/07 10:06
35	7	NTIP02E	2	26.9	0.6	08/28/07 10:06	08/28/07 10:40
36	1	NTIP02E/NTIP02F	2	141.9	5.2	08/28/07 10:40	08/28/07 15:50
36	2	NTIP02E/NTIP02F	2	268.7	6.5	08/28/07 15:50	08/28/07 22:20
36	3	NTIP02E/NTIP02F	2	99.7	2.1	08/28/07 22:20	08/29/07 00:25
36	4	NTIP02E	2	132.2	2.7	08/29/07 00:25	08/29/07 03:10
36	5	NTIP02E	2	20.7	0.4	08/29/07 03:10	08/29/07 03:35
36	7	NTIP02F	2	89.7	1.9	08/30/07 00:00	08/30/07 01:51
37	1	NTIP02F	2	160.2	3.9	08/30/07 01:51	08/30/07 05:44
37	2	NTIP02F	2	267.8	6.5	08/30/07 05:44	08/30/07 12:14
37	3	NTIP02F	2	335.6	14.1	08/30/07 12:14	08/31/07 02:23
37	4	NTIP02F	2	73.9	1.5	08/31/07 02:23	08/31/07 03:55
37	5	NTIP02F	2	25.9	0.5	08/31/07 03:55	08/31/07 04:27
37	6	NTIP02F	2	195.6	4.1	08/31/07 04:27	08/31/07 08:31
38	0	NTIP02F	2	7.7	0.3	08/31/07 08:31	08/31/07 08:48
38	1	NTIP02F	2	305.0	11.1	08/31/07 08:48	08/31/07 19:54
38	2	NTIP02F	2	264.7	6.4	08/31/07 19:54	09/01/07 02:19
38	3	NTIP02F	2	226.5	4.7	09/01/07 02:19	09/01/07 07:01
38	4	NTIP02F	2	299.9	6.2	09/01/07 07:01	09/02/07 13:15
38	5	NTIP02F	2	375.5	7.8	09/02/07 13:15	09/02/07 21:03
38	6	NTIP02F	2	498.9	10.4	09/02/07 21:03	09/04/07 07:25
39	0	NTIP02F	2	1.1	0.0	09/04/07 07:25	09/04/07 07:28
39	1	NTIP02F	2	137.6	5.0	09/04/07 07:28	09/04/07 12:28
39	2	NTIP02F	2	305.9	15.0	09/04/07 12:28	09/05/07 03:31
39	3	NTIP02F	2	311.8	6.5	09/05/07 03:31	09/05/07 09:59
39	4	NTIP02F	2	447.2	9.3	09/05/07 09:59	09/05/07 19:17

Grid ID		Dredge Area	Dredge ID (1,2,3,4)	Eng. Consideration Dredge Weight (tons)	Design Factored Time (hr)	Start Time	Finish Time
I	J						
39	5	NTIP02F	2	376.0	7.8	09/05/07 19:17	09/06/07 03:06
39	6	NTIP02F	2	355.0	7.4	09/06/07 03:06	09/06/07 10:29
39	7	NTIP02F	2	383.3	8.0	09/06/07 10:29	09/06/07 18:27
40	1	NTIP02F	2	10.6	0.4	09/06/07 18:27	09/06/07 18:50
40	2	NTIP02F	2	22.7	0.5	09/06/07 18:50	09/06/07 19:23
40	3	NTIP02F	2	33.6	0.7	09/06/07 19:23	09/06/07 20:04
40	4	NTIP02F	2	41.7	0.9	09/06/07 20:04	09/06/07 20:56
40	5	NTIP02F	2	187.8	3.9	09/06/07 20:56	09/07/07 00:51
40	6	NTIP02F	2	314.4	13.3	09/07/07 00:51	09/07/07 14:06
40	7	NTIP02F	2	352.9	7.3	09/07/07 14:06	09/07/07 21:26
40	8	NTIP02F	2	434.8	9.0	09/07/07 21:26	09/08/07 06:28
41	1	NTIP02F	2	63.4	2.3	09/08/07 06:28	09/08/07 08:47
41	2	NTIP02F	2	196.7	4.8	09/08/07 08:47	09/08/07 13:33
41	3	NTIP02F	2	113.5	4.8	09/08/07 13:33	09/08/07 18:20
41	4	NTIP02F	2	17.6	0.4	09/08/07 18:20	09/08/07 18:42
41	5	NTIP02F	2	21.5	0.4	09/08/07 18:42	09/08/07 19:09
41	6	NTIP02F	2	70.4	1.5	09/08/07 19:09	09/08/07 20:37
41	7	NTIP02F	2	125.3	2.6	09/08/07 20:37	09/08/07 23:13
41	8	NTIP02F	2	194.9	4.1	09/08/07 23:13	09/10/07 03:16
41	9	NTIP02F	2	191.7	4.0	09/10/07 03:16	09/10/07 07:15
41	10	NTIP02F	2	57.0	1.9	09/10/07 07:15	09/10/07 09:10
41	11	NTIP02F	2	178.2	3.7	09/10/07 09:10	09/10/07 12:53
41	12	NTIP02F	2	323.0	6.7	09/10/07 12:53	09/10/07 19:35
41	13	NTIP02F	2	406.5	17.1	09/10/07 19:35	09/11/07 12:43
41	14	NTIP02F	2	431.8	9.0	09/11/07 12:43	09/11/07 21:42
41	15	NTIP02F	2	295.5	6.1	09/11/07 21:42	09/12/07 03:50
42	0	NTIP02F	2	0.0	0.0	09/12/07 03:50	09/12/07 03:50
42	1	NTIP02F	2	179.7	6.5	09/12/07 03:50	09/12/07 10:22
42	2	NTIP02F	2	173.2	4.2	09/12/07 10:22	09/12/07 14:34
42	3	NTIP02F	2	305.0	6.3	09/12/07 14:34	09/12/07 20:55
42	4	NTIP02F	2	345.7	14.6	09/12/07 20:55	09/13/07 11:29
42	5	NTIP02F	2	262.1	5.4	09/13/07 11:29	09/13/07 16:56
42	6	NTIP02F	2	206.7	4.3	09/13/07 16:56	09/13/07 21:13
42	7	NTIP02F	2	240.0	5.0	09/13/07 21:13	09/14/07 02:13
42	8	NTIP02F	2	213.1	4.4	09/14/07 02:13	09/14/07 06:38
42	9	NTIP02F	2	290.3	6.0	09/14/07 06:38	09/14/07 12:40
42	10	NTIP02F	2	368.6	7.7	09/14/07 12:40	09/14/07 20:20
42	11	NTIP02F	2	380.6	7.9	09/14/07 20:20	09/15/07 04:14
42	12	NTIP02F	2	285.3	5.9	09/15/07 04:14	09/15/07 10:10
42	13	NTIP02F	2	309.4	6.4	09/15/07 10:10	09/15/07 16:36
43	0	NTIP02F	2	3.7	0.1	09/15/07 16:36	09/15/07 16:44
43	1	NTIP02F	2	206.0	7.5	09/15/07 16:44	09/17/07 00:13
43	2	NTIP02F	2	82.3	2.0	09/17/07 00:13	09/17/07 02:13
43	3	NTIP02F	2	27.7	0.7	09/17/07 02:13	09/17/07 02:54
43	4	NTIP02F	2	105.1	2.2	09/17/07 02:54	09/17/07 05:05
43	5	NTIP02F	2	126.2	2.6	09/17/07 05:05	09/17/07 07:42
43	6	NTIP02F	2	222.2	4.6	09/17/07 07:42	09/17/07 12:19
43	7	NTIP02F	2	224.4	4.7	09/17/07 12:19	09/17/07 16:59
43	8	NTIP02F	2	172.9	3.6	09/17/07 16:59	09/17/07 20:34

Grid ID		Dredge Area	Dredge ID (1,2,3,4)	Eng. Consideration Dredge Weight (tons)	Design Factored Time (hr)	Start Time	Finish Time
I	J						
43	9	NTIP02F	2	237.9	4.9	09/17/07 20:34	09/18/07 01:31
43	10	NTIP02F	2	201.5	4.2	09/18/07 01:31	09/18/07 05:42
43	11	NTIP02F	2	157.6	3.3	09/18/07 05:42	09/18/07 08:59
44	1	NTIP02F	2	6.7	0.2	09/18/07 08:59	09/18/07 09:13
44	2	NTIP02F	2	77.3	2.8	09/18/07 09:13	09/18/07 12:02
44	3	NTIP02F	2	214.3	5.2	09/18/07 12:02	09/18/07 17:14
44	4	NTIP02F	2	221.9	4.6	09/18/07 17:14	09/18/07 21:51
44	5	NTIP02F	2	93.0	1.9	09/18/07 21:51	09/18/07 23:47
44	6	NTIP02F	2	85.7	1.8	09/18/07 23:47	09/19/07 01:33
44	7	NTIP02F	2	143.3	3.0	09/19/07 01:33	09/19/07 04:32
44	8	NTIP02F	2	175.1	3.6	09/19/07 04:32	09/19/07 08:10
44	9	NTIP02F	2	202.0	4.2	09/19/07 08:10	09/19/07 12:22
44	10	NTIP02F	2	163.9	3.4	09/19/07 12:22	09/19/07 15:47
45	0	NTIP02F	2	0.0	0.0	09/19/07 15:47	09/19/07 15:47
45	1	NTIP02F	2	19.5	0.7	09/19/07 15:47	09/19/07 16:29
45	2	NTIP02F	2	64.2	2.3	09/19/07 16:29	09/19/07 18:49
45	3	NTIP02F	2	83.2	2.0	09/19/07 18:49	09/19/07 20:50
45	4	NTIP02F	2	144.1	3.5	09/19/07 20:50	09/20/07 00:20
45	5	NTIP02F	2	47.7	1.0	09/20/07 00:20	09/20/07 01:20
45	6	NTIP02F	2	0.7	0.0	09/20/07 01:20	09/20/07 01:21
46	3	NTIP02G	2	0.0	0.0	09/21/07 00:00	09/21/07 00:00
46	4	NTIP02G	2	73.4	1.5	09/21/07 00:00	09/21/07 01:31
46	5	NTIP02G	2	217.5	9.2	09/21/07 01:31	09/21/07 10:41
46	6	NTIP02G	2	368.3	7.7	09/21/07 10:41	09/21/07 18:20
47	0	NTIP02G	2	0.0	0.0	09/21/07 18:20	09/21/07 18:20
47	1	NTIP02G	2	22.0	0.5	09/21/07 18:20	09/21/07 18:52
47	2	NTIP02G	2	52.3	1.3	09/21/07 18:52	09/21/07 20:08
47	3	NTIP02G	2	64.7	1.6	09/21/07 20:08	09/21/07 21:43
47	4	NTIP02G	2	114.1	2.8	09/21/07 21:43	09/22/07 00:28
47	5	NTIP02G	2	121.9	2.5	09/22/07 00:28	09/22/07 03:00
47	6	NTIP02G	2	137.5	5.8	09/22/07 03:00	09/22/07 08:48
47	7	NTIP02G	2	132.7	2.8	09/22/07 08:48	09/22/07 11:34
47	8	NTIP02G	2	164.2	3.4	09/22/07 11:34	09/22/07 14:59
48	1	NTIP02G	2	49.4	1.2	09/22/07 14:59	09/22/07 16:10
48	2	NTIP02G	2	85.4	2.1	09/22/07 16:10	09/22/07 18:15
48	3	NTIP02G	2	120.8	2.9	09/22/07 18:15	09/22/07 21:10
48	4	NTIP02G	2	137.5	5.8	09/22/07 21:10	09/24/07 02:58
48	5	NTIP02G	2	154.2	3.2	09/24/07 02:58	09/24/07 06:10
48	6	NTIP02G	2	118.5	2.5	09/24/07 06:10	09/24/07 08:38
48	7	NTIP02G	2	144.6	3.0	09/24/07 08:38	09/24/07 11:38
48	8	NTIP02G	2	234.2	4.9	09/24/07 11:38	09/24/07 16:30
48	9	NTIP02G	2	334.8	7.0	09/24/07 16:30	09/24/07 23:28
48	10	NTIP02G	2	284.1	5.9	09/24/07 23:28	09/25/07 05:22
48	11	NTIP02G	2	299.6	6.2	09/25/07 05:22	09/25/07 11:36
49	0	NTIP02G	2	0.0	0.0	09/25/07 11:36	09/25/07 11:36
49	1	NTIP02G	2	156.3	3.8	09/25/07 11:36	09/25/07 15:23
49	2	NTIP02G	2	235.6	5.7	09/25/07 15:23	09/25/07 21:06
49	3	NTIP02G	2	231.1	5.6	09/25/07 21:06	09/26/07 02:42
49	4	NTIP02G	2	263.0	5.5	09/26/07 02:42	09/26/07 08:10

Grid ID I	Grid ID J	Dredge Area	Dredge ID (1,2,3,4)	Eng. Consideration Dredge Weight (tons)	Design Factored Time (hr)	Start Time	Finish Time
49	5	NTIP02G	2	215.9	4.5	09/26/07 08:10	09/26/07 12:39
49	6	NTIP02G	2	198.5	4.1	09/26/07 12:39	09/26/07 16:47
49	7	NTIP02G	2	193.2	4.0	09/26/07 16:47	09/26/07 20:48
50	0	NTIP02G	2	11.7	0.3	09/26/07 20:48	09/26/07 21:05
50	1	NTIP02G	2	259.5	6.3	09/26/07 21:05	09/27/07 03:23
50	2	NTIP02G	2	379.0	9.2	09/27/07 03:23	09/27/07 12:34
50	3	NTIP02G	2	374.8	7.8	09/27/07 12:34	09/27/07 20:21
50	4	NTIP02G	2	288.3	6.0	09/27/07 20:21	09/28/07 02:21
50	5	NTIP02G	2	289.6	6.0	09/28/07 02:21	09/28/07 08:22
50	6	NTIP02G	2	347.4	7.2	09/28/07 08:22	09/28/07 15:35
51	0	NTIP02G	2	0.0	0.0	09/28/07 15:35	09/28/07 15:35
51	1	NTIP02G	2	199.4	4.8	09/28/07 15:35	09/28/07 20:25
51	2	NTIP02G	2	336.5	8.2	09/28/07 20:25	09/29/07 04:35
51	3	NTIP02G	2	362.3	8.8	09/29/07 04:35	09/29/07 13:22
51	4	NTIP02G	2	284.3	5.9	09/29/07 13:22	09/29/07 19:16
51	5	NTIP02G	2	310.9	6.5	09/29/07 19:16	10/01/07 01:44
51	6	NTIP02G	2	297.5	6.2	10/01/07 01:44	10/01/07 07:55
52	1	NTIP02G	2	145.0	3.5	10/01/07 07:55	10/01/07 11:26
52	2	NTIP02G	2	332.4	8.1	10/01/07 11:26	10/01/07 19:30
52	3	NTIP02G	2	364.0	8.8	10/01/07 19:30	10/02/07 04:19
52	4	NTIP02G	2	372.2	7.7	10/02/07 04:19	10/02/07 12:03
52	5	NTIP02G	2	397.1	8.3	10/02/07 12:03	10/02/07 20:19
14	9	NTIP02C	3	50.6	4.3	06/18/07 00:00	06/18/07 04:16
14	10	NTIP02C	3	0.1	0.0	06/18/07 04:16	06/18/07 04:16
15	7	NTIP02C	3	180.4	7.5	06/18/07 04:16	06/18/07 11:46
15	8	NTIP02C	3	224.7	18.9	06/18/07 11:46	06/19/07 06:42
15	9	NTIP02C	3	196.3	8.2	06/19/07 06:42	06/19/07 14:52
15	10	NTIP02C	3	51.8	2.2	06/19/07 14:52	06/19/07 17:01
16	7	NTIP02C	3	282.1	11.7	06/19/07 17:01	06/20/07 04:45
16	8	NTIP02C	3	282.8	11.8	06/20/07 04:45	06/20/07 16:30
16	9	NTIP02C	3	249.0	10.3	06/20/07 16:30	06/21/07 02:51
16	10	NTIP02C	3	208.0	17.5	06/21/07 02:51	06/21/07 20:23
16	11	NTIP02C	3	257.8	21.7	06/21/07 20:23	06/22/07 18:07
16	12	NTIP02C	3	188.0	7.8	06/22/07 18:07	06/23/07 01:56
16	13	NTIP02C	3	32.8	1.4	06/23/07 01:56	06/23/07 03:18
17	7	NTIP02C	3	281.8	11.7	06/23/07 03:18	06/23/07 15:00
17	8	NTIP02C	3	424.6	17.6	06/23/07 15:00	06/25/07 08:39
17	9	NTIP02C	3	378.5	15.7	06/25/07 08:39	06/26/07 00:23
17	10	NTIP02C	3	324.5	13.5	06/26/07 00:23	06/26/07 13:52
17	11	NTIP02C	3	240.2	10.0	06/26/07 13:52	06/26/07 23:51
17	12	NTIP02C	3	6.9	0.3	06/26/07 23:51	06/27/07 00:08
18	6	NTIP02C	3	190.2	16.0	06/27/07 00:08	06/27/07 16:11
18	7	NTIP02C	3	191.3	8.0	06/27/07 16:11	06/28/07 00:08
18	8	NTIP02C	3	143.8	6.0	06/28/07 00:08	06/28/07 06:06
18	9	NTIP02C	3	7.3	0.3	06/28/07 06:06	06/28/07 06:25
19	5	NTIP02C	3	358.2	30.2	06/28/07 06:25	06/29/07 12:37
19	6	NTIP02C	3	321.0	27.1	06/29/07 12:37	06/30/07 15:41
19	7	NTIP02C	3	73.3	6.2	06/30/07 15:41	06/30/07 21:52
19	8	NTIP02C	3	41.6	2.8	06/30/07 21:52	07/02/07 00:40

Grid ID		Dredge Area	Dredge ID (1,2,3,4)	Eng. Consideration Dredge Weight (tons)	Design Factored Time (hr)	Start Time	Finish Time
I	J						
19	9	NTIP02C	3	10.0	0.4	07/02/07 00:40	07/02/07 01:05
20	5	NTIP02C	3	390.9	33.0	07/02/07 01:05	07/03/07 10:03
20	6	NTIP02C	3	295.0	12.3	07/03/07 10:03	07/03/07 22:18
21	6	NTIP02C	3	307.7	25.9	07/03/07 22:18	07/06/07 00:15
21	7	NTIP02C	3	159.8	7.8	07/06/07 00:15	07/06/07 08:00
21	8	NTIP02C	3	81.2	5.9	07/06/07 08:00	07/06/07 13:54
22	6	NTIP02C	3	569.9	41.4	07/06/07 13:54	07/09/07 07:21
22	7	NTIP02C	3	839.7	123.9	07/09/07 07:21	07/14/07 11:15
22	8	NTIP02C	3	277.2	20.2	07/14/07 11:15	07/16/07 07:26
23	6	NTIP02C	3	791.3	16.4	07/16/07 07:26	07/16/07 23:52
23	7	NTIP02C	3	736.1	31.0	07/16/07 23:52	07/18/07 06:54
23	8	NTIP02C	3	396.2	29.2	07/18/07 06:54	07/19/07 12:08
23	9	NTIP02C	3	66.9	1.6	07/19/07 12:08	07/19/07 13:45
24	6	NTIP02C	3	746.5	36.7	07/19/07 13:45	07/21/07 02:28
24	7	NTIP02C	3	656.3	32.3	07/21/07 02:28	07/23/07 10:45
24	8	NTIP02C/NTIP02D	3	672.7	33.1	07/23/07 10:45	07/24/07 19:50
24	9	NTIP02C/NTIP02D	3	426.5	10.3	07/24/07 19:50	07/25/07 06:11
25	6	NTIP02C	3	267.7	9.7	07/25/07 06:11	07/25/07 15:55
25	7	NTIP02C	3	257.2	9.4	07/25/07 15:55	07/26/07 01:16
25	8	NTIP02C/NTIP02D	3	304.8	22.5	07/26/07 01:16	07/26/07 23:45
26	6	NTIP02C	3	412.1	8.6	07/26/07 23:45	07/27/07 08:19
26	7	NTIP02C	3	441.4	9.2	07/27/07 08:19	07/27/07 17:29
26	8	NTIP02C	3	155.9	6.1	07/27/07 17:29	07/27/07 23:37
26	9	NTIP02C	3	101.0	2.4	07/27/07 23:37	07/28/07 02:04
27	6	NTIP02C	3	330.9	8.0	07/28/07 02:04	07/28/07 10:06
27	7	NTIP02C	3	191.1	4.0	07/28/07 10:06	07/28/07 14:04
27	8	NTIP02C	3	144.4	3.0	07/28/07 14:04	07/28/07 17:04
27	9	NTIP02C	3	444.9	9.2	07/28/07 17:04	07/30/07 02:19
27	10	NTIP02C/NTIP02D	3	256.5	6.2	07/30/07 02:19	07/30/07 08:32
27	11	NTIP02C/NTIP02D	3	622.2	30.6	07/30/07 08:32	07/31/07 15:08
28	8	NTIP02C/NTIP02E	3	133.0	3.2	07/31/07 15:08	07/31/07 18:21
28	9	NTIP02C/NTIP02E	3	493.8	10.3	07/31/07 18:21	08/01/07 04:37
28	10	NTIP02C	3	386.1	9.4	08/01/07 04:37	08/01/07 13:59
28	11	NTIP02C	3	392.5	9.5	08/01/07 13:59	08/01/07 23:30
29	10	NTIP02C	3	129.4	3.1	08/01/07 23:30	08/02/07 02:38
29	11	NTIP02C	3	165.4	4.0	08/02/07 02:38	08/02/07 06:39
25	9	NTIP02D	3	543.0	19.7	08/03/07 00:00	08/03/07 19:44
25	10	NTIP02D	3	954.2	70.4	08/03/07 19:44	08/07/07 18:08
25	11	NTIP02D	3	387.8	28.6	08/07/07 18:08	08/08/07 22:45
26	10	NTIP02D	3	303.3	7.4	08/08/07 22:45	08/09/07 06:06
26	11	NTIP02D	3	622.4	15.1	08/09/07 06:06	08/09/07 21:13
29	7	NTIP02E	3	212.5	5.2	08/10/07 00:00	08/10/07 05:09
29	8	NTIP02E	3	598.9	29.5	08/10/07 05:09	08/11/07 10:36
29	9	NTIP02E	3	27.6	0.6	08/11/07 10:36	08/11/07 11:11
30	6	NTIP02E	3	14.8	0.4	08/11/07 11:11	08/11/07 11:32
30	7	NTIP02E	3	667.4	16.2	08/11/07 11:32	08/13/07 03:43
30	8	NTIP02E	3	785.3	16.3	08/13/07 03:43	08/13/07 20:02
30	9	NTIP02E	3	218.0	9.2	08/13/07 20:02	08/14/07 05:14
31	6	NTIP02E	3	939.4	22.8	08/14/07 05:14	08/15/07 04:00

Grid ID I	Grid ID J	Dredge Area	Dredge ID (1,2,3,4)	Eng. Consideration Dredge Weight (tons)	Design Factored Time (hr)	Start Time	Finish Time
31	7	NTIP02E	3	1176.5	57.9	08/15/07 04:00	08/17/07 13:52
31	8	NTIP02E	3	385.0	8.0	08/17/07 13:52	08/17/07 21:52
32	6	NTIP02E	3	1139.2	23.7	08/17/07 21:52	08/18/07 21:33
32	7	NTIP02E	3	1167.1	24.3	08/18/07 21:33	08/20/07 21:48
32	8	NTIP02E	3	76.4	1.6	08/20/07 21:48	08/20/07 23:23
33	7	NTIP02E	3	2164.3	45.0	08/20/07 23:23	08/22/07 20:22
33	8	NTIP02E	3	1445.2	35.0	08/22/07 20:22	08/24/07 07:24
33	9	NTIP02E	3	238.5	5.8	08/24/07 07:24	08/24/07 13:11
34	7	NTIP02E	3	1819.1	37.8	08/24/07 13:11	08/27/07 02:59
34	8	NTIP02E	3	1033.1	25.0	08/27/07 02:59	08/28/07 04:02
34	9	NTIP02E	3	488.0	11.8	08/28/07 04:02	08/28/07 15:52
36	8	NTIP02F	3	915.7	33.3	08/29/07 00:00	08/30/07 09:18
36	9	NTIP02F	3	541.4	13.1	08/30/07 09:18	08/30/07 22:25
37	7	NTIP02F	3	1237.3	25.7	08/30/07 22:25	09/01/07 00:08
37	8	NTIP02F	3	865.0	18.0	09/01/07 00:08	09/02/07 18:07
38	7	NTIP02F	3	575.2	24.2	09/02/07 18:07	09/04/07 18:21
38	8	NTIP02F	3	368.3	7.7	09/04/07 18:21	09/05/07 02:01
38	9	NTIP02F	3	214.3	7.8	09/05/07 02:01	09/05/07 09:48
38	10	NTIP02F	3	20.7	0.5	09/05/07 09:48	09/05/07 10:18
39	8	NTIP02F	3	406.2	8.4	09/05/07 10:18	09/05/07 18:45
39	9	NTIP02F	3	432.1	15.7	09/05/07 18:45	09/06/07 10:28
39	10	NTIP02F	3	479.8	17.4	09/06/07 10:28	09/07/07 03:55
39	11	NTIP02F	3	369.6	13.4	09/07/07 03:55	09/07/07 17:21
39	12	NTIP02F	3	21.1	0.8	09/07/07 17:21	09/07/07 18:07
40	9	NTIP02F	3	282.2	5.9	09/07/07 18:07	09/07/07 23:59
40	10	NTIP02F	3	118.7	4.3	09/07/07 23:59	09/08/07 04:18
40	11	NTIP02F	3	197.2	4.8	09/08/07 04:18	09/08/07 09:05
40	12	NTIP02F	3	319.2	7.7	09/08/07 09:05	09/08/07 16:49
40	13	NTIP02F	3	238.6	5.8	09/08/07 16:49	09/08/07 22:36
40	14	NTIP02F	3	282.6	6.9	09/08/07 22:36	09/10/07 05:27
41	16	NTIP02F	3	287.3	6.0	09/10/07 05:27	09/10/07 11:26
41	17	NTIP02F	3	251.4	5.2	09/10/07 11:26	09/10/07 16:39
41	18	NTIP02F	3	203.4	4.2	09/10/07 16:39	09/10/07 20:53
41	19	NTIP02F	3	180.7	3.8	09/10/07 20:53	09/11/07 00:38
41	20	NTIP02F	3	148.0	3.1	09/11/07 00:38	09/11/07 03:43
41	21	NTIP02F	3	177.0	6.4	09/11/07 03:43	09/11/07 10:09
41	22	NTIP02F	3	138.0	5.0	09/11/07 10:09	09/11/07 15:10
41	23	NTIP02F	3	680.3	24.7	09/11/07 15:10	09/12/07 15:55
42	14	NTIP02F	3	310.7	6.5	09/12/07 15:55	09/12/07 22:22
42	15	NTIP02F	3	227.6	4.7	09/12/07 22:22	09/13/07 03:06
42	16	NTIP02F	3	231.2	4.8	09/13/07 03:06	09/13/07 07:54
42	17	NTIP02F	3	248.4	5.2	09/13/07 07:54	09/13/07 13:04
42	18	NTIP02F	3	203.7	4.2	09/13/07 13:04	09/13/07 17:18
42	19	NTIP02F	3	157.4	3.3	09/13/07 17:18	09/13/07 20:34
42	20	NTIP02F	3	135.5	2.8	09/13/07 20:34	09/13/07 23:23
42	21	NTIP02F	3	132.2	2.7	09/13/07 23:23	09/14/07 02:08
42	22	NTIP02F	3	99.3	2.1	09/14/07 02:08	09/14/07 04:12
42	23	NTIP02F	3	1488.3	36.1	09/14/07 04:12	09/15/07 16:17
43	12	NTIP02F	3	128.3	2.7	09/15/07 16:17	09/15/07 18:57

Grid ID I	Grid ID J	Dredge Area	Dredge ID (1,2,3,4)	Eng. Consideration Dredge Weight (tons)	Design Factored Time (hr)	Start Time	Finish Time
43	13	NTIP02F	3	136.0	2.8	09/15/07 18:57	09/15/07 21:46
43	14	NTIP02F	3	160.4	3.3	09/15/07 21:46	09/17/07 01:06
43	15	NTIP02F	3	117.3	2.4	09/17/07 01:06	09/17/07 03:32
43	16	NTIP02F	3	128.6	2.7	09/17/07 03:32	09/17/07 06:13
43	17	NTIP02F	3	149.6	6.3	09/17/07 06:13	09/17/07 12:31
43	18	NTIP02F	3	126.0	2.6	09/17/07 12:31	09/17/07 15:08
43	19	NTIP02F	3	87.6	1.8	09/17/07 15:08	09/17/07 16:58
43	20	NTIP02F	3	76.5	1.6	09/17/07 16:58	09/17/07 18:33
43	21	NTIP02F	3	59.1	1.2	09/17/07 18:33	09/17/07 19:47
43	22	NTIP02F	3	34.3	0.7	09/17/07 19:47	09/17/07 20:29
43	23	NTIP02F	3	203.7	4.9	09/17/07 20:29	09/18/07 01:26
44	11	NTIP02F	3	189.8	3.9	09/18/07 01:26	09/18/07 05:23
44	12	NTIP02F	3	202.6	4.2	09/18/07 05:23	09/18/07 09:35
44	13	NTIP02F	3	224.6	4.7	09/18/07 09:35	09/18/07 14:15
44	14	NTIP02F	3	187.5	7.9	09/18/07 14:15	09/18/07 22:10
44	15	NTIP02F	3	142.7	3.0	09/18/07 22:10	09/19/07 01:07
44	16	NTIP02F	3	88.3	1.8	09/19/07 01:07	09/19/07 02:58
44	17	NTIP02F	3	63.0	1.3	09/19/07 02:58	09/19/07 04:16
44	18	NTIP02F	3	49.6	1.0	09/19/07 04:16	09/19/07 05:18
44	19	NTIP02F	3	38.4	0.8	09/19/07 05:18	09/19/07 06:06
44	20	NTIP02F	3	16.3	0.3	09/19/07 06:06	09/19/07 06:26
44	21	NTIP02F	3	0.8	0.0	09/19/07 06:26	09/19/07 06:27
45	8	NTIP02F/NTIP02G	3	240.7	5.0	09/19/07 06:27	09/19/07 11:27
45	9	NTIP02F/NTIP02G	3	174.4	3.6	09/19/07 11:27	09/19/07 15:05
45	10	NTIP02F/NTIP02G	3	103.2	2.1	09/19/07 15:05	09/19/07 17:13
45	11	NTIP02F/NTIP02G	3	70.5	1.5	09/19/07 17:13	09/19/07 18:41
45	12	NTIP02F/NTIP02G	3	44.6	0.9	09/19/07 18:41	09/19/07 19:37
45	13	NTIP02F	3	40.2	0.8	09/19/07 19:37	09/19/07 20:27
45	14	NTIP02F	3	43.1	1.8	09/19/07 20:27	09/19/07 22:16
45	15	NTIP02F	3	0.6	0.0	09/19/07 22:16	09/19/07 22:17
46	7	NTIP02G	3	344.1	7.2	09/20/07 00:00	09/20/07 07:09
46	8	NTIP02G	3	319.4	6.6	09/20/07 07:09	09/20/07 13:47
46	9	NTIP02G	3	195.8	4.1	09/20/07 13:47	09/20/07 17:51
46	10	NTIP02G	3	86.9	3.7	09/20/07 17:51	09/20/07 21:31
46	11	NTIP02G	3	48.2	1.6	09/20/07 21:31	09/20/07 23:08
46	12	NTIP02G	3	21.0	0.7	09/20/07 23:08	09/20/07 23:51
46	13	NTIP02G	3	0.7	0.0	09/20/07 23:51	09/20/07 23:52
47	9	NTIP02G	3	195.3	4.1	09/20/07 23:52	09/21/07 03:56
47	10	NTIP02G	3	122.1	2.5	09/21/07 03:56	09/21/07 06:28
47	11	NTIP02G	3	131.8	5.6	09/21/07 06:28	09/21/07 12:01
47	12	NTIP02G	3	157.9	3.3	09/21/07 12:01	09/21/07 15:18
47	13	NTIP02G	3	140.0	2.9	09/21/07 15:18	09/21/07 18:13
47	14	NTIP02G	3	124.4	2.6	09/21/07 18:13	09/21/07 20:48
47	15	NTIP02G	3	49.0	1.0	09/21/07 20:48	09/21/07 21:49
47	16	NTIP02G	3	19.2	0.4	09/21/07 21:49	09/21/07 22:13
47	17	NTIP02G	3	2.4	0.0	09/21/07 22:13	09/21/07 22:16
48	12	NTIP02G	3	351.6	7.3	09/21/07 22:16	09/22/07 05:34
48	13	NTIP02G	3	392.4	8.2	09/22/07 05:34	09/22/07 13:44
48	14	NTIP02G	3	416.5	8.7	09/22/07 13:44	09/22/07 22:23

Grid ID		Dredge Area	Dredge ID (1,2,3,4)	Eng. Consideration Dredge Weight (tons)	Design Factored Time (hr)	Start Time	Finish Time
I	J						
48	15	NTIP02G	3	305.5	6.3	09/22/07 22:23	09/24/07 04:44
48	16	NTIP02G	3	227.3	4.7	09/24/07 04:44	09/24/07 09:27
48	17	NTIP02G	3	77.1	1.6	09/24/07 09:27	09/24/07 11:03
49	8	NTIP02G	3	168.2	3.5	09/24/07 11:03	09/24/07 14:33
49	9	NTIP02G	3	157.1	3.3	09/24/07 14:33	09/24/07 17:49
49	10	NTIP02G	3	192.4	4.0	09/24/07 17:49	09/24/07 21:49
49	11	NTIP02G	3	175.4	3.6	09/24/07 21:49	09/25/07 01:28
49	12	NTIP02G	3	182.0	3.8	09/25/07 01:28	09/25/07 05:15
49	13	NTIP02G	3	183.5	3.8	09/25/07 05:15	09/25/07 09:03
49	14	NTIP02G	3	187.8	3.9	09/25/07 09:03	09/25/07 12:58
49	15	NTIP02G	3	172.8	3.6	09/25/07 12:58	09/25/07 16:33
49	16	NTIP02G	3	106.0	2.2	09/25/07 16:33	09/25/07 18:45
49	17	NTIP02G	3	29.0	0.6	09/25/07 18:45	09/25/07 19:21
50	7	NTIP02G	3	260.1	5.4	09/25/07 19:21	09/26/07 00:46
50	8	NTIP02G	3	255.3	5.3	09/26/07 00:46	09/26/07 06:04
50	9	NTIP02G	3	225.1	4.7	09/26/07 06:04	09/26/07 10:45
50	10	NTIP02G	3	148.0	3.1	09/26/07 10:45	09/26/07 13:49
50	11	NTIP02G	3	125.5	2.6	09/26/07 13:49	09/26/07 16:26
50	12	NTIP02G	3	140.0	2.9	09/26/07 16:26	09/26/07 19:20
50	13	NTIP02G	3	146.6	3.0	09/26/07 19:20	09/26/07 22:23
50	14	NTIP02G	3	261.9	5.4	09/26/07 22:23	09/27/07 03:50
50	15	NTIP02G	3	215.8	4.5	09/27/07 03:50	09/27/07 08:19
50	16	NTIP02G	3	54.2	1.1	09/27/07 08:19	09/27/07 09:26
51	7	NTIP02G	3	235.8	4.9	09/27/07 09:26	09/27/07 14:20
51	8	NTIP02G	3	239.9	5.0	09/27/07 14:20	09/27/07 19:19
51	9	NTIP02G	3	200.5	4.2	09/27/07 19:19	09/27/07 23:29
51	10	NTIP02G	3	189.4	3.9	09/27/07 23:29	09/28/07 03:26
51	11	NTIP02G	3	192.3	4.0	09/28/07 03:26	09/28/07 07:25
51	12	NTIP02G	3	266.8	5.5	09/28/07 07:25	09/28/07 12:58
51	13	NTIP02G	3	289.7	6.0	09/28/07 12:58	09/28/07 18:59
51	14	NTIP02G	3	243.7	5.1	09/28/07 18:59	09/29/07 00:03
51	15	NTIP02G	3	140.5	2.9	09/29/07 00:03	09/29/07 02:58
51	16	NTIP02G	3	12.3	0.3	09/29/07 02:58	09/29/07 03:14
51	17	NTIP02G	3	1.7	0.0	09/29/07 03:14	09/29/07 03:16
52	7	NTIP02G	3	256.6	5.3	09/29/07 03:16	09/29/07 08:36
52	8	NTIP02G	3	265.0	5.5	09/29/07 08:36	09/29/07 14:06
52	9	NTIP02G	3	286.4	6.0	09/29/07 14:06	09/29/07 20:03
52	10	NTIP02G	3	277.7	5.8	09/29/07 20:03	10/01/07 01:49
52	11	NTIP02G	3	230.2	4.8	10/01/07 01:49	10/01/07 06:37
52	12	NTIP02G	3	218.6	4.5	10/01/07 06:37	10/01/07 11:09
52	13	NTIP02G	3	224.9	4.7	10/01/07 11:09	10/01/07 15:50
52	14	NTIP02G	3	194.6	4.0	10/01/07 15:50	10/01/07 19:52
52	15	NTIP02G	3	123.3	2.6	10/01/07 19:52	10/01/07 22:26
52	16	NTIP02G	3	42.6	0.9	10/01/07 22:26	10/01/07 23:19
53	8	NTIP02G	3	290.1	6.0	10/01/07 23:19	10/02/07 05:21
53	9	NTIP02G	3	314.4	6.5	10/02/07 05:21	10/02/07 11:53
173	10	EGIA01A	4	0.9	0.0	06/04/07 00:00	06/04/07 00:01
173	11	EGIA01A	4	58.2	1.2	06/04/07 00:01	06/04/07 01:13
173	12	EGIA01A	4	56.6	1.2	06/04/07 01:13	06/04/07 02:24

Grid ID		Dredge Area	Dredge ID (1,2,3,4)	Eng. Consideration Dredge Weight (tons)	Design Factored Time (hr)	Start Time	Finish Time
I	J						
173	13	EGIA01A	4	0.8	0.0	06/04/07 02:24	06/04/07 02:25
174	8	EGIA01A	4	6.4	0.1	06/04/07 02:25	06/04/07 02:33
174	9	EGIA01A	4	28.6	1.0	06/04/07 02:33	06/04/07 03:30
174	10	EGIA01A	4	53.9	2.3	06/04/07 03:30	06/04/07 05:47
174	11	EGIA01A	4	209.4	8.8	06/04/07 05:47	06/04/07 14:36
174	12	EGIA01A	4	54.9	1.1	06/04/07 14:36	06/04/07 15:45
175	7	EGIA01A	4	22.3	0.5	06/04/07 15:45	06/04/07 16:13
175	8	EGIA01A	4	211.1	4.4	06/04/07 16:13	06/04/07 20:36
175	9	EGIA01A	4	245.9	10.4	06/04/07 20:36	06/05/07 06:58
175	10	EGIA01A	4	194.1	4.0	06/05/07 06:58	06/05/07 11:00
175	11	EGIA01A	4	189.8	3.9	06/05/07 11:00	06/05/07 14:57
175	12	EGIA01A	4	102.5	2.1	06/05/07 14:57	06/05/07 17:04
175	13	EGIA01A/EGIA01B	4	25.0	0.5	06/05/07 17:04	06/05/07 17:35
175	14	EGIA01A/EGIA01B	4	39.4	0.8	06/05/07 17:35	06/05/07 18:25
176	6	EGIA01A	4	17.5	0.4	06/05/07 18:25	06/05/07 18:46
176	7	EGIA01A	4	105.4	2.2	06/05/07 18:46	06/05/07 20:58
176	8	EGIA01A	4	229.8	4.8	06/05/07 20:58	06/06/07 01:44
176	9	EGIA01A	4	237.6	4.9	06/06/07 01:44	06/06/07 06:41
176	10	EGIA01A	4	131.0	2.7	06/06/07 06:41	06/06/07 09:24
176	11	EGIA01A	4	130.3	2.7	06/06/07 09:24	06/06/07 12:07
176	12	EGIA01A	4	192.4	4.0	06/06/07 12:07	06/06/07 16:07
176	13	EGIA01A/EGIA01B	4	146.5	3.0	06/06/07 16:07	06/06/07 19:09
177	11	EGIA01A	4	95.3	2.0	06/06/07 19:09	06/06/07 21:08
177	12	EGIA01A/EGIA01B	4	41.3	0.9	06/06/07 21:08	06/06/07 22:00
173	20	EGIA01B	4	2.9	0.1	06/07/07 00:00	06/07/07 00:03
173	21	EGIA01B	4	136.3	3.3	06/07/07 00:03	06/07/07 03:21
173	22	EGIA01B	4	90.9	2.2	06/07/07 03:21	06/07/07 05:34
173	23	EGIA01B	4	2.5	0.1	06/07/07 05:34	06/07/07 05:37
174	20	EGIA01B	4	43.5	0.9	06/07/07 05:37	06/07/07 06:32
174	21	EGIA01B	4	169.5	4.1	06/07/07 06:32	06/07/07 10:38
174	22	EGIA01B	4	97.2	2.4	06/07/07 10:38	06/07/07 13:00
174	23	EGIA01B	4	2.8	0.1	06/07/07 13:00	06/07/07 13:04
175	15	EGIA01B	4	58.1	1.2	06/07/07 13:04	06/07/07 14:16
175	16	EGIA01B	4	53.8	1.1	06/07/07 14:16	06/07/07 15:23
175	17	EGIA01B	4	48.0	1.0	06/07/07 15:23	06/07/07 16:23
175	18	EGIA01B	4	15.0	0.3	06/07/07 16:23	06/07/07 16:42
175	19	EGIA01B	4	70.1	1.5	06/07/07 16:42	06/07/07 18:09
175	20	EGIA01B	4	159.9	3.3	06/07/07 18:09	06/07/07 21:29
175	21	EGIA01B	4	118.8	2.9	06/07/07 21:29	06/08/07 00:22
175	22	EGIA01B	4	26.1	1.0	06/08/07 00:22	06/08/07 01:19
176	14	EGIA01B	4	86.4	1.8	06/08/07 01:19	06/08/07 03:07
176	15	EGIA01B	4	131.7	2.7	06/08/07 03:07	06/08/07 05:51
176	16	EGIA01B	4	177.4	3.7	06/08/07 05:51	06/08/07 09:32
176	17	EGIA01B	4	194.7	4.0	06/08/07 09:32	06/08/07 13:35
176	18	EGIA01B	4	338.2	7.0	06/08/07 13:35	06/08/07 20:36
176	19	EGIA01B	4	324.7	6.7	06/08/07 20:36	06/09/07 03:21
176	20	EGIA01B	4	307.6	6.4	06/09/07 03:21	06/09/07 09:45
176	21	EGIA01B	4	320.4	7.8	06/09/07 09:45	06/09/07 17:31
176	22	EGIA01B	4	136.5	5.0	06/09/07 17:31	06/09/07 22:29

Grid ID		Dredge Area	Dredge ID (1,2,3,4)	Eng. Consideration Dredge Weight (tons)	Design Factored Time (hr)	Start Time	Finish Time
I	J						
177	13	EGIA01B	4	164.1	3.4	06/09/07 22:29	06/11/07 01:54
177	14	EGIA01B	4	275.5	5.7	06/11/07 01:54	06/11/07 07:37
177	15	EGIA01B	4	273.5	5.7	06/11/07 07:37	06/11/07 13:18
177	16	EGIA01B	4	106.1	2.2	06/11/07 13:18	06/11/07 15:30
177	17	EGIA01B	4	2.4	0.0	06/11/07 15:30	06/11/07 15:33
177	18	EGIA01B	4	121.4	2.5	06/11/07 15:33	06/11/07 18:05
177	19	EGIA01B	4	324.9	6.8	06/11/07 18:05	06/12/07 00:50
177	20	EGIA01B	4	344.3	7.2	06/12/07 00:50	06/12/07 07:59
177	21	EGIA01B	4	465.2	11.3	06/12/07 07:59	06/12/07 19:16
177	22	EGIA01B	4	363.0	8.8	06/12/07 19:16	06/13/07 04:04
178	12	EGIA01B	4	110.2	2.3	06/13/07 04:04	06/13/07 06:22
178	13	EGIA01B	4	157.7	3.3	06/13/07 06:22	06/13/07 09:38
178	14	EGIA01B	4	114.6	2.4	06/13/07 09:38	06/13/07 12:01
178	15	EGIA01B	4	24.8	0.5	06/13/07 12:01	06/13/07 12:32
178	16	EGIA01B	4	39.6	0.8	06/13/07 12:32	06/13/07 13:22
178	17	EGIA01B	4	150.1	3.1	06/13/07 13:22	06/13/07 16:29
178	18	EGIA01B	4	294.4	6.1	06/13/07 16:29	06/13/07 22:36
178	19	EGIA01B	4	386.6	8.0	06/13/07 22:36	06/14/07 06:38
178	20	EGIA01B	4	476.3	9.9	06/14/07 06:38	06/14/07 16:32
178	21	EGIA01B	4	537.4	13.0	06/14/07 16:32	06/15/07 05:34
178	22	EGIA01B	4	538.3	13.1	06/15/07 05:34	06/15/07 18:37
178	23	EGIA01B	4	37.2	0.9	06/15/07 18:37	06/15/07 19:31
179	16	EGIA01B	4	61.9	1.3	06/15/07 19:31	06/15/07 20:48
179	17	EGIA01B	4	158.7	3.3	06/15/07 20:48	06/16/07 00:06
179	18	EGIA01B	4	279.6	5.8	06/16/07 00:06	06/16/07 05:54
179	19	EGIA01B	4	531.7	11.0	06/16/07 05:54	06/16/07 16:57
180	17	EGIA01B	4	43.5	0.9	07/02/07 00:00	07/02/07 00:54
180	18	EGIA01B	4	563.1	11.7	07/02/07 00:54	07/02/07 12:36
180	19	EGIA01B	4	615.7	22.4	07/02/07 12:36	07/03/07 10:59
181	17	EGIA01B	4	197.6	4.1	07/03/07 10:59	07/03/07 15:06
181	18	EGIA01B	4	654.5	27.6	07/03/07 15:06	07/05/07 18:41
181	19	EGIA01B	4	700.6	14.6	07/05/07 18:41	07/06/07 09:15
181	20	EGIA01B	4	601.0	21.9	07/06/07 09:15	07/07/07 07:06
182	16	EGIA01B/EGIA01C	4	178.1	3.7	07/07/07 07:06	07/07/07 10:48
182	17	EGIA01B	4	508.2	21.4	07/07/07 10:48	07/09/07 08:13
182	18	EGIA01B	4	846.2	17.6	07/09/07 08:13	07/10/07 01:48
182	19	EGIA01B	4	643.5	27.1	07/10/07 01:48	07/11/07 04:56
182	20	EGIA01B	4	564.4	11.7	07/11/07 04:56	07/11/07 16:40
182	21	EGIA01B	4	814.3	60.1	07/11/07 16:40	07/14/07 04:45
182	22	EGIA01B	4	922.3	33.5	07/14/07 04:45	07/16/07 14:17
182	23	EGIA01B	4	124.7	3.0	07/16/07 14:17	07/16/07 17:19
179	20	EGIA01B	4	558.6	20.3	07/17/07 00:00	07/17/07 20:18
179	21	EGIA01B	4	416.4	8.7	07/17/07 20:18	07/18/07 04:58
179	22	EGIA01B	4	372.1	13.5	07/18/07 04:58	07/18/07 18:30
179	23	EGIA01B	4	27.5	1.0	07/18/07 18:30	07/18/07 19:30
180	20	EGIA01B	4	611.9	22.3	07/18/07 19:30	07/19/07 17:45
180	21	EGIA01B	4	661.7	16.0	07/19/07 17:45	07/20/07 09:47
180	22	EGIA01B	4	523.0	19.0	07/20/07 09:47	07/21/07 04:50
180	23	EGIA01B	4	0.0	0.0	07/21/07 04:50	07/21/07 04:50

Grid ID		Dredge Area	Dredge ID (1,2,3,4)	Eng. Consideration Dredge Weight (tons)	Design Factored Time (hr)	Start Time	Finish Time
I	J						
181	21	EGIA01B	4	624.0	22.7	07/21/07 04:50	07/23/07 03:31
181	22	EGIA01B	4	728.5	26.5	07/23/07 03:31	07/24/07 06:02
34	21	NTIP02B	4	1028.5	21.4	07/25/07 00:00	07/25/07 21:22
34	22	NTIP02B	4	1319.4	48.0	07/25/07 21:22	07/27/07 21:23
34	23	NTIP02B	4	8.0	0.3	07/27/07 21:23	07/27/07 21:41
35	21	NTIP02B	4	1905.0	46.2	07/27/07 21:41	07/30/07 19:52
35	22	NTIP02B	4	1032.5	37.5	07/30/07 19:52	08/01/07 09:25
35	23	NTIP02B	4	31.3	1.1	08/01/07 09:25	08/01/07 10:33
36	21	NTIP02B	4	2380.9	49.5	08/01/07 10:33	08/03/07 12:02
36	22	NTIP02B	4	1584.2	38.4	08/03/07 12:02	08/06/07 02:26
36	23	NTIP02B	4	425.5	15.5	08/06/07 02:26	08/06/07 17:56
37	21	NTIP02B	4	1145.6	23.8	08/06/07 17:56	08/07/07 17:44
37	22	NTIP02B	4	911.0	44.8	08/07/07 17:44	08/09/07 14:32
38	20	NTIP02B	4	658.7	13.7	08/09/07 14:32	08/10/07 04:14
38	21	NTIP02B	4	641.5	15.6	08/10/07 04:14	08/10/07 19:47
38	22	NTIP02B	4	488.8	17.8	08/10/07 19:47	08/11/07 13:33
38	23	NTIP02B	4	14.5	0.5	08/11/07 13:33	08/11/07 14:05
39	19	NTIP02B	4	465.0	9.7	08/11/07 14:05	08/11/07 23:45
39	20	NTIP02B	4	459.7	19.4	08/11/07 23:45	08/13/07 19:08
39	21	NTIP02B	4	426.4	18.0	08/13/07 19:08	08/14/07 13:06
39	22	NTIP02B	4	299.6	22.1	08/14/07 13:06	08/15/07 11:12
39	23	NTIP02B	4	50.3	1.8	08/15/07 11:12	08/15/07 13:02
40	16	NTIP02B/NTIP02F	4	309.7	15.2	08/15/07 13:02	08/16/07 04:16
40	17	NTIP02B/NTIP02F	4	343.6	8.3	08/16/07 04:16	08/16/07 12:36
40	18	NTIP02B/NTIP02F	4	307.1	6.4	08/16/07 12:36	08/16/07 18:59
40	19	NTIP02B/NTIP02F	4	278.4	5.8	08/16/07 18:59	08/17/07 00:46
40	20	NTIP02B/NTIP02F	4	288.8	6.0	08/17/07 00:46	08/17/07 06:46
40	21	NTIP02B/NTIP02F	4	211.0	7.7	08/17/07 06:46	08/17/07 14:27
40	22	NTIP02B/NTIP02F	4	44.4	1.6	08/17/07 14:27	08/17/07 16:03

E.6.2 Incorporation of a Dredge Plan into a Simulation

The total sediment mass removed and dredge duration were used to calculate the average sediment mass removal rate for each grid cell. The fraction of the sediment volume attributable to each of the three suspendable sediment fractions was used to calculate the individual sediment class mass removal rates. The sediment mass removal rates were then multiplied by the overall dredge resuspension loss rate (0.35% for the base case) to calculate the rate of sediment resuspended. The Total PCB concentrations of each sediment fraction (computed as described in Section E.5.3) were applied to estimate the mass rate of PCB resuspended for each sediment class. These mass loading rates were input to the water column grid cell above the sediment being dredged. The loading rates for each grid cell were applied with the exact duration and timing as specified in the dredge plan.

E.6.3 Overview of Control Systems

Various control systems have been considered as possible methods for reducing the downstream transport of solids and PCBs released during dredging operations. The control systems presently being investigated are "hard" control structures that offer physical barriers to the transport of resuspended material. Two types of control structures are considered: sheet piling and silt curtains. Sheet piling involves construction of a hard barrier that is designed to cut off flow and prevent transport of solids and PCBs. A silt curtain is a flexible barrier that reduces flow and transport; a silt curtain is not as effective as a rigid barrier (i.e., sheet piling) at reducing flow and transport of solids and PCBs.

Currently, control structures are being considered for use at two TIP locations. A combination of sheet piling and silt curtains are planned for use in the East Channel at Rogers Island (Figure E-6-2). At this location, one sheet pile structure is proposed at the northern entrance to the East Channel, with structure length of 220 ft. This structure will block flow from entering the East Channel, diverting it to the West Channel. A silt curtain, approximate length of 230 ft., is proposed at the southern end of the East Channel (Figure E-6-2) to reduce downstream transport of resuspended sediment. The second control structure is proposed along the eastern shoreline near Griffin Island (Figure E-6-3). A sheet pile and three silt curtains are being considered at this location. The sheet pile will extend approximately 125 ft. into the channel from the shoreline and encloses about 1.7 acres; about 6% of the total flow in the river will be diverted by the structure. Silt curtains are proposed to extend an additional approximately 100 ft into the channel from the sheet pile, continue approximately 600 ft. parallel to the river channel, then extend back to the shoreline to fully enclose an area of about 2.9 acres (Figure E-6-3).

The dredging schedule, which extends from May through October, specifies the following schedule for the use of control structures. The Rogers Island sheet pile will be in place for 122 days, from May 21 to September 19. The Rogers Island silt curtain will be in place for

91 days, from May 21 to August 19. The sheet pile in the vicinity of Griffin Island will be place for 40 days, from July 17 to August 25. The East Griffin Island silt curtains will be placed for 9 days, from July 17 to July 25. Note that silt curtains are taken down shortly after completion of dredging of enclosed sediments. Sheet piles remain in place for an additional month to ensure ample time for settling of residual sediment and PCB.

E.6.4 Simulation of Control Structure Effects

The effects of control structures on flow and transport are incorporated into the model as follows. At the location of a sheet pile structure, the grid cells along the boundary of the structure are treated as a solid boundary, with zero flow and transport across that boundary. At the location of a silt curtain, flow is allowed across the grid cells at the structure boundary; flow is conserved at a silt curtain boundary. The flux of suspended sediment across a silt curtain boundary is modified, with the flux of cohesive (Class 1) sediment being reduced by 70% of the flux encountering the structure. It is assumed that the flux of coarse (Classes 2 and 3) sediment is zero across the silt curtain. The transport of dissolved PCBs is unaffected by the silt curtain structure, but the transport of PCBs sorbed to sediment is adjusted in the same manner as the suspended sediment fluxes.

E.7 RESULTS OF MODEL SIMULATIONS

E.7.1 Baseline Far-Field Concentrations

The RPS threshold and control levels for far-field PCB concentration criteria are absolute concentrations. In order to evaluate the ability of proposed dredging alternatives to maintain PCB levels below these standards, it was necessary to estimate the value of the baseline concentration that would exist in addition to the PCB concentrations resulting from dredging. For the Phase 1 dredging of River Section 1, the location of the far-field station is at the TID. In June 2004, the BMP was set up with the purpose of establishing these non-dredging related PCB concentrations. Inspection of this data as well as the previous Hudson River Monitoring (HRM) Program in the West Channel of Thompson Island shows a strong seasonal dependence of the levels. For this reason the BMP data were analyzed on a monthly basis and average monthly Total PCB concentrations were used to establish the baseline concentration. These values are given in Table E-7-1. These concentrations were added to the PCB concentrations predicted by the resuspension modeling to estimate absolute Total PCB at the TID for comparison to RPS standards.

Table E-7-1. Baseline TID Total PCB concentration.

Month	PCB Concentration (ng/L)
May	34.5
June	63.1
July	52.5
August	21.3
September	29.0
October	58.5

E.7.2 Overview of Model Simulations

Two basic model simulations are presented here. The base dredging plan with no control systems was initially run to evaluate the ability to meet RPS criteria without such structures. The results of this simulation were used to identify time periods (and the associated dredge locations) when RPS criteria were exceeded. After analysis of this base case, control systems were proposed that would address and confine the releases from dredging of areas that are responsible for the exceedance of RPS criteria. The other primary model simulation includes the final set of control systems chosen and serves to demonstrate the ability of such controls to maintain levels below the standards.

For these base scenarios, assumptions were made regarding the dredging loss rate and river flow conditions. The loss rate was assumed to be 0.35% of resuspendable material. The river flow conditions were considered to be median values for the particular time of year based on ten-day intervals. Sensitivity runs are also presented to show the effects on PCB and TSS levels of variations of river flow, resuspension loss rate, as well as desorption capacity.

E.7.3 General Results and Insights

Plume Characteristics

The plume of suspended sediment and PCBs downstream of an operating dredge exhibits certain common characteristics. Near the dredge head, the plume width is relatively narrow and water column concentrations are at maximum levels. Moving downstream from the dredge head, the plume widens as suspended sediment and PCBs are dispersed in the lateral (cross-channel) direction. Water column concentrations decrease due to dispersive dilution and deposition of suspended sediment. Figure E-7-1 shows the development of a typical PCB plume during dredge operation.

The relative location of the dredge head in the channel (e.g., shallow near-shore area or deeper navigation channel) affects the general structure of the plume. Figure E-7-2 demonstrates the form of a fully developed dredge plume of Total PCBs for a mid-channel dredge operation near the southern end of Rogers Island. The plume quickly disperses across the channel within a mile of the dredge head. When the plume reaches the TID, the PCBs are well mixed with only small lateral gradients. By contrast, the plume from a near-shore dredge operation (Figure E-7-3) exhibits much higher cross-channel gradients. These gradients persist for a much longer distance downstream and retain significant lateral variations at the TID. It is also evident from comparison of these two figures that for a given distance downstream, the maximum plume concentration of a near-shore release can be much higher than for a mid-channel release.

Sediment Transport

Under median flow conditions, only fine sediments (Class 1 – clay and silt) are carried in suspension to the far-field station. The resuspended sand (Classes 2 and 3) settles out in the near-field. Figure E-7-4 shows the normalized suspended sediment concentration of the three classes as the plume travels downstream from a near-shore dredging operation. Class 3 sediment settles out within approximately 50 m of the dredge (i.e., within the grid cell in which dredging occurs). The Class 2 sediment travels a longer distance, nearly twice as far, but it is typically redeposited within 100 m of the dredge. The normalized suspended sediment profile for a mid-channel dredge operation is shown in Figure E-7-5. Class 3 sediment travels further but still deposits within a relatively short distance (100 m). Similarly, Class 2 sediments also travel further. The longer travel distance of these two classes is due to the higher velocities and deeper depths associated with the navigation channel. Under high-flow conditions, these sediments can remain in suspension for a considerable distance downstream. Some fraction of Class 2 sediment can often reach the far-field station.

Class 1 sediment deposits much more slowly and a significant portion will stay in suspension for miles from the dredge. Redeposition of fine (Class 1) sediment varies widely; it is largely dependent on the flow conditions and location of the release. Anywhere from 0% to 75% of the resuspended fine sediment redeposits before reaching the far-field station. Generally, redeposition is highest for near-shore releases under low flow conditions and lowest for releases near or in the navigational channel under high flow conditions. For example, a typical dredge release was simulated in the near-shore region just below Rogers Island using average sediment composition, 0.35% release rate, and median flow conditions. Under these conditions, 58% of the resuspended fine sediment and 0% of the resuspended sand reach the far-field station.

TSS concentrations at the far-field station are relatively low under all conditions as a result of the lateral mixing and dilution of the plume and the redeposition of resuspended sediments. Even with relatively high resuspension rates, the far-field TSS concentrations remain below 5 mg/L.

PCB Transport

The contribution of each sediment class to PCB transport differs significantly due to the interplay between redeposition rates, particle size and the magnitude of the labile and refractory components of sorbed PCB. Nearly all of the PCBs associated with resuspended Class 3 sediments do not reach the far-field station. These PCBs redeposit because the sediments settle much quicker than the time scales of either labile or refractory desorption. Class 2 sediment, while not generally reaching the far-field station, does contribute to the PCBs downstream as a result of the longer time that this sediment spends in suspension as well as the higher rates of desorption (compared to Class 3) due to smaller particle diameters. Nearly all of this contribution comes from the labile sorbed PCBs. The refractory component on this sediment does not have sufficient time to desorb. The extent of labile desorption depends on local conditions which determine the amount of time sediments spend in suspension. Fine sediment is the main source of PCBs reaching the far-field station. Nearly the entire labile component desorbs from these particles and transports downstream as dissolved PCBs. Much of the refractory component remains sorbed, but contributes to the far-field PCB levels due to the significant transport of fine sediments to the far-field station. During a typical near-shore dredge release just below Rogers Island using average PCB concentrations, 0.35% loss rate, and median flow, 78% of PCBs initially sorbed to Class 1 sediment were transported past the TID, whereas only 7.6% and 1.7% of the PCBs initially sorbed to Class 2 and 3 sediment, respectively, passed the TID.

The bulk of the desorption occurs in the vicinity of the dredge operation. Figure E-7-6 shows the spatial profile of a typical mid-channel dredge PCB plume. After the first initial decline in total PCB in the first approximately 200 m due to dilution and deposition, the PCB concentration declines much more slowly, primarily as a result of fine sediment deposition. The dissolved PCB component shows that a rapid desorption occurs in the first 100 m, a slower portion continues to desorb until about 0.5 mi. after which the fraction of the PCBs that are dissolved remains relatively constant. For a typical release as described above, nearly two-thirds of the PCB flux at TID is in the dissolved phase.

E.7.4 Dredging With No Control Structures

The modeling indicates that far-field PCB levels will vary greatly during the course of Phase 1 dredging due to variations in the PCB concentration and grain size distribution of the sediment being dredged. Distinct peaks in PCB release are predicted to occur during mid-June, the first half of July and the first half of August. The first peak is associated with dredging in the East Griffin Island area. The second peak primarily comes from dredging in the East Channel at Rogers Island with a smaller contribution from the East Griffin Island area. The third peak is produced by the dredging occurring in the East Channel at Rogers Island. The East Channel at Rogers Island contribution to the second peak results from dredging in just downstream of Bond Creek, whereas the third peak occurs due to dredging further downstream just above where the channel bends to the west. All of these areas contain high PCB concentrations and high percentages of fine grained sediments.

The design resuspension loss rate (0.35%) produces Total PCB concentrations at TID that remain below the Control Level (seven-day average concentration of 350 ng/L) and the Primary Standard (24-hour average of 500 ng/L) for the entire season. The seven-day average Total PCB concentration at TID fluctuates between about 25 ng/L and 200 ng/L (Figure E-7-7). The 24-hour average concentration at this location ranges between 25 ng/L and 260 ng/L.

The seven-day average net PCB flux at TID resulting from 0.35% release varies from near zero to about 1,030 g/d (Figure E-7-8). It exceeds the Evaluation Level of 300 g/d for about 34% of the dredging season. The Control Level of 600 g/d is exceeded for about 18% of the dredging season. Despite the period of elevated seven-day average fluxes, the total flux over the dredging season remains below the Control Level of 65 kg (Figure E-7-9). The total downstream flux is about 40 kg.

The elevated Total PCB concentrations and fluxes at TID are not associated with elevated TSS. The model indicates that six-hour average net TSS concentrations never exceed 1 mg/L

(Figure E-7-10). Similarly, near-field net TSS concentrations remain relatively low and always below the RPS criteria. At the station 300 m downstream of the dredging, TSS concentrations are typically less than 10 mg/L (Figure E-7-11). The highest concentration of about 20 mg/L occurs when dredging fine sediments along the western shore in NTIP02G (Dredge 2 in Figure E-7-11) and in East Griffin Island (Dredge 4 in Figure E-7-11). At the station 100 m downstream of the dredging, TSS concentrations do not exceed about 50 mg/L (Figure E-7-12).

E.7.5 Dredging With Control Structures

The addition of the resuspension controls in East Channel at Rogers Island and East Griffin Island that are described in Section E.6.3 reduces downstream PCB fluxes by about a quarter. The flux of Total PCBs past TID over the entire Phase 1 program declines from about 40 kg to about 31 kg (Figure E-7-15) with the reduction about equally attributable to the two areas where controls are deployed. The seven-day average Total PCB concentration at TID remains below 170 ng/L for the entire season, whereas it reached about 200 ng/L without controls (Figure E-7-13). The 24-hour average concentration exhibits a greater reduction overall and exhibits less variability than was predicted to occur without controls. For the entire season the 24-hour average is below 200 ng/L.

The resuspension controls are predicted to be moderately effective in reducing the seven-day average net PCB flux at TID resulting from 0.35% release to levels below the Control Level (Figure E-7-14). The maximum flux is reduced from about 1,030 g/d to about 700 g/d and the peaks associated with dredging in the East Channel at Rogers Island are greatly reduced, but the fluxes remain above the Evaluation Level for about 26% of the dredging season and above the Control Level for about 7% of the dredging season. This is largely because reducing flow through the East Channel at Rogers Island by cutting off of the upstream entrance reduces the PCB flux from the channel only by about a third because the lower flow is compensated by a buildup of PCB concentrations within the channel. The remaining low flow carrying this more highly contaminated water remains a significant flux. In contrast, the elimination of flow in the sheet piled area at East Griffin Island reduces the flux from this area by about 75%.

The ability of the dredge plan with control structures to keep PCB levels under the standards was evaluated assuming higher loss rate of dredged material. For a loss rate of 0.70%, the seven-day average concentration past TID varied from about 40 ng/L to about 220 ng/L, well below the Control Level (Figure E-7-16). The daily average remained below the 500 ng/L threshold throughout the season, only reaching a maximum of about 330 ng/L.

The seven-day average net PCB flux at TID resulting from 0.70% release varies from about 50 g/d to about 1,400 g/d (Figure E-7-17). It exceeds the Evaluation Level for about 43% of the dredging season and the Control Level for about 29% of the dredging season. Despite these elevated fluxes, the total flux for the dredging season reaches only 56 kg, remaining below the Control Level (Figure E-7-18).

E.7.6 Sensitivity Analysis

Model runs were conducted to access the sensitivity of the model to river flow conditions and desorption capacity. While the median flow was used in the development of the dredge plan, low flow and high flow conditions were also evaluated. The dredge plan with the control structures in the East Channel at Rogers Island and East Griffin Island were run using low and high flow values at the 10 and 90 percentile from the historical flow distribution for each of the ten day intervals. Under high flow conditions, the total predicted PCB flux past the TID is increased by about 3 kg (Figure E-7-19). Conversely, low flow conditions decreased the seasonal flux by about 3 kg due to the increased settling of suspended sediment resulting from lower water velocities and bottom shear stresses. This represents about +/-10% about the median flow. It should be noted that the dredge plan shown in Figure E-7-19 is different than the dredge plan presented in Section E.7.5 and is only meant to show the relative sensitivity of the model.

Sensitivity to the desorption capacity of the sediments was evaluated by varying the initial labile/refractory split of sorbed PCBs. As presented in Section E.5.4, the calibrated value of the initial fraction labile was 53%. Assuming that the sorbed PCBs were much less labile at 20%, the overall season flux of PCB past the TID would be reduced by about 5 kg (Figure E-7-20). Although the labile component is reduced by more than 50%, the overall transport is only reduced by about 16% because of the desorption of some refractory PCBs and because a significant portion of the flux is from PCB sorbed to fine grained sediment. Again, it should be noted that these runs are for a different dredge plan as presented in Section E.7.5, but the relative sensitivity will be the same.

E.8 SUMMARY AND CONCLUSIONS

A mathematical modeling framework, consisting of linked hydrodynamic, sediment transport and PCB fate and transport sub-models, has been developed and it is used to simulate the transport and fate of sediment and PCBs released during dredging operations. The two-dimensional, vertically-averaged hydrodynamic model predicts stage height and current velocity in the TIP, over a range of flow rates, with good accuracy. The sediment transport model simulates the transport and deposition of three classes of suspended sediment: 1) flocculating sediment (clay and silt); 2) very fine sand; and 3) fine and medium sands. The PCB fate and transport model incorporates these chemical transport processes into the modeling framework: 1) water column transport of dissolved and particle-associated PCBs; 2) deposition of particle-associated chemical; 3) sorption and desorption; and 4) volatilization.

Application of the sediment transport model to the simulation of the fate of sediment released during dredging operations provides the following general insights. First, coarse sediment (i.e., sand, which is represented as Class 2 and 3 sediment in the model) settles quickly and redeposits relatively close to the dredge head. This behavior is caused by two factors: 1) relatively high settling speed of sands (typically greater than 500 m/d); and 2) high probability of deposition for flow conditions in the river during typical dredging operations. Second, fine sediment (i.e., flocculating clay and silt, which is represented by Class 1 sediment in the model) settles slowly and is transported long distances downstream of the dredge head. In contrast to sand, fine sediment has a relatively low settling speed (i.e., range of 1 to 10 m/d) and the probability of deposition is relatively low.

Model results were used to evaluate PCB concentrations in the river caused by releases during dredging operations without and with control structures. For dredging with no control structures and 0.35% resuspension loss rate, the following conclusions are developed from the model results:

- Total PCB concentrations at TID remain below the Control Level (seven-day average concentration of 350 ng/L) and the Primary Standard (24-hour average of 500 ng/L) for the entire dredging season.
- The total flux over the dredging season (40 kg) is below the Control Level (65 kg).
- The PCB flux at TID consists on average of about two-thirds dissolved phase and one third particulate phase PCB.
- The seven-day average net PCB flux at TID exceeds the Evaluation Level (300 g/d) for about 34% of the dredging season. The Control Level (600 g/d) is exceeded for about 18% of the dredging season.
- Elevated Total PCB concentrations and fluxes at TID are not associated with elevated TSS concentrations.

For dredging with control structures (i.e., controls at East Channel at Rogers Island and East Griffin Island) and 0.35% resuspension loss rate, model results indicate that:

- The addition of resuspension controls reduces downstream PCB releases by about 25%. The flux of Total PCBs past TID during the dredging seasons declines from about 40 kg with no controls to about 31 kg with controls.
- The resuspension controls are moderately effective in reducing the seven-day average net PCB flux at TID to levels below the Control Level. The fluxes remain above the Evaluation Level for about 26% of the dredging season and above the Control Level for about 7% of the dredging season.
- Higher loss rates of dredge material will result in higher net PCB fluxes at TID. The season flux increases by 80% from 31 kg to 56 kg as the loss rate doubles from 0.35 to 0.70%.
- High flow conditions will result in higher net PCB fluxes at TID of about 10%. Similarly, low flow conditions will decrease net PCB fluxes by about 10%.
- Lower desorption capacity of the dredged sediments will result in lower PCB fluxes at TID. The overall season flux is reduced by about 16% as the labile PCB component is reduced from 53% to 20%.

E.9 REFERENCES

Baker, J.R., J.R. Mihelcic, D.C. Luehrs and J.P. Hickey, 1997. Evaluation of estimation methods for organic carbon normalized sorption coefficients. *Water Environ. Res.* 69:136-145.

Bopp, R.F., 1983. Revised parameters for modeling the transport of PCB components across an air-water interface. *J. Geophys. Res.* 88:2521-2529.

Brunner, S., E. Hornung, H. Santi, E. Wolff, O.G. Piringer, J. Altschuh and T. Brüggemann, 1990. Henry's Law constants for polychlorinated biphenyls: experimental determination and structure-property relationships. *Environ. Sci. Technol.* 24:1751-1754.

Burban, P.Y., Y.J. Xu, J. McNeil, and W. Lick, 1990. Settling speeds of flocs in fresh water and seawater. *J. Geophys. Res.* 95(C10):18213-18220.

Burkhard, L., D.E. Armstrong, and A.W. Anderson, 1985. Henry's Law constants for the polychlorinated biphenyls. *Environ. Sci. Technol.* 19:590-596.

Carroll, K.M., M.R. Harkness, A.A. Bracco and R.R. Balcarcel, 1994. Application of a permeant/polymer diffusional model to the desorption of polychlorinated biphenyls from Hudson River sediments. *Environ. Sci. Technol.* 28:253-258

Cheng, N.S., 1997. Simplified settling velocity formula for sediment particle. *ASCE J. Hydr. Engrg.* 123(2):149-152.

Connolly, J.P., N.E. Armstrong, and R.W. Miksad, 1983. Adsorption of Hydrophobic Pollutants in Estuaries. *ASCE J. Envir. Eng. Div.* 109(1):17-35.

Connolly, J.P., H.A. Zahakos, J. Benaman, C.K. Ziegler, J.R. Rhea and K. Russell, 2000. A model of PCB fate in the Upper Hudson River. *Environ. Sci. Technol.* 34(19):4076-4087.

Dunnivant, F.M. and A.W. Elzerman, 1988. Aqueous Solubility and Henry's Law constant data for PCB congeners for evaluation of quantitative structure-property relationships (QSPRs). *Chemosphere* 17:525-541.

Famularo, J., Pannu, A.S. and Mueller, J.A., 1980. Prediction of Carbon Column Performance from Pure Solute Data. *JWPCF* 52:2019-2032.

Gailani, J., W. Lick, C.K. Ziegler, and D. Endicott, 1996. Development and calibration of a fine-grained sediment transport model for the Buffalo River. *J. Great Lakes Res.* 22:765-778.

Gessler, J., 1967. *The Beginning of Bedload Movement of Mixtures Investigated as Natural Armoring in Channels.* Translated by E.A. Prych, Translation T-5, W. M. Keck Laboratory of Hydraulics and Water Research, California Institute of Technology, Pasadena, CA.

Hamrick, J.M., 1992. *A Three-Dimensional Environmental Fluid Dynamics Code: Theoretical and Computational Aspects*. Special Report 317 in Applied Marine Science and Ocean Engineering, Virginia Institute of Marine Science, VA.

Karickhoff, S.W., 1984. Organic pollutant sorption in aquatic systems. *J. Hydr. Eng.* 110:707-735.

Karickhoff, S.W., 1981. Semi-empirical estimation of sorption of hydrophobic pollutants on natural sediments and soils. *Chemosphere* 10:833-846.

Kan, A.T., G. Fu, M.A. Hunter and M.B. Tomson, 1997. Irreversible adsorption of naphthalene and tetrachlorobiphenyl to Lula and surrogate sediments. *Environ. Sci. Technol.* 2176-2185.

Krone, R.B., 1962. *Flume Studies of the Transport of Sediment in Estuarial Processes: Final Report.* Hydraulic Engineering Laboratory and Sanitary Engineering Research Laboratory, University of California, Berkeley, California.

Malcolm Pirnie, Inc. and TAMS Consultants, Inc., 2004. *Engineering Performance Standards Hudson River PCBs Superfund Site, Volume 2: Technical Basis of the Performance Standard for Dredging Resuspension.* Prepared for U.S. Army Corps of Engineers, Kansas City District on behalf of U.S. Environmental Protection Agency, Region 2. April 2004.

Murphy, T.J., M.D. Mullin and J.A. Meyer, 1987. Equilibration of polychlorinated biphenyls and toxaphene with air and water. *Environ. Sci. Technol.* 21:155-162.

O'Connor, D.J., 1984. The significance of gas exchange in water quality assessment and planning. In *Gas Transfer at Water Surfaces*, Edited by W. Brutsaert, and G. H. Jirka. Dordrecht, Holland: D. Reidel Publishing Company, 559-576.

O'Connor, D.J., 1983. The effects of wind on the gas-liquid transfer coefficients. *J. Environ. Eng. Div. ASCE* 109:731-752.

Partheniades, E., 1992. Estuarine sediment dynamics and shoaling processes. In: *Handbook of Coastal and Ocean Engineering, Volume 3*, edited by J. Herbick. Houston, TX: Gulf Publishing Company, 985-1071.

Pignatello, J.J. and B. Xing, 1996. Mechanisms of slow sorption of organic chemicals to natural particles. *Environ. Sci. Technol.* 30:1-11.

Pignatello, J.J., 1990. Slow-reversible Sorption of Aliphatic Halocarbons in Soils. II. Mechanistic Aspects. *Environ. Toxicol. Chem.* 9:1116-1124.

Quantitative Environmental Analysis, LLC, 2004. *Baseline Monitoring Program – Data Summary Report for 2004.* Hudson River PCBs Site. Prepared for General Electric Company, Albany, NY.

Quantitative Environmental Analysis, LLC, 1999. *PCBs in the Upper Hudson River – Volume 2.* Prepared for General Electric Company, Albany, NY. June 1999.

Rutherford, J.C., 1994. *River Mixing.* New York: John Wiley and Sons.

Schneider, A., Porter, E. and Baker, J., 2004. PCB Desorption from Hudson River Sediments During Realistic Bottom Shear and Water Column Turbulence. Paper presented at the SETAC 25th Annual Meeting.

Tateya, S., S. Tanabe and R. Tatsulawa, 1988. PCBs on the Globe: Possible trend of future levels in the open ocean environment. In *Toxic Contamination in Large Lakes, Volume 3*, edited by M.W. Schmidtke. Chelsea, MI: Lewis Publishers, 237-281.

ten Hulscher, Th.E.M., L.E. van der Velde and W.A. Bruggman, 1992. Temperature dependence of Henry's Law constants for selected chlorobenzenes, polychlorinated biphenyls and polycyclic aromatic hydrocarbons. *Environ. Tox. Chem.* 11:1595-1603.

USEPA 2002. *Record of Decision, Hudson River PCBs Reassessment RI/FS, USEPA Region 2, New York.*

USEPA 2000. *Phase 3 Report: Feasibility Study, Hudson River PCBs Reassessment RI/FS.* Prepared for U.S. EPA Region 2 and the U.S. Army Corps of Engineers (USACE), Kansas City District by TAMS Consultants, Inc. December 2000.

van Rijn, L.C., 1984. Sediment Transport, Part II: Suspended Load Transport. *ASCE J. Hydr. Engrg.* 110(11):1612-1638.

Wu, S. and Gschwend, P.M., 1986. Sorption Kinetics of Hydrophobic Organic Compounds to Natural Sediments and Soils. *Environ. Sci. Technol.* 20:717-725.

Ziegler, C.K., P.H. Israelsson, and J.P. Connolly, 2000. Modeling sediment transport dynamics in Thompson Island Pool, Upper Hudson River. *Water Quality and Ecosystem Modeling* 1:193-222.

Ziegler, C.K. and B.S. Nisbet, 1995. Long-term simulation of fine-grained sediment transport in large reservoir. *ASCE J. Hydr. Engrg.* 121(11):773-781.

Ziegler, C.K. and B.S. Nisbet, 1994. Fine-grained sediment transport in Pawtuxet River, Rhode Island. *ASCE J. Hydr. Engrg.* 120(5):561-576.

FIGURES

Quantitative Environmental Analysis, LLC
∂c/∂t

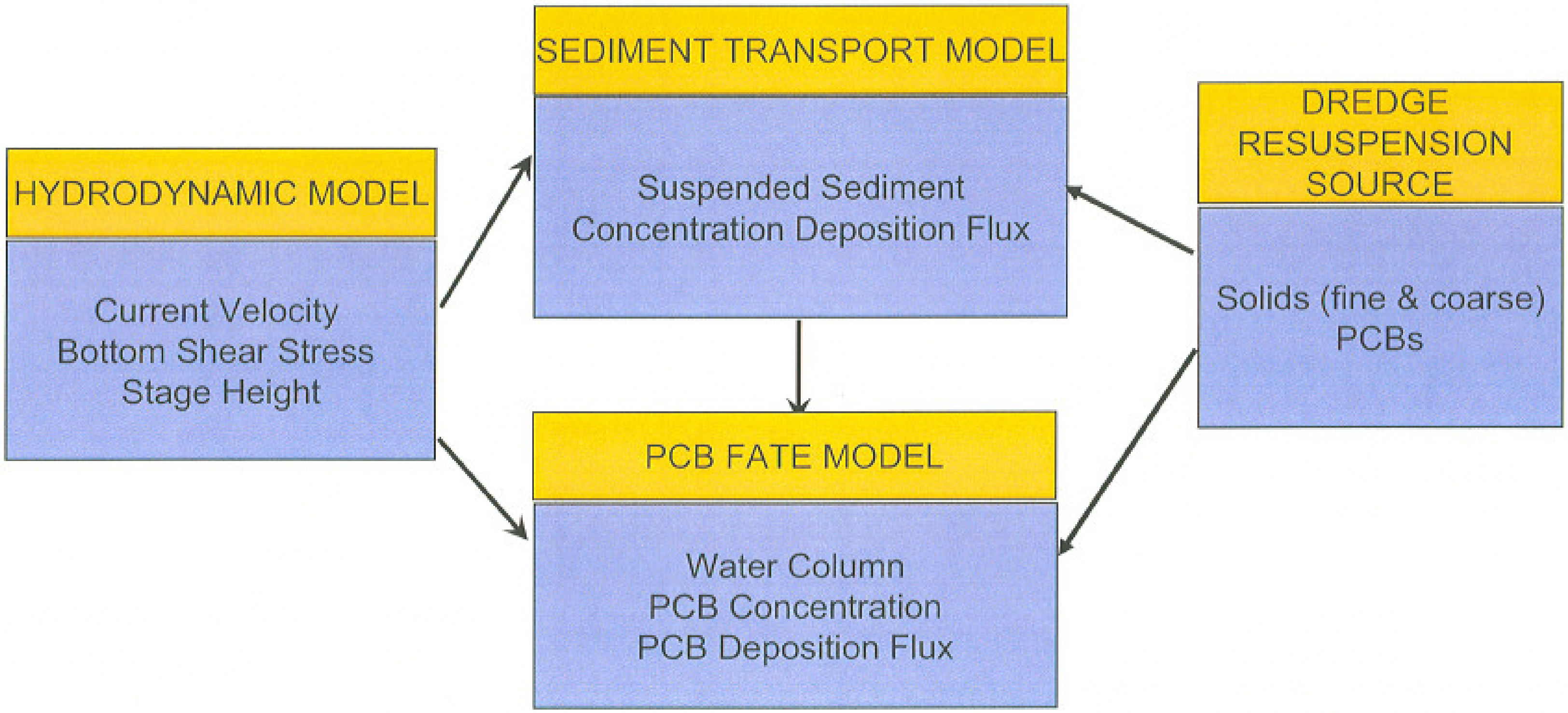

Figure E-1-1. Structure of dredge resuspension modeling framework.

DN - \\Dalee\D_DRIVE\GENdes\Documents\Reports\IDR\Figure_A1-1.ppt
8/18/2005 10:00 AM

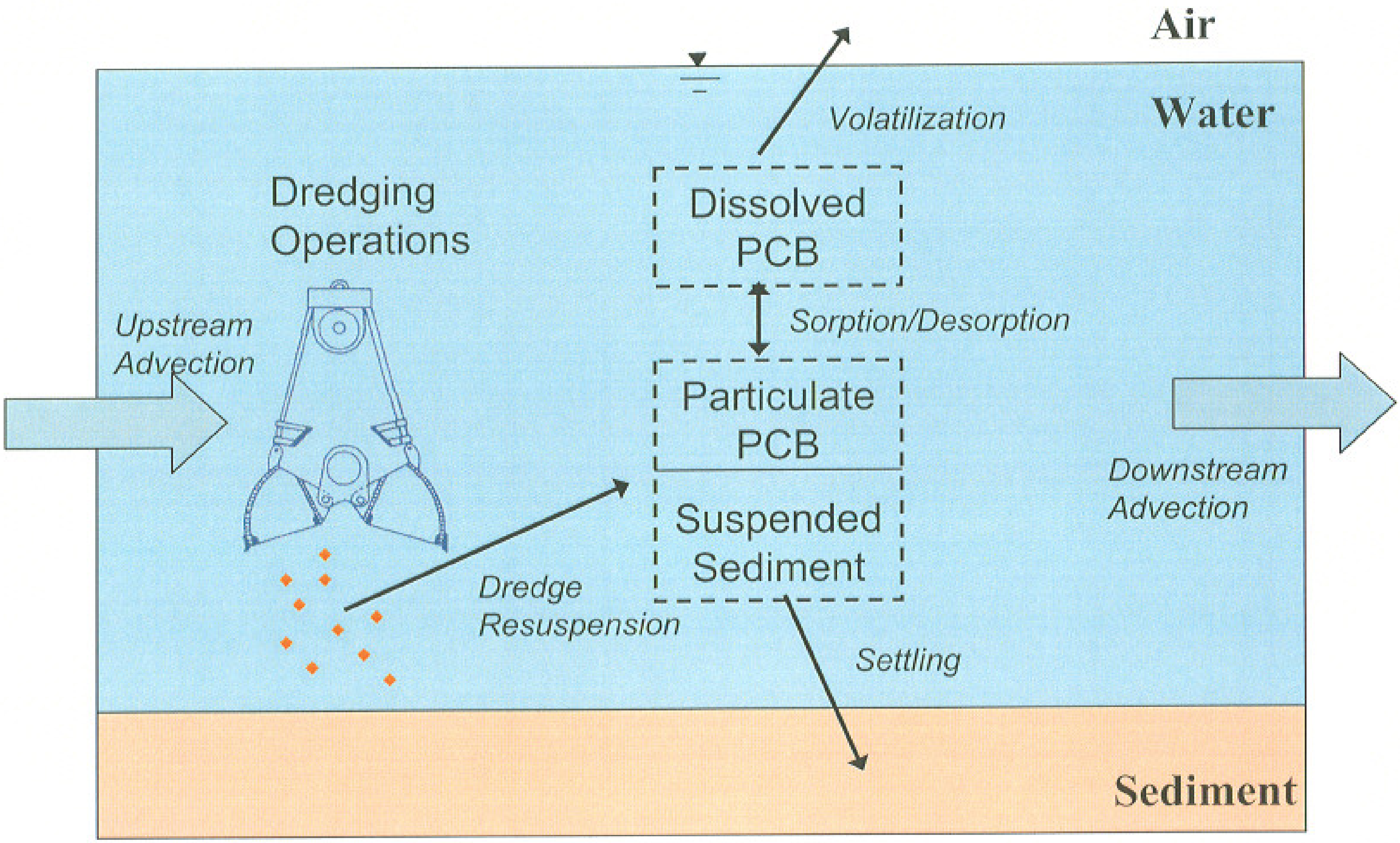

Figure E-1-2. Generalized conceptual diagram of resuspension modeling.

\\daleef\d_drive\GENdes\Documents\Reports\IDR\Figure_E-1-2_pcb_fate.ppt

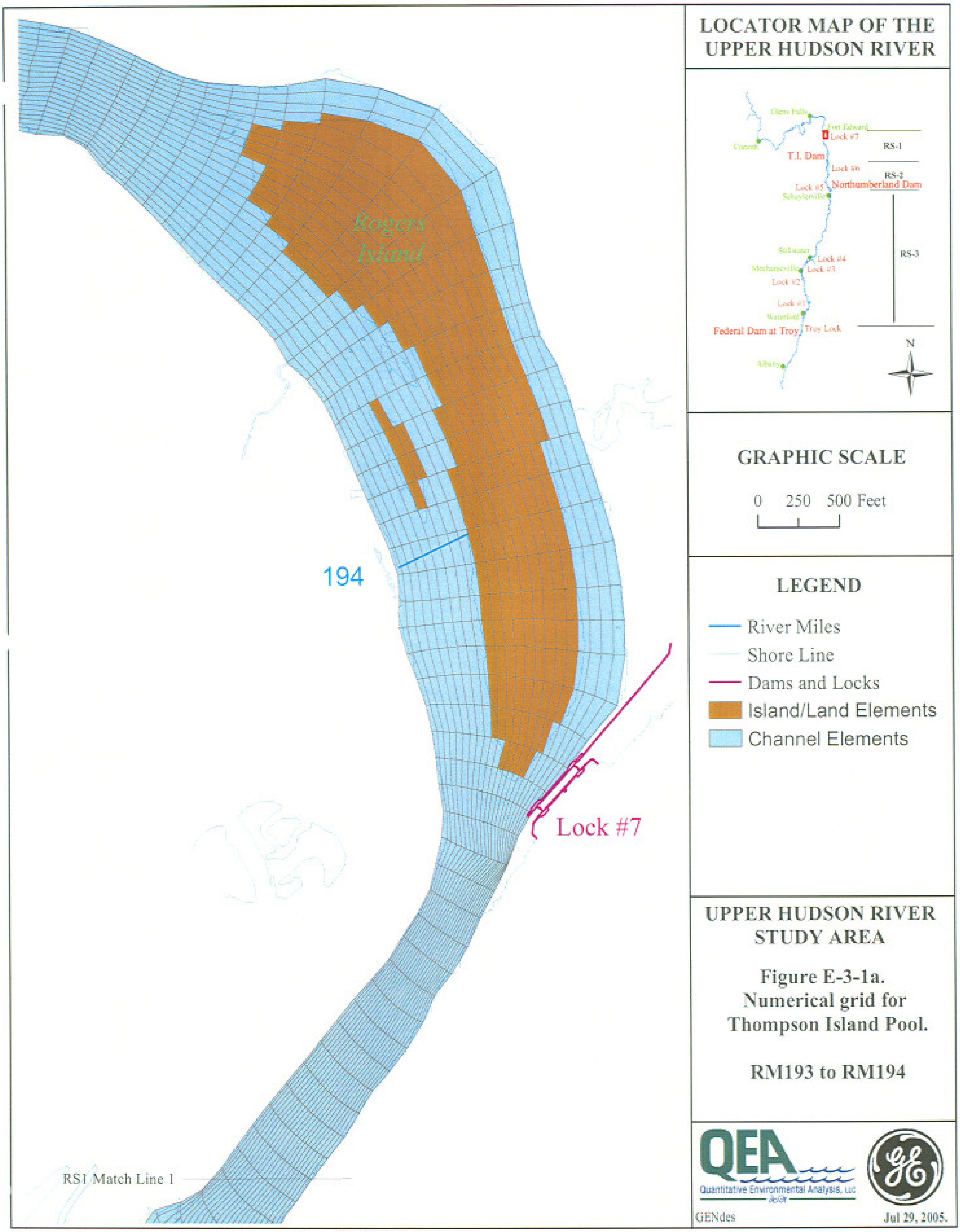

UPPER HUDSON RIVER STUDY AREA

Figure E-3-1a. Numerical grid for Thompson Island Pool.

RM193 to RM194

DN - \\Daleel\D_DRIVE\GENdes\Documents\Reports\IDR\Figure_E-3-1.mxd

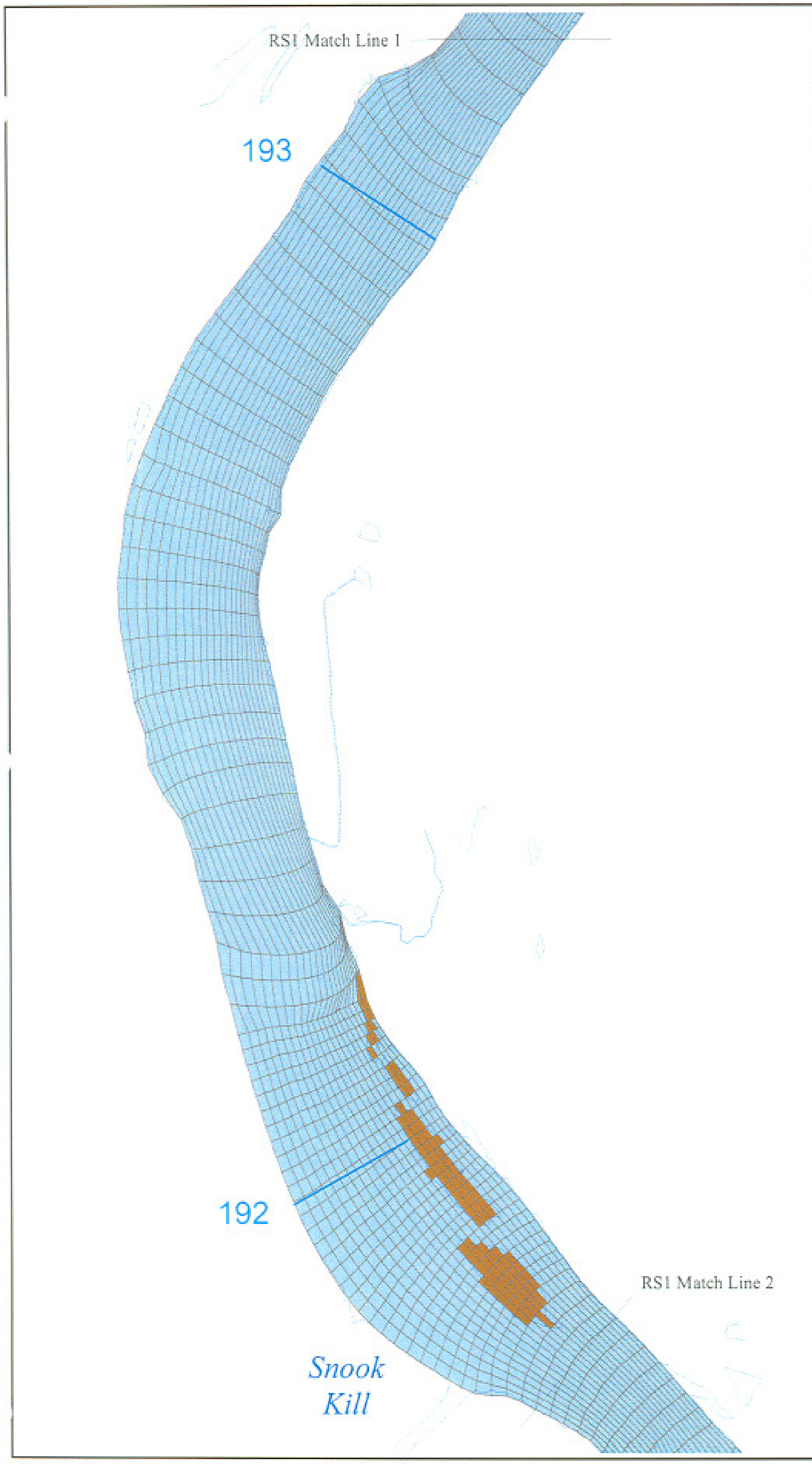

LOCATOR MAP OF THE UPPER HUDSON RIVER

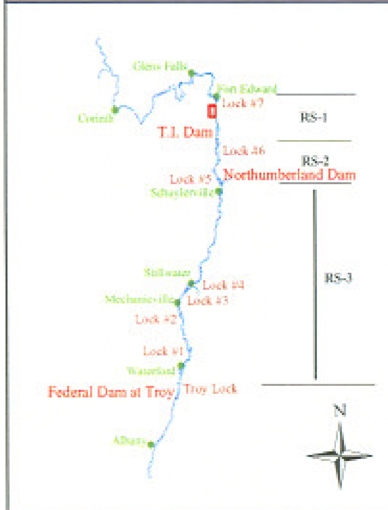

GRAPHIC SCALE

0 250 500 Feet

LEGEND

- River Miles
- Shore Line
- Dams and Locks
- Island/Land Elements
- Channel Elements

UPPER HUDSON RIVER STUDY AREA

Figure E-3-1b. Numerical grid for Thompson Island Pool.

RM191 to RM193

QEA Quantitative Environmental Analysis, LLC

GENdes

Jul 29, 2005.

DN - \\Daleel\D_DRIVE\GENdes\Documents\Reports\IDR\Figure_E-3-1.mxd

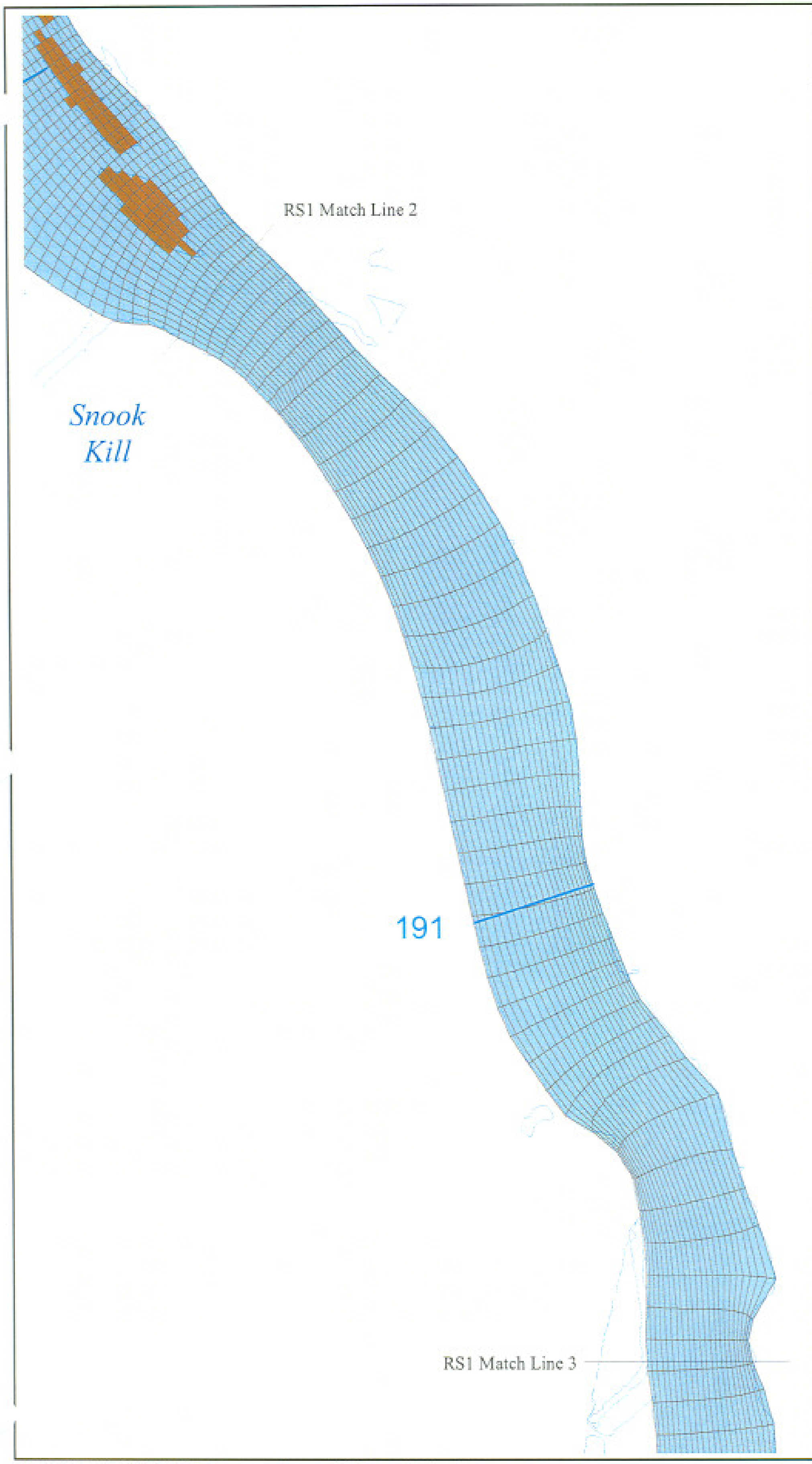

LOCATOR MAP OF THE UPPER HUDSON RIVER

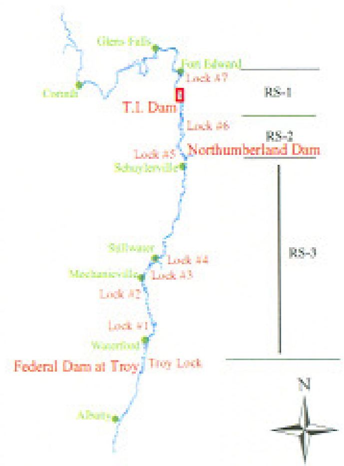

GRAPHIC SCALE

0 250 500 Feet

LEGEND

- River Miles
- Shore Line
- Dams and Locks
- Island/Land Elements
- Channel Elements

UPPER HUDSON RIVER STUDY AREA

Figure E-3-1c. Numerical grid for Thompson Island Pool.

RM190 to RM191

Quantitative Environmental Analysis, LLC

GENdes Jul 29, 2005.

DN - \\Dalecl\D_DRIVE\GENdes\Documents\Reports\IDR\Figure_E-3-1.mxd

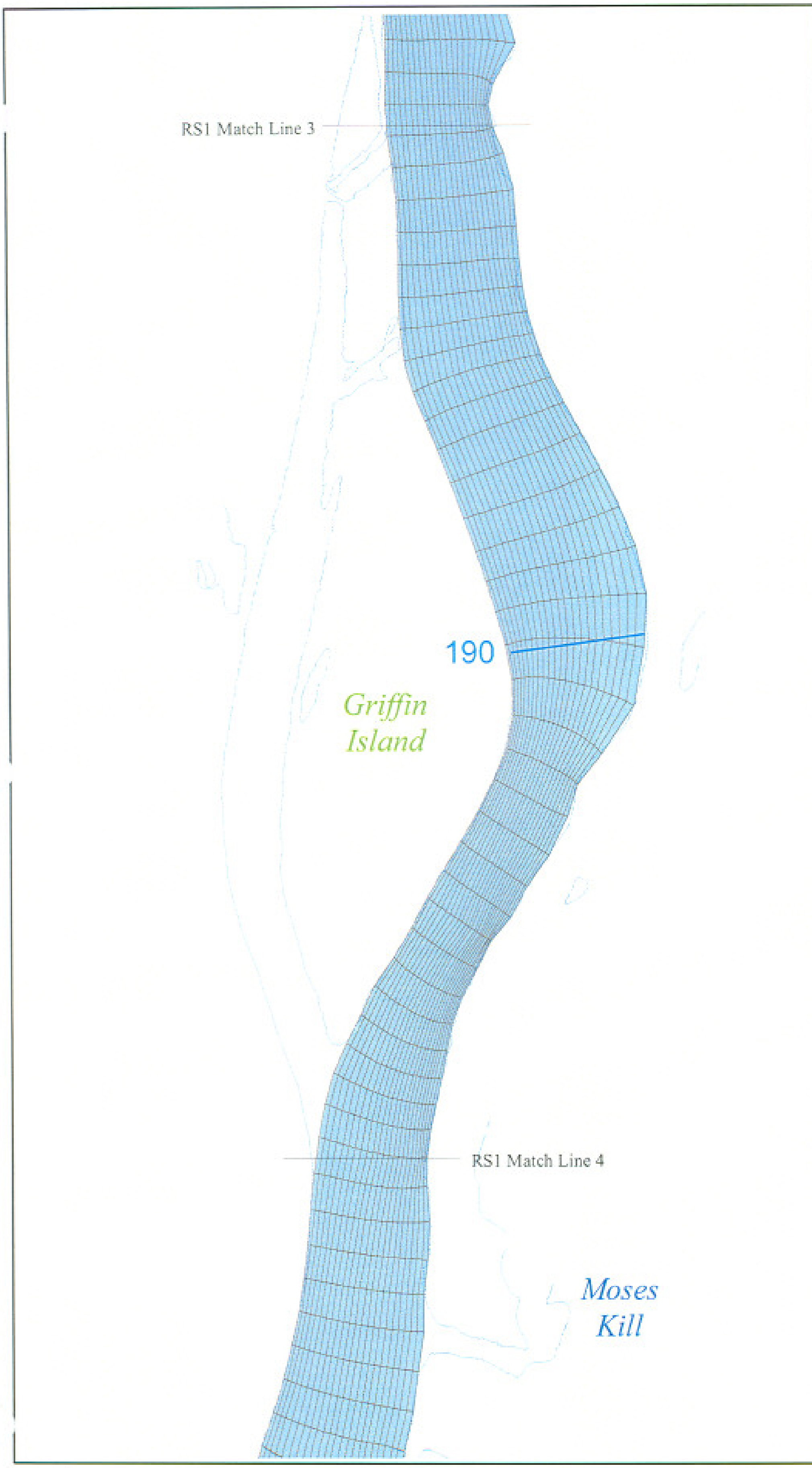

LOCATOR MAP OF THE UPPER HUDSON RIVER

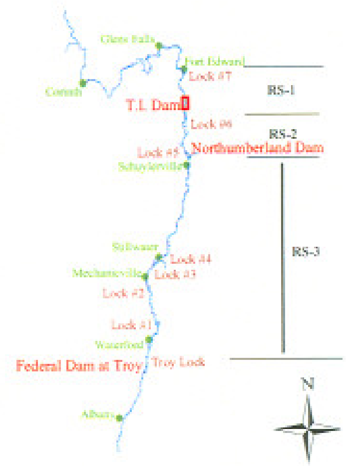

GRAPHIC SCALE

0 250 500 Feet

LEGEND

- River Miles
- Shore Line
- Dams and Locks
- Island/Land Elements
- Channel Elements

UPPER HUDSON RIVER STUDY AREA

Figure E-3-1d. Numerical grid for Thompson Island Pool.

RM189 to RM190

Quantitative Environmental Analysis, LLC

GENdes Jul 29, 2005.

DN - \\Daleel\D_DRIVE\GENdes\Documents\Reports\IDR\Figure_E-3-1.mxd

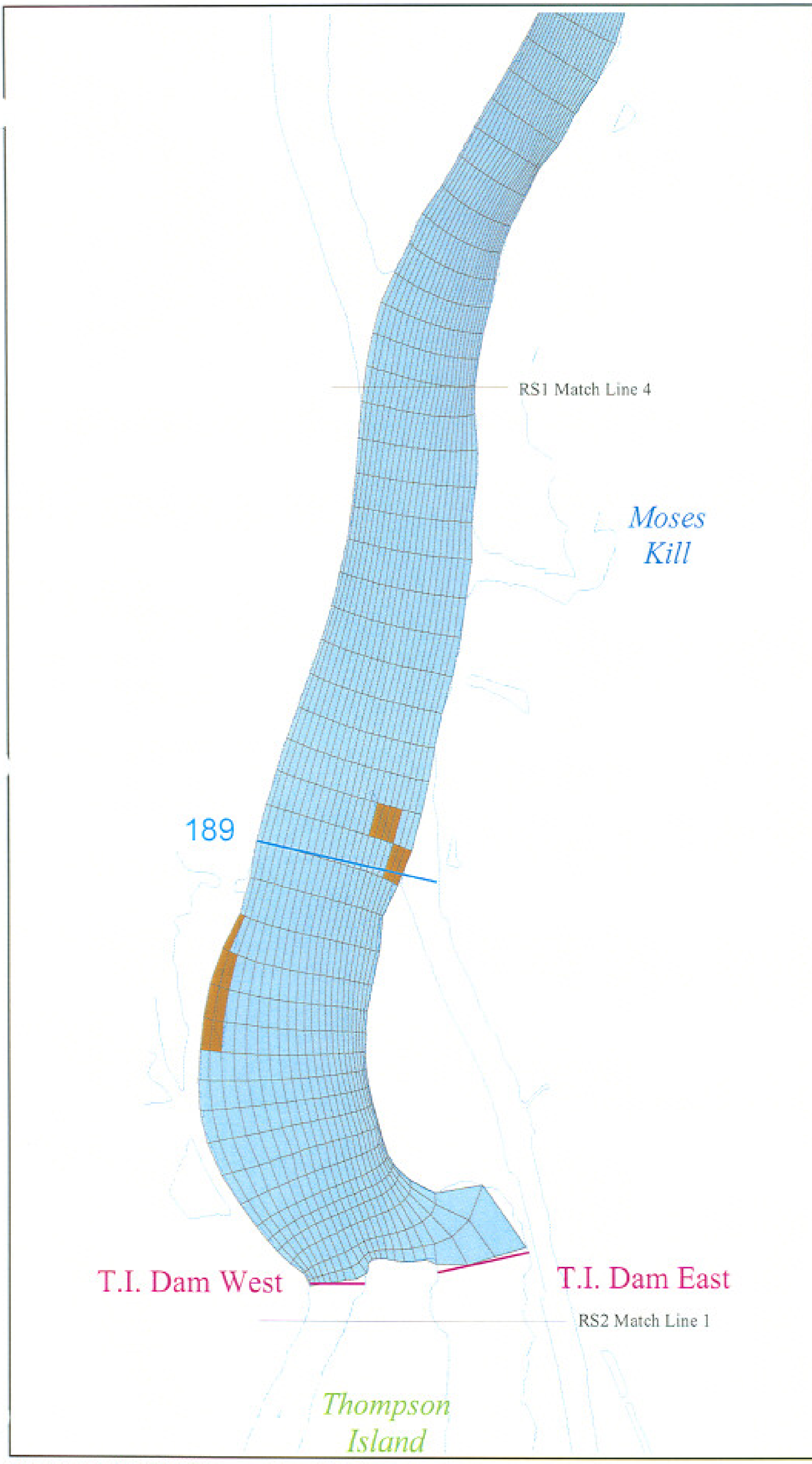

LOCATOR MAP OF THE UPPER HUDSON RIVER

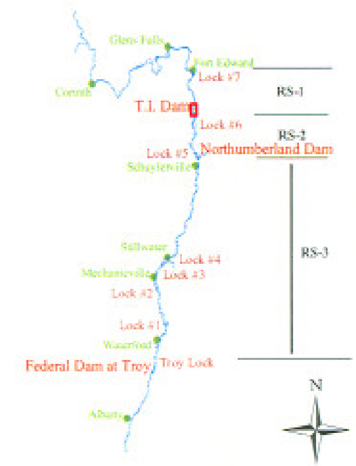

GRAPHIC SCALE

0 250 500 Feet

LEGEND

- River Miles
- Shore Line
- Dams and Locks
- Island/Land Elements
- Channel Elements

UPPER HUDSON RIVER STUDY AREA

Figure E-3-1e. Numerical grid for Thompson Island Pool.

RM188 to RM189

QEA Quantitative Environmental Analysis, LLC

GENdes

Jul 29, 2005.

DN - \\Daleel\D_DRIVE\GENdes\Documents\Reports\IDR\Figure_E-3-1.mxd

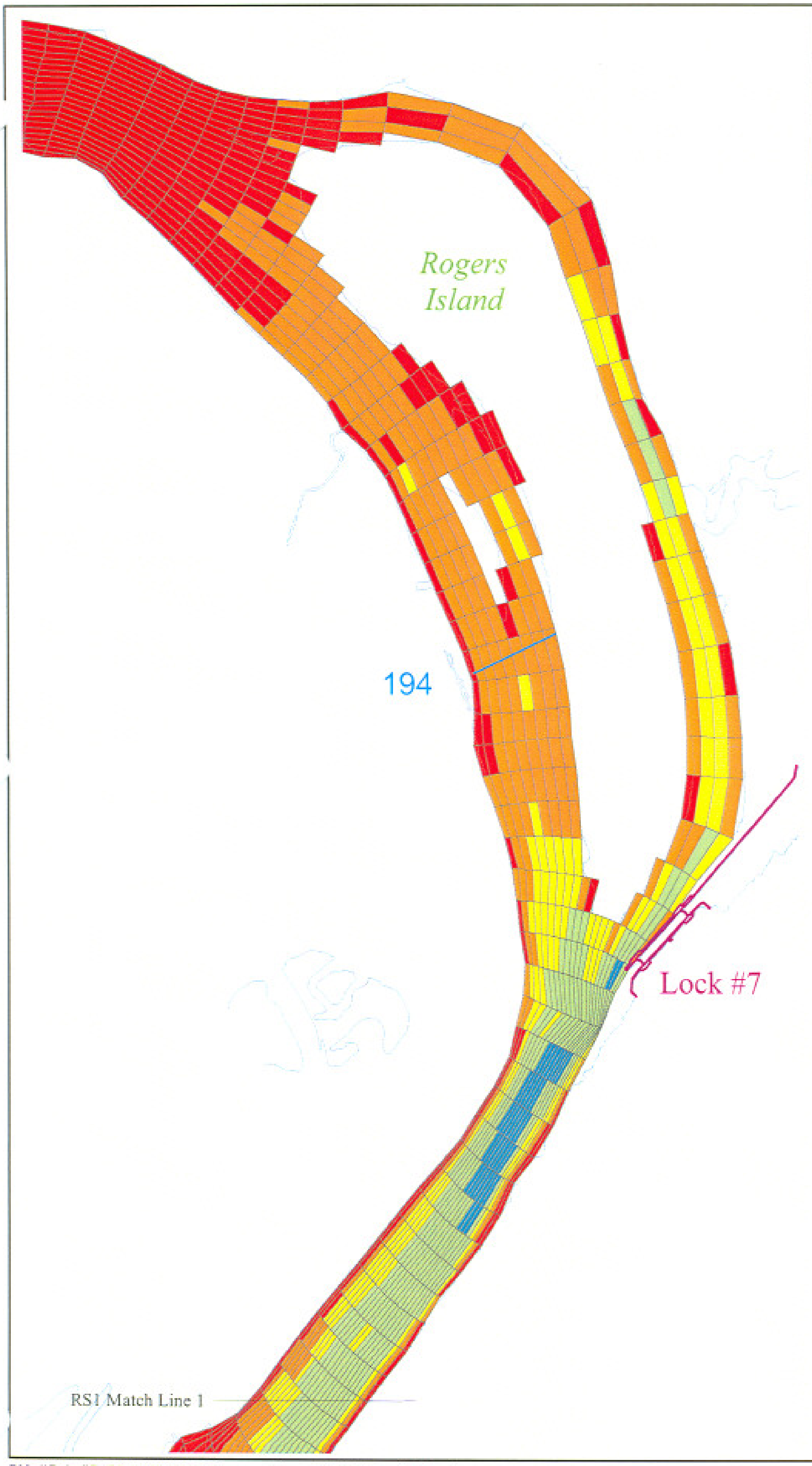

LOCATOR MAP OF THE UPPER HUDSON RIVER

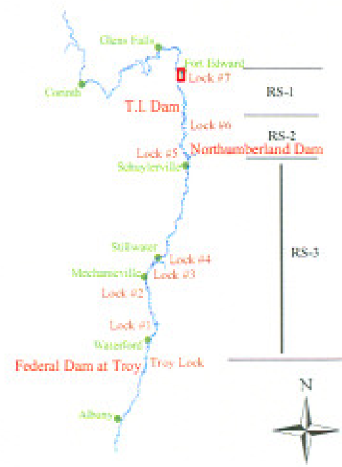

GRAPHIC SCALE

0 250 500 Feet

LEGEND

- River Miles
- Shore Line
- Dams and Locks

Sediment Elev. (ft NAVD88)

- < 90
- 90 - 95
- 95 - 100
- 100 - 105
- 105 - 110
- 110 - 115
- > 115

UPPER HUDSON RIVER STUDY AREA

Figure E-3-2a. Bathymetry for Thompson Island Pool.

RM193 to RM194

QEA Quantitative Environmental Analysis, LLC

GENdes

Jul 29, 2005.

DN - \\Daleel\D_DRIVE\GENdes\Documents\Reports\IDR\Figure_E-3-2.mxd

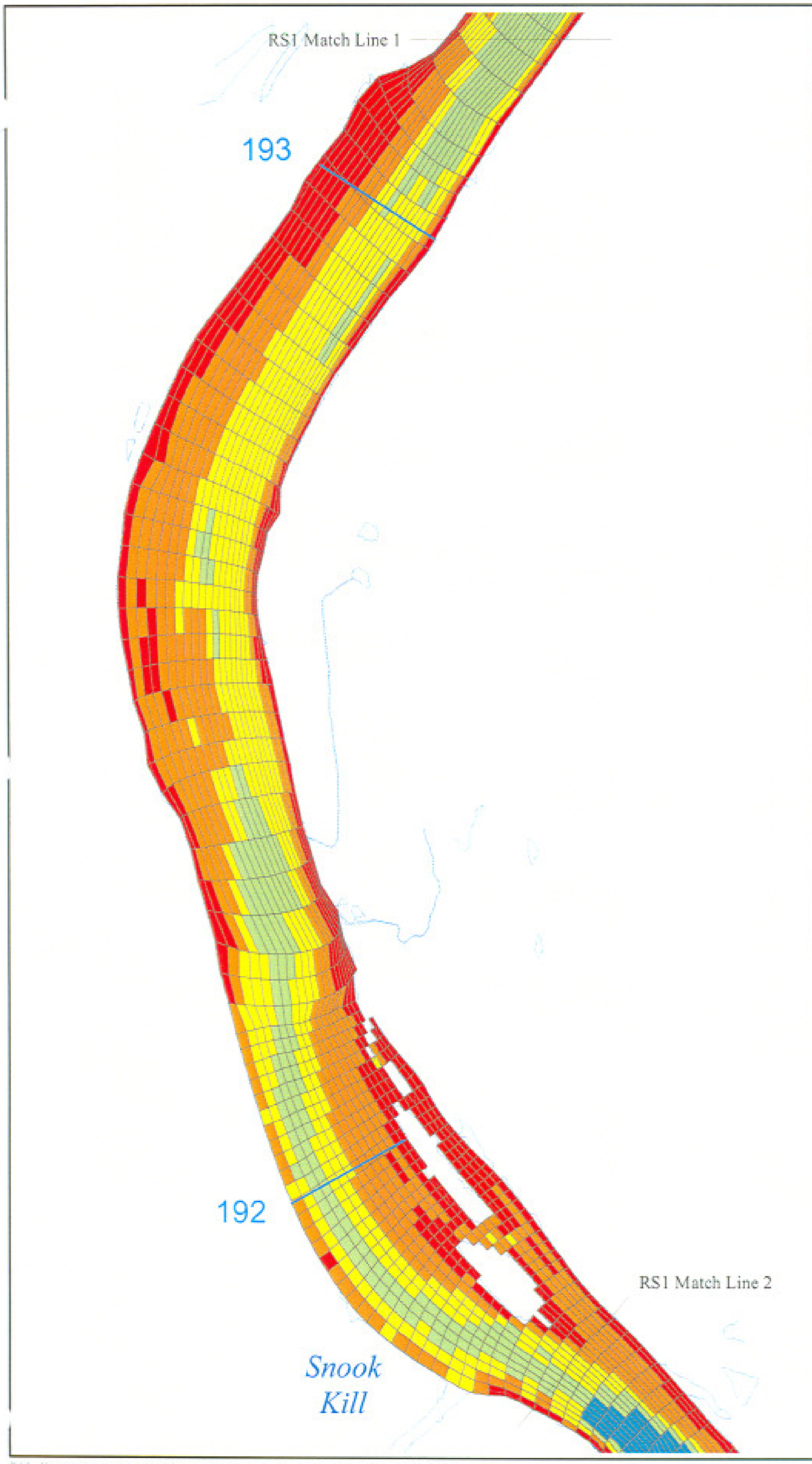

LOCATOR MAP OF THE UPPER HUDSON RIVER

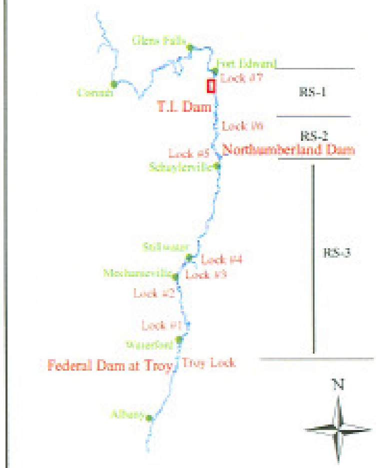

GRAPHIC SCALE

0 250 500 Feet

LEGEND

- River Miles
- Shore Line
- Dams and Locks

Sediment Elev. (ft NAVD88)

- < 90
- 90 - 95
- 95 - 100
- 100 - 105
- 105 - 110
- 110 - 115
- > 115

UPPER HUDSON RIVER STUDY AREA

Figure E-3-2b. Bathymetry for Thompson Island Pool.

RM191 to RM193

QEA Quantitative Environmental Analysis, LLC

GENdes

Jul 29, 2005.

DN - \\DaleeJ\D_DRIVE\GENdes\Documents\Reports\IDR\Figure_E-3-2.mxd

LOCATOR MAP OF THE UPPER HUDSON RIVER

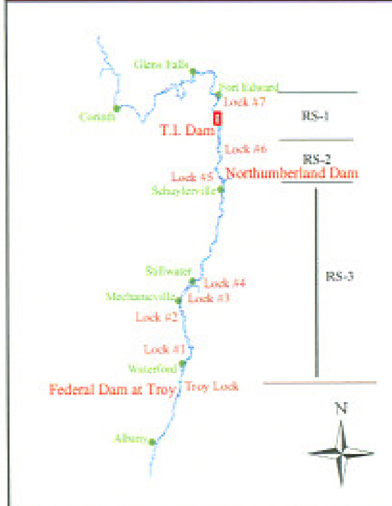

GRAPHIC SCALE

0 250 500 Feet

LEGEND

- River Miles
- Shore Line
- Dams and Locks

Sediment Elev. (ft NAVD88)

- < 90
- 90 - 95
- 95 - 100
- 100 - 105
- 105 - 110
- 110 - 115
- > 115

UPPER HUDSON RIVER STUDY AREA

Figure E-3-2c. Bathymetry for Thompson Island Pool.

RM190 to RM191

QEA Quantitative Environmental Analysis, LLC

GENdes Jul 29, 2005.

DN - \\Daleel\D_DRIVE\GENdes\Documents\Reports\IDR\Figure_E-3-2.mxd

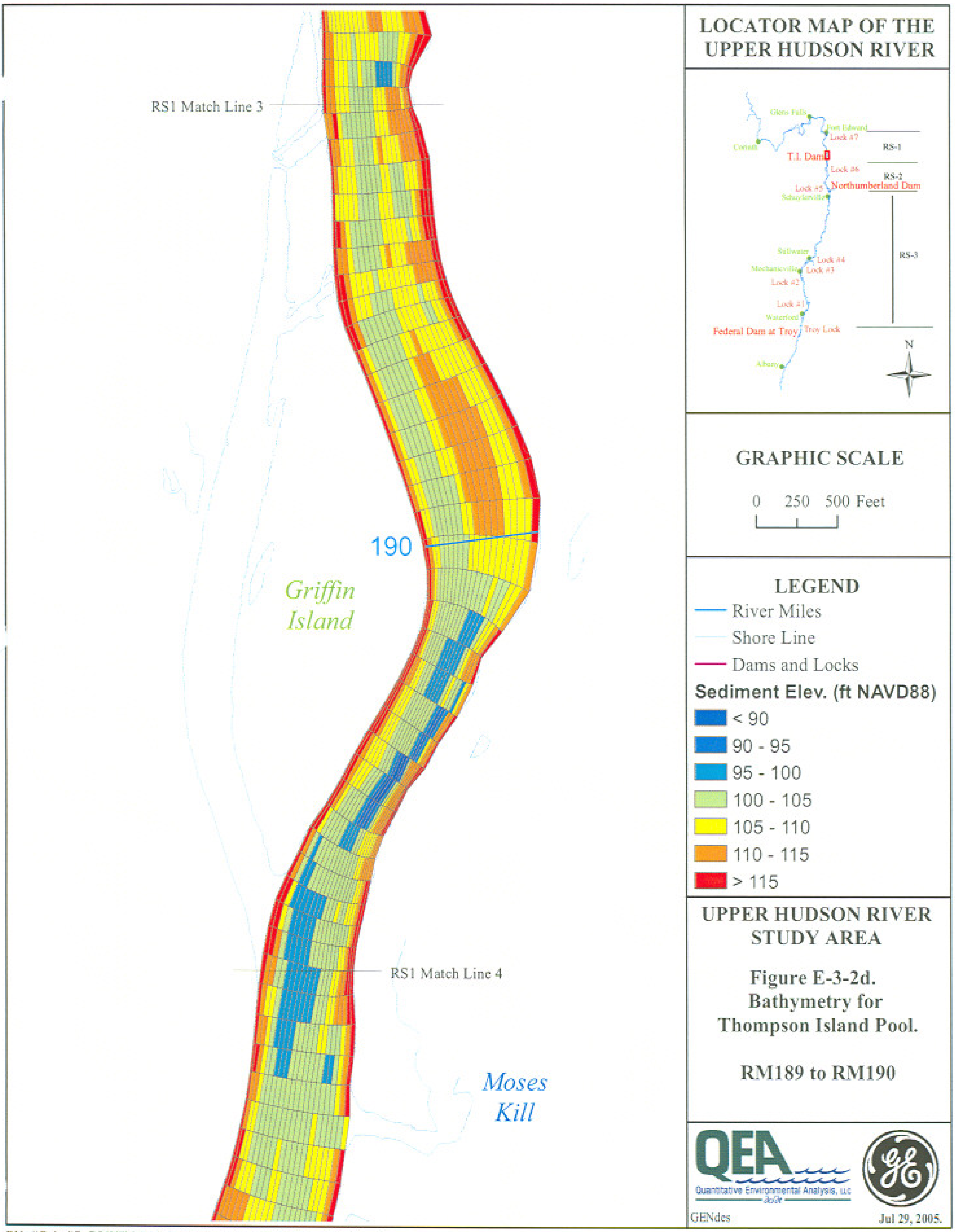

Figure E-3-2d. Bathymetry for Thompson Island Pool.

RM189 to RM190

DN - \\Dalcel\D_DRIVE\GENdes\Documents\Reports\IDR\Figure_E-3-2.mxd

LOCATOR MAP OF THE UPPER HUDSON RIVER

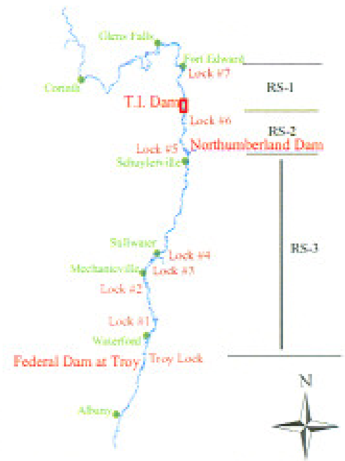

GRAPHIC SCALE

0 250 500 Feet

LEGEND

- River Miles
- Shore Line
- Dams and Locks

Sediment Elev. (ft NAVD88)

- < 90
- 90 - 95
- 95 - 100
- 100 - 105
- 105 - 110
- 110 - 115
- > 115

UPPER HUDSON RIVER STUDY AREA

Figure E-3-2e. Bathymetry for Thompson Island Pool.

RM188 to RM189

QEA Quantitative Environmental Analysis, LLC

GENdes

Jul 29, 2005.

DN - \\Daleel\D_DRIVE\GENdes\Documents\Reports\IDR\Figure_E-3-2.mxd

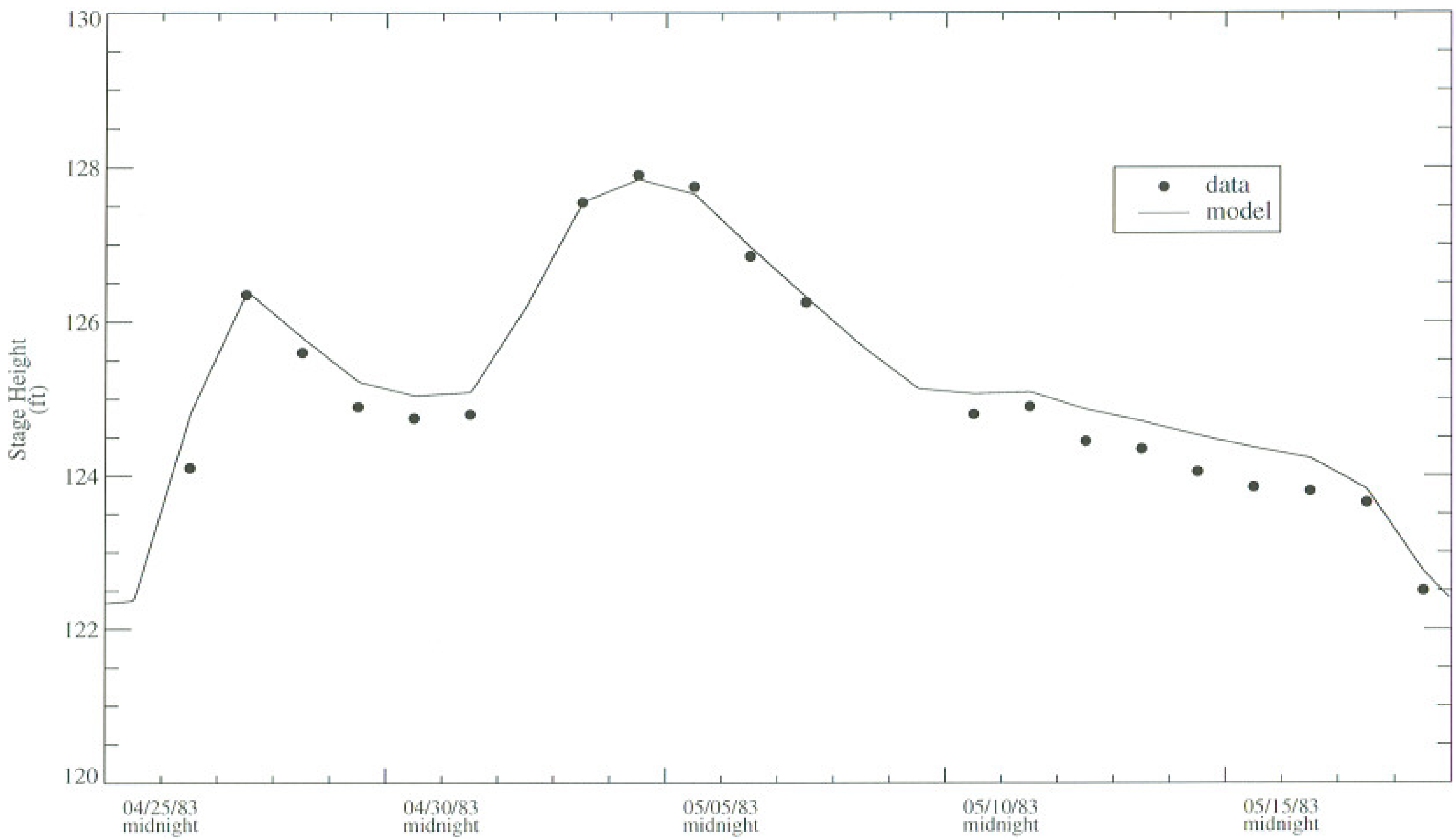

Figure E-3-3. Comparison of predicted and observed stage height at gauge 119 (at the entrance to Lock 7) during Spring 1983 flood.

lz - D:\GENdes\Analysis\Model_Outputs\EFDC_Outputs\Plot_stage83\plot_stage83.pro
Thu Aug 18 13:21:37 2005

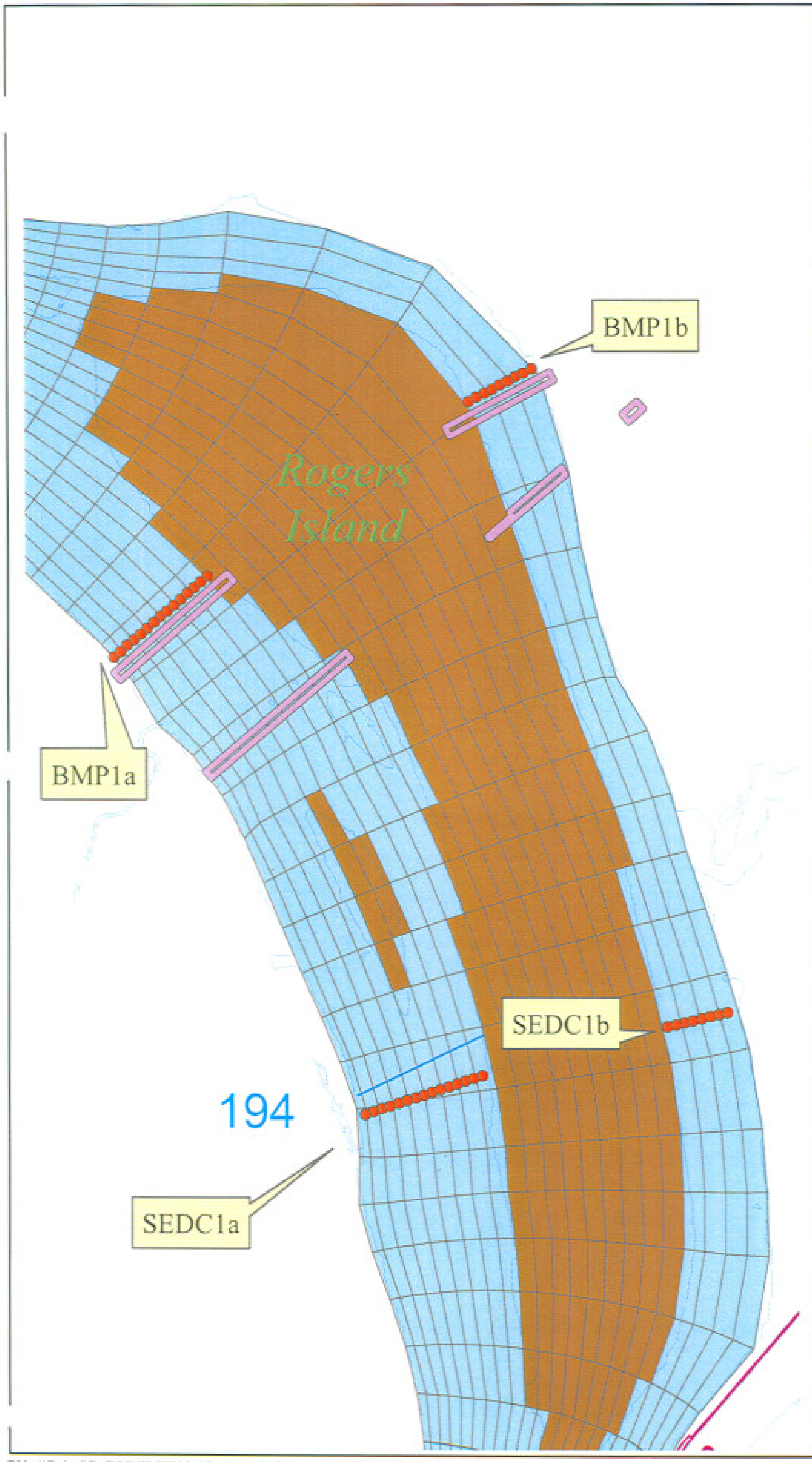

LOCATOR MAP OF THE UPPER HUDSON RIVER

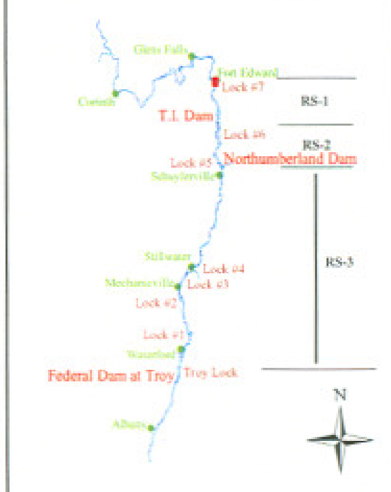

GRAPHIC SCALE

0 250 500 Feet

LEGEND

- ADCP Data
- River Miles
- Shore Line
- Dams and Locks
- Island/Land Elements
- Channel Elements
- Bridges

UPPER HUDSON RIVER STUDY AREA

Figure E-3-4. Locations of transects BMP1 and SEDC1 at which ADCP data were collected during June 2004.

QEA Quantitative Environmental Analysis, LLC

GENdes

Jul 29, 2005.

DN - \\Daleel\D_DRIVE\GENdes\Documents\Reports\IDR\Figure_E-3-4_5_6_7.mxd

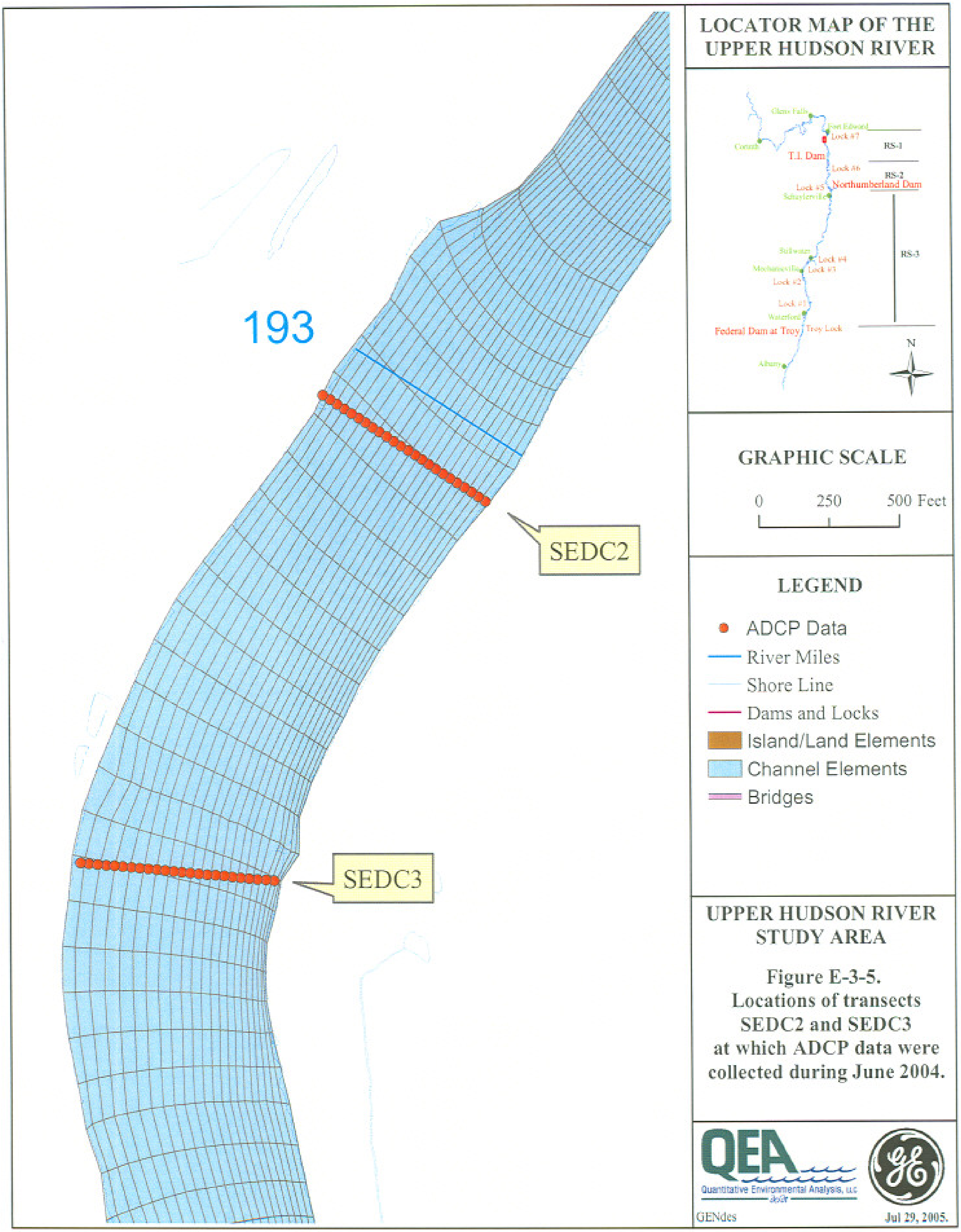

Figure E-3-5.
Locations of transects SEDC2 and SEDC3 at which ADCP data were collected during June 2004.

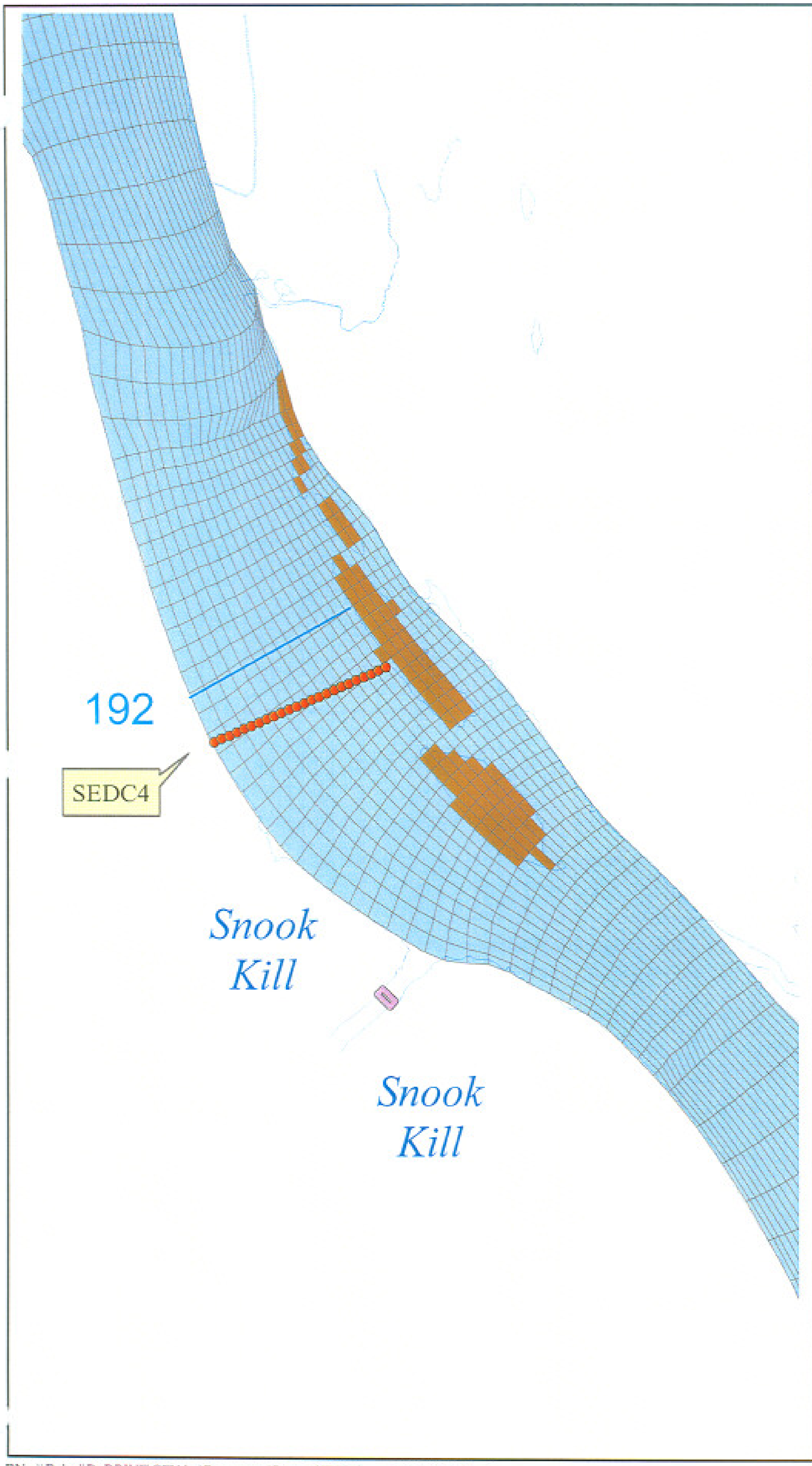

LOCATOR MAP OF THE UPPER HUDSON RIVER

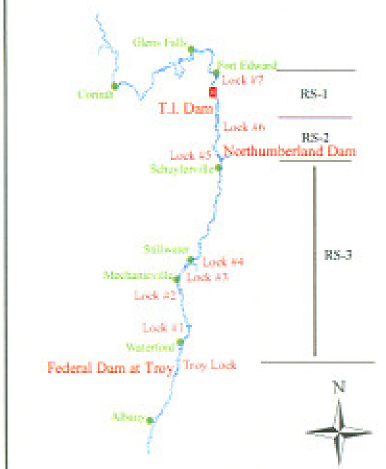

GRAPHIC SCALE

0 250 500 Feet

LEGEND

- ADCP Data
- River Miles
- Shore Line
- Dams and Locks
- Island/Land Elements
- Channel Elements
- Bridges

UPPER HUDSON RIVER STUDY AREA

Figure E-3-6. Location of transect SEDC4 at which ADCP data were collected during June 2004.

QEA Quantitative Environmental Analysis, LLC

GENdes

Jul 29, 2005.

DN - \\Daleel\D_DRIVE\GENdes\Documents\Reports\IDR\Figure_E-3-4_5_6_7.mxd

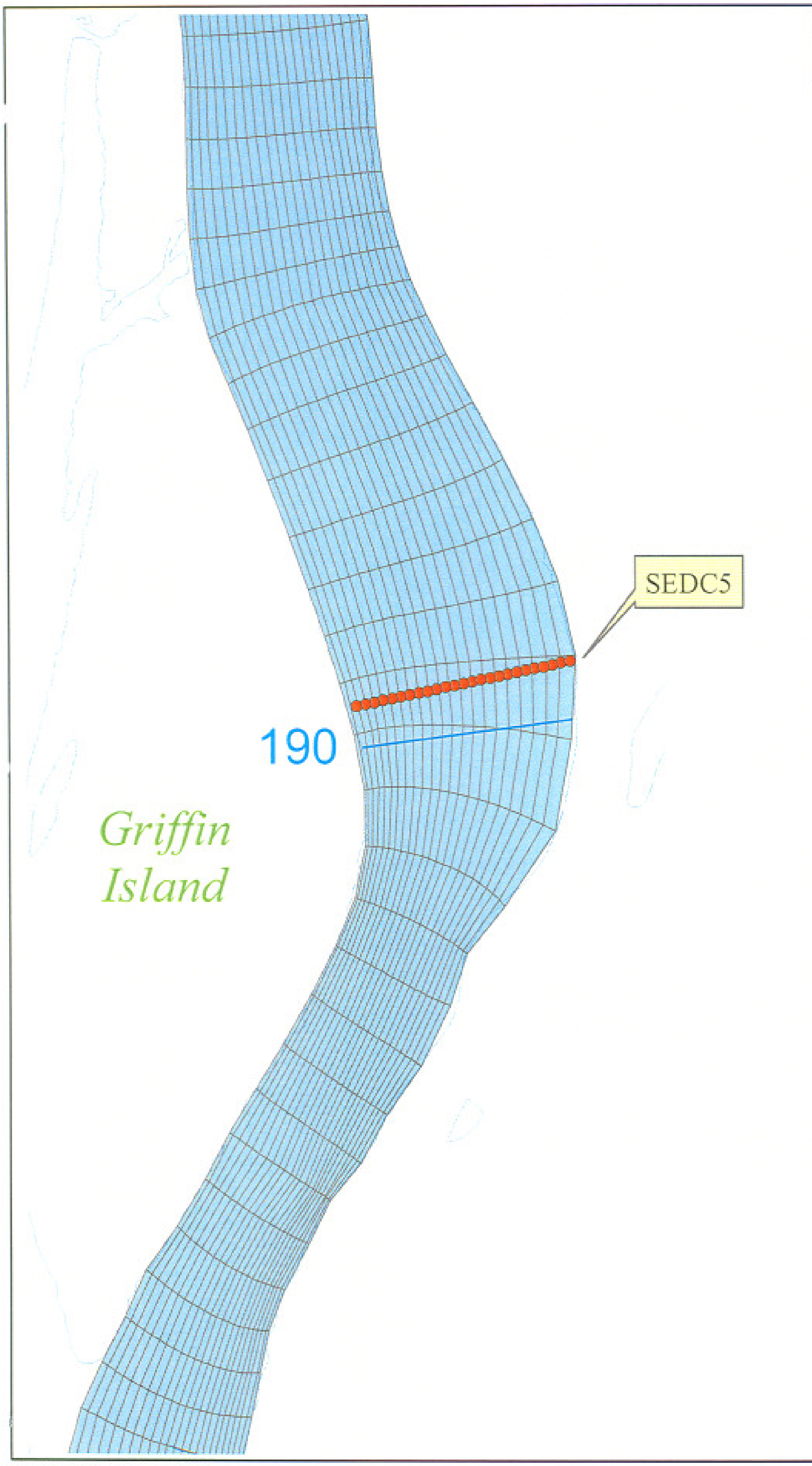

LOCATOR MAP OF THE UPPER HUDSON RIVER

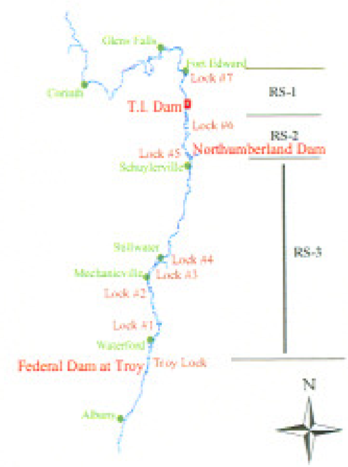

GRAPHIC SCALE

0 250 500 Feet

LEGEND

- ADCP Data
- River Miles
- Shore Line
- Dams and Locks
- Island/Land Elements
- Channel Elements
- Bridges

UPPER HUDSON RIVER STUDY AREA

Figure E-3-7. Location of transect SEDC5 at which ADCP data were collected during June 2004.

QEA Quantitative Environmental Analysis, LLC

GENdes Jul 29, 2005.

DN - \\Daleel\D_DRIVE\GENdes\Documents\Reports\IDR\Figure_E-3-4_5_6_7.mxd

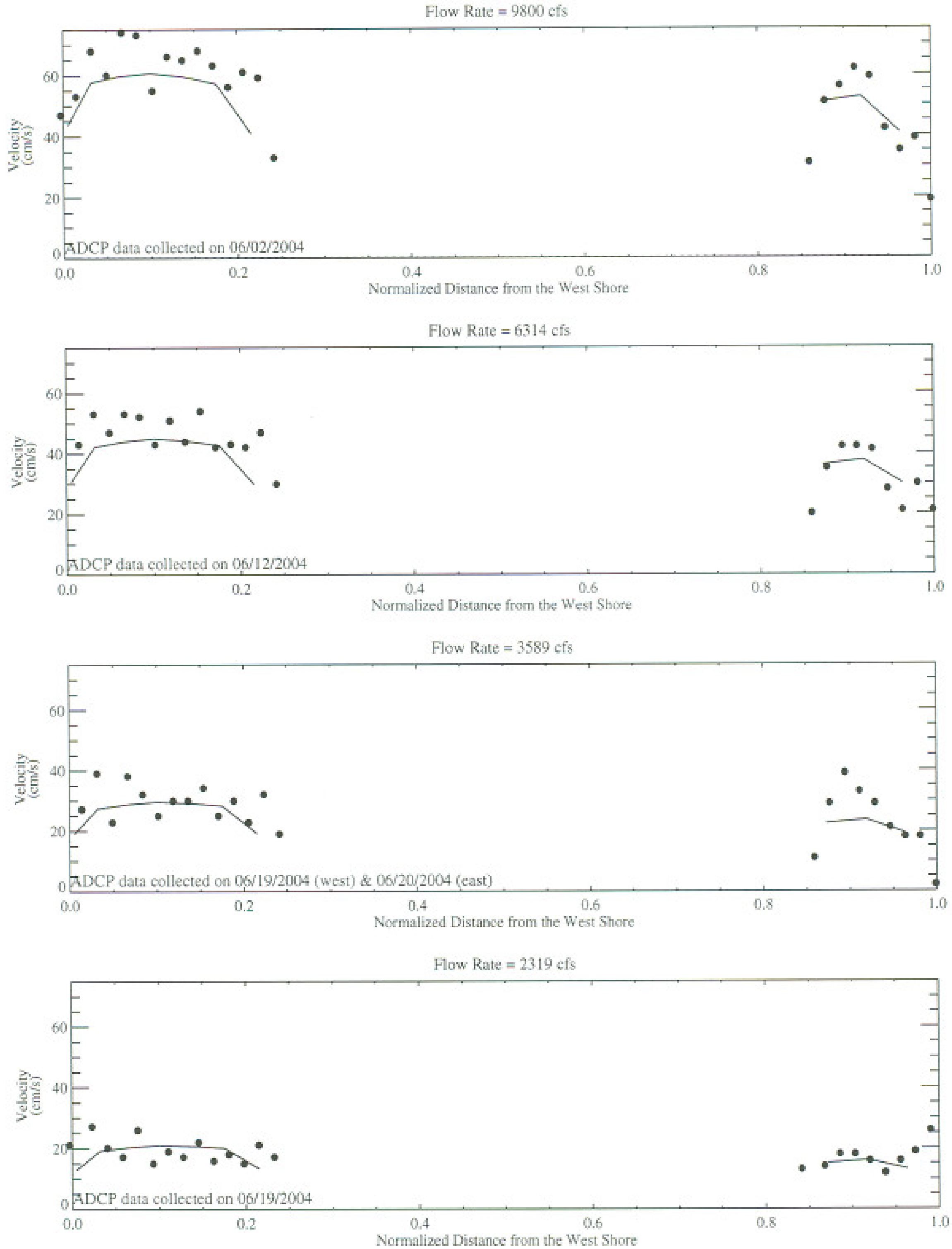

Figure E-3-8. Comparison of predicted and measured current velocity at transect BMP1 during June 2004.

cfo - C:\GENdes\Analysis\Model\plot_vel_adcp.pro
Wed Oct 27 11:07:35 2004

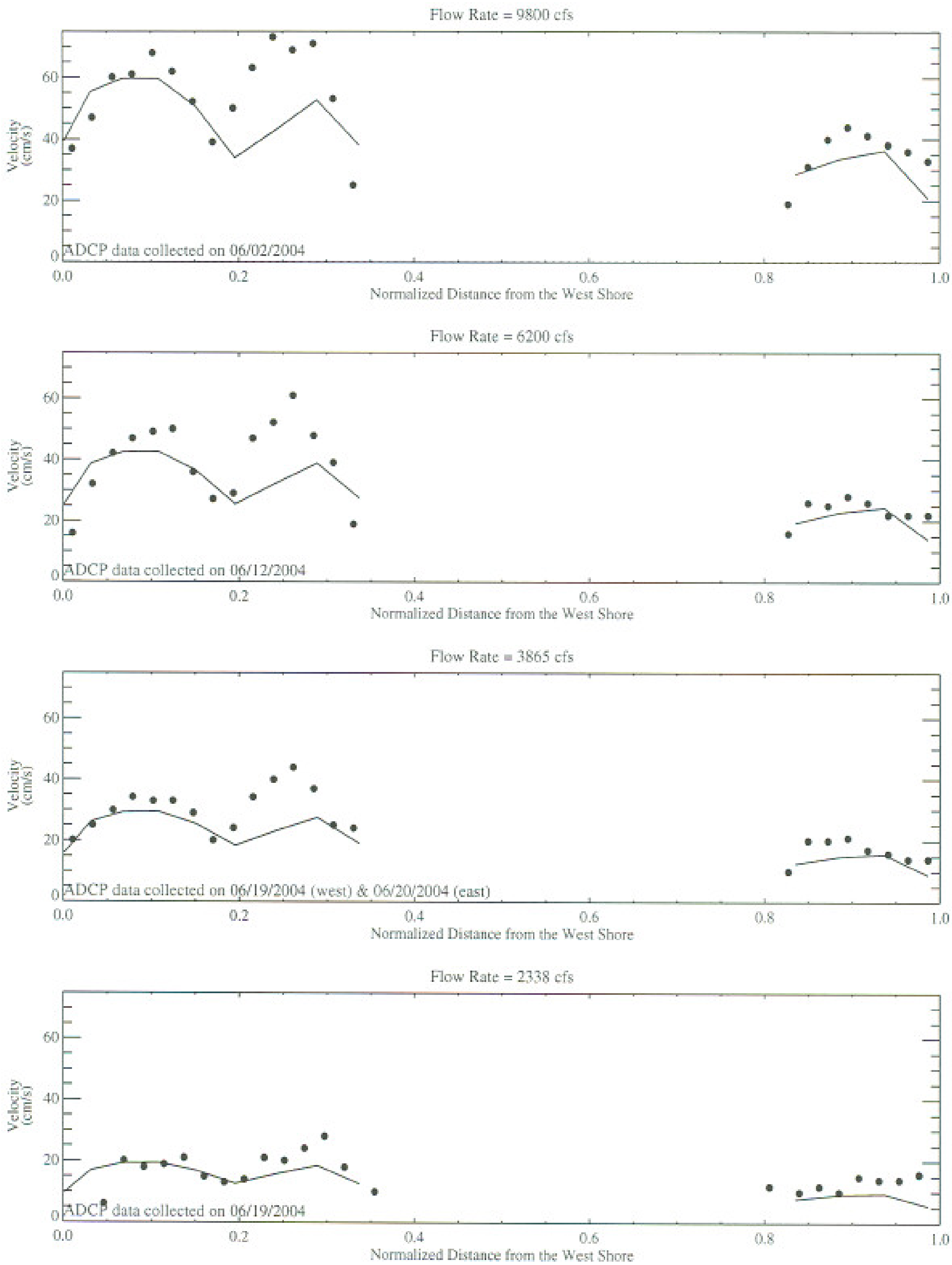

Figure E-3-9. Comparison of predicted and measured current velocity at transect SEDC1 during June 2004.

cfo - C:\GENdes\Analysis\Model\plot_vel_adcp.pro
Wed Oct 27 11:07:35 2004

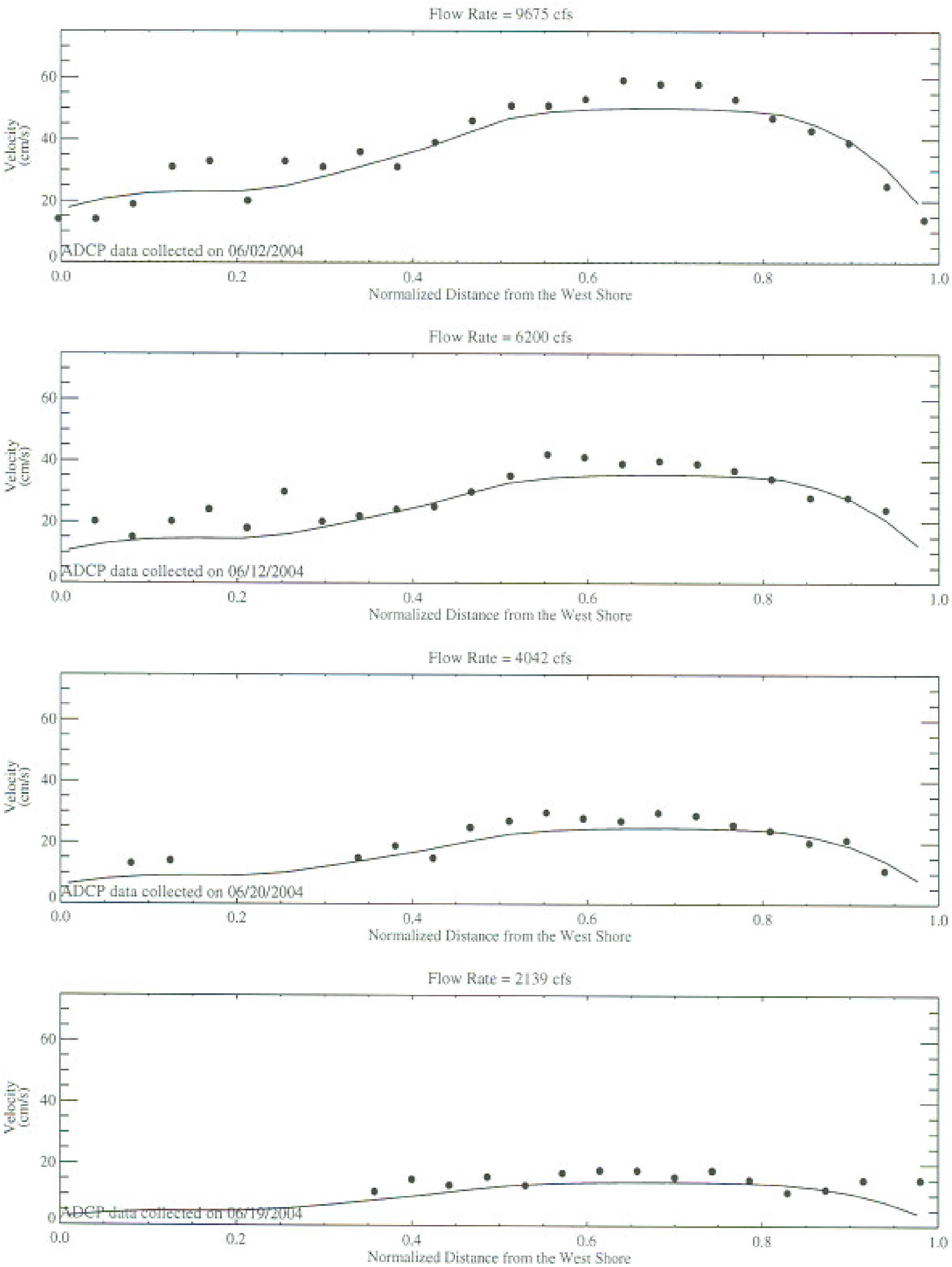

Figure E-3-10. Comparison of predicted and measured current velocity at transect SEDC2 during June 2004.

cfo - C:\GENdes\Analysis\Model\plot_vel_adcp.pro
Wed Oct 27 11:07:35 2004

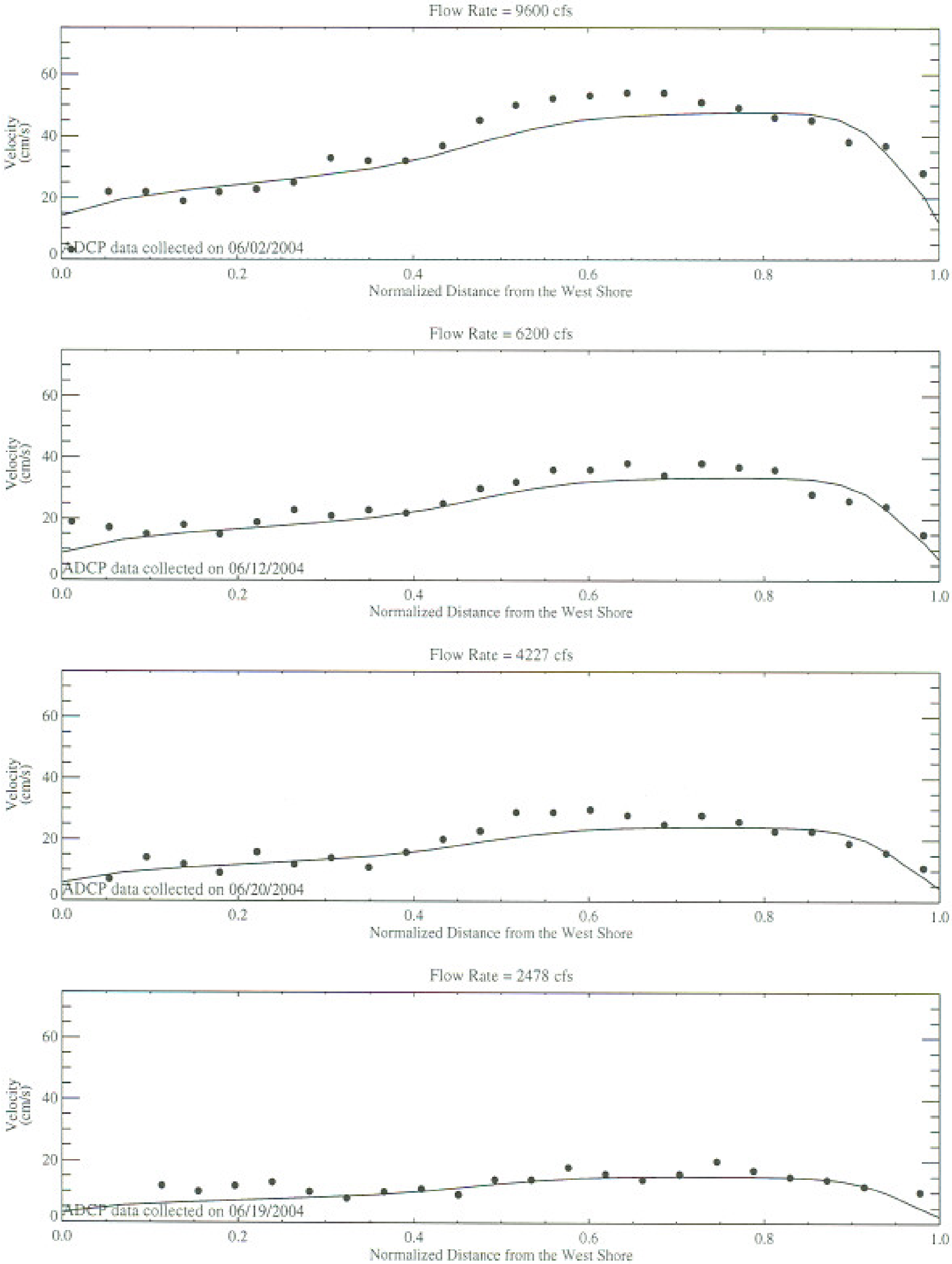

Figure E-3-11. Comparison of predicted and measured current velocity at transect SEDC3 during June 2004.

cfo - C:\GENdes\Analysis\Model\plot_vel_adcp.pro
Wed Oct 27 11:07:35 2004

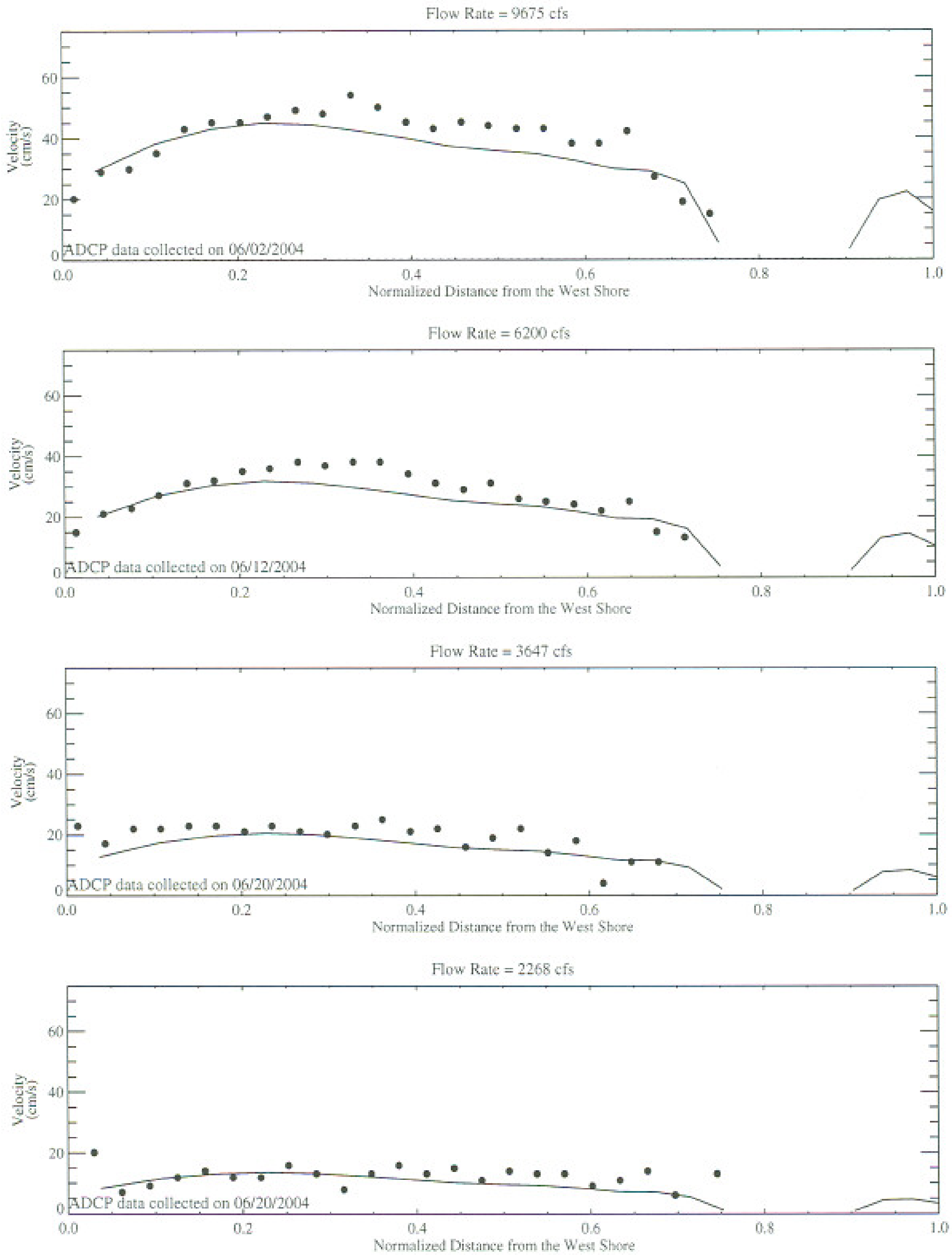

Figure E-3-12. Comparison of predicted and measured current velocity at transect SEDC4 during June 2004.

cfo - C:\GENdes\Analysis\Model\plot_vel_adcp.pro
Wed Oct 27 11:07:35 2004

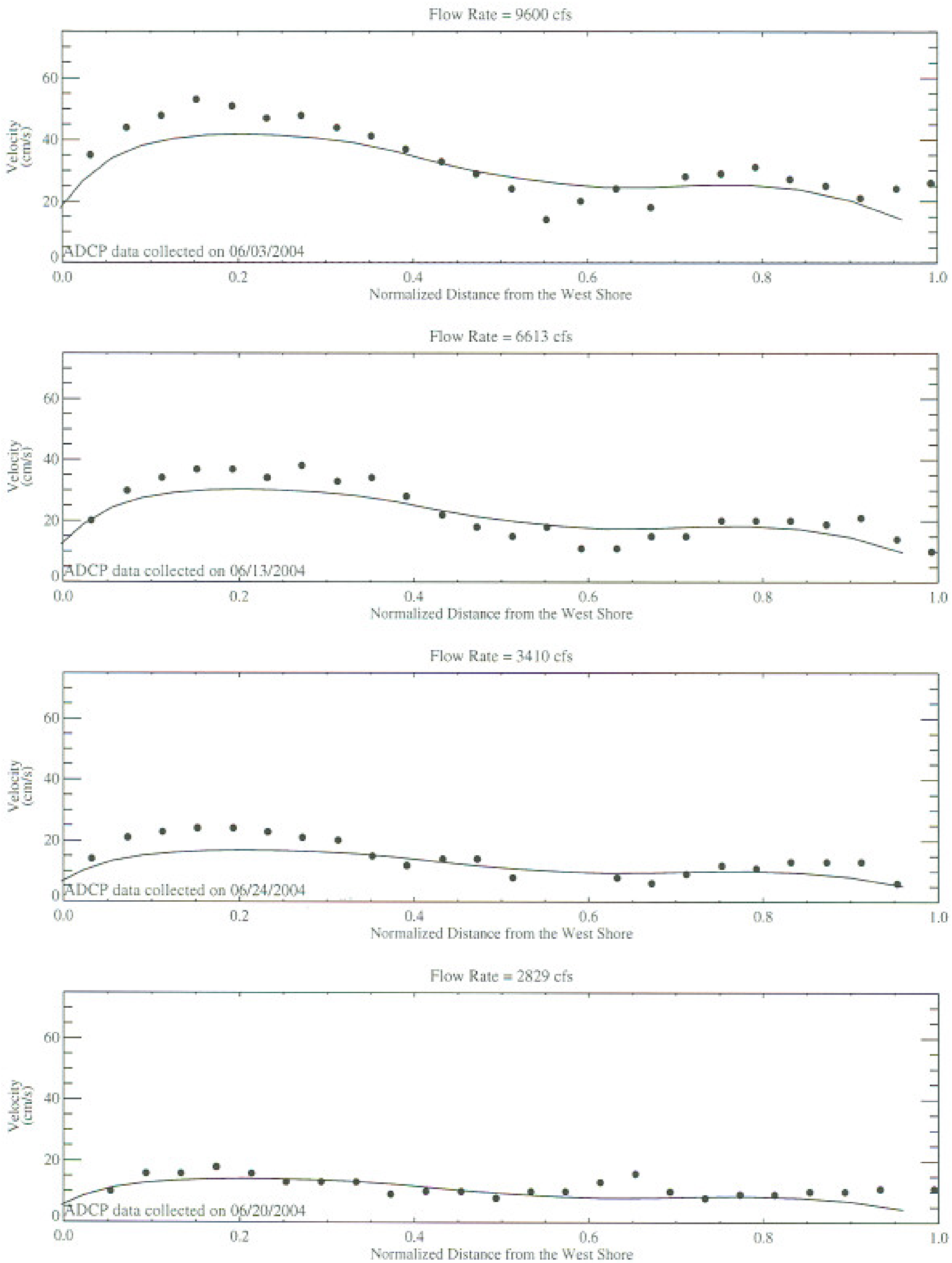

Figure E-3-13. Comparison of predicted and measured current velocity at transect SEDC5 during June 2004.

cfo - C:\GENdes\Analysis\Model\plot_vel_adcp.pro
Wed Oct 27 11:07:36 2004

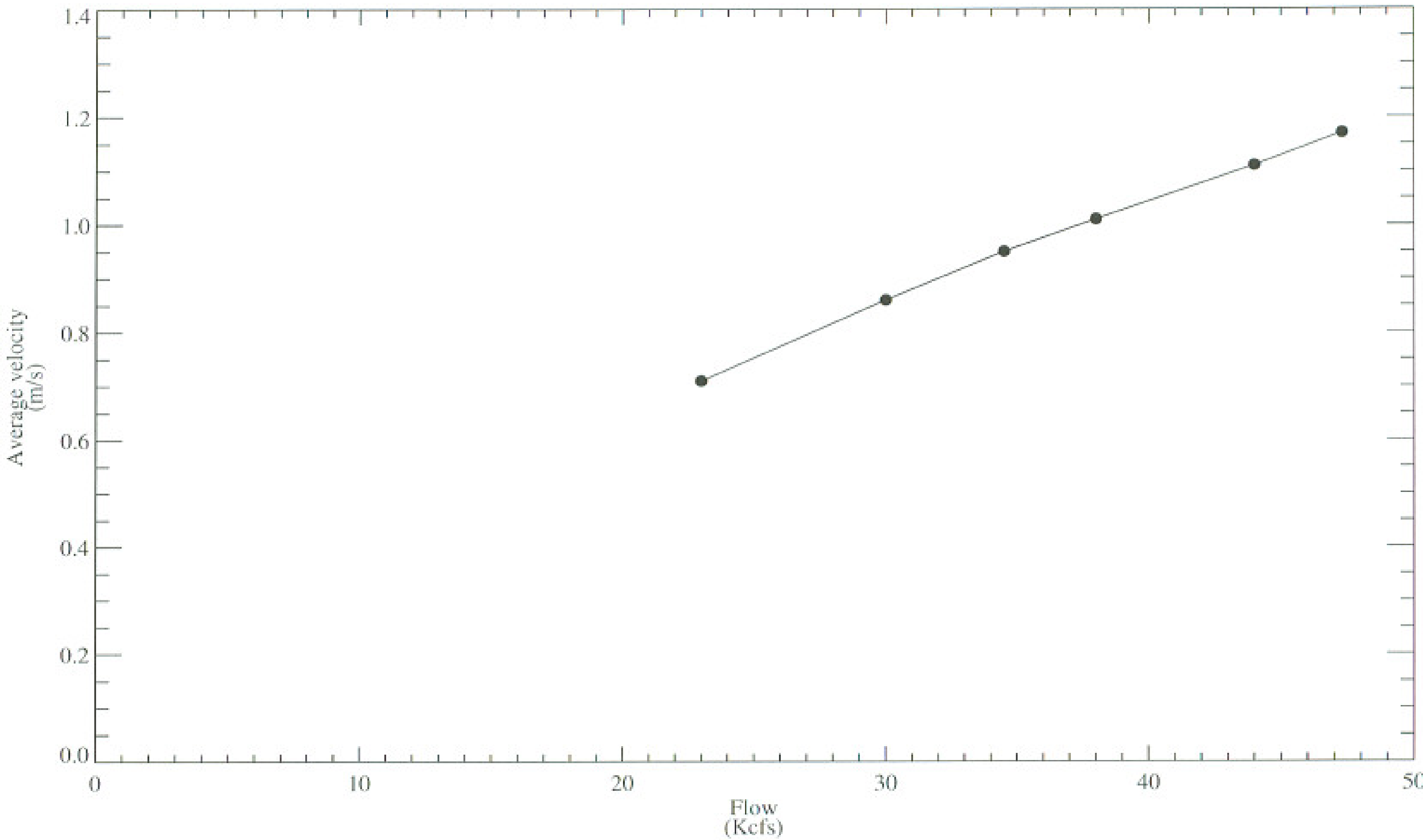

Figure E-3-14. Average current velocity in TIP as a function of flow rate at Fort Edward.

lz - D:\GENdes\Analysis\Model_Outputs\EFDC_Outputs\Get_ave_vel\plot_ave_vel.pro
Wed Aug 17 16:34:14 2005

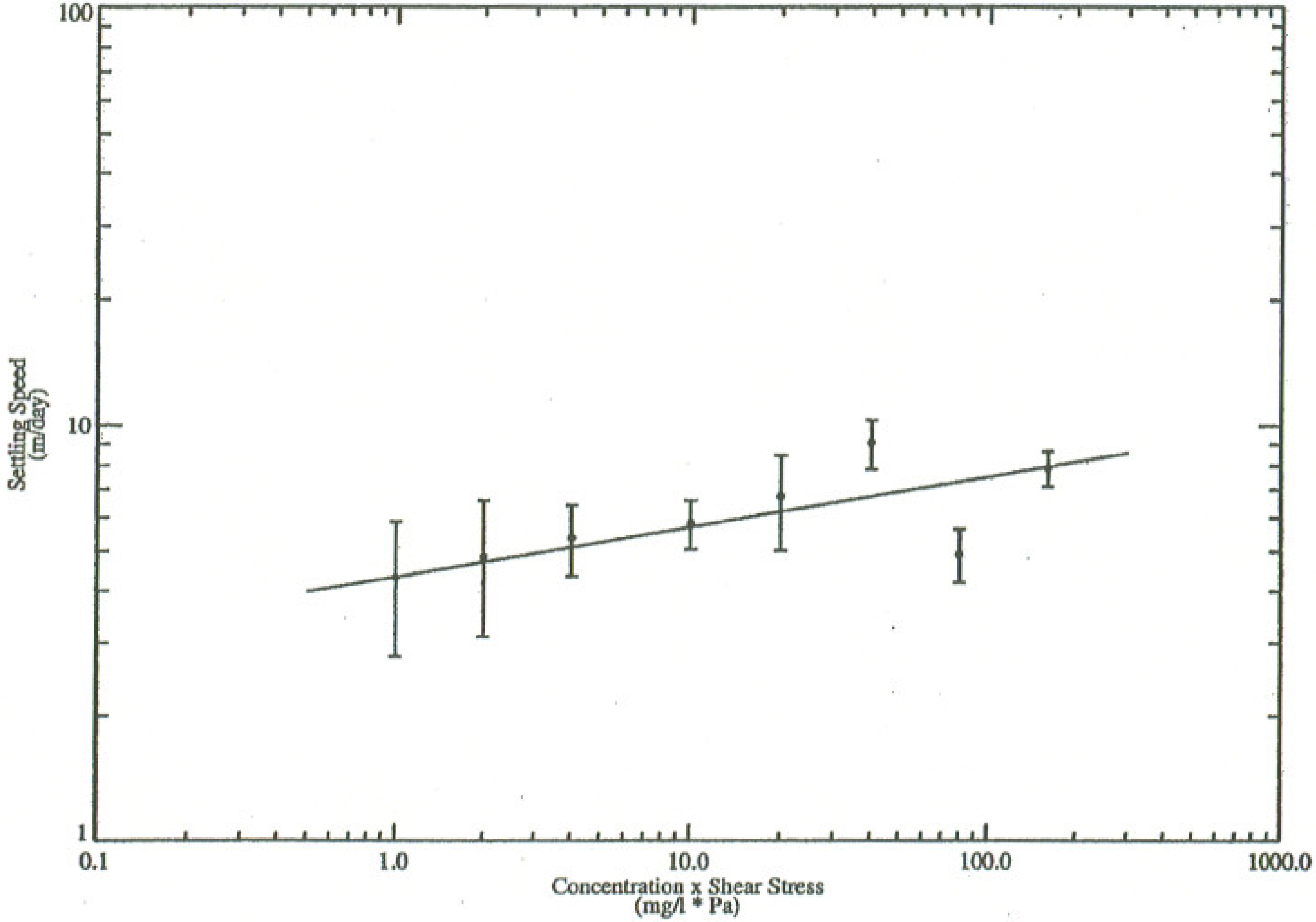

Figure E-4-1. Settling speed of flocculating cohesive (class 1) sediment (solid line) and floc settling speed data (mean + 95% confidence interval, Burban et al. 1990) as a function of sediment concentration and shear stress.

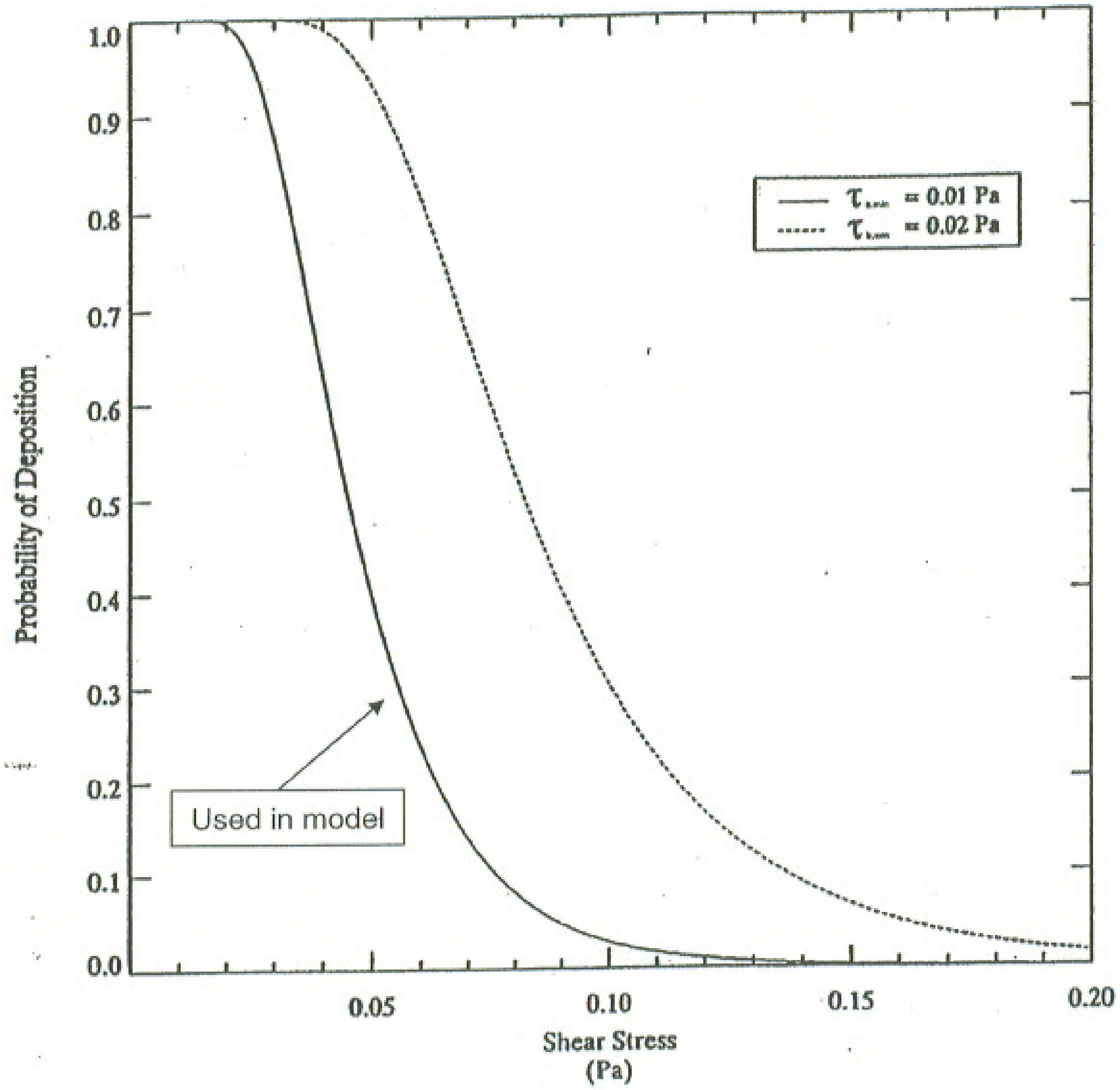

Figure E-4-2. Probability of deposition of cohesive (class 1) sediment as a function of bottom shear stress.

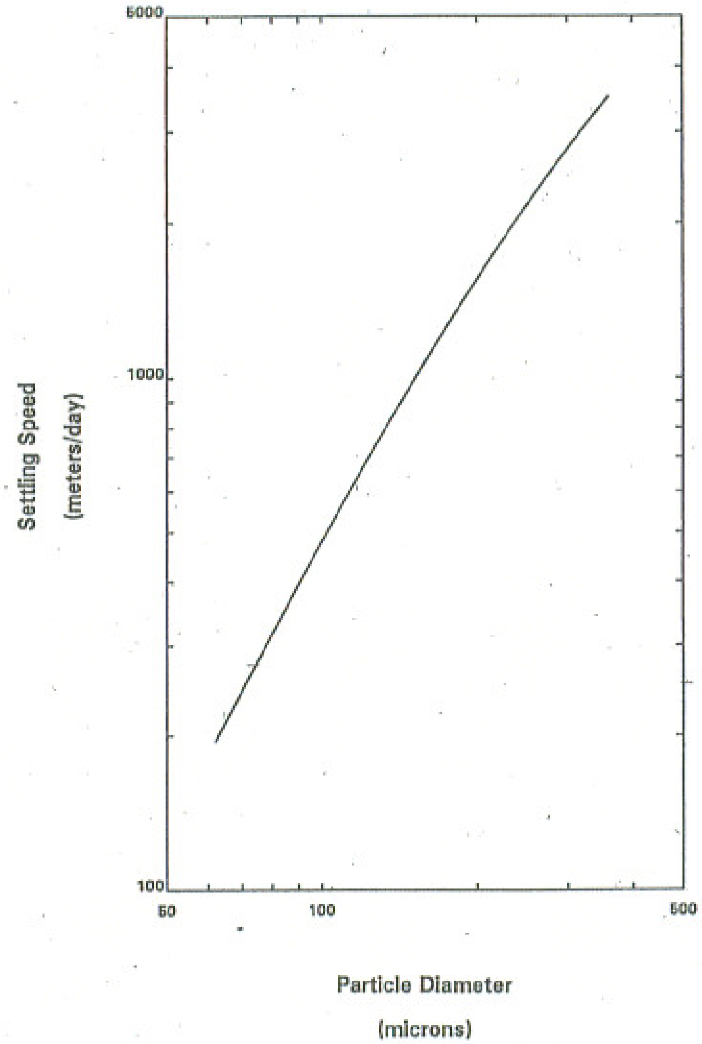

Figure E-4-3. Settling speed of noncohesive (classes 2 and 3) sediment as a function of particle diameter (Cheng 1997).

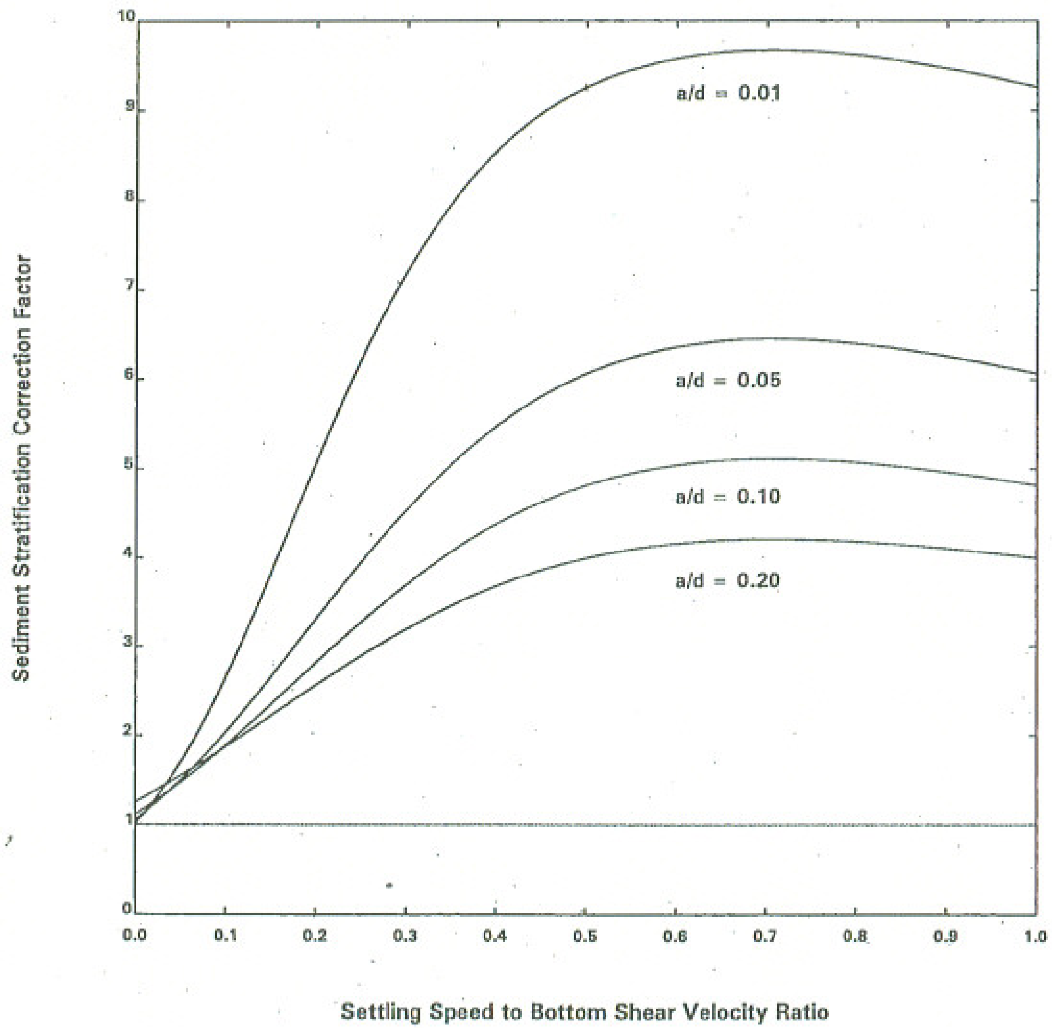

Figure E-4-4. Stratification correction factor (Γ) for noncohesive (classes 2 and 3) sediment as function of W_s/u^* for various reference heights (normalized with respect to water depth).

DN - \\Daleel\D_DRIVE\GENdes\Documents\Reports\IDR\Figure_E-4-1_2_3_4_5.ppt
8/18/2005 10:55 AM

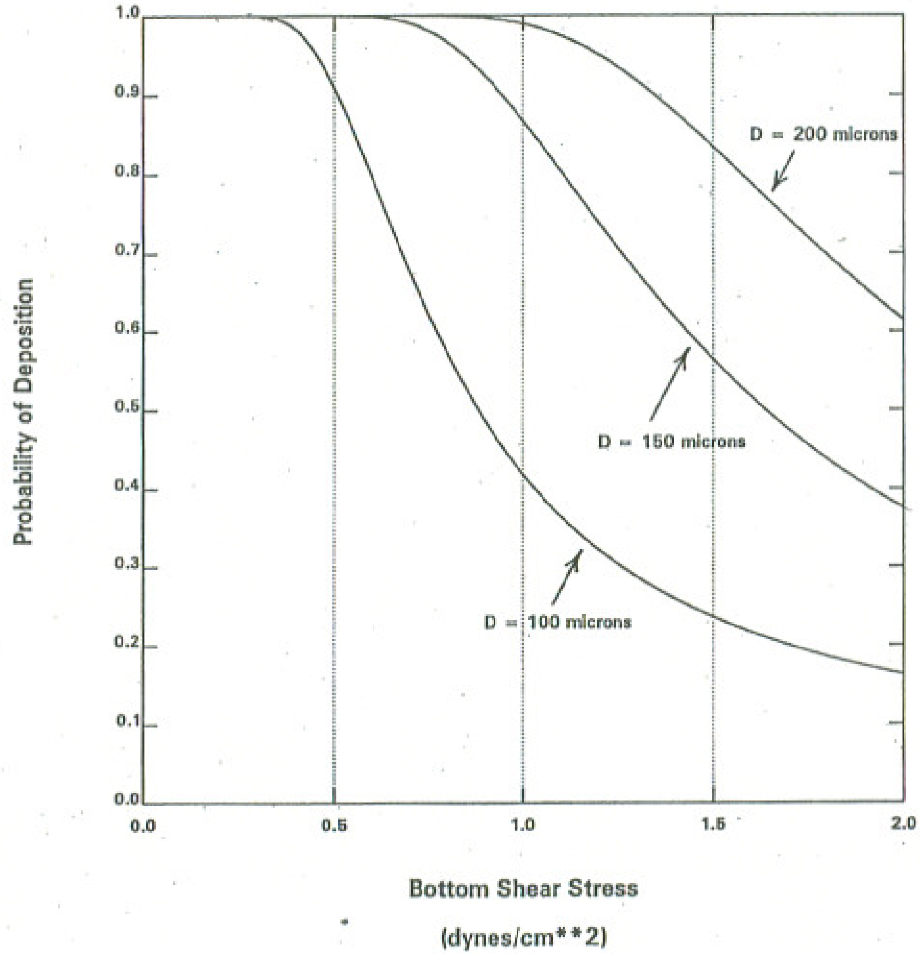

Figure E-4-5. Probability of deposition of noncohesive (classes 2 and 3) sediment as function of bottom shear stress for different particle diameters.

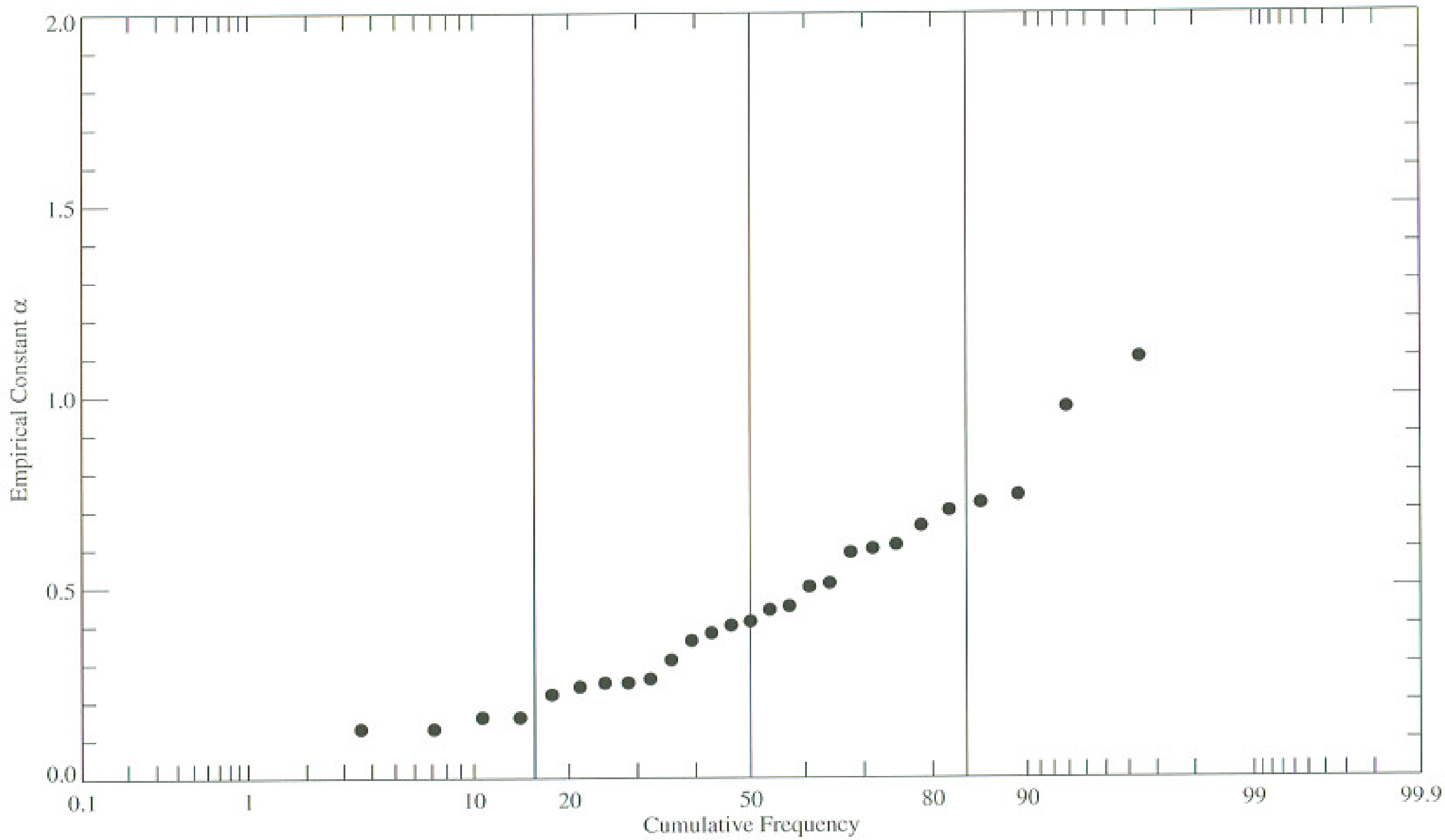

Figure E-4-6. Frequency distribution of empirical constant (α) in lateral dispersion coefficient formulation. Empirical constant values based on data cited in Rutherford (1994).

lz - D:\GENdes\Data\Tran_dispersion_coef\probplot_tran_disp_coef_meander.pro
Wed Aug 17 16:38:56 2005

LOCATOR MAP OF THE UPPER HUDSON RIVER

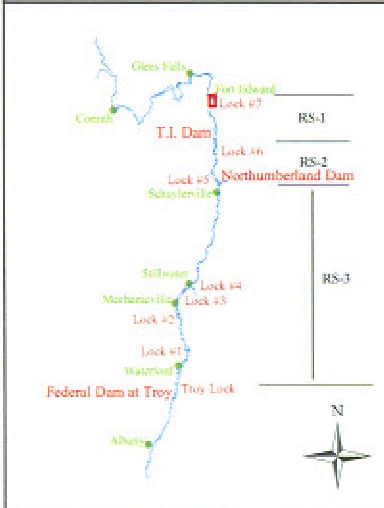

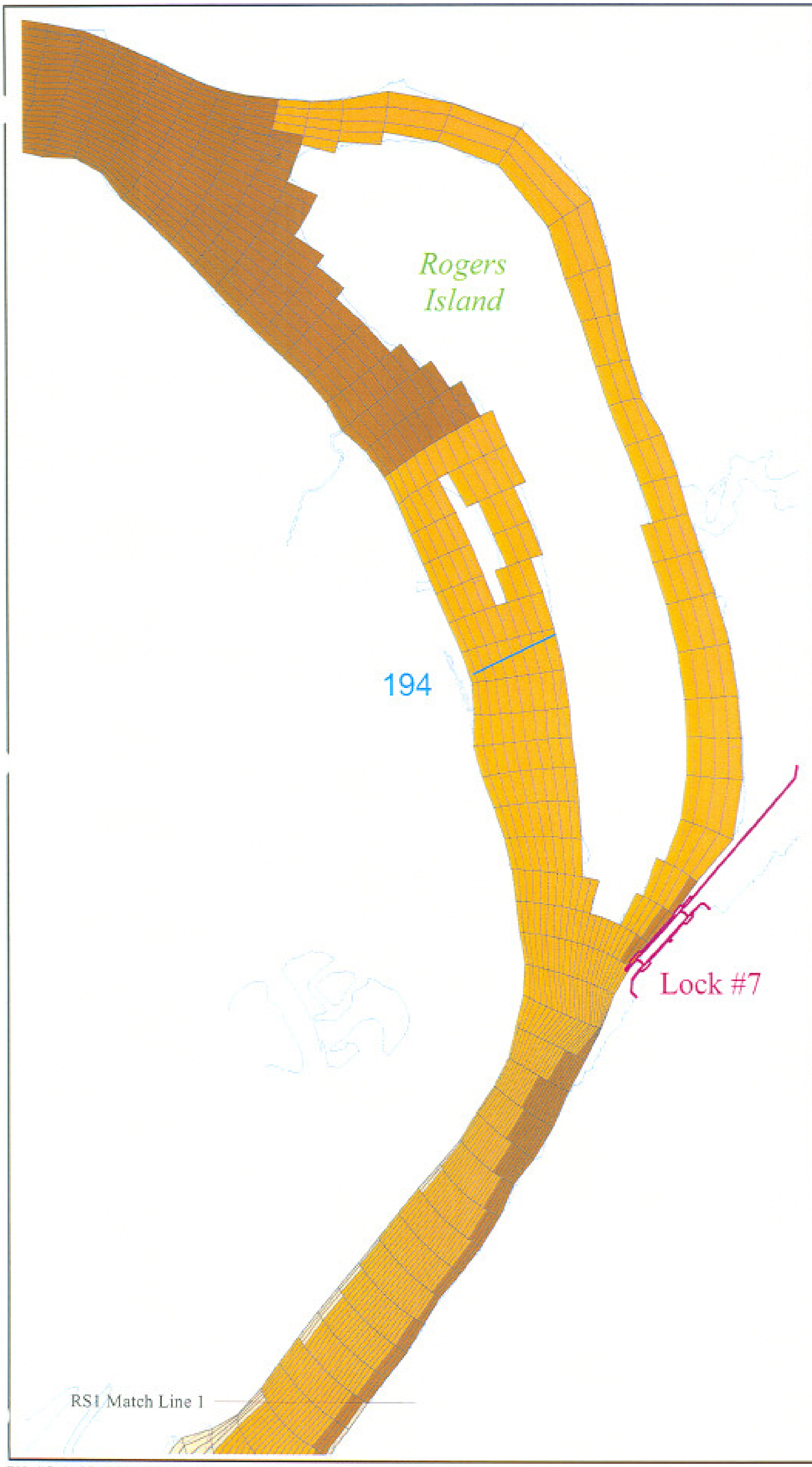

GRAPHIC SCALE

0 250 500 Feet

LEGEND

- River Miles
- Shore Line
- Dams and Locks
- Hard-Bottom
- Cohesive Sediment
- Non-Cohesive Sediment

UPPER HUDSON RIVER STUDY AREA

Figure E-4-7a. Sediment bed map for Thompson Island Pool.

RM193 to RM194

QEA Quantitative Environmental Analysis, LLC

GENdes

Jul 29, 2005.

DN - \\Daleel\D_DRIVE\GENdes\Documents\Reports\IDR\Figure_E-4-7.mxd

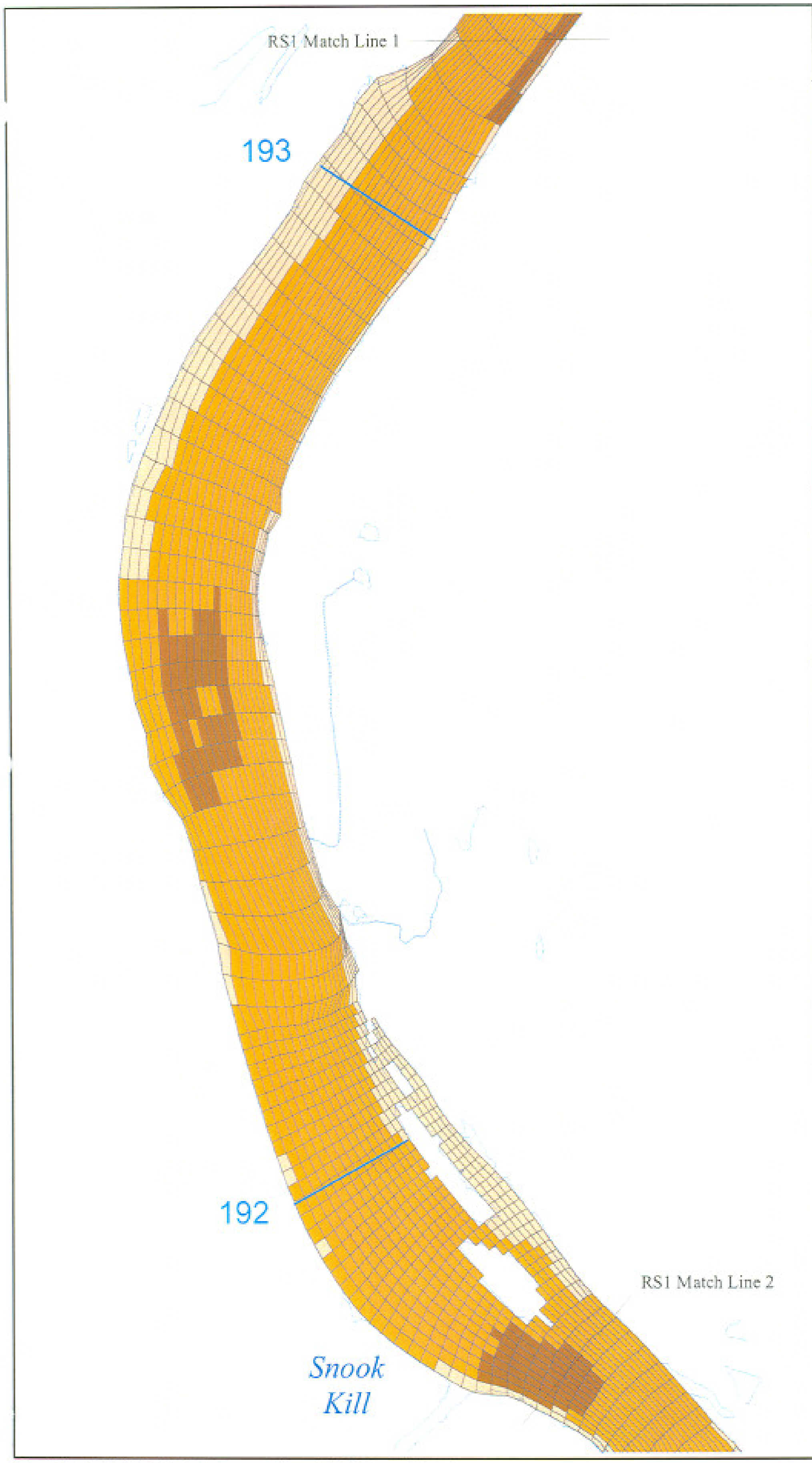

LOCATOR MAP OF THE UPPER HUDSON RIVER

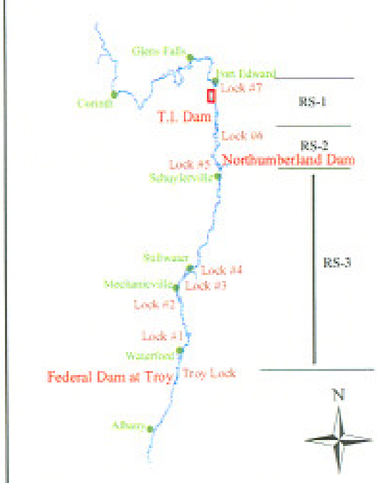

GRAPHIC SCALE

0 250 500 Feet

LEGEND

- River Miles
- Shore Line
- Dams and Locks
- Hard-Bottom
- Cohesive Sediment
- Non-Cohesive Sediment

UPPER HUDSON RIVER STUDY AREA

Figure E-4-7b. Sediment bed map for Thompson Island Pool.

RM191 to RM193

Quantitative Environmental Analysis, LLC

GENdes

Jul 29, 2005.

DN - \\Daleel\D_DRIVE\GENdes\Documents\Reports\IDR\Figure_E-4-7.mxd

LOCATOR MAP OF THE UPPER HUDSON RIVER

GRAPHIC SCALE

0 250 500 Feet

LEGEND

- River Miles
- Shore Line
- Dams and Locks
- Hard-Bottom
- Cohesive Sediment
- Non-Cohesive Sediment

UPPER HUDSON RIVER STUDY AREA

Figure E-4-7c.
Sediment bed map for Thompson Island Pool.

RM190 to RM191

QEA Quantitative Environmental Analysis, LLC

GENdes

Jul 29, 2005.

DN - \\Daleel\D_DRIVE\GENdes\Documents\Reports\IDR\Figure_E-4-7.mxd

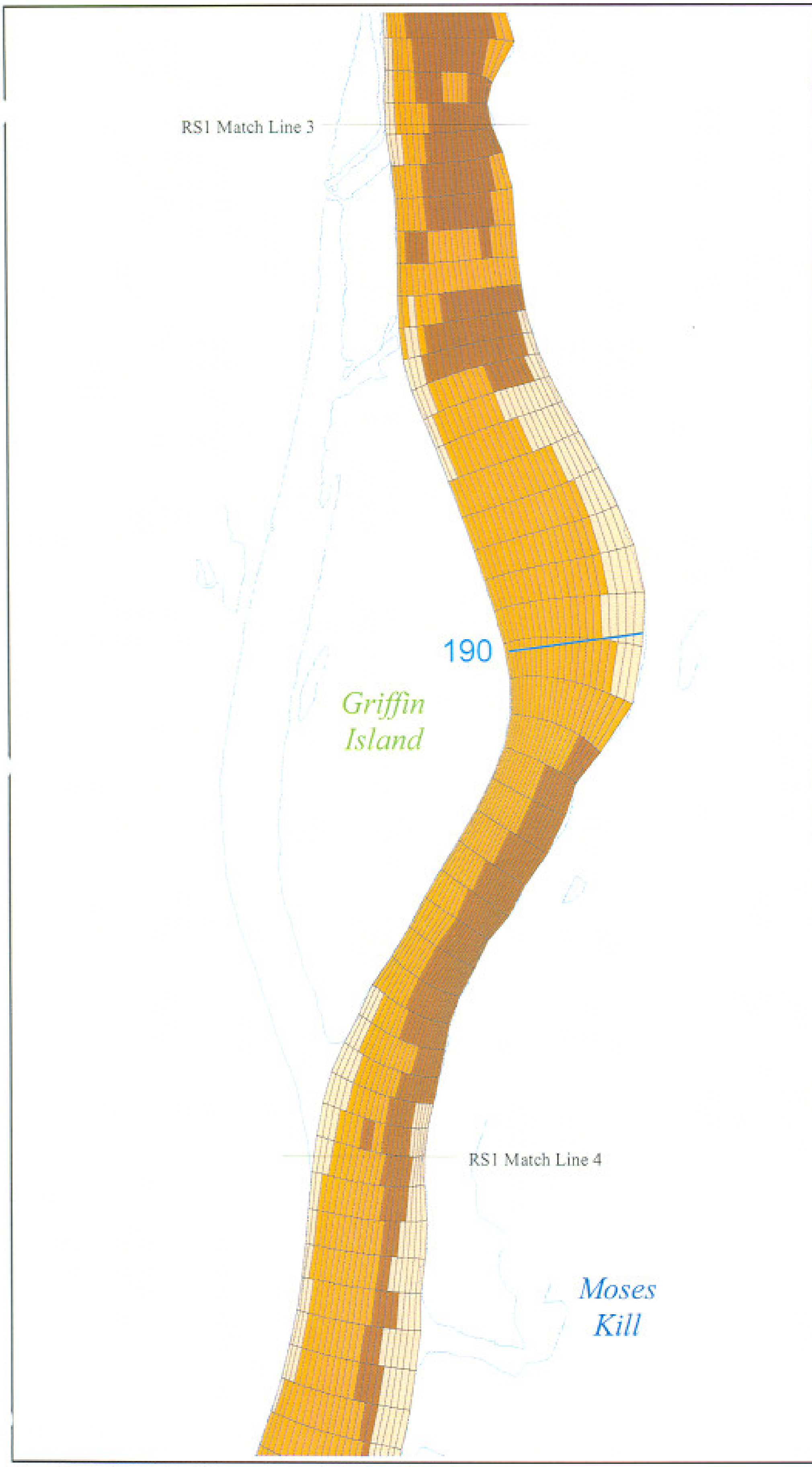

LOCATOR MAP OF THE UPPER HUDSON RIVER

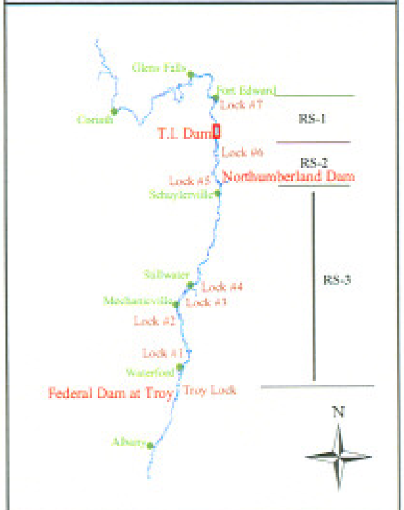

GRAPHIC SCALE

0 250 500 Feet

LEGEND

- River Miles
- Shore Line
- Dams and Locks
- Hard-Bottom
- Cohesive Sediment
- Non-Cohesive Sediment

UPPER HUDSON RIVER STUDY AREA

Figure E-4-7d. Sediment bed map for Thompson Island Pool.

RM189 to RM190

QEA Quantitative Environmental Analysis, LLC

GENdes

Jul 29, 2005.

DN - \\Daleel\D_DRIVE\GENdes\Documents\Reports\IDR\Figure_E-4-7.mxd

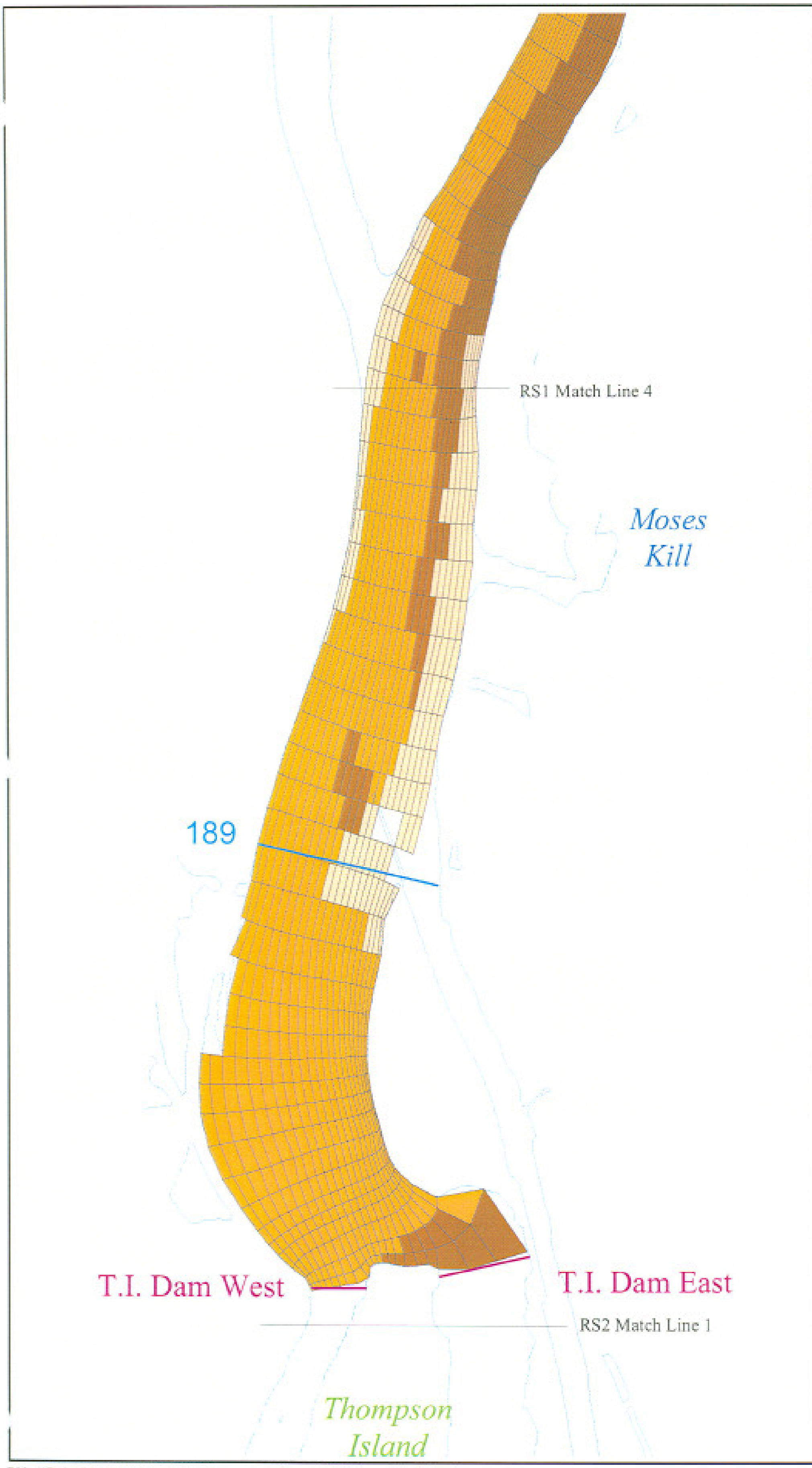

LOCATOR MAP OF THE UPPER HUDSON RIVER

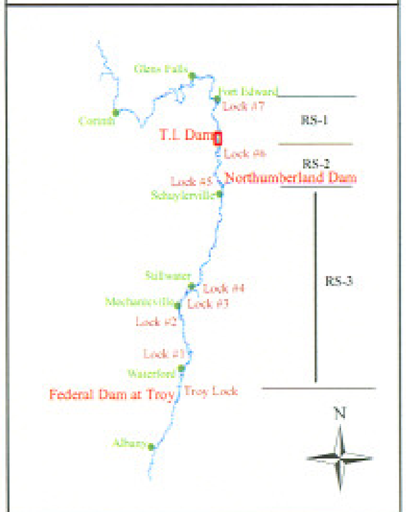

GRAPHIC SCALE

0 250 500 Feet

LEGEND

- River Miles
- Shore Line
- Dams and Locks
- Hard-Bottom
- Cohesive Sediment
- Non-Cohesive Sediment

UPPER HUDSON RIVER STUDY AREA

Figure E-4-7e. Sediment bed map for Thompson Island Pool.

RM188 to RM189

QEA Quantitative Environmental Analysis, LLC

GENdes

Jul 29, 2005.

DN - \\Daleel\D_DRIVE\GENdes\Documents\Reports\IDR\Figure_E-4-7.mxd

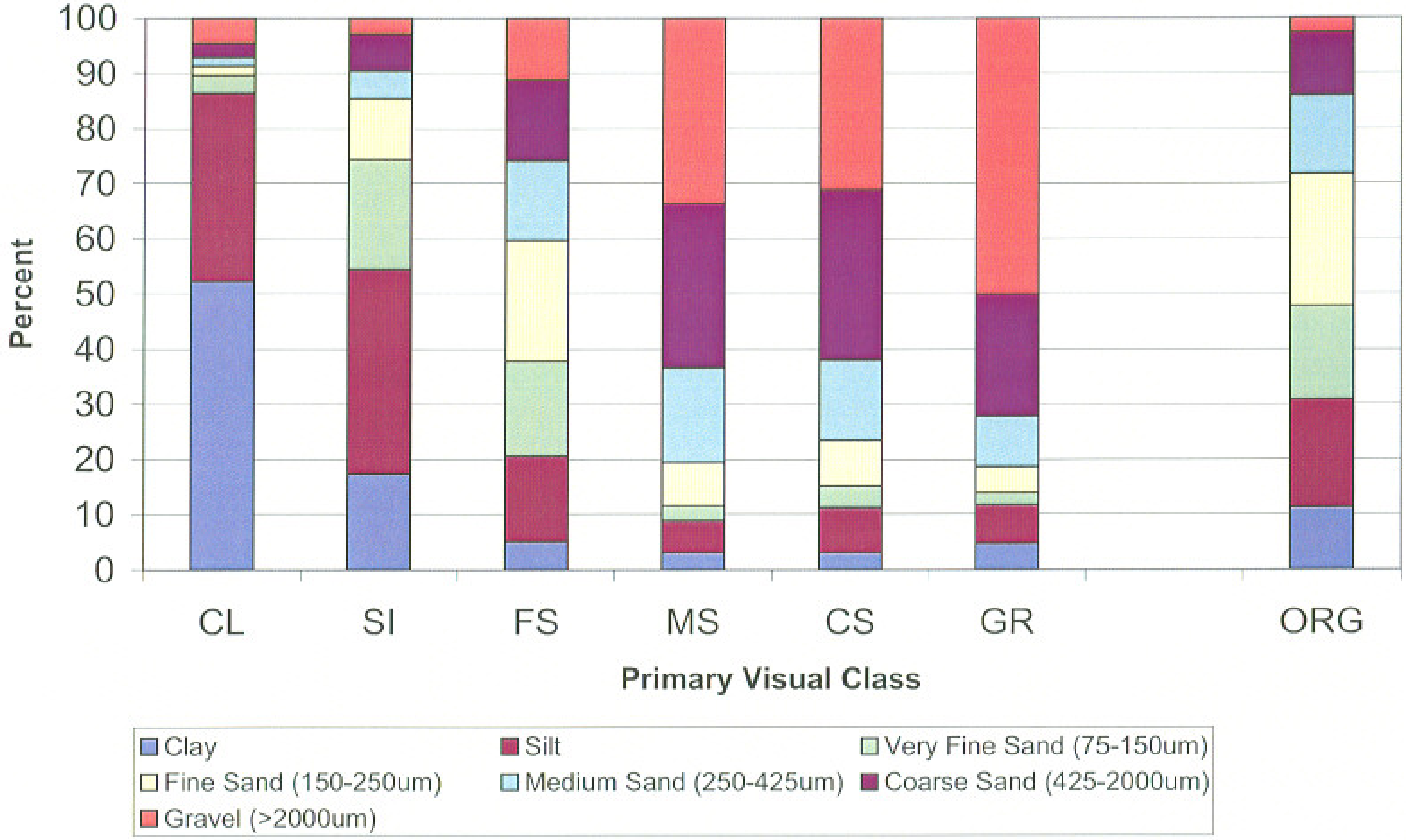

Figure E-4-8. Average Grainsize Composition of SSAP Primary Visual Classes

\\dalee\\d_drive\\GENdes\\Documents\\Reports\\IDR\\Figure_E-4-8_Phase1_GS_VIS_Results_050505.xls

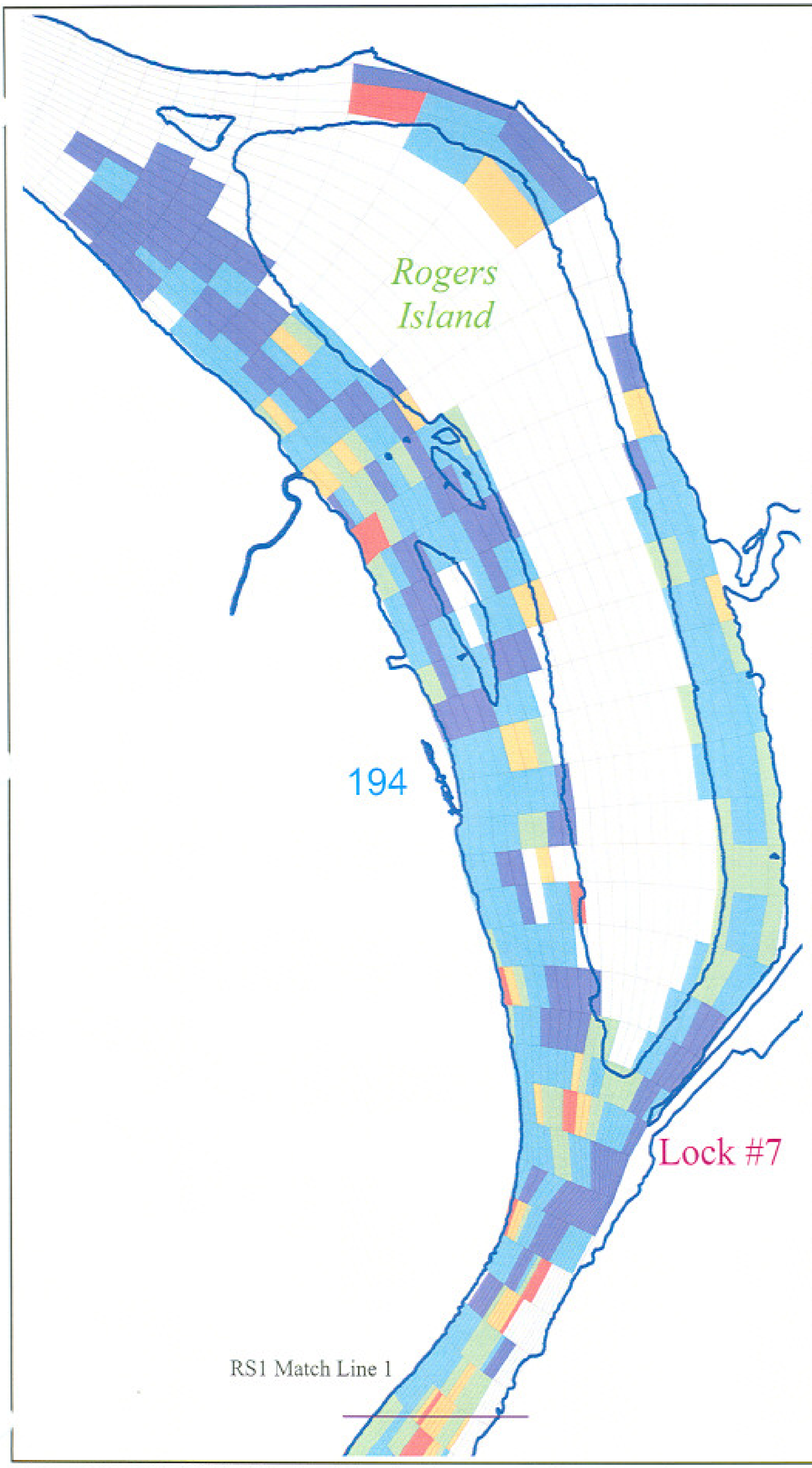

LOCATOR MAP OF THE UPPER HUDSON RIVER

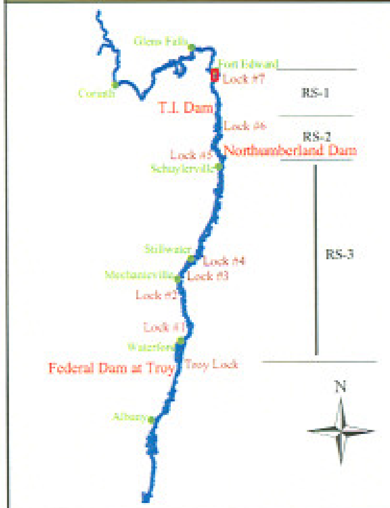

GRAPHIC SCALE

0 250 500 Feet

LEGEND

Percent Clay and Silt

- 0 - 15
- 15 - 30
- 30 - 45
- 45 - 60
- > 60
- Shoreline
- Model Grid

Figure E-4-9a.

Percent Clay and Silt in Total Sediment Bed by Model Grid Cell.

QEA Quantitative Environmental Analysis, LLC

GENdes: 232

Aug 17, 2005.

MS - \\Zeus\E_Drive\GENrem\Working\GIS\maps\ArcGIS8_maps\model\maps\resuspension\PCB_Frac_Map.mxd

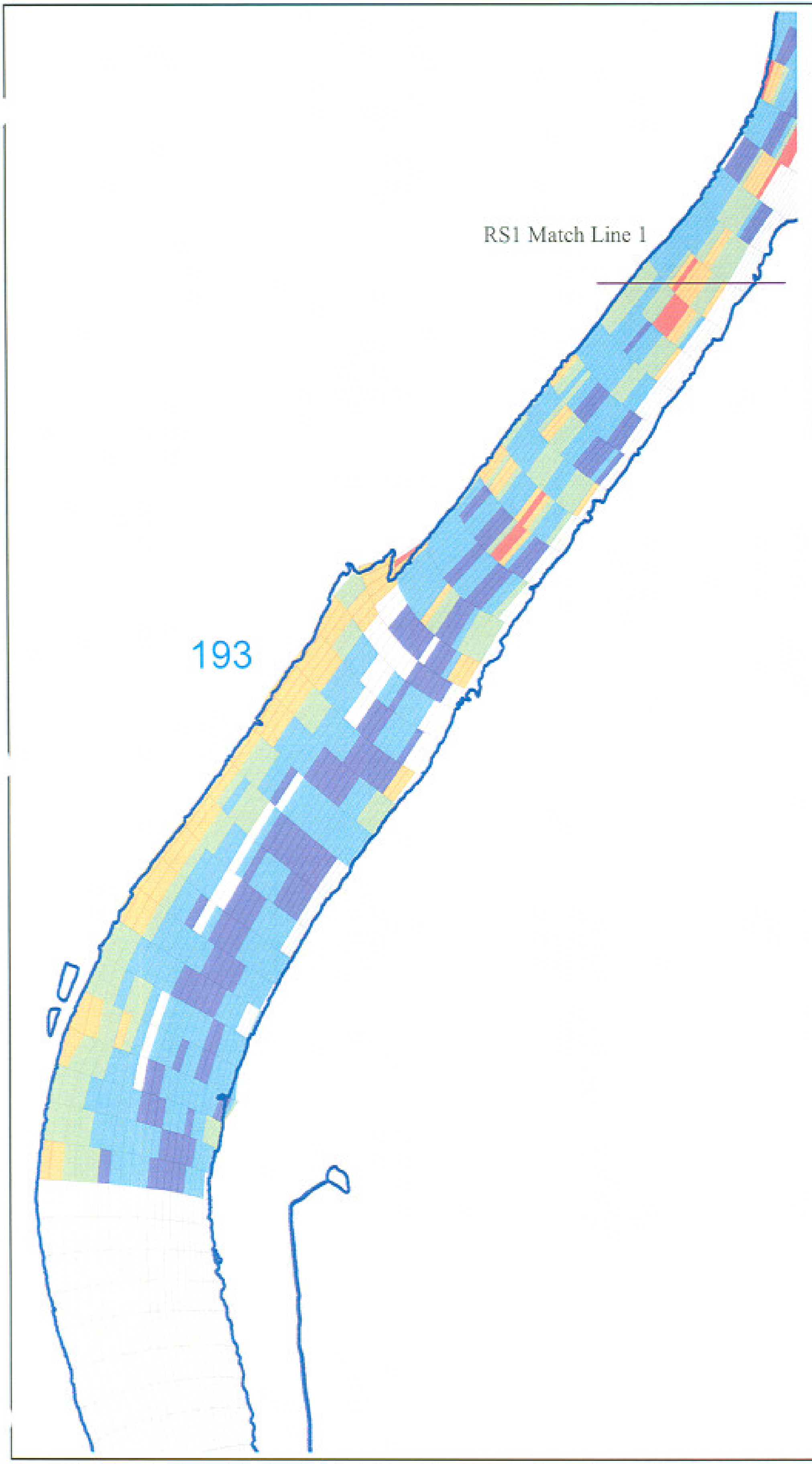

LOCATOR MAP OF THE UPPER HUDSON RIVER

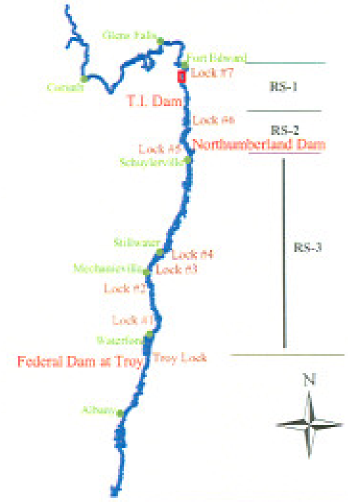

GRAPHIC SCALE

0 250 500Feet

LEGEND

Percent Clay and Silt

- 0 - 15
- 15 - 30
- 30 - 45
- 45 - 60
- > 60
- Shoreline
- Model Grid

Figure E-4-9b.

Percent Clay and Silt in Total Sediment Bed by Model Grid Cell.

QEA Quantitative Environmental Analysis, LLC

GENdes: 232

Aug 17, 2005.

MS - \\Zeus\E_Drive\GENrem\Working\GIS\maps\ArcGIS8_maps\model\maps\resuspension\PCB_Frac_Map.mxd

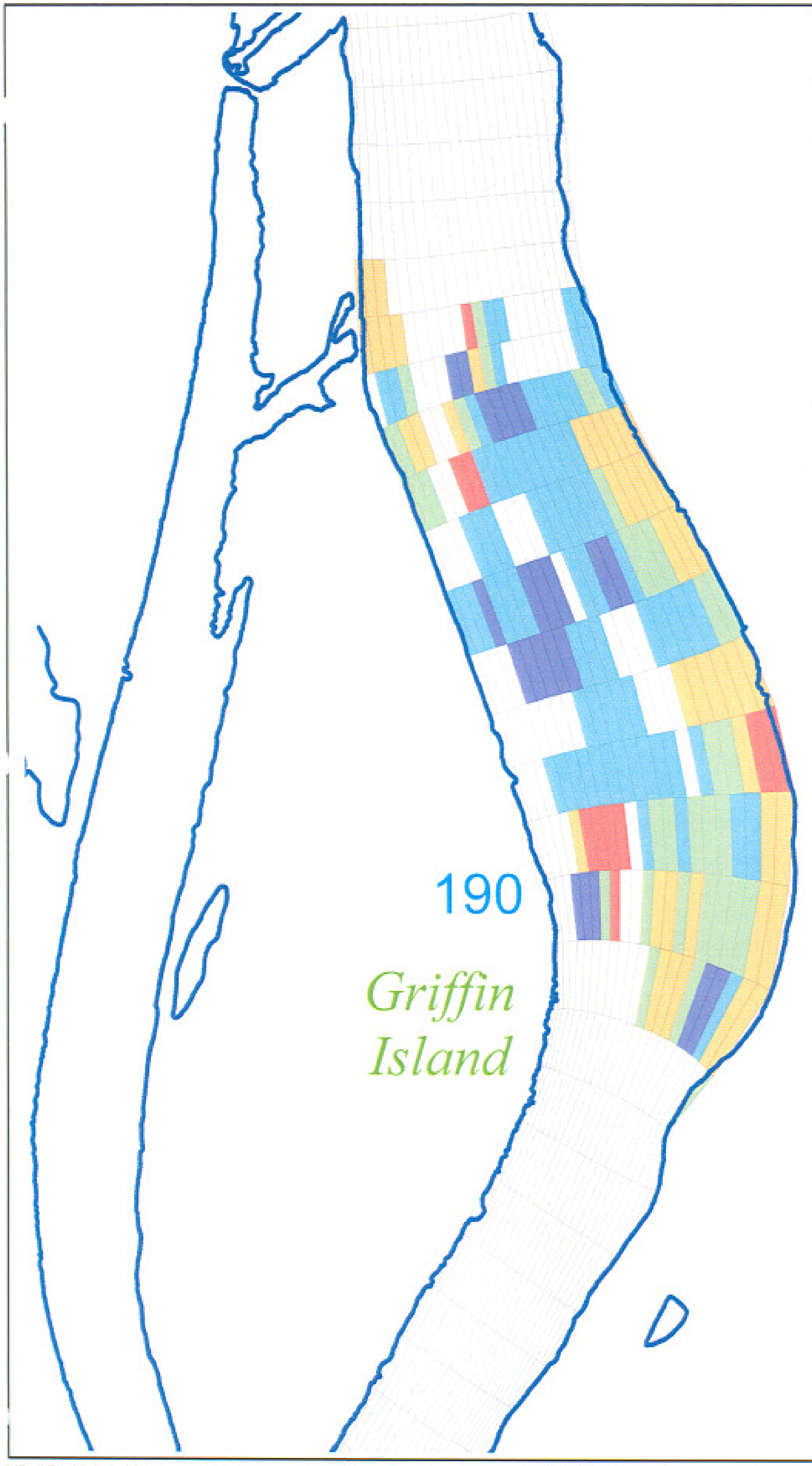

LOCATOR MAP OF THE UPPER HUDSON RIVER

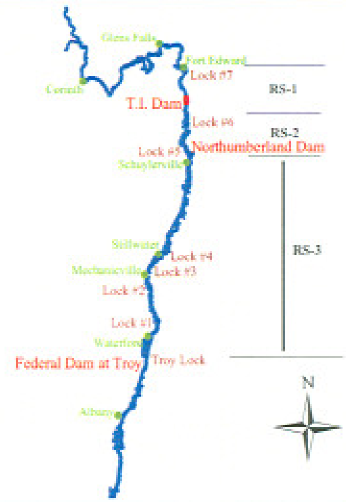

GRAPHIC SCALE

0 250 500 Feet

LEGEND

Percent Clay and Silt

- 0 - 15
- 15 - 30
- 30 - 45
- 45 - 60
- > 60
- Shoreline
- Model Grid

Figure E-4-9c.

Percent Clay and Silt in Total Sediment Bed by Model Grid Cell.

QEA Quantitative Environmental Analysis, LLC

GENdes: 232

Aug 17, 2005.

MS - \\Zeus\E_Drive\GENrem\Working\GIS\maps\ArcGIS8_maps\model\maps\resuspension\PCB_Frac_Map.mxd

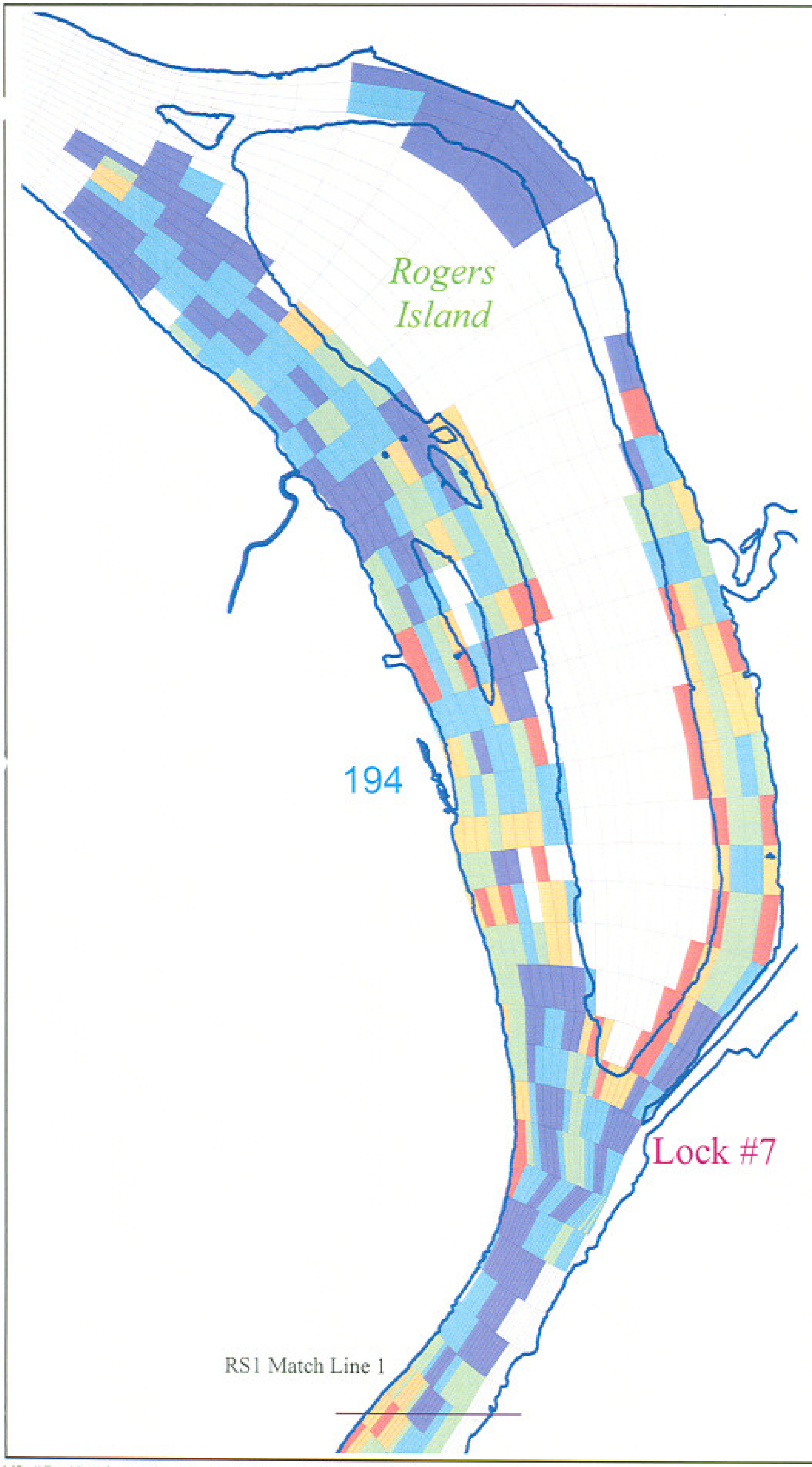

LOCATOR MAP OF THE UPPER HUDSON RIVER

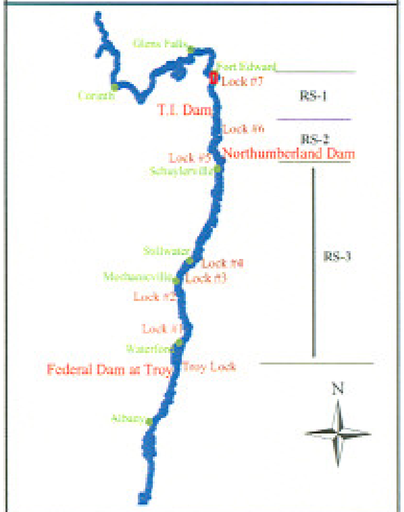

GRAPHIC SCALE

0 250 500 Feet

LEGEND

Percent Very Fine Sand

- 0 - 4
- 4 - 8
- 8 - 12
- 12 - 16
- 16 - 20
- Shoreline
- Model Grid

Figure E-4-10a.

Percent Very Fine Sand in Total Sediment Bed by Model Grid Cell.

QEA Quantitative Environmental Analysis, LLC

GENdes: 232 Aug 17, 2005.

MS - \\Zeus\E_Drive\GENrem\Working\GIS\maps\ArcGIS8_maps\model\maps\resuspension\PCB_Frac_Map.mxd

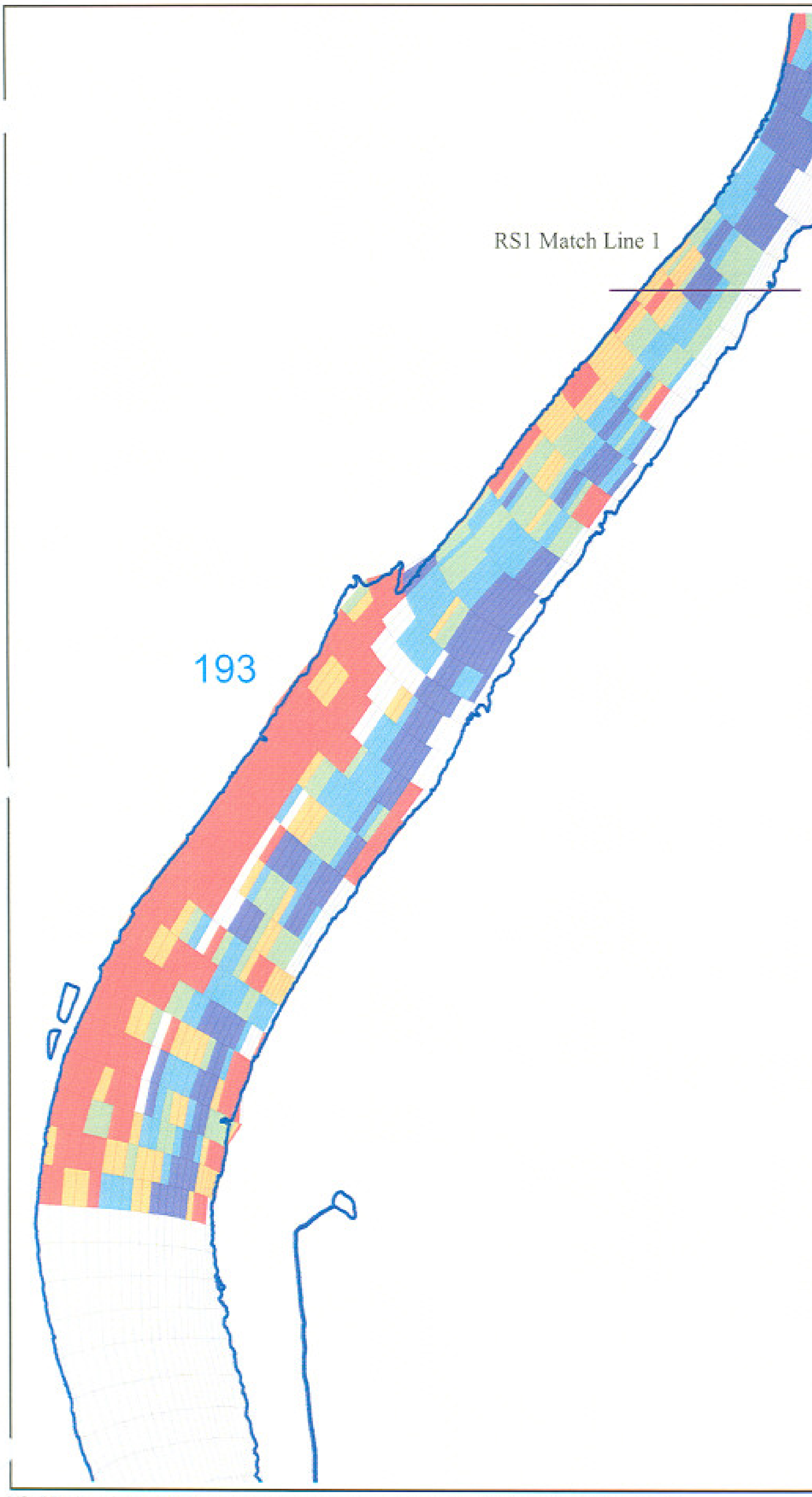

LOCATOR MAP OF THE UPPER HUDSON RIVER

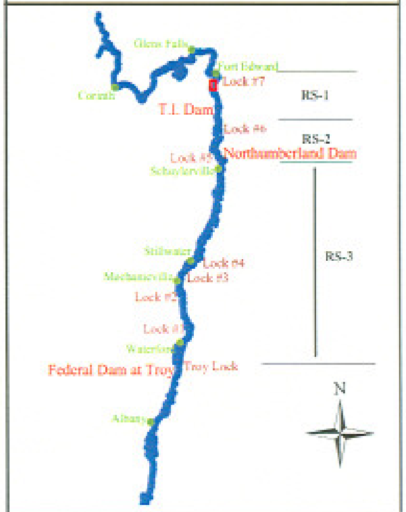

GRAPHIC SCALE

0 250 500 Feet

LEGEND

Percent Very Fine Sand

- 0 - 4
- 4 - 8
- 8 - 12
- 12 - 16
- 16 - 20
- Shoreline
- Model Grid

Figure E-4-10b.

Percent Very Fine Sand in Total Sediment Bed by Model Grid Cell.

QEA Quantitative Environmental Analysis, LLC

GENdes: 232

Aug 17, 2005.

MS - \\Zeus\E_Drive\GENrem\Working\GIS\maps\ArcGIS8_maps\model\maps\resuspension\PCB_Frac_Map.mxd

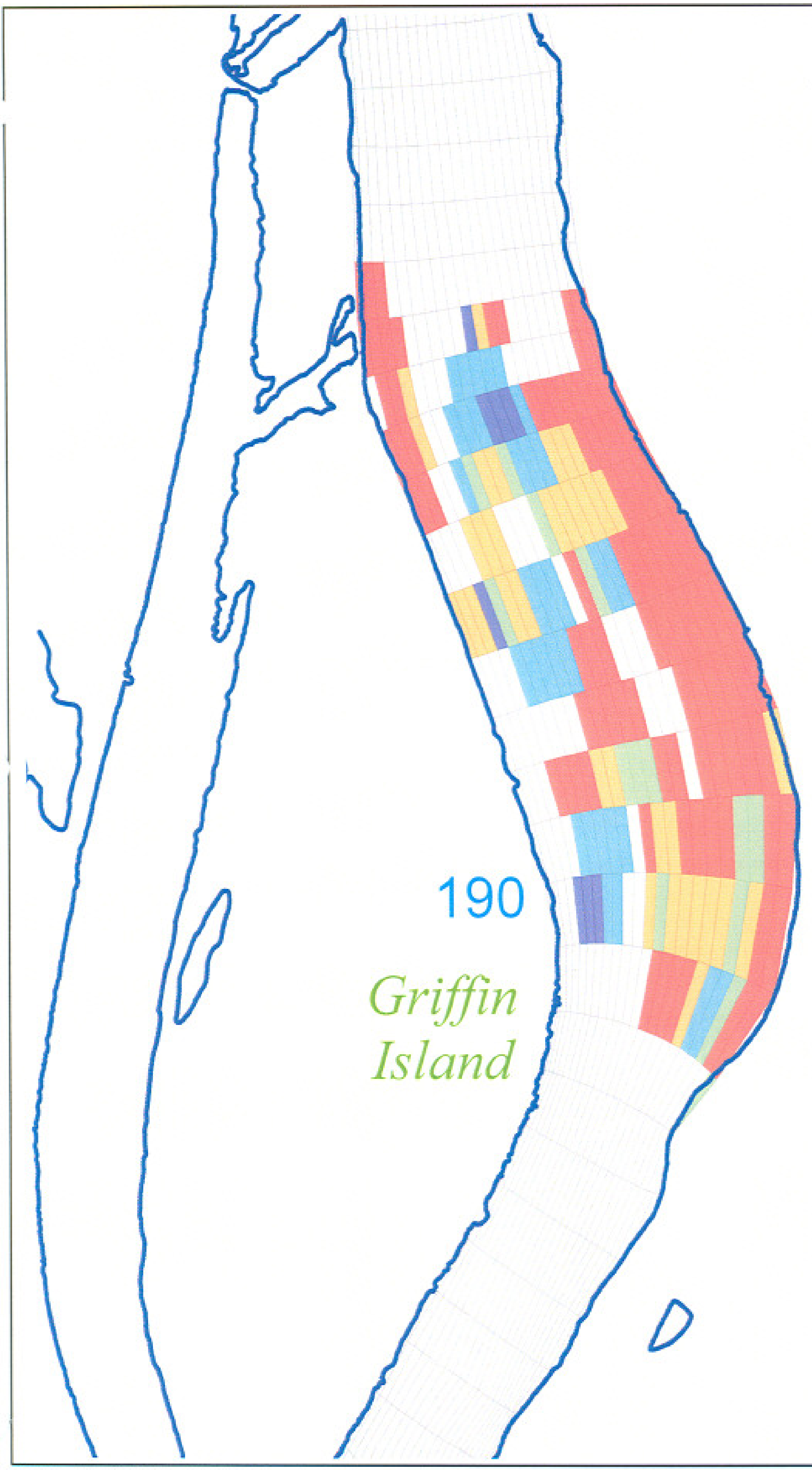

LOCATOR MAP OF THE UPPER HUDSON RIVER

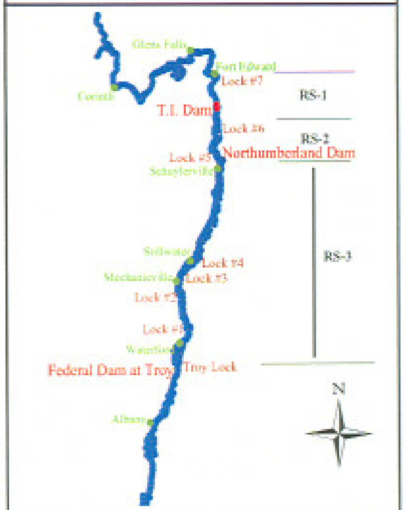

GRAPHIC SCALE

0 250 500 Feet

LEGEND

Percent Very Fine Sand

- 0 - 4
- 4 - 8
- 8 - 12
- 12 - 16
- 16 - 20
- Shoreline
- Model Grid

Figure E-4-10c.

Percent Very Fine Sand in Total Sediment Bed by Model Grid Cell.

Quantitative Environmental Analysis, LLC

GENdes: 232 Aug 17, 2005.

MS - \\Zeus\E_Drive\GENrem\Working\GIS\maps\ArcGIS8_maps\model\maps\resuspension\PCB_Frac_Map.mxd

LOCATOR MAP OF THE UPPER HUDSON RIVER

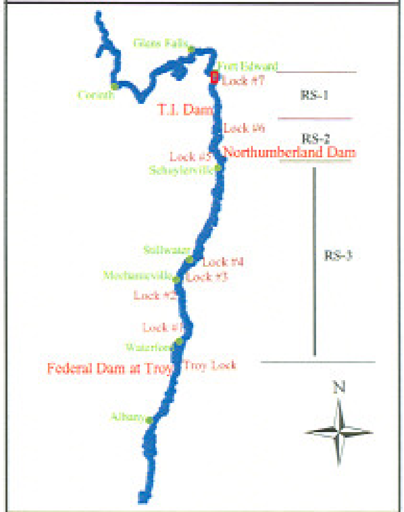

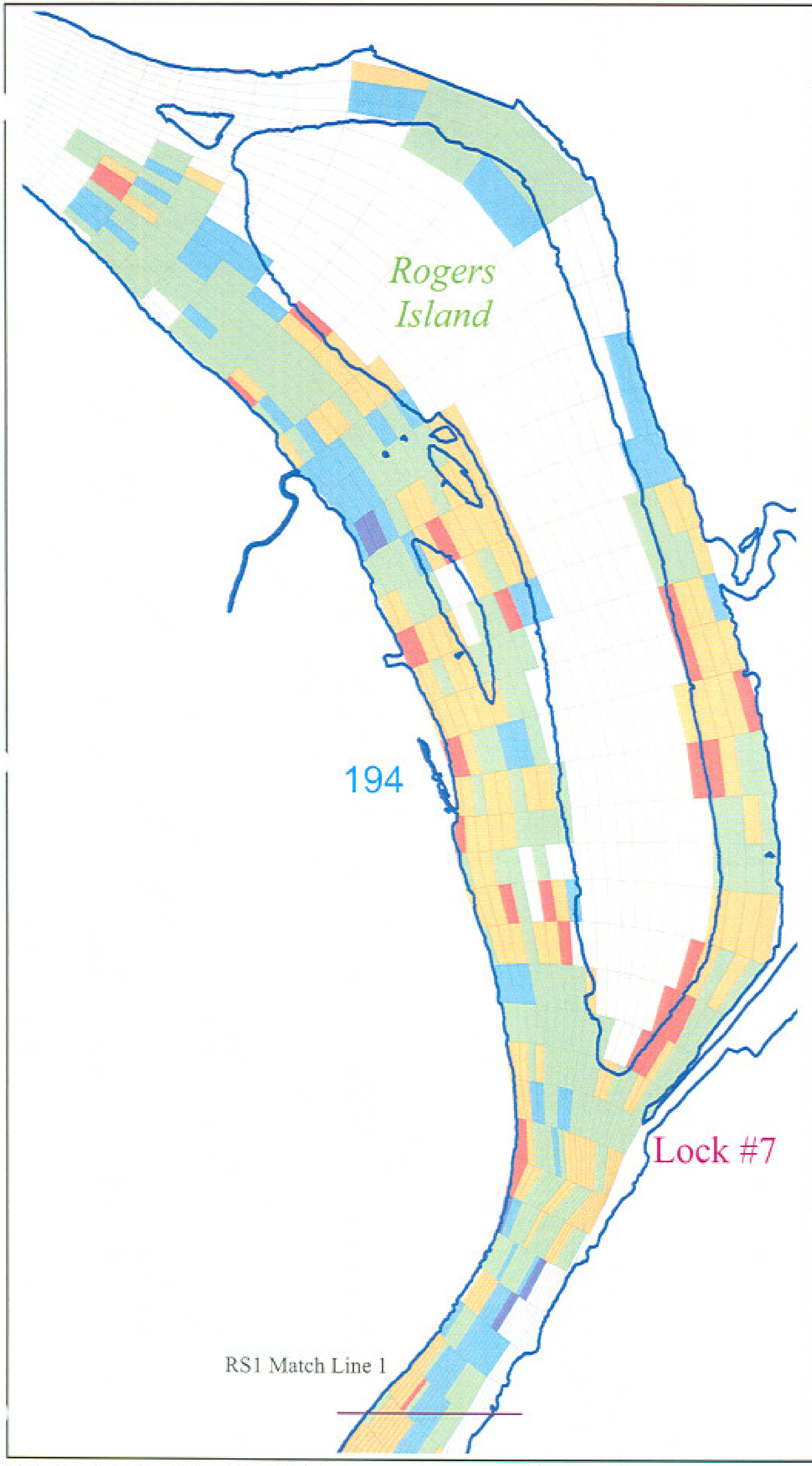

GRAPHIC SCALE

0 250 500 Feet

LEGEND

Percent Fine and Medium Sand

- 0 - 8
- 8 - 16
- 16 - 24
- 24 - 32
- 32 - 40
- Shoreline
- Model Grid

Figure E-4-11a.

Percent Fine and Medium Sand in Total Sediment Bed by Model Grid Cell.

QEA Quantitative Environmental Analysis, LLC

GENdes: 232

Aug 17, 2005.

MS - \\Zeus\E_Drive\GENrem\Working\GIS\maps\ArcGIS8_maps\model\maps\resuspension\PCB_Frac_Map.mxd

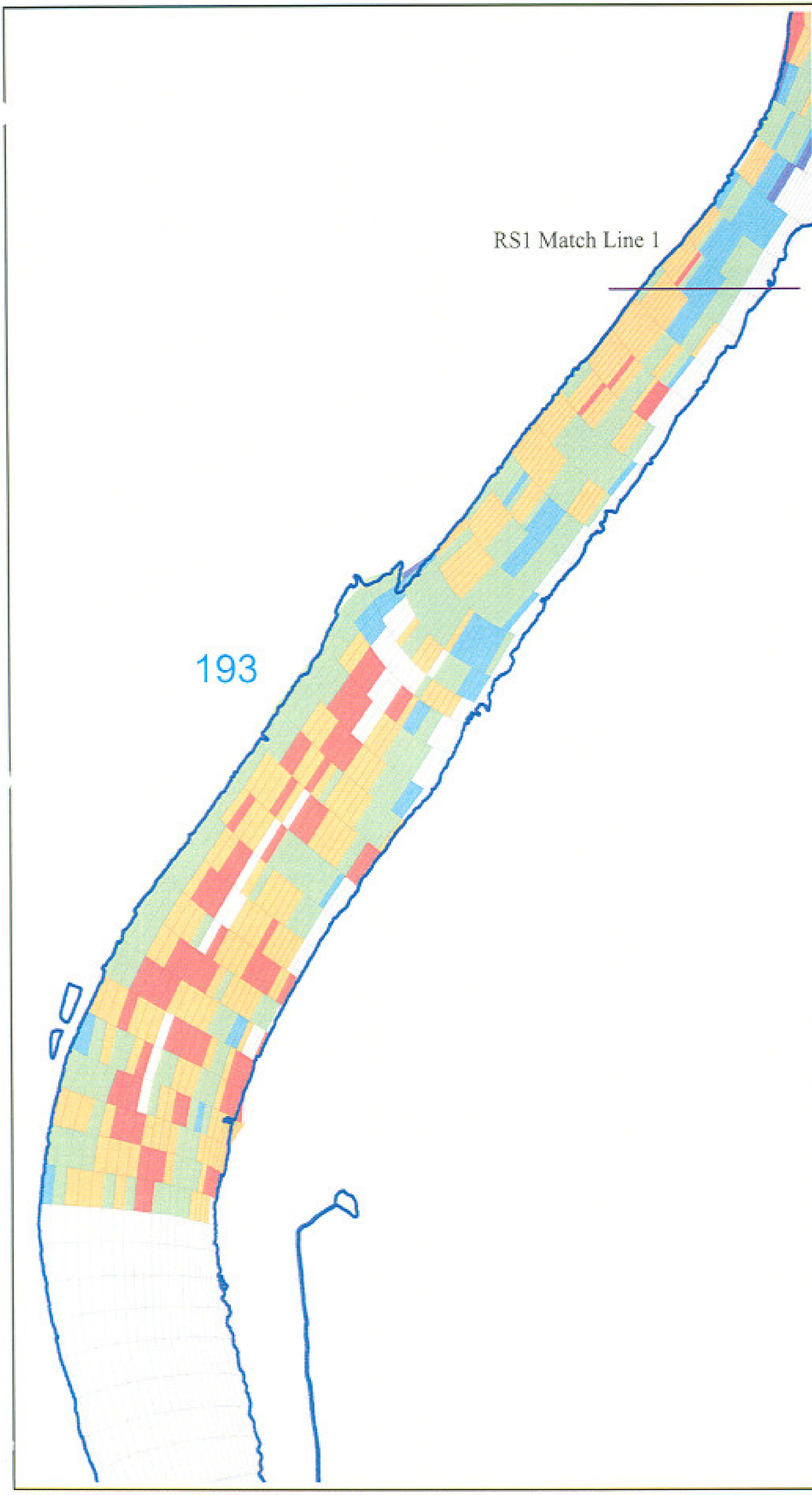

LOCATOR MAP OF THE UPPER HUDSON RIVER

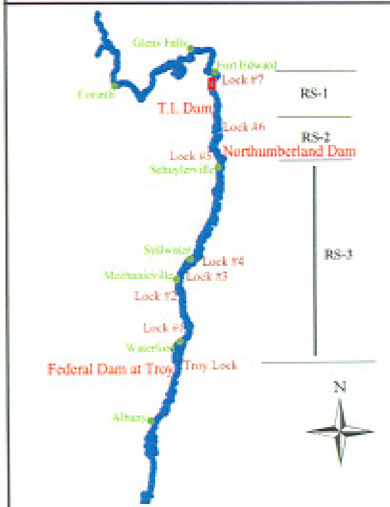

GRAPHIC SCALE

0 250 500 Feet

LEGEND

Percent

Fine and Medium Sand

- 0 - 8
- 8 - 16
- 16 - 24
- 24 - 32
- 32 - 40
- Shoreline
- Model Grid

Figure E-4-11b.

Percent Fine and Medium Sand in Total Sediment Bed by Model Grid Cell.

GENdes: 232 Aug 17, 2005.

MS - \\Zeus\E_Drive\GENrem\Working\GIS\maps\ArcGIS8_maps\model\maps\resuspension\PCB_Frac_Map.mxd

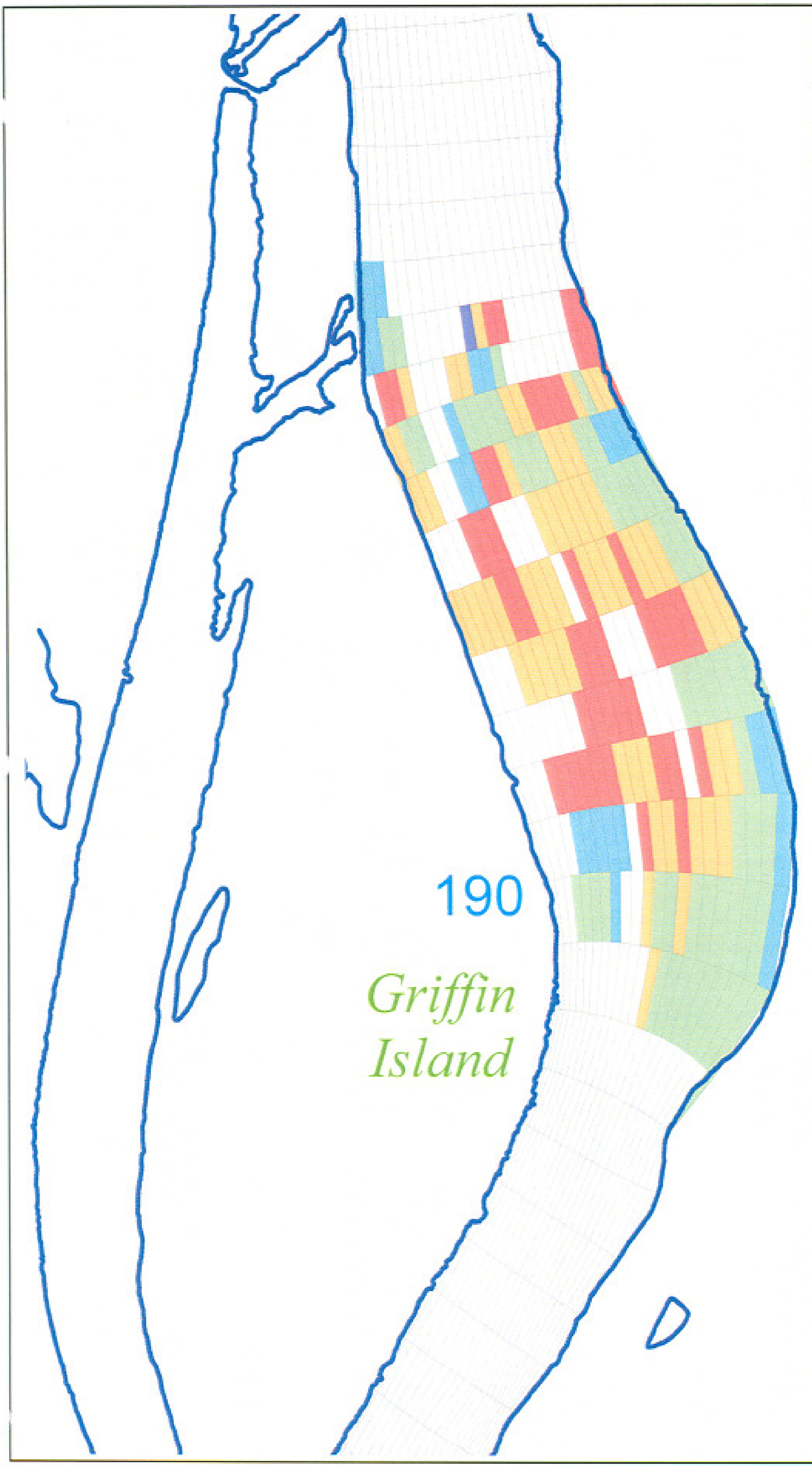

LOCATOR MAP OF THE UPPER HUDSON RIVER

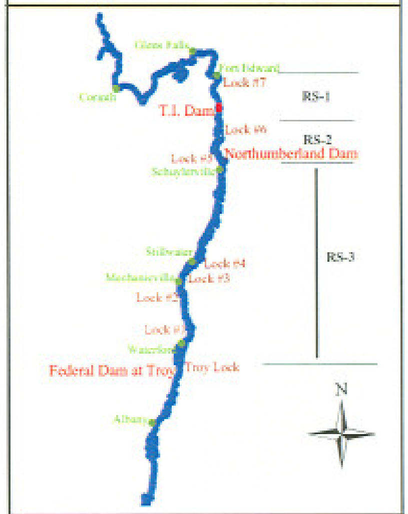

GRAPHIC SCALE

0 250 500 Feet

LEGEND

Percent Fine and Medium Sand

- 0 - 8
- 8 - 16
- 16 - 24
- 24 - 32
- 32 - 40
- Shoreline
- Model Grid

Figure E-4-11c.

Percent Fine and Medium Sand in Total Sediment Bed by Model Grid Cell.

QEA Quantitative Environmental Analysis, LLC

GENdes: 232 Aug 17, 2005.

MS - \\Zeus\E_Drive\GENrem\Working\GIS\maps\ArcGIS8_maps\model\maps\resuspension\PCB_Frac_Map.mxd

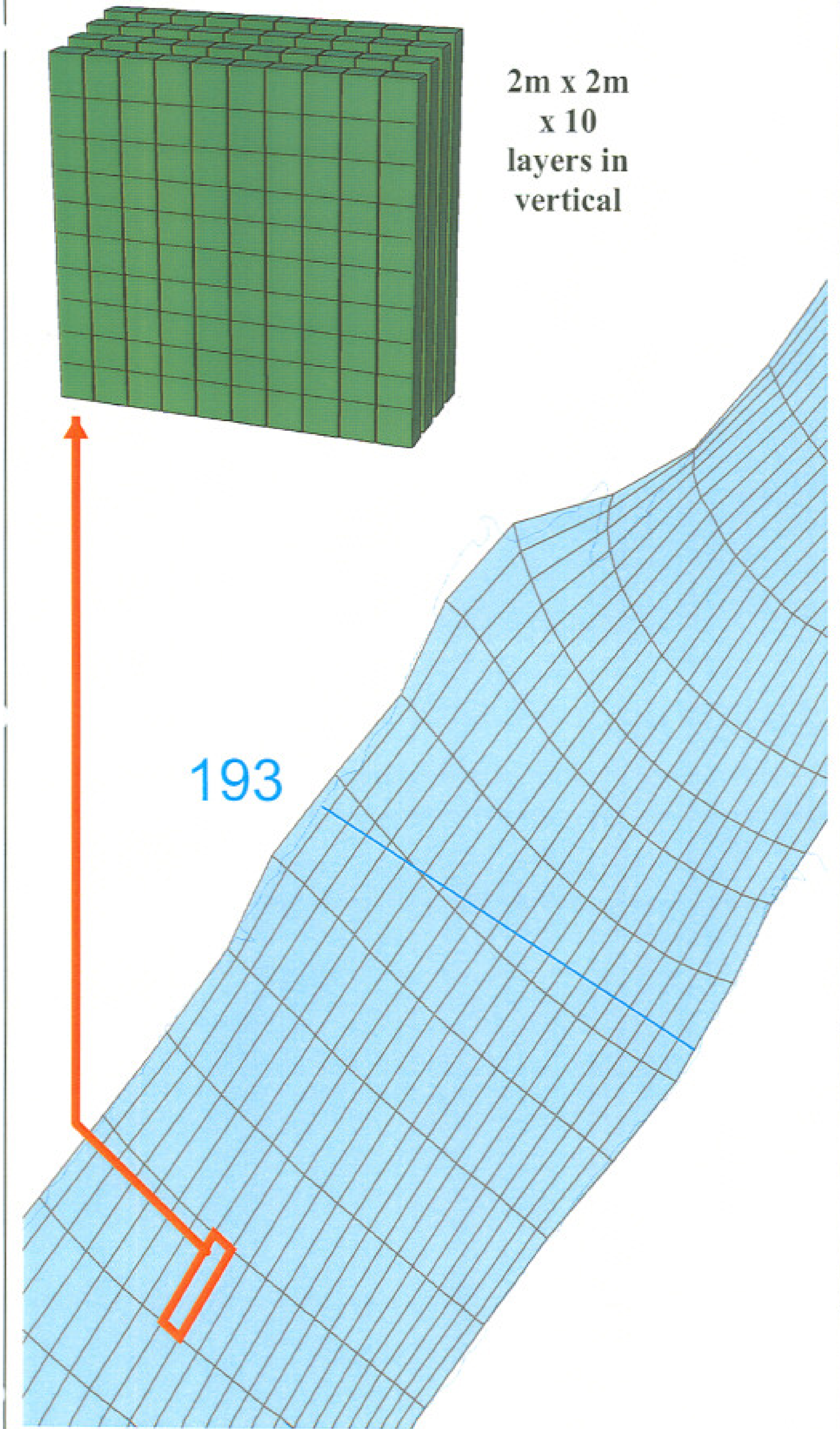

LOCATOR MAP OF THE UPPER HUDSON RIVER

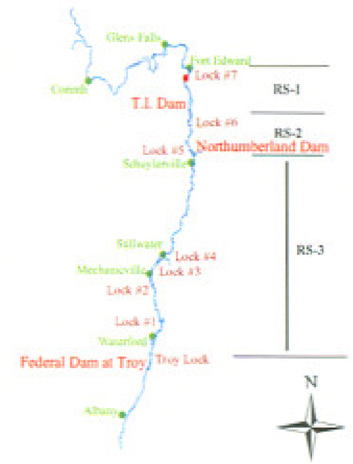

GRAPHIC SCALE

0 100 200 Feet

LEGEND

- River Miles
- Shore Line
- Dams and Locks
- Island/Land Elements
- Channel Elements

UPPER HUDSON RIVER STUDY AREA

Figure E.4-12.

Relationship between numerical grids used for 2-D far-field and 3-D near-field models.

QEA Quantitative Environmental Analysis, LLC

GENdes

Jul 29, 2005.

DN - \\Daleel\D_DRIVE\GENdes\Documents\Reports\IDR\Figure_E-4-12.mxd

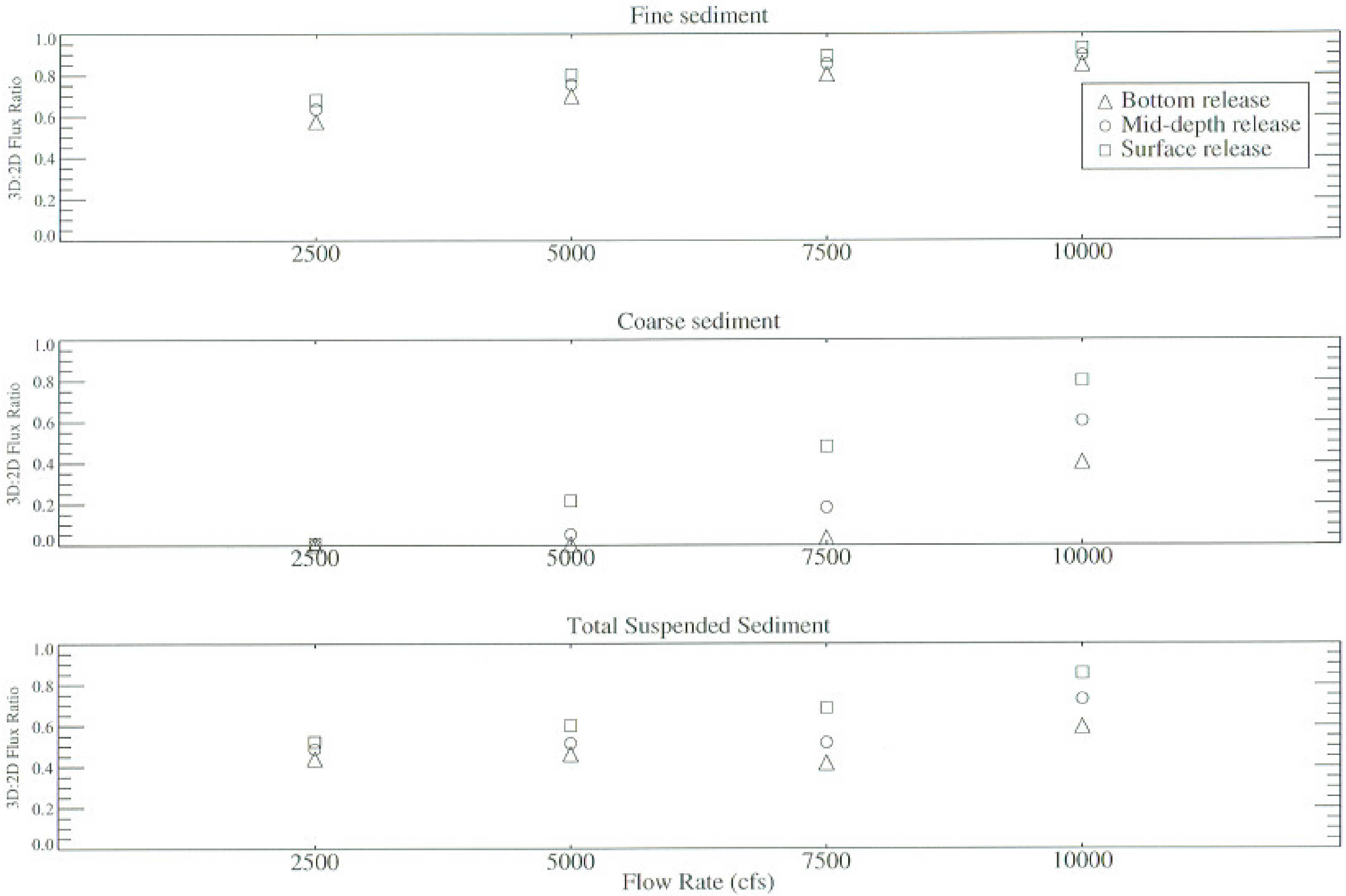

Figure E-4-13. Effect of river flow rate on 2-D/3-D model results: ratio of 3-D to 2-D sediment flux transported out of 2-D grid cell.

lz - C:\GENdes\Analysis\Model_Outputs\EFDC_Outputs\3d_vs_2d_flux\present_3d_2d_flux_f.pro
Sun Jan 09 19:06:59 2005

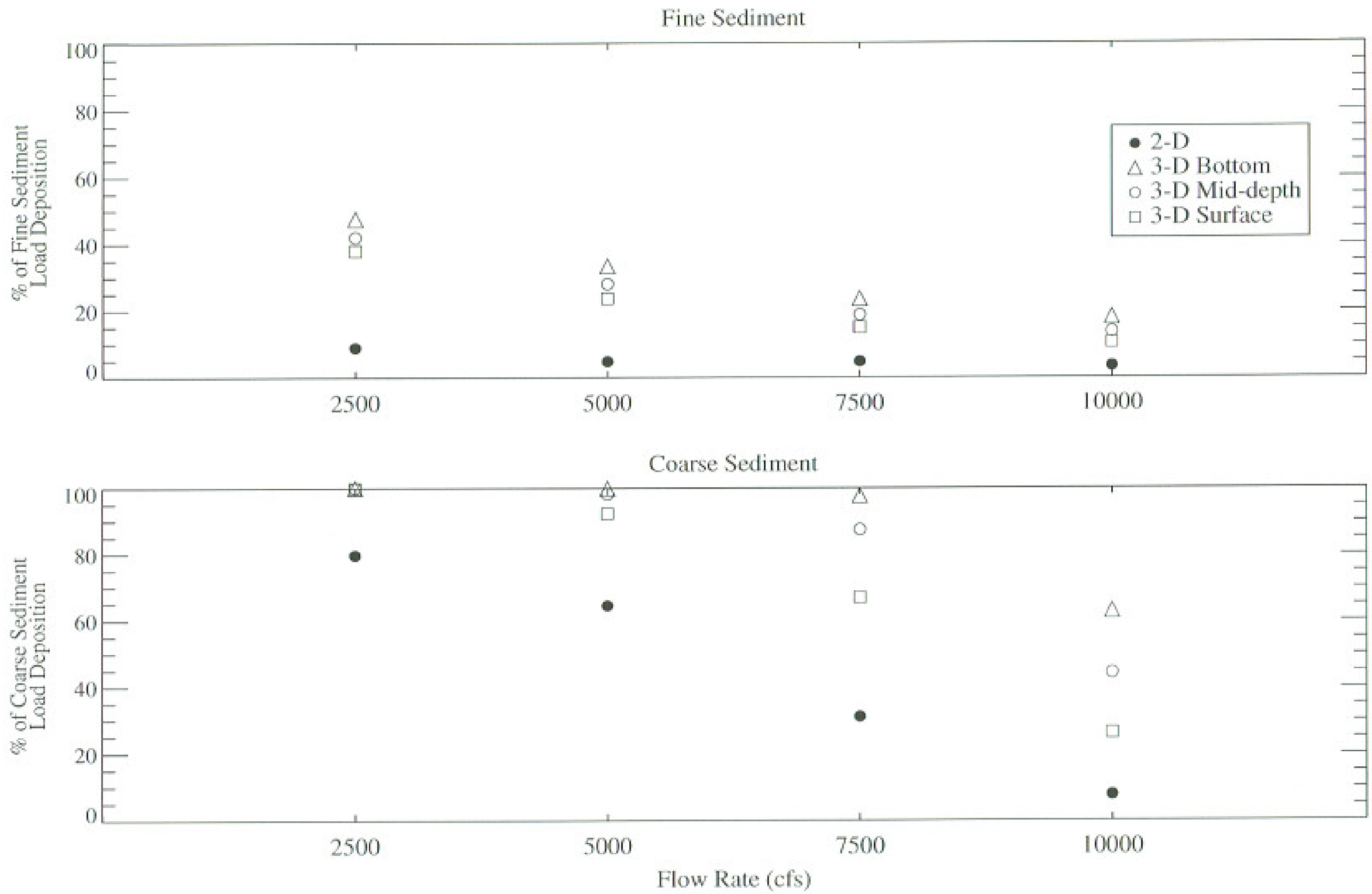

Figure E-4-14. Effect of river flow rate on 2-D/3-D model results: percent of released load deposited within 2-D grid cell.

lz - C:\GENdes\Analysis\Model_Outputs\EFDC_Outputs\3d_vs_2d_flux\present_3d_2d_dep_f.pro
Sun Jan 09 19:04:53 2005

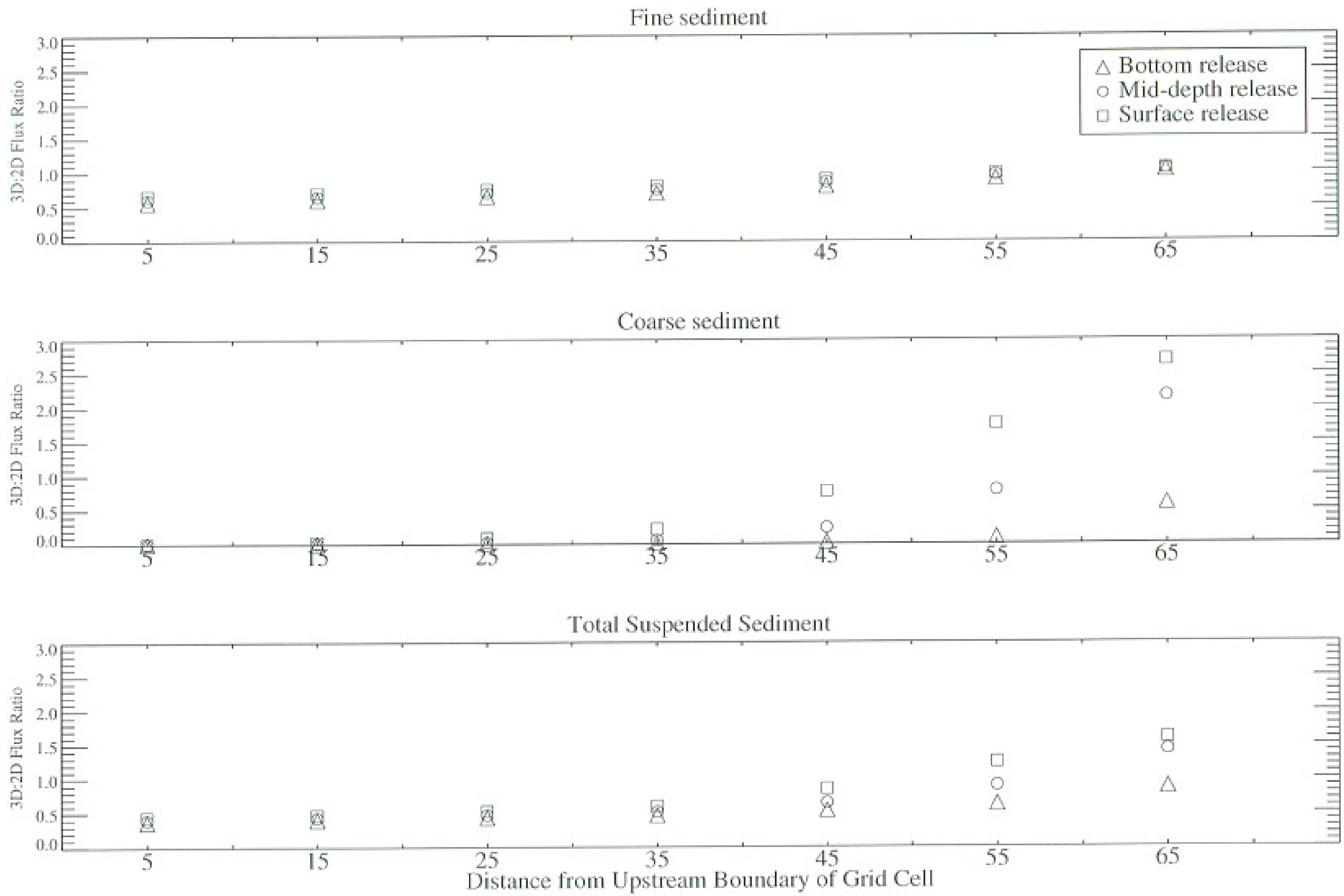

Figure E-4-15. Effect of load release location in 3-D grid on 2-D/3-D model results: ratio of 3-D to 2-D sediment flux transported out of 2-D grid cell.

lz - C:\GENdev\Analysis\Model_Outputs\EFDC_Outputs\3d_vs_2d_flux\present_3d_2d_flux_h.pro
Sun Jan 09 19:04:00 2005

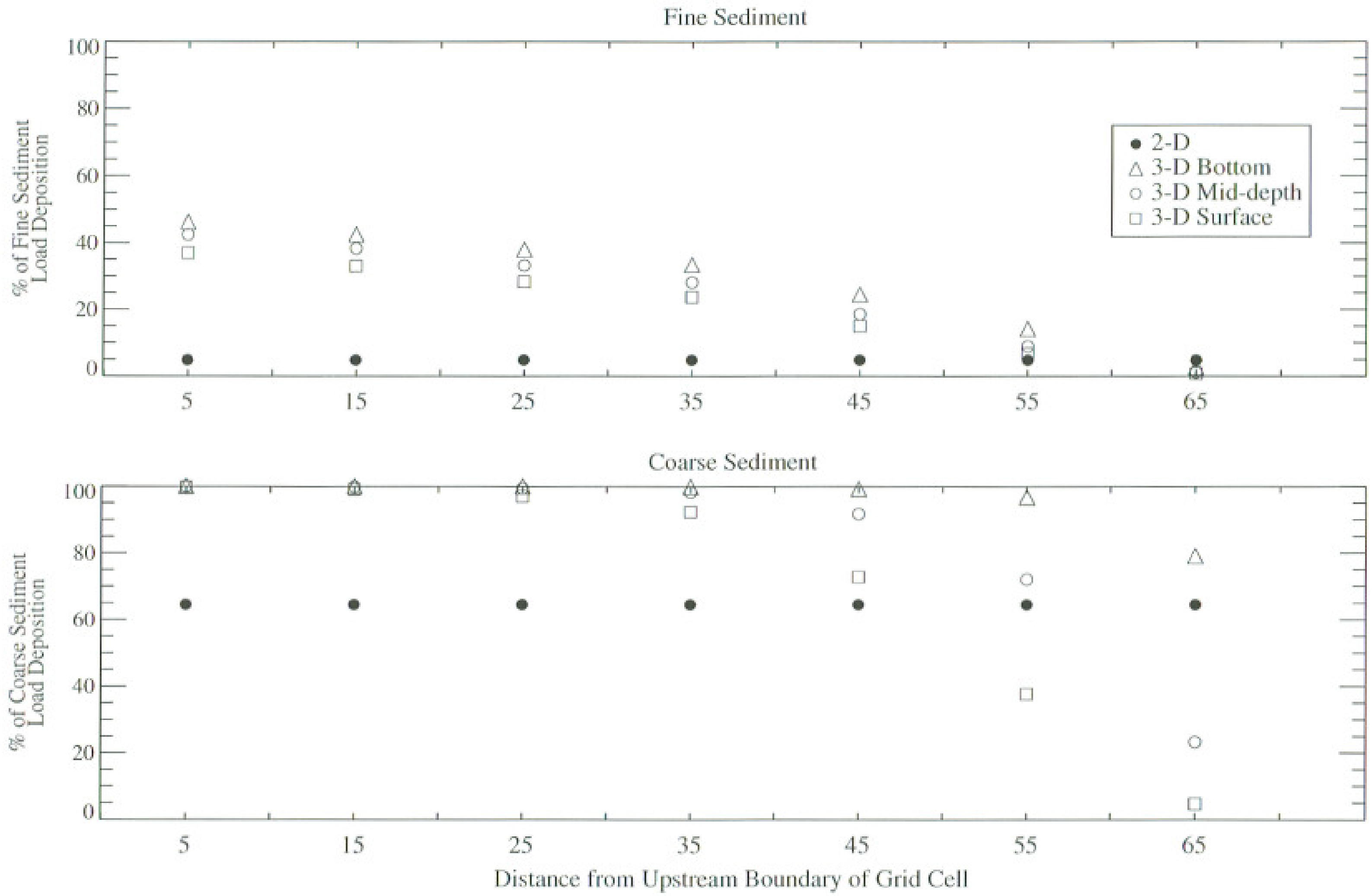

Figure E-4-16. Effect of load release location in 3-D grid on 2-D/3-D model results: percent of released load deposited within 2-D grid cell.

lz - C:\GENdes\Analysis\Model_Outputs\EFDC_Outputs\3d_vs_2d_flux\present_3d_2d_dep_h.pro
Sun Jan 09 19:06:00 2005

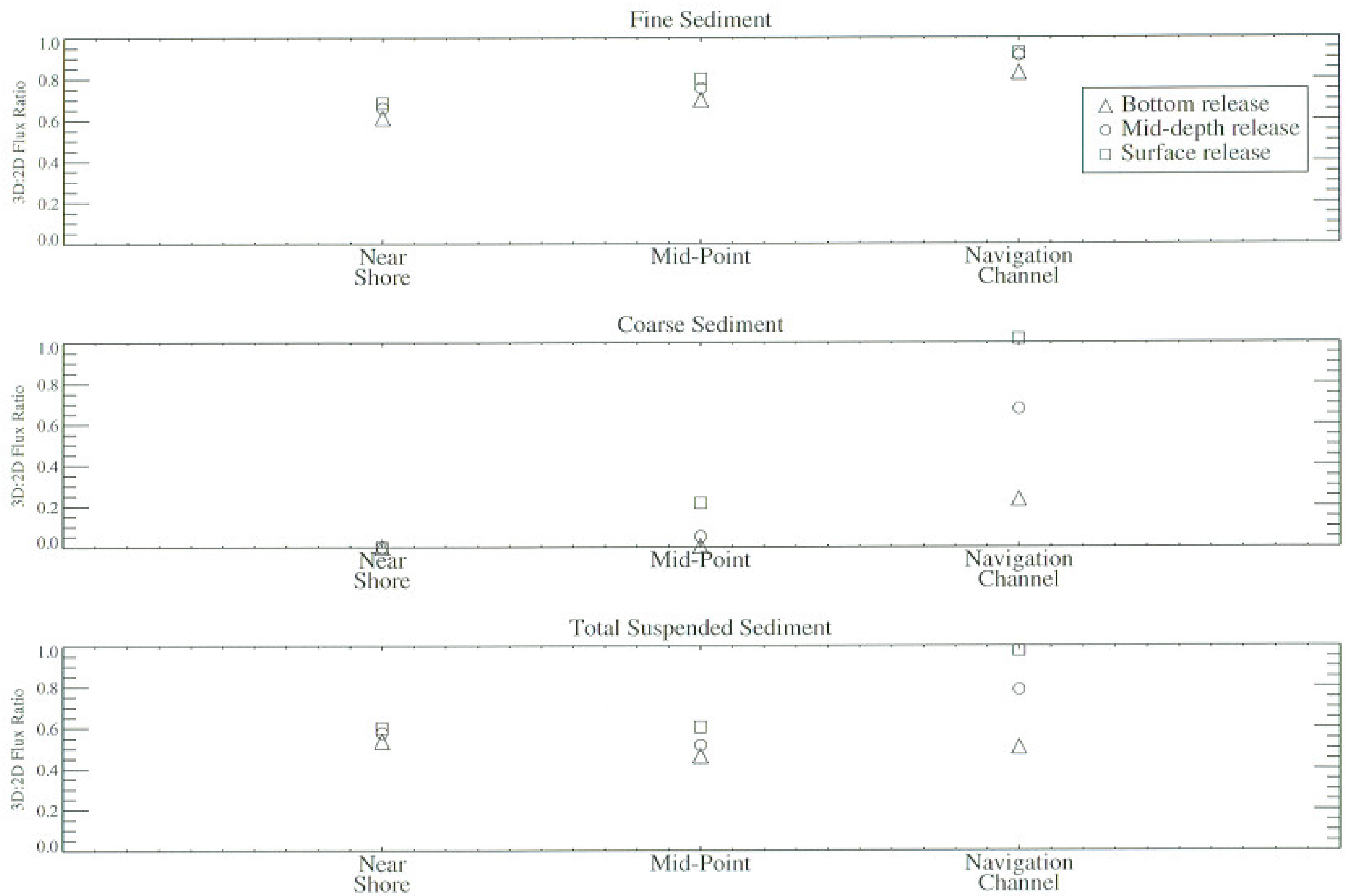

Figure E-4-17. Effect of 2-D grid cell location in the TIP channel (near RM 193) on 2-D/3-D model results: ratio of 3-D to 2-D sediment flux transported out of 2-D grid cell.

lz - D:\GENdes\Analysis\Model_Outputs\EFDC_Outputs\3d_vs_2d_flux\present_3d_2d_flux.pro
Wed Aug 17 20:29:53 2005

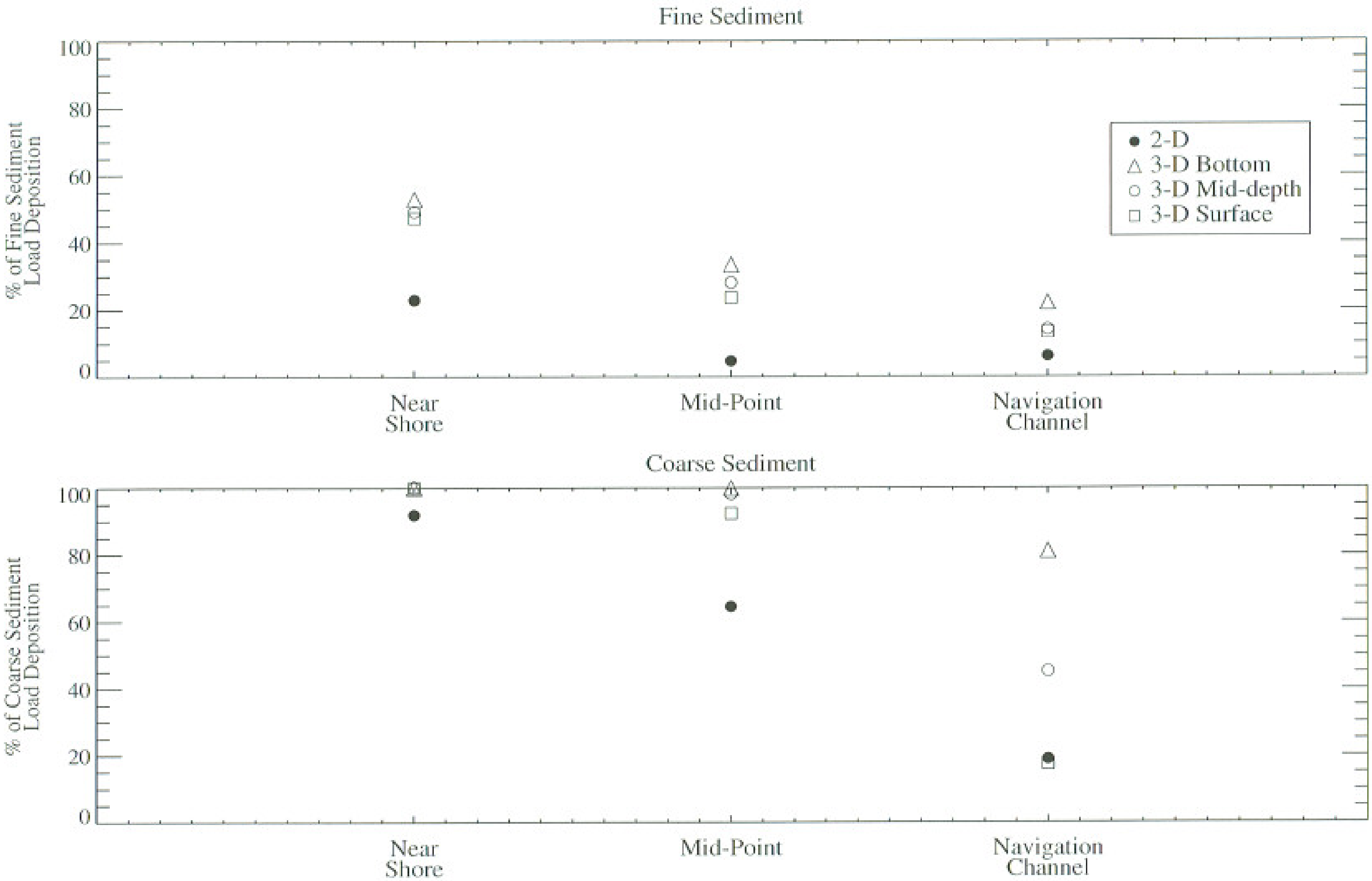

Figure E-4-18. Effect of 2-D grid cell location in the TIP channel (near RM 193) on 2-D/3-D model results: percent of released load deposited within 2-D grid cell.

lz - D:\GENdes\Analysis\Model_Outputs\EFDC_Outputs\3d_vs_2d_flux\present_3d_2d_dep.pro
Wed Aug 17 20:57:05 2005

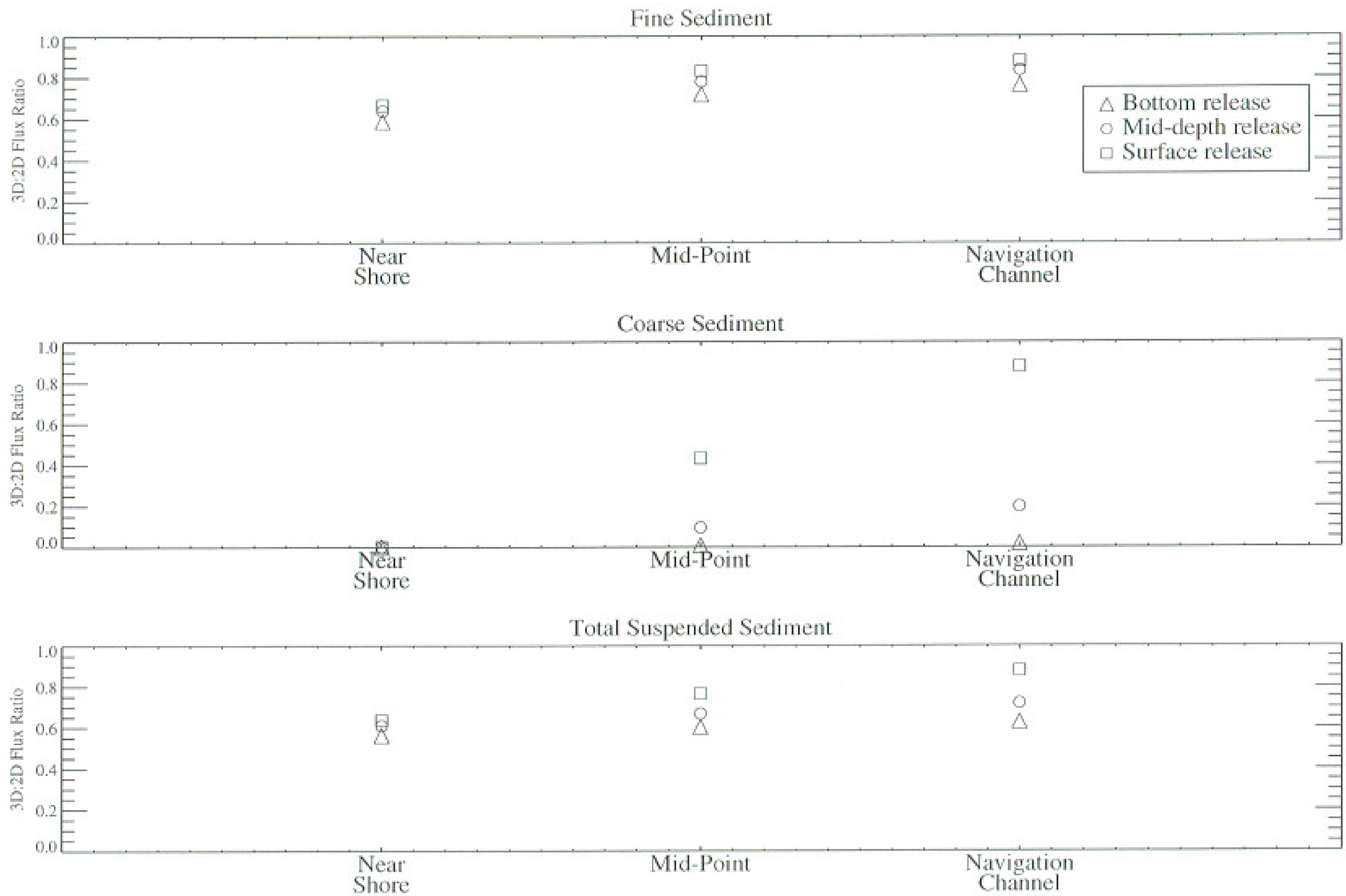

Figure E-4-19. Effect of 2-D grid cell location in the TIP channel (near Griffin Island) on 2-D/3-D model results: ratio of 3-D to 2-D sediment flux transported out of 2-D grid cell.

lz - D:\GENdes\Analysis\Model_Outputs\EFDC_Outputs\3d_vs_2d_flux\present_3d_2d_flux.pro
Wed Aug 17 20:41:43 2005

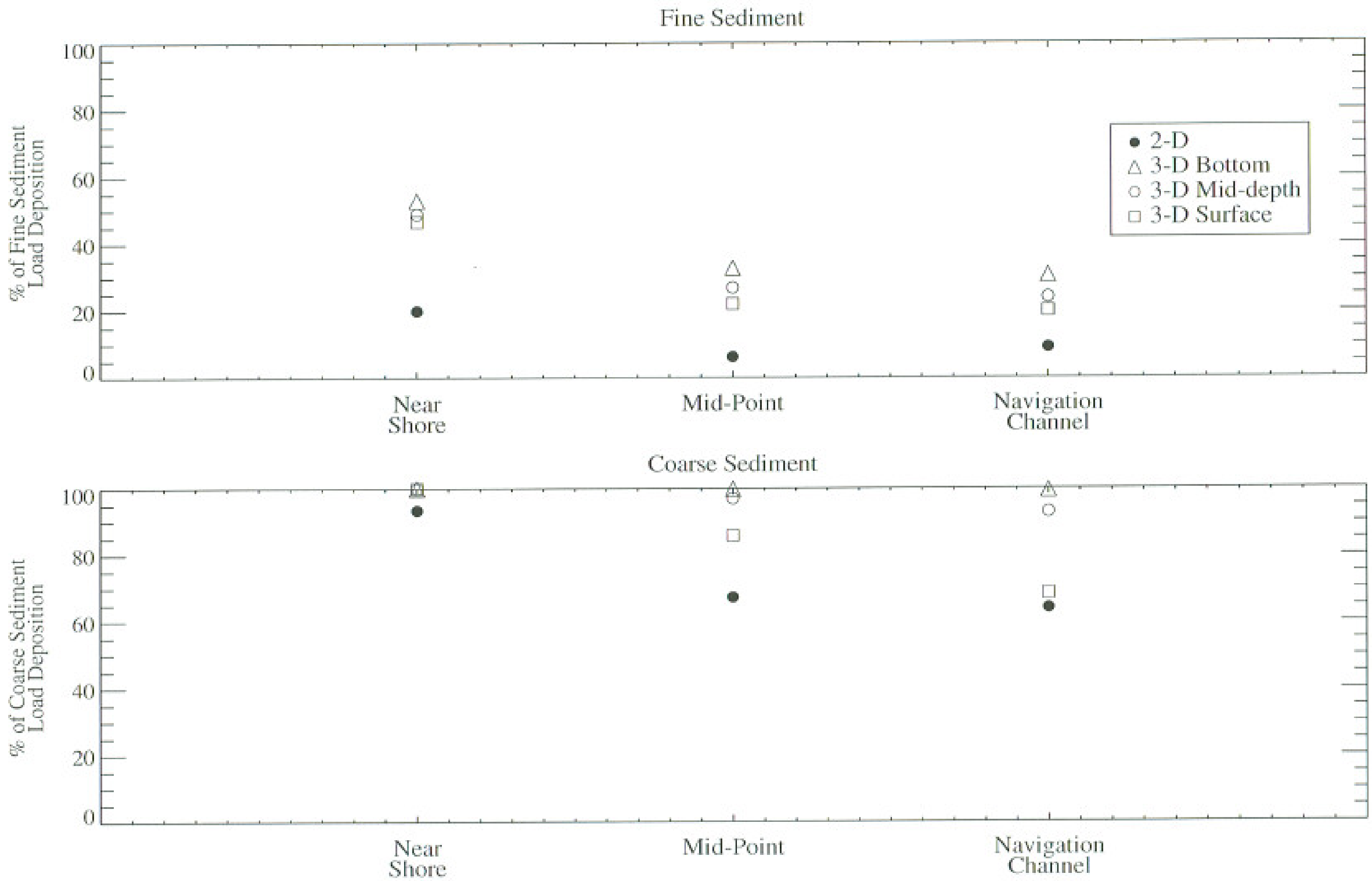

Figure E-4-20. Effect of 2-D grid cell location in the TIP channel (near Griffin Island) on 2-D/3-D model results: percent of released load deposited within 2-D grid cell.

lz - D:\GENdes\Analysis\Model_Outputs\EFDC_Outputs\3d_vs_2d_flux\present_3d_2d_dep.pro
Wed Aug 17 20:49:31 2005

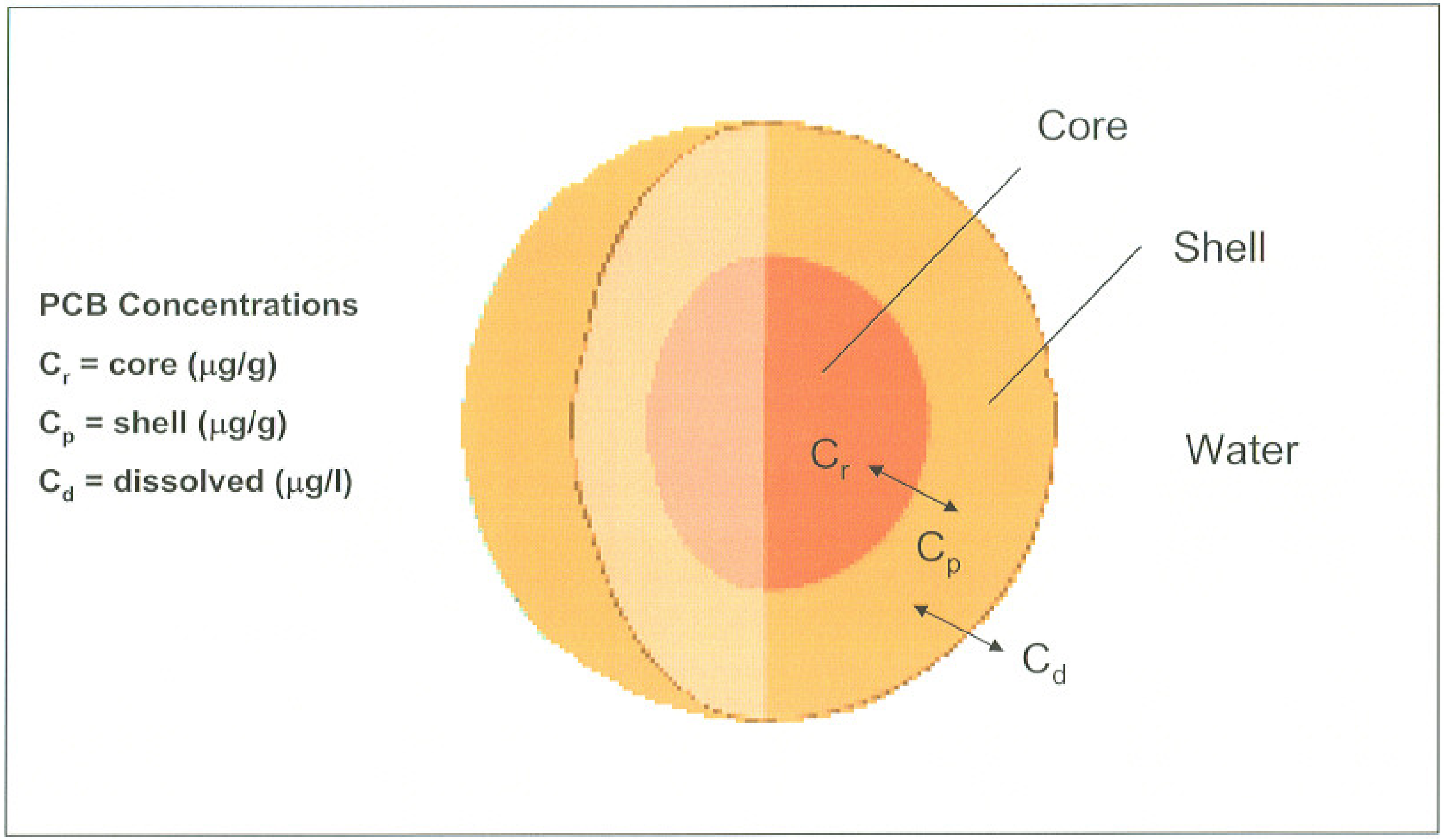

Figure E-5-1. Conceptual diagram of dual compartment radial diffusive PCB sorption sub-model

\\dalee\d_drive\GENdes\Documents\Reports\IDR\Figure_E-5-1_desorption_model_fig.ppt

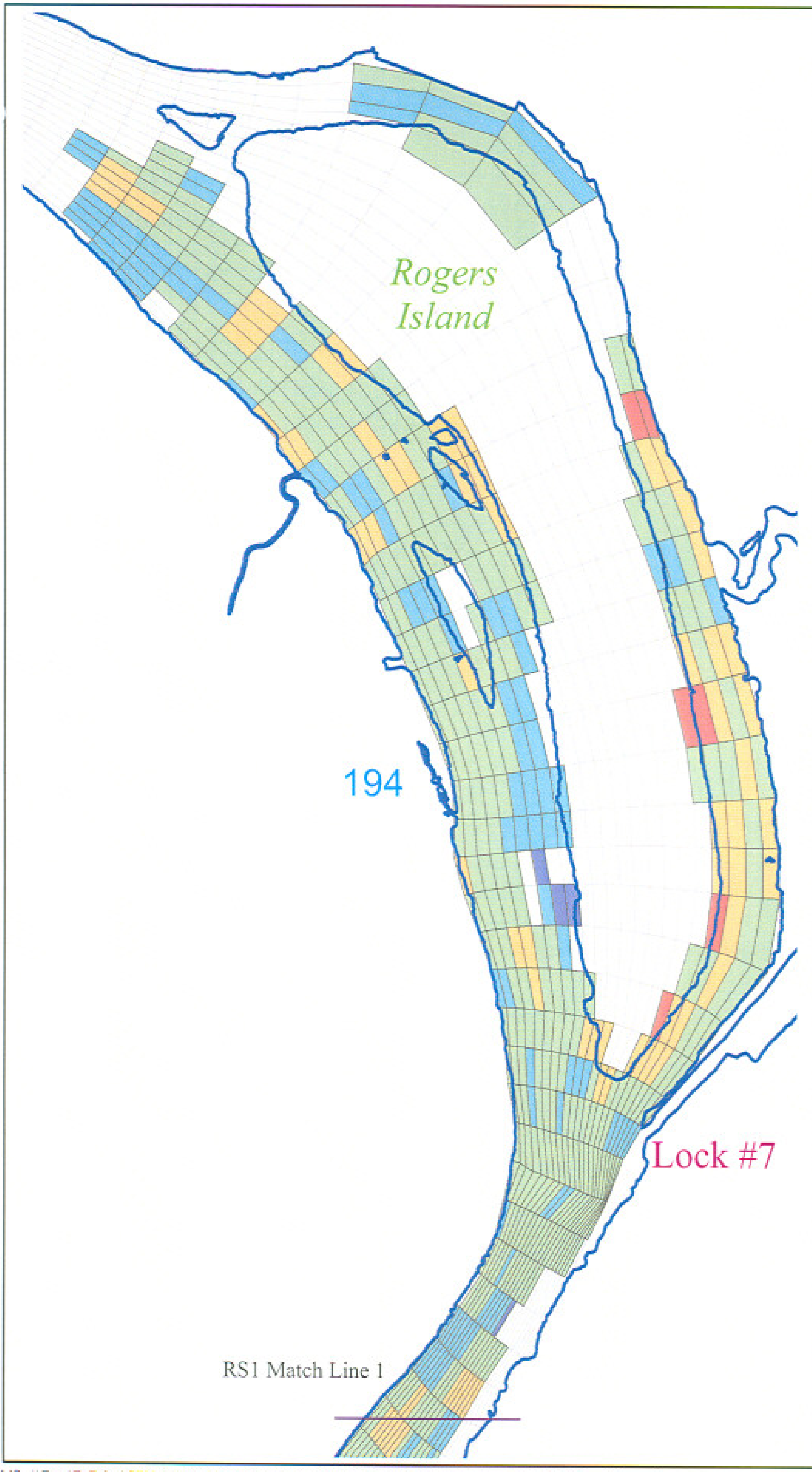

LOCATOR MAP OF THE UPPER HUDSON RIVER

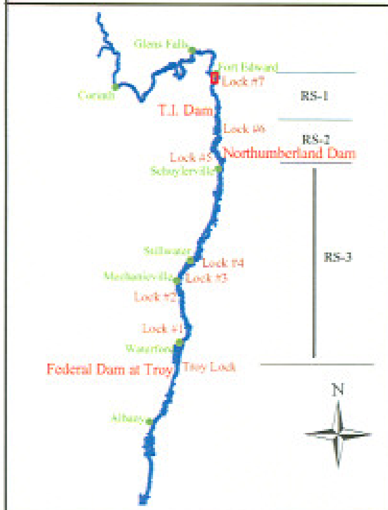

GRAPHIC SCALE

0 250 500 Feet

LEGEND

Avg. Total PCB Concentration (µg/g)

Clay and Silt

- 0 - 1
- 1 - 10
- 10 - 100
- 100 - 1000
- >1000
- Shoreline
- Model Grid

Figure E-5-2a.

Average Total PCB Concentration in Clay and Silt by Model Grid Cell.

GENdes: 232

Aug 17, 2005.

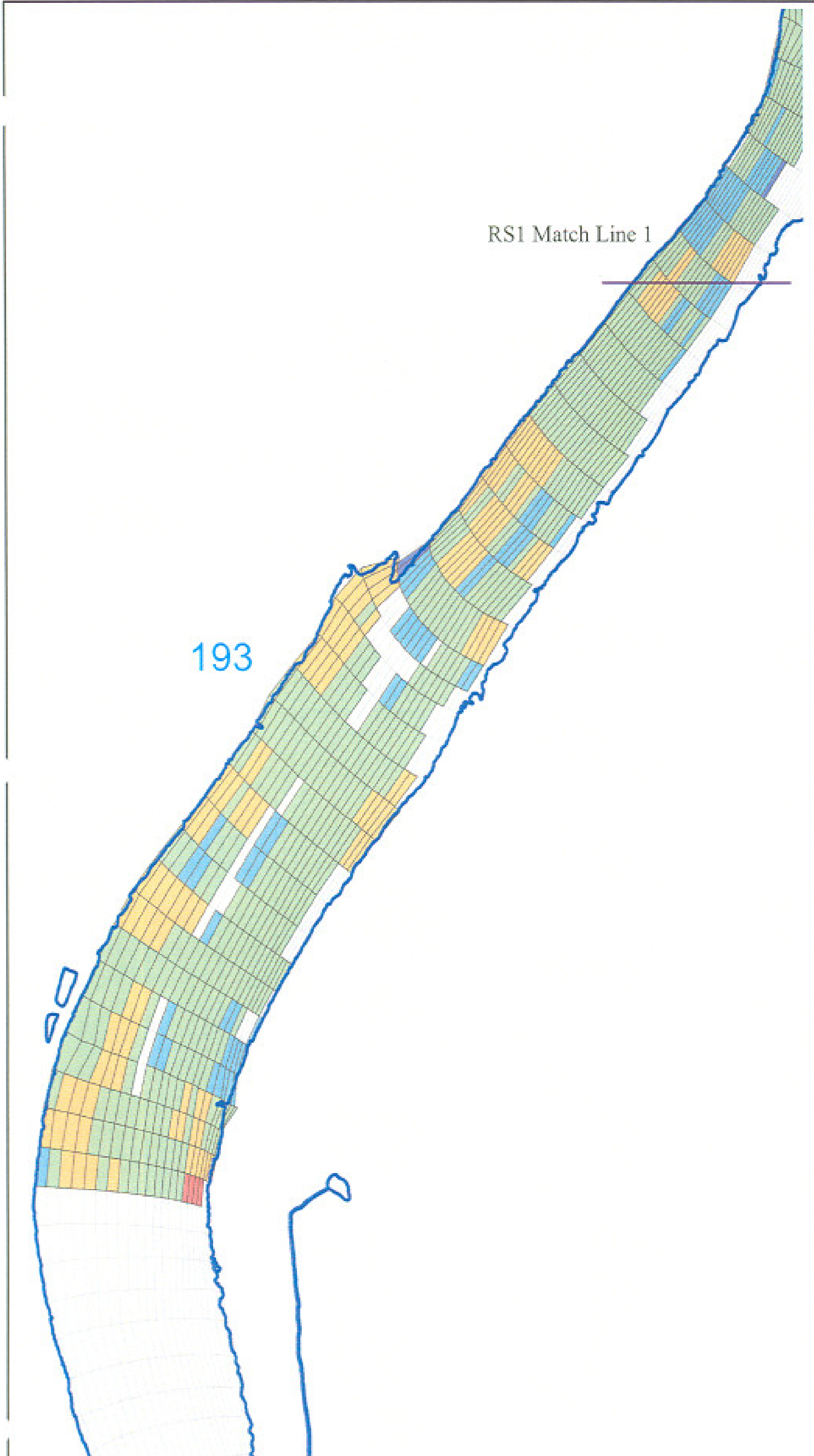

LOCATOR MAP OF THE UPPER HUDSON RIVER

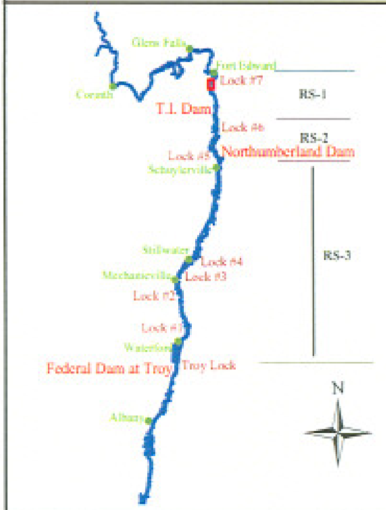

GRAPHIC SCALE

0 250 500 Feet

LEGEND

Avg. Total PCB Concentration (µg/g)

Clay and Silt

- 0 - 1
- 1 - 10
- 10 - 100
- 100 - 1000
- >1000
- Shoreline
- Model Grid

Figure E-5-2b.

Average Total PCB Concentration in Clay and Silt by Model Grid Cell.

QEA Quantitative Environmental Analysis, LLC

GENdes: 232 Aug 17, 2005.

MS - \\Zeus\E_Drive\GENrem\Working\GIS\maps\ArcGIS8_maps\model\maps\resuspension\PCB_Frac_Map.mxd

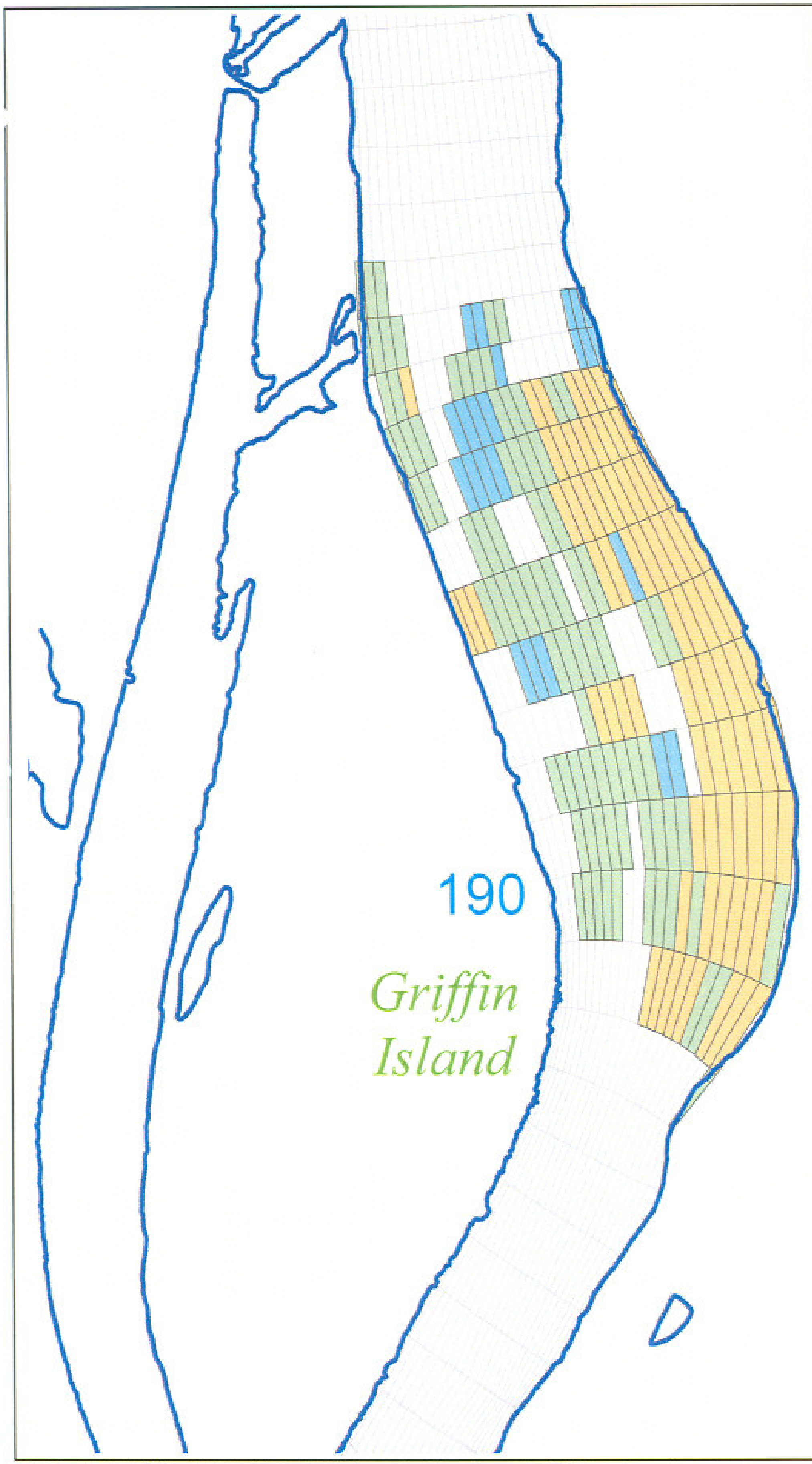

LOCATOR MAP OF THE UPPER HUDSON RIVER

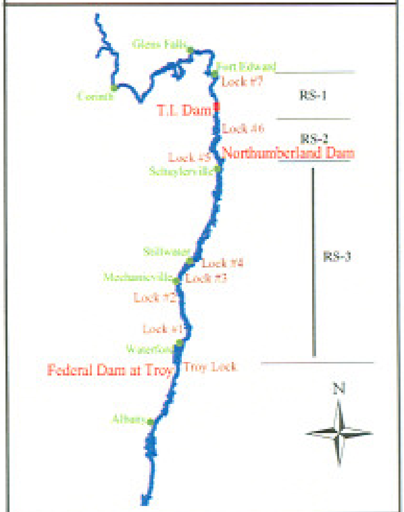

GRAPHIC SCALE

0 250 500 Feet

LEGEND

Avg. Total PCB Concentration (µg/g)

Clay and Silt

- 0 - 1
- 1 - 10
- 10 - 100
- 100 - 1000
- >1000
- Shoreline
- Model Grid

Figure E-5-2c.

Average Total PCB Concentration in Clay and Silt by Model Grid Cell.

QEA Quantitative Environmental Analysis, LLC

GENdes: 232 Aug 17, 2005.

MS - \\Zeus\E_Drive\GENrem\Working\GIS\maps\ArcGIS8_maps\model\maps\resuspension\PCB_Frac_Map.mxd

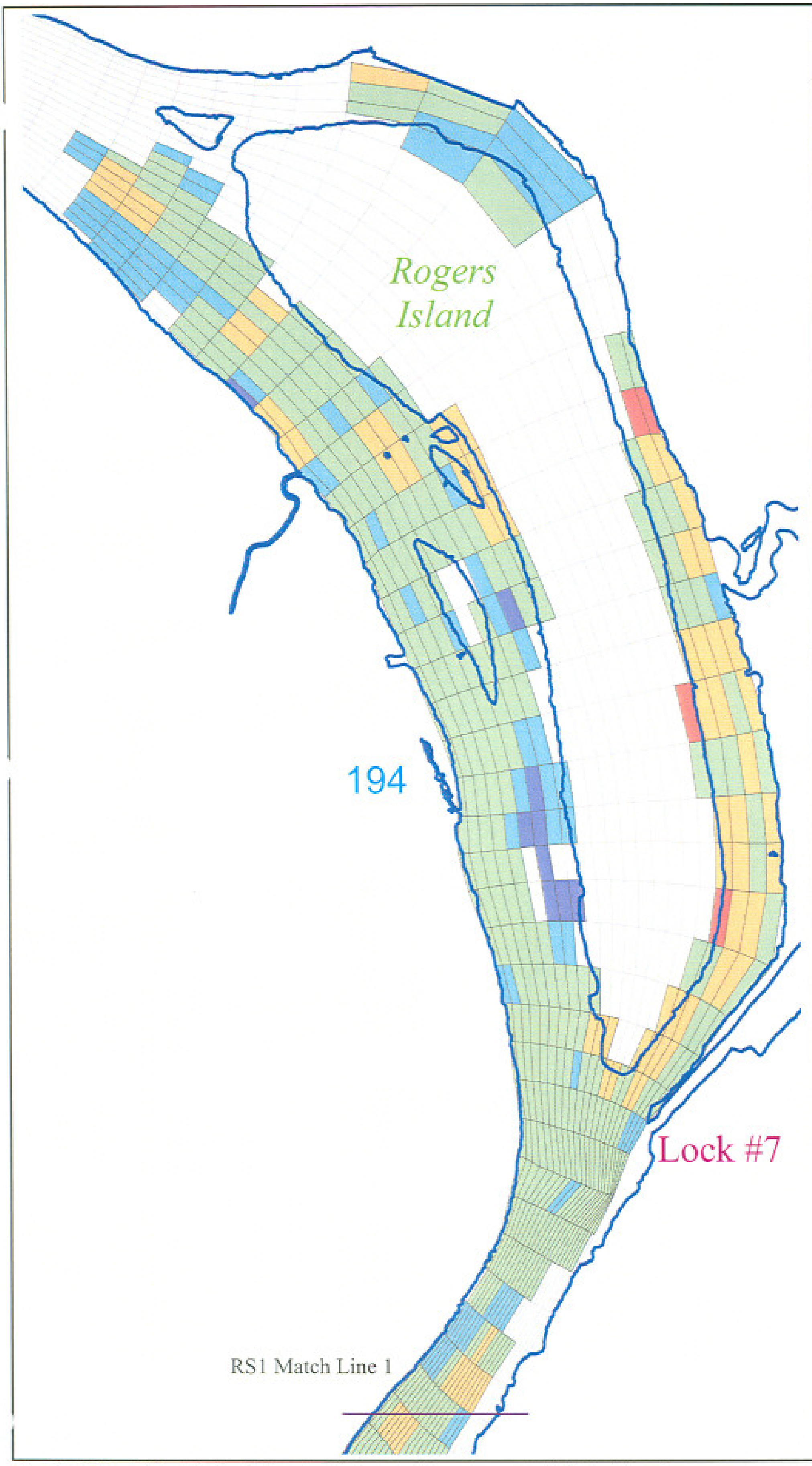

LOCATOR MAP OF THE UPPER HUDSON RIVER

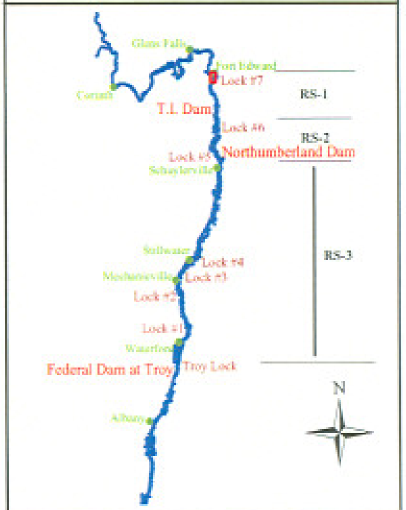

GRAPHIC SCALE

0 250 500 Feet

LEGEND

Avg. Total PCB Concentration (µg/g)

Very Fine Sand

- 0 - 1
- 1 - 10
- 10 - 100
- 100 - 1000
- >1000
- Shoreline
- Model Grid

Figure E-5-3a.

Average Total PCB Concentration in Very Fine Sand by Model Grid Cell.

QEA Quantitative Environmental Analysis, LLC

GENdes: 232

Aug 17, 2005.

MS - \\Zeus\E_Drive\GENrem\Working\GIS\maps\ArcGIS8_maps\model\maps\resuspension\PCB_Frac_Map.mxd

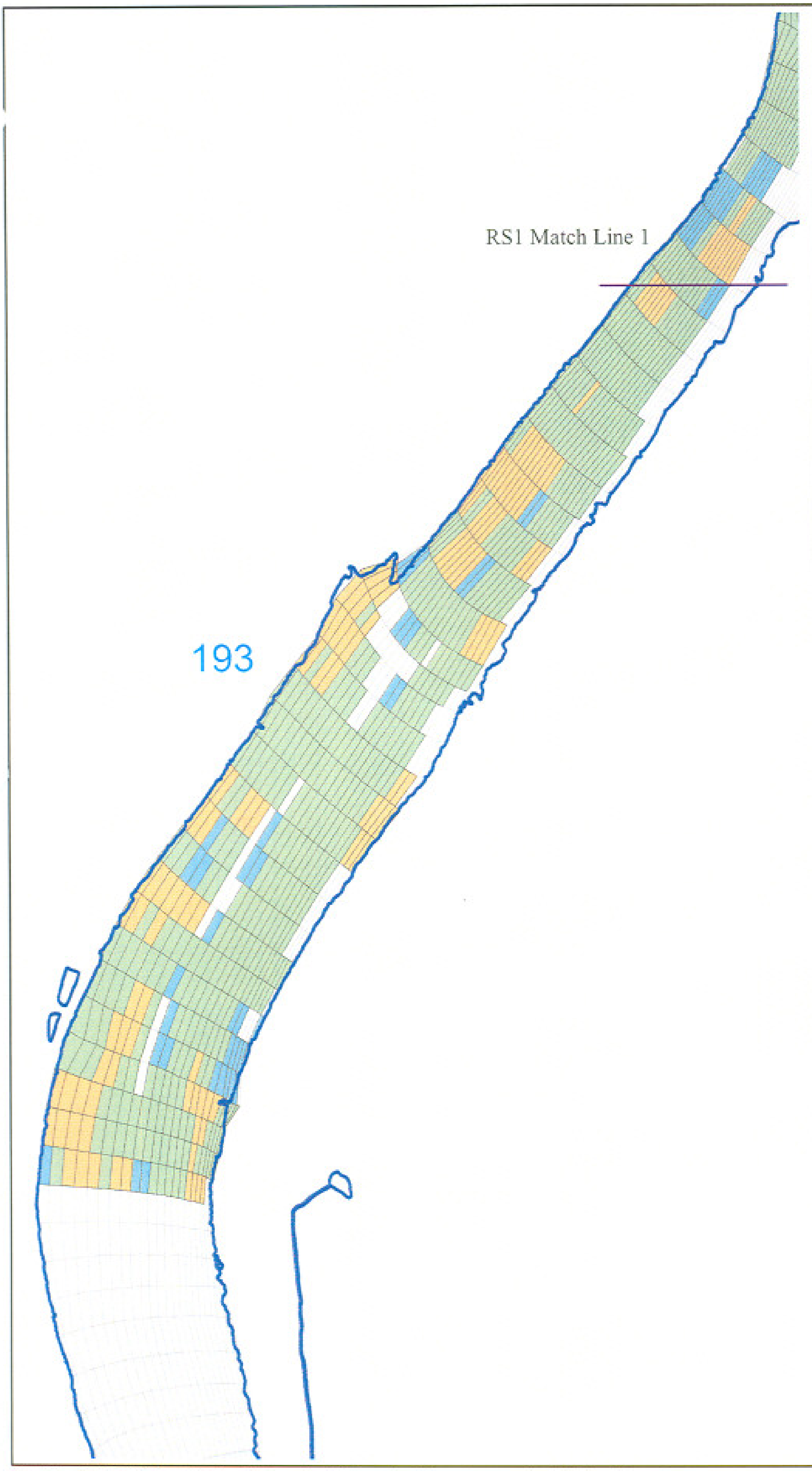

LOCATOR MAP OF THE UPPER HUDSON RIVER

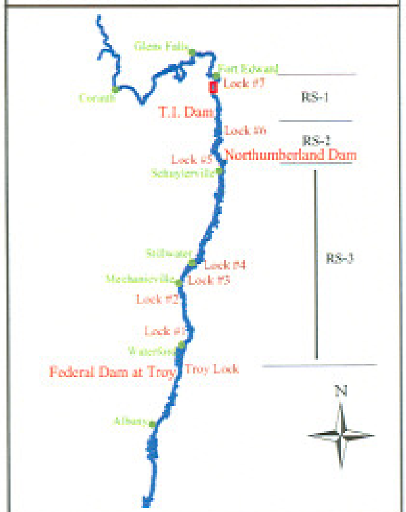

GRAPHIC SCALE

0 250 500Feet

LEGEND

Avg. Total PCB Concentration (µg/g)

Very Fine Sand

- 0 - 1
- 1 - 10
- 10 - 100
- 100 - 1000
- >1000
- Shoreline
- Model Grid

Figure E-5-3b.

Average Total PCB Concentration in Very Fine Sand by Model Grid Cell.

Quantitative Environmental Analysis, LLC

GENdes: 232 Aug 17, 2005.

MS - \\Zeus\E_Drive\GENrem\Working\GIS\maps\ArcGIS8_maps\model\maps\resuspension\PCB_Frac_Map.mxd

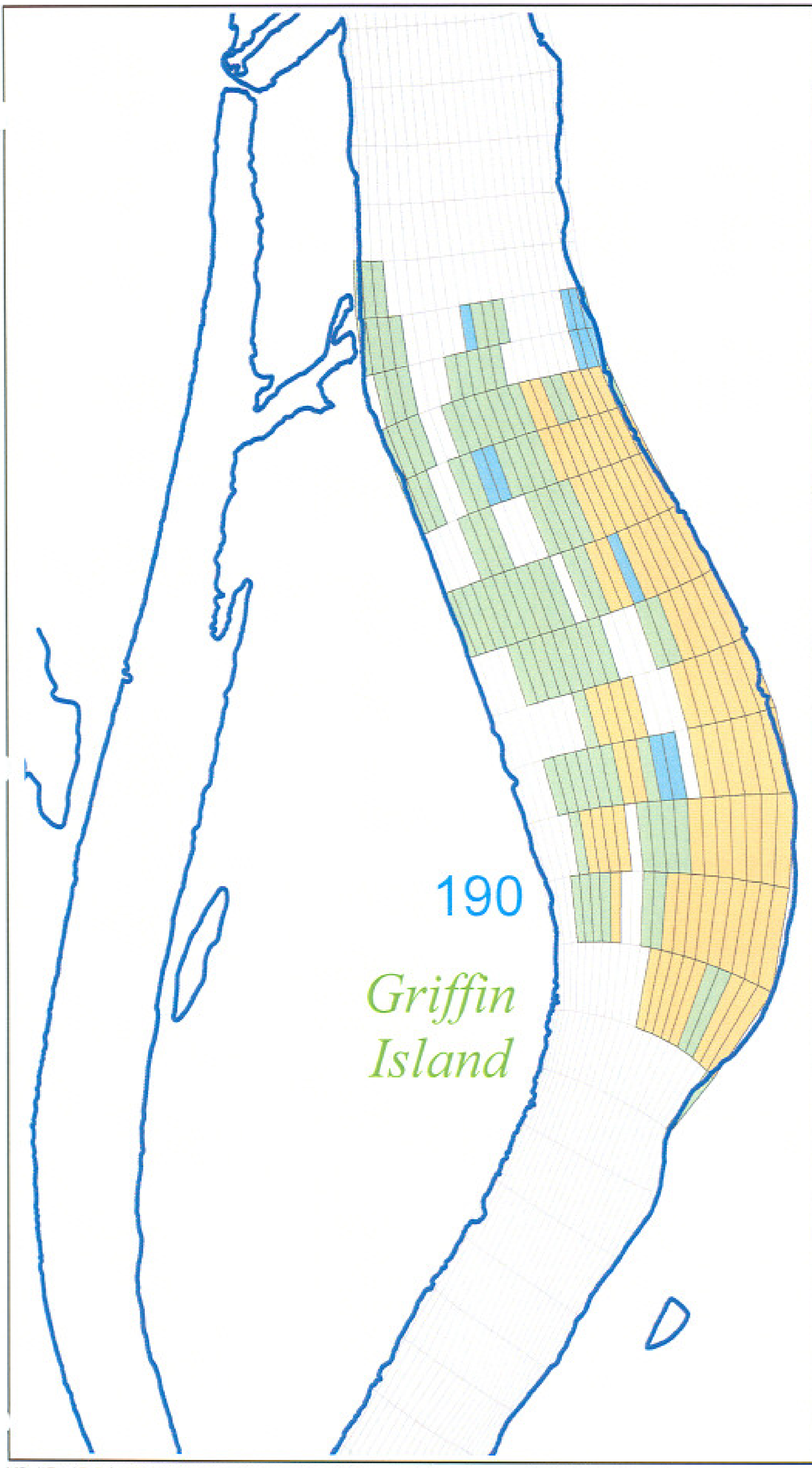

LOCATOR MAP OF THE UPPER HUDSON RIVER

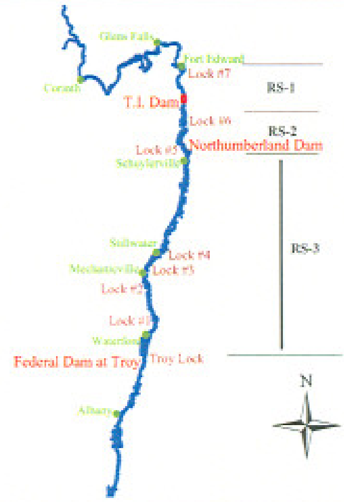

GRAPHIC SCALE

0 250 500 Feet

LEGEND

Avg. Total PCB Concentration (µg/g)

Very Fine Sand

- 0 - 1
- 1 - 10
- 10 - 100
- 100 - 1000
- >1000
- Shoreline
- Model Grid

Figure E-5-3c.

Average Total PCB Concentration in Very Fine Sand by Model Grid Cell.

QEA Quantitative Environmental Analysis, LLC

GENdes: 232

Aug 17, 2005.

MS - \\Zeus\E_Drive\GENrem\Working\GIS\maps\ArcGIS8_maps\model\maps\resuspension\PCB_Frac_Map.mxd

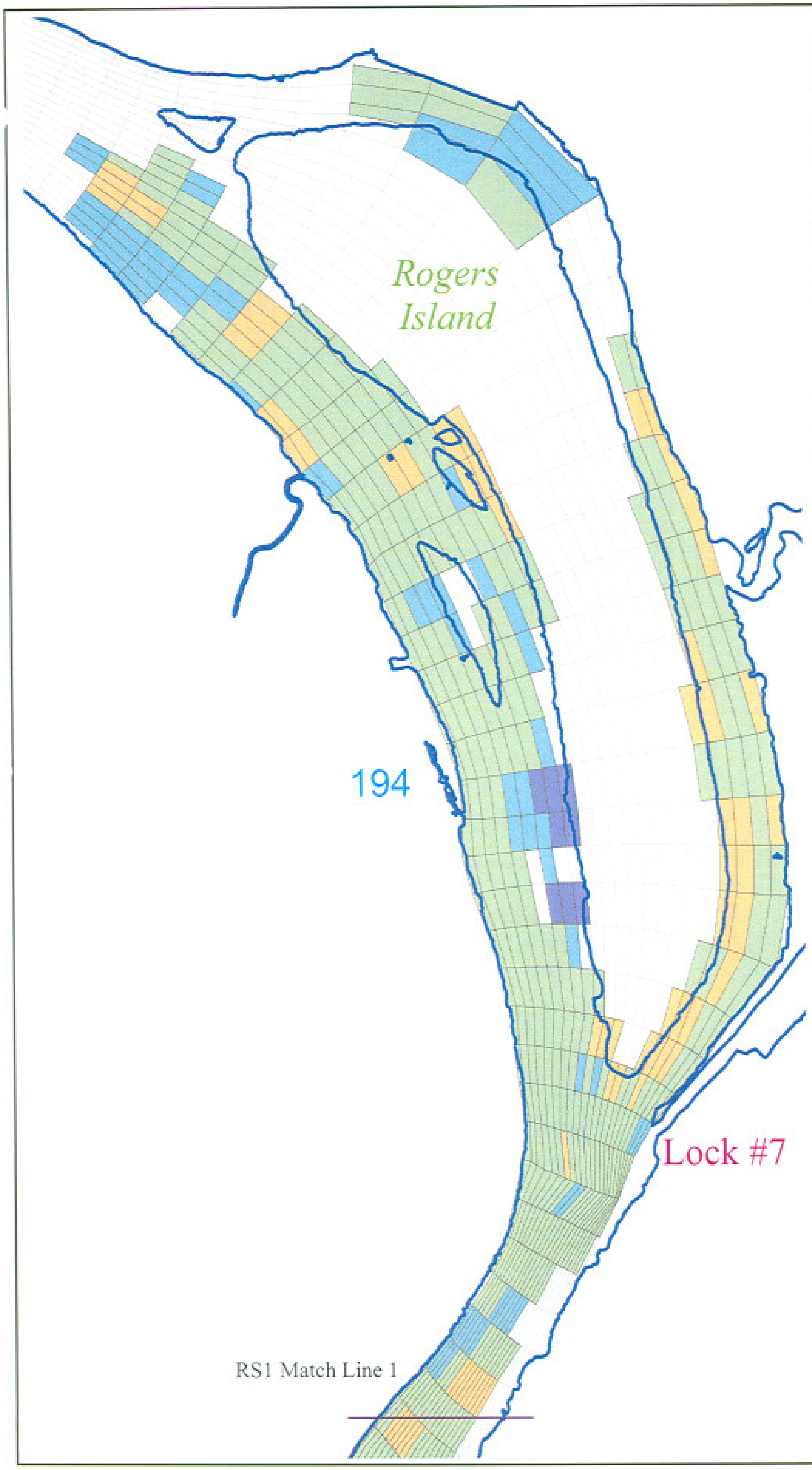

LOCATOR MAP OF THE UPPER HUDSON RIVER

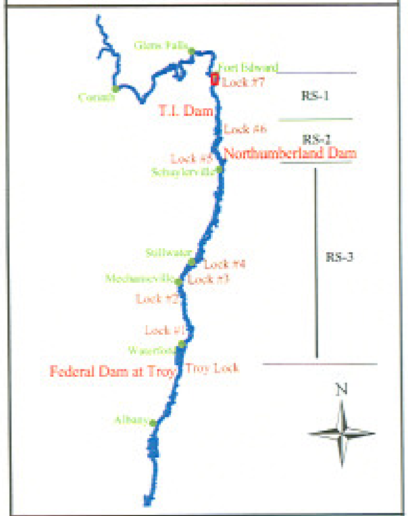

GRAPHIC SCALE

0 250 500 Feet

LEGEND

Avg. Total PCB Concentration (µg/g)

Fine and Medium Sand

- 0 - 1
- 1 - 10
- 10 - 100
- 100 - 1000
- >1000
- Shoreline
- Model Grid

Figure E-5-4a.

Average Total PCB Concentration in Fine and Medium Sand by Model Grid Cell.

QEA Quantitative Environmental Analysis, LLC

GENdes: 232

Aug 17, 2005.

MS - \\Zeus\E_Drive\GENrem\Working\GIS\maps\ArcGIS8_maps\model\maps\resuspension\PCB_Frac_Map.mxd

LOCATOR MAP OF THE UPPER HUDSON RIVER

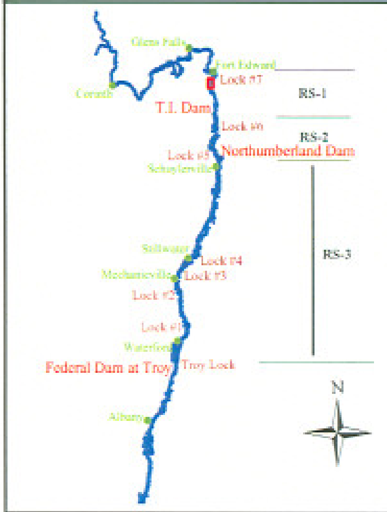

GRAPHIC SCALE

0 250 500 Feet

LEGEND

Avg. Total PCB Concentration (μg/g)

Fine and Medium Sand

- 0 - 1
- 1 - 10
- 10 - 100
- 100 - 1000
- >1000
- Shoreline
- Model Grid

Figure E-5-4b.

Average Total PCB Concentration in Fine and Medium Sand by Model Grid Cell.

GENdes: 232 Aug 17, 2005.

MS - \\Zeus\E_Drive\GENrem\Working\GIS\maps\ArcGIS8_maps\model\maps\resuspension\PCB_Frac_Map.mxd

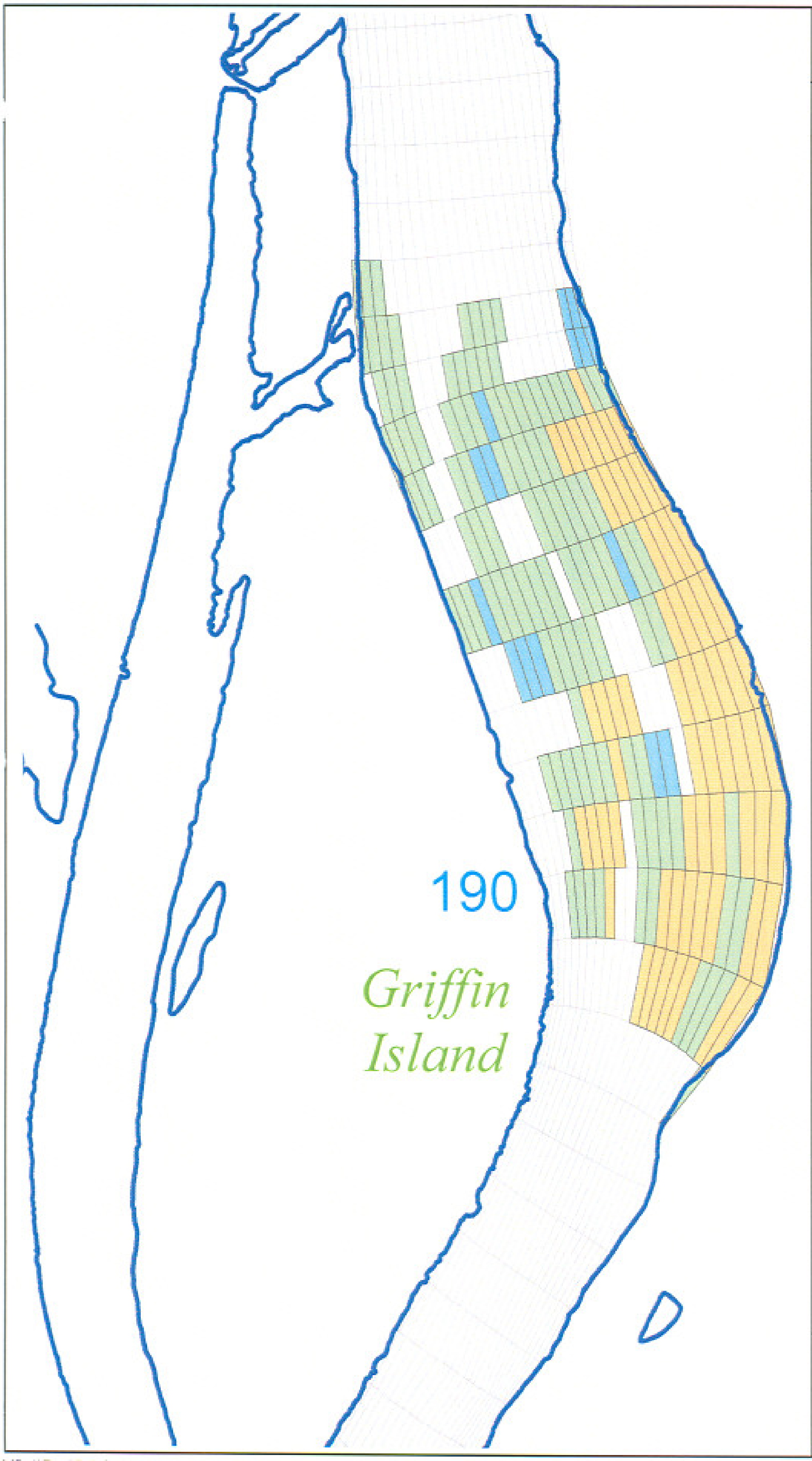

LOCATOR MAP OF THE UPPER HUDSON RIVER

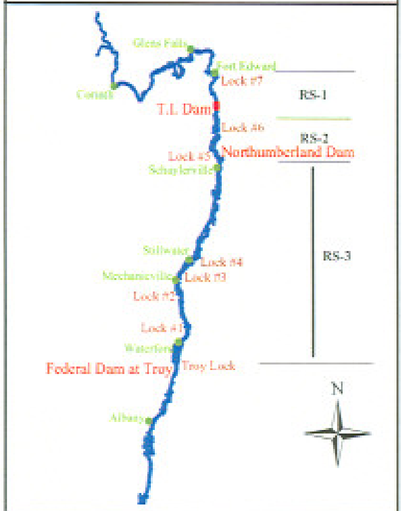

GRAPHIC SCALE

0 250 500 Feet

LEGEND

Avg. Total PCB Concentration (µg/g)

Fine and Medium Sand

- 0 - 1
- 1 - 10
- 10 - 100
- 100 - 1000
- >1000
- Shoreline
- Model Grid

Figure E-5-4c.

Average Total PCB Concentration in Fine and Medium Sand by Model Grid Cell.

QEA Quantitative Environmental Analysis, LLC

GENdes: 232 Aug 17, 2005.

MS - \\Zeus\E_Drive\GENrem\Working\GIS\maps\ArcGIS8_maps\model\maps\resuspension\PCB_Frac_Map.mxd

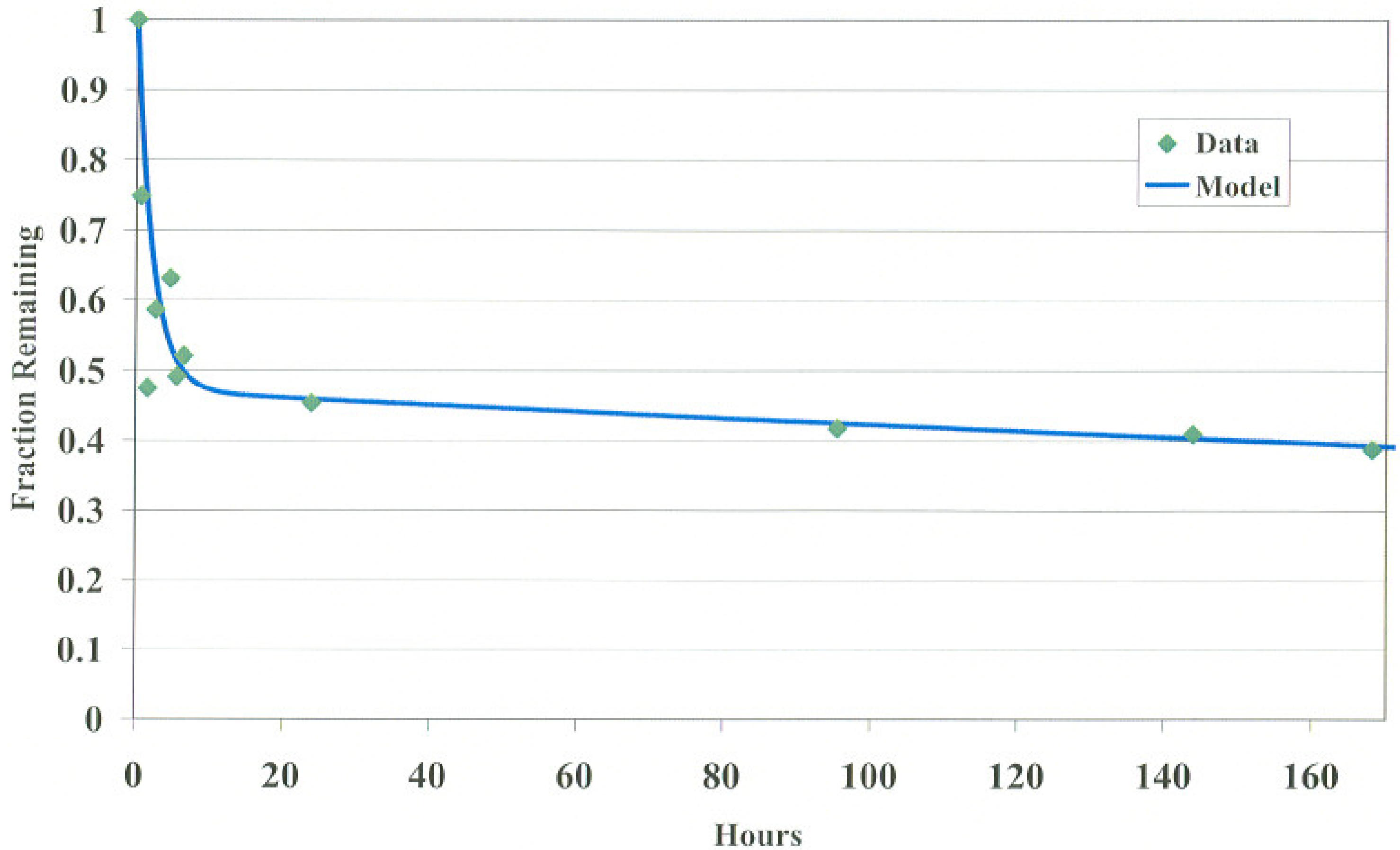

Figure E-5-5. Hudson River Sediment PCB desorption. Comparison of results of Carroll, et.al. (1994) and desorption sub-model calibration

\\dataw\d_drive\GENdas\Documents\Reports\IDR\Figure_E-5-5_model.xls

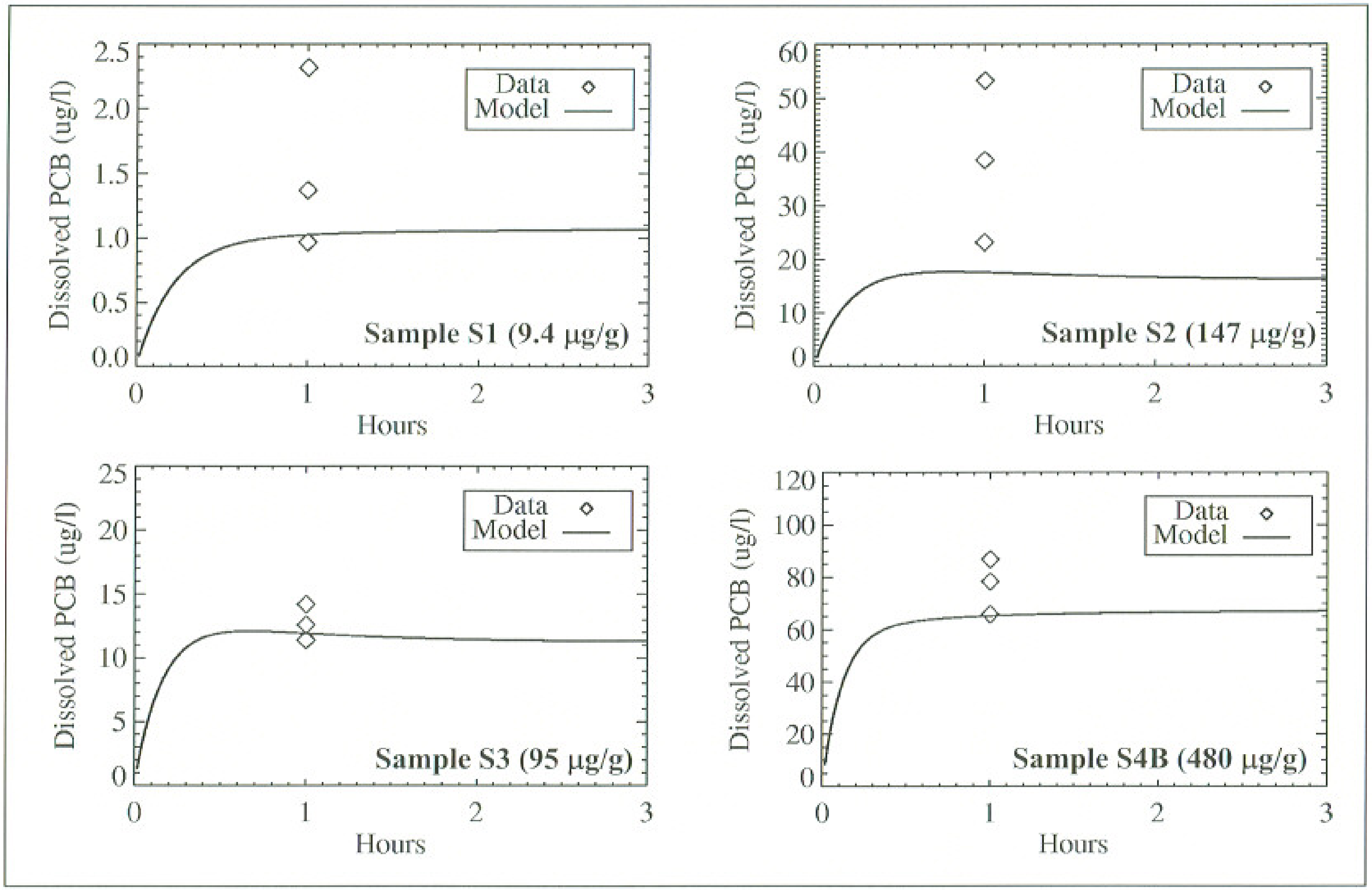

Figure E-5-6. Comparison of DRET Study results to desorption sub-model predictions

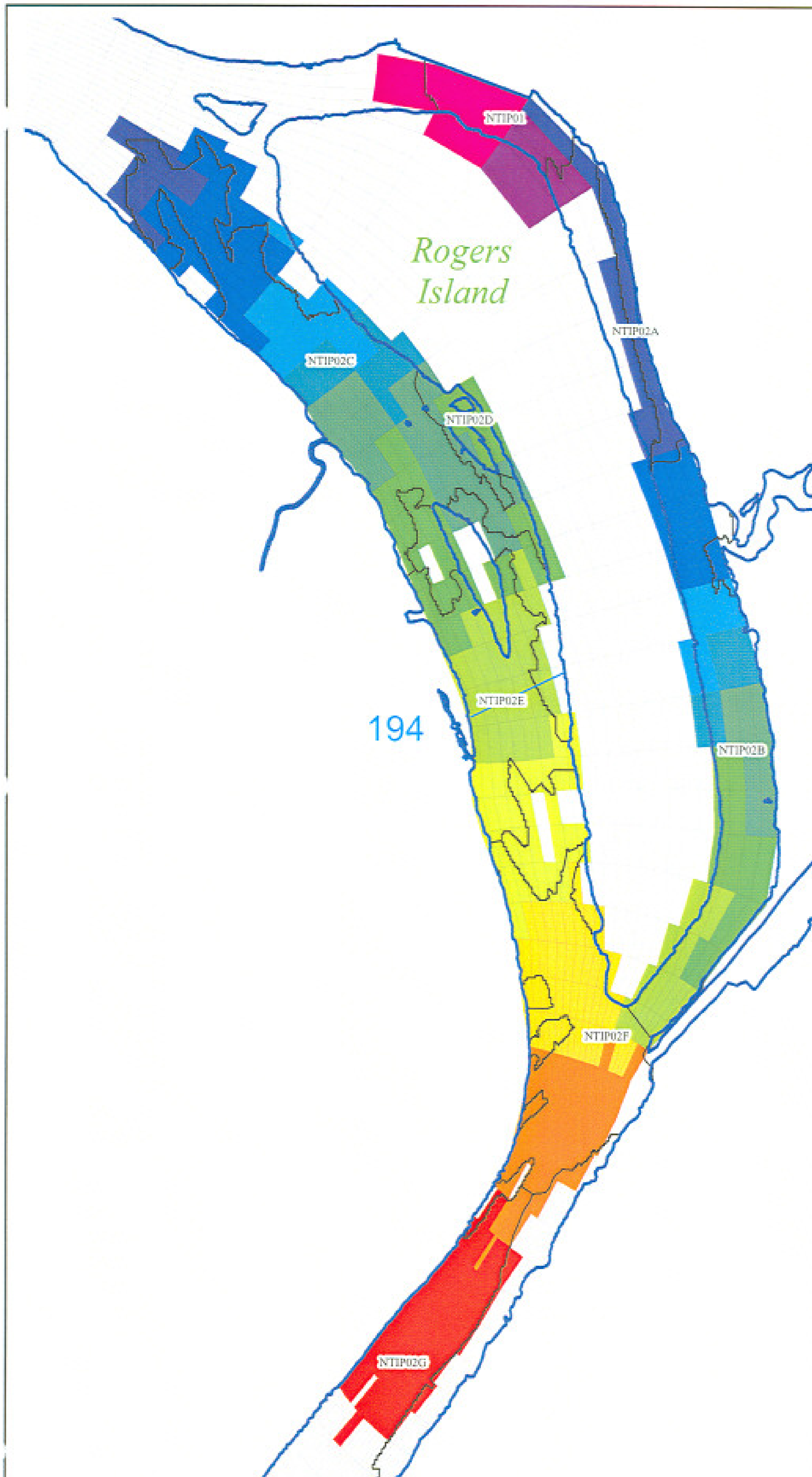

OCATOR MAP OF THE PPER HUDSON RIVER

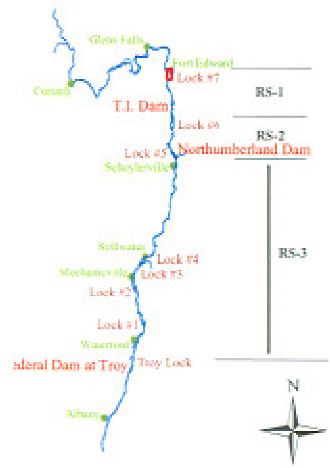

GRAPHIC SCALE

0 250 500 Feet

LEGEND

2007 Dredge Dates

- May 21 - May 31
- June 1 - June 10
- June 11 - June 20
- June 21 - June 30
- July 1 - July 10
- July 11 - July 20
- July 21 - July 31
- Aug 1 - Aug 10
- Aug 11 - Aug 20
- Aug 21 - Aug 31
- Sep 1 - Sep 10
- Sep 11 - Sep 20
- Sep 21 - Oct 2
- Dredge Areas

Figure E-6-1a.

Phase 1 Dredging Schedule Northern TIP

GE es:221

Aug 17, 2005

MS - \\Zeus\c_drive\GENrem\Working\GIS\maps\ArcGIS8_maps\model\maps\resuspension\Dredge_schedule_for_report_20050808.mxd

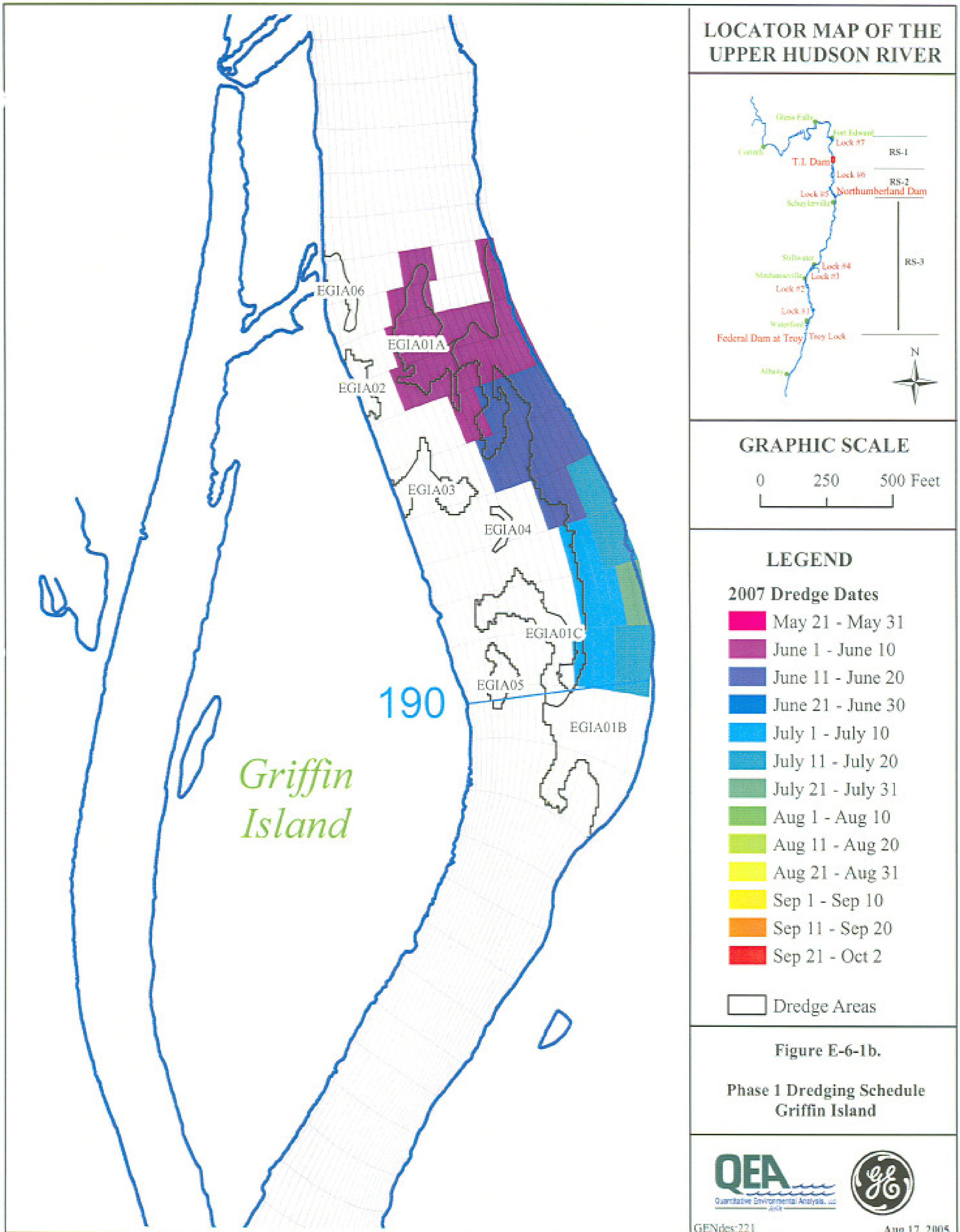

Figure E-6-1b.

Phase 1 Dredging Schedule Griffin Island

MS - \\Zeus\e_drive\GENrem\Working\GIS\maps\ArcGIS8_maps\model\maps\resuspension\Dredge_schedule_for_report_20050808.mxd

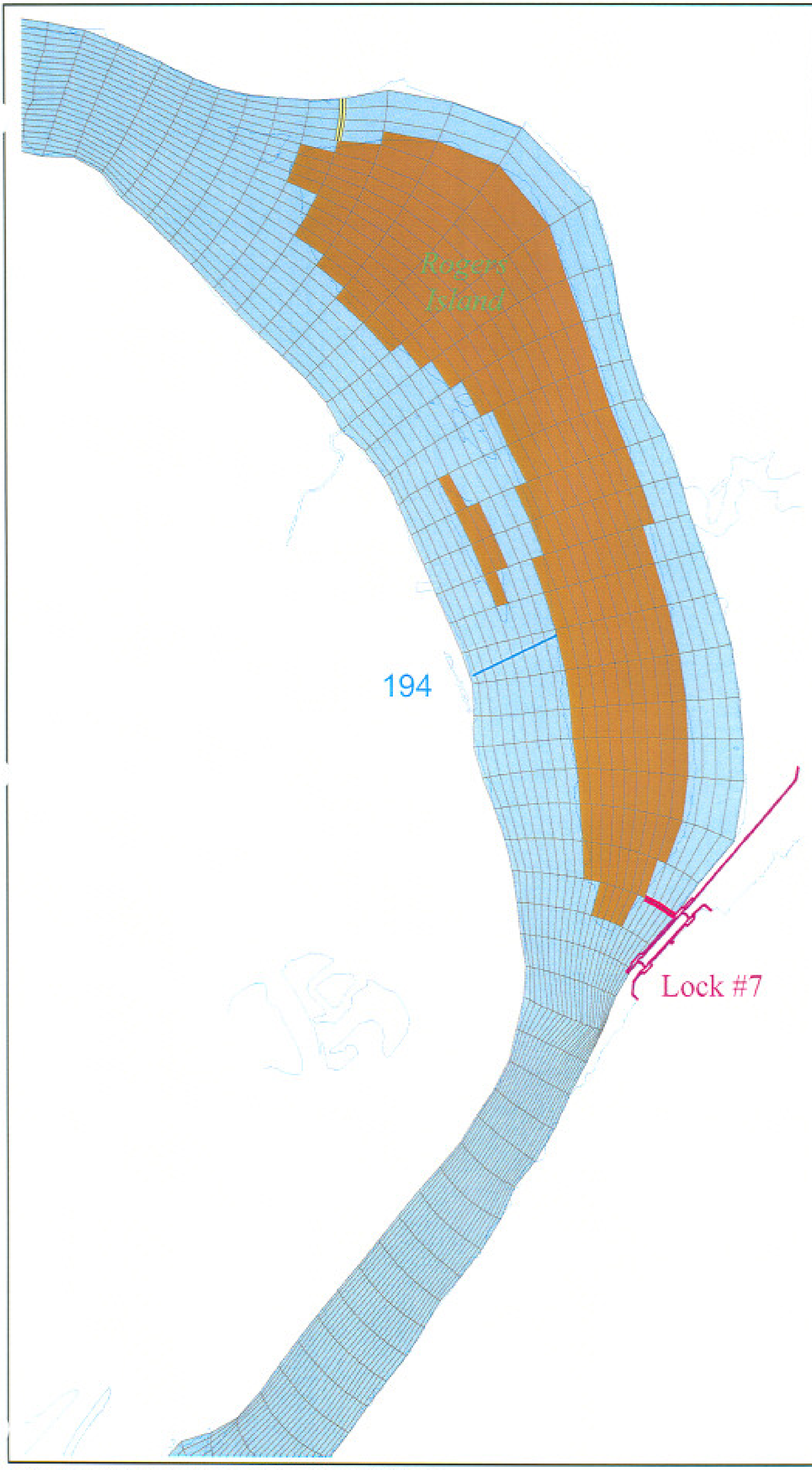

LOCATOR MAP OF THE UPPER HUDSON RIVER

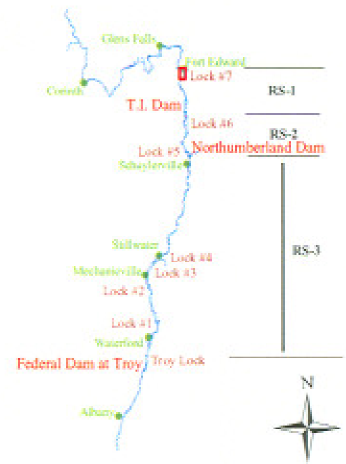

GRAPHIC SCALE

0 250 500 Feet

LEGEND

- River Miles
- Shore Line
- Dams and Locks
- Island/Land Elements
- Channel Elements
- Silt Curtain
- Sheetpile

UPPER HUDSON RIVER STUDY AREA

Figure E-6-2.

Model Implementation of the Sheet Pile and Silt Curtain near Rogers Island

QEA Quantitative Environmental Analysis, LLC

GENdes

Jul 29, 2005.

DN - \\daleel\d_drive\GENdes\Documents\Reports\IDR\Figure_E-6-2.mxd

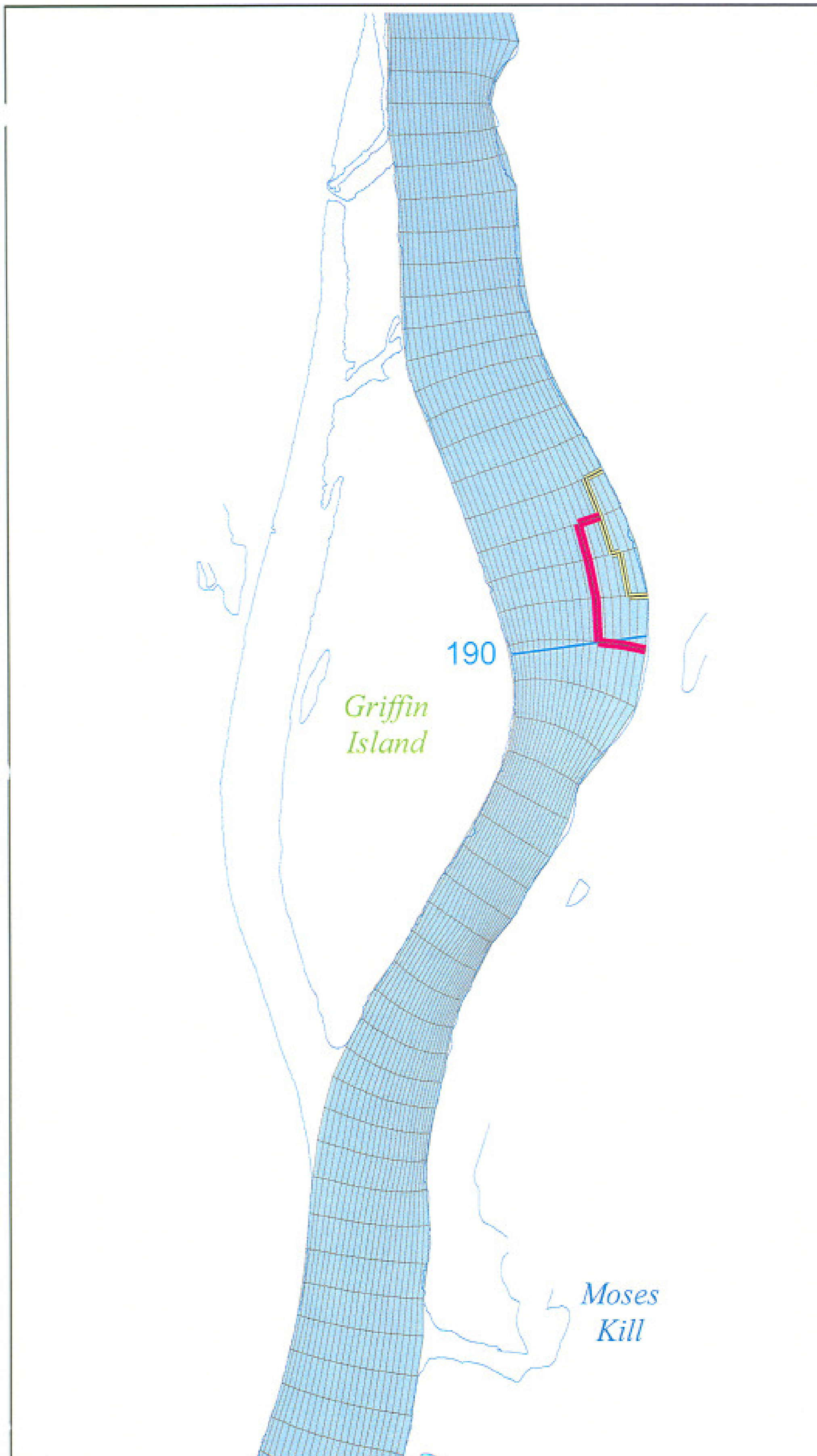

LOCATOR MAP OF THE UPPER HUDSON RIVER

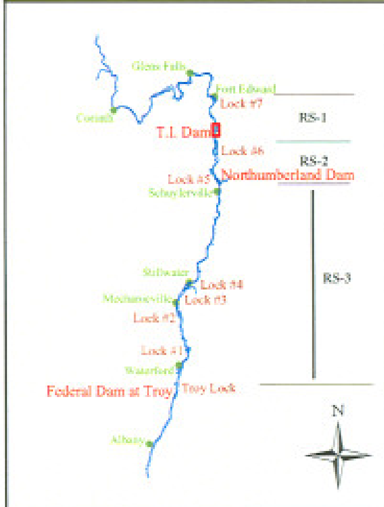

GRAPHIC SCALE

0 250 500 Feet

LEGEND

- River Miles
- Shore Line
- Dams and Locks
- Island/Land Elements
- Channel Elements
- Sheetpile
- Silt Curtain

UPPER HUDSON RIVER STUDY AREA

Figure E-6-3.

Model Implementation of the Sheet Pile and Silt Curtain near Griffin Island

QEA Quantitative Environmental Analysis, LLC

GENdes

Jul 29, 2005.

DN - \\Daleel\D_DRIVE\GENdes\Documents\Reports\IDR\Figure_E-6-3.mxd

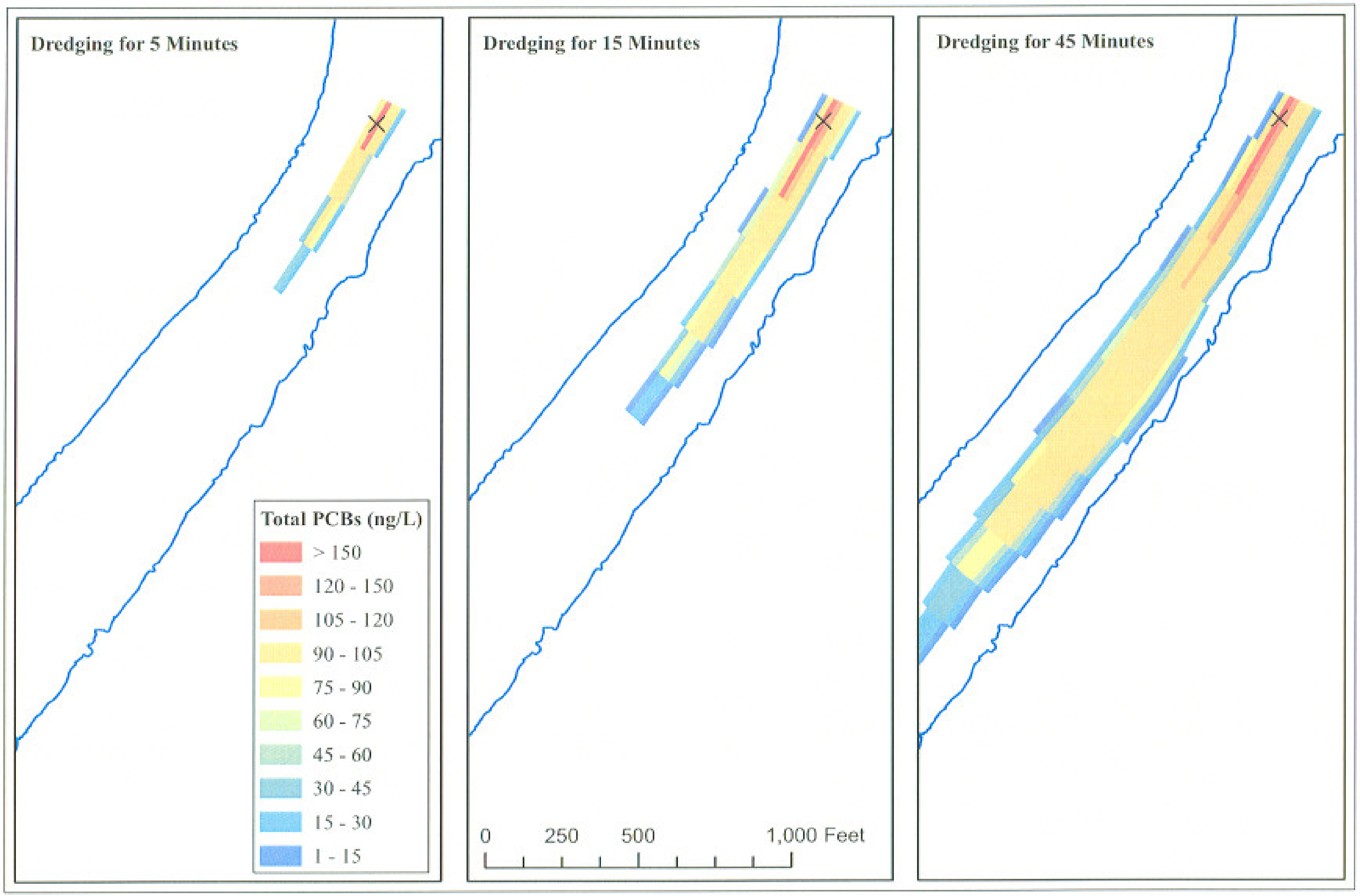

Figure E-7-1. Development of Typical Dredge Resuspension PCB Plume.

Location of dredge head is mid-channel and denoted by 'X'

\\Sam\d_drive\jobs\gendes\analysis\plume_figures\gis\plume_development.mxd

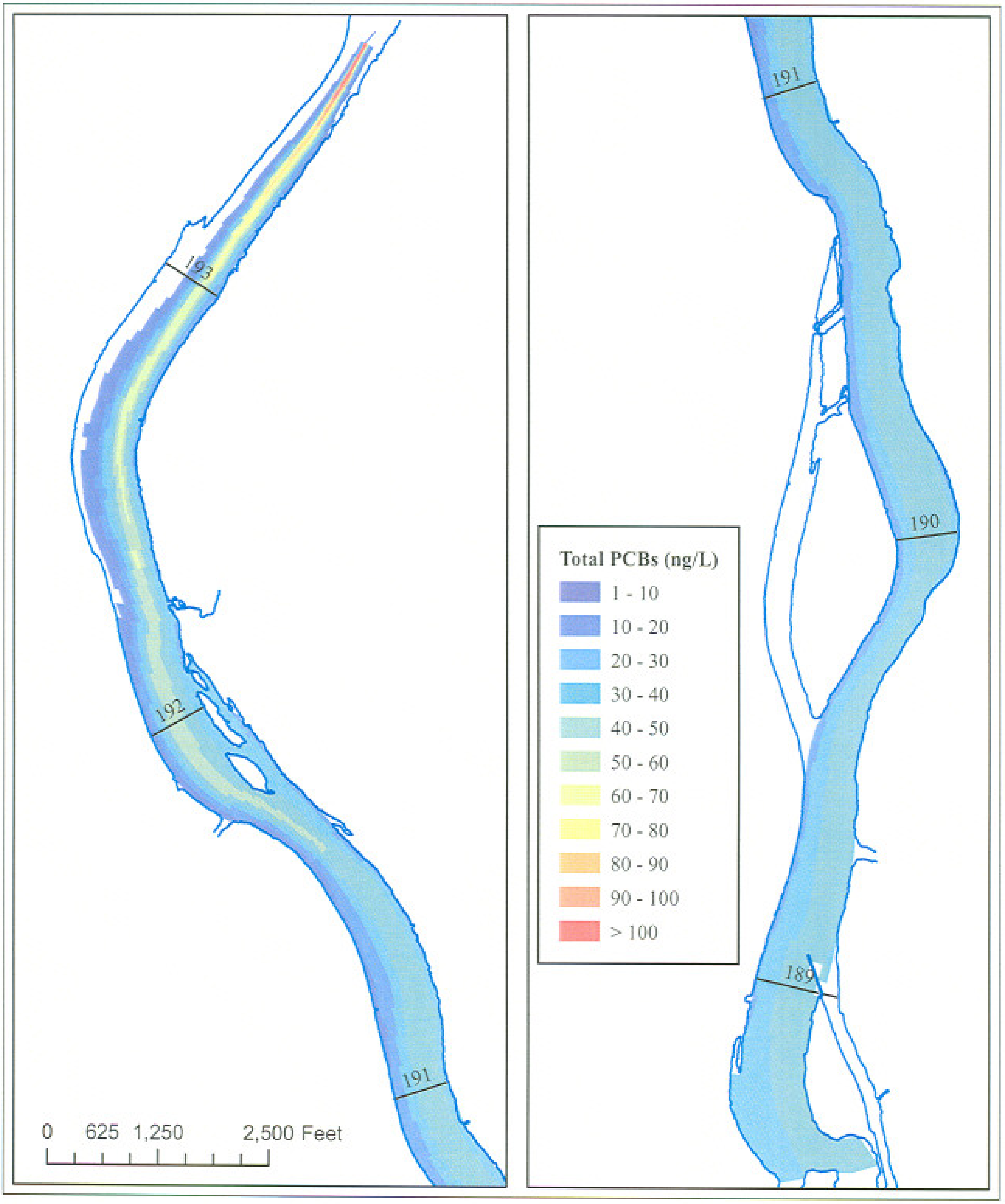

Figure E-7-2. Fully Developed Dredge Resuspension PCB Plume for a Mid-Channel Operation.

\\Sam\d_drive\jobs\gendes\analysis\plume_figures\gis\plume_steady_state_bank_release.mxd

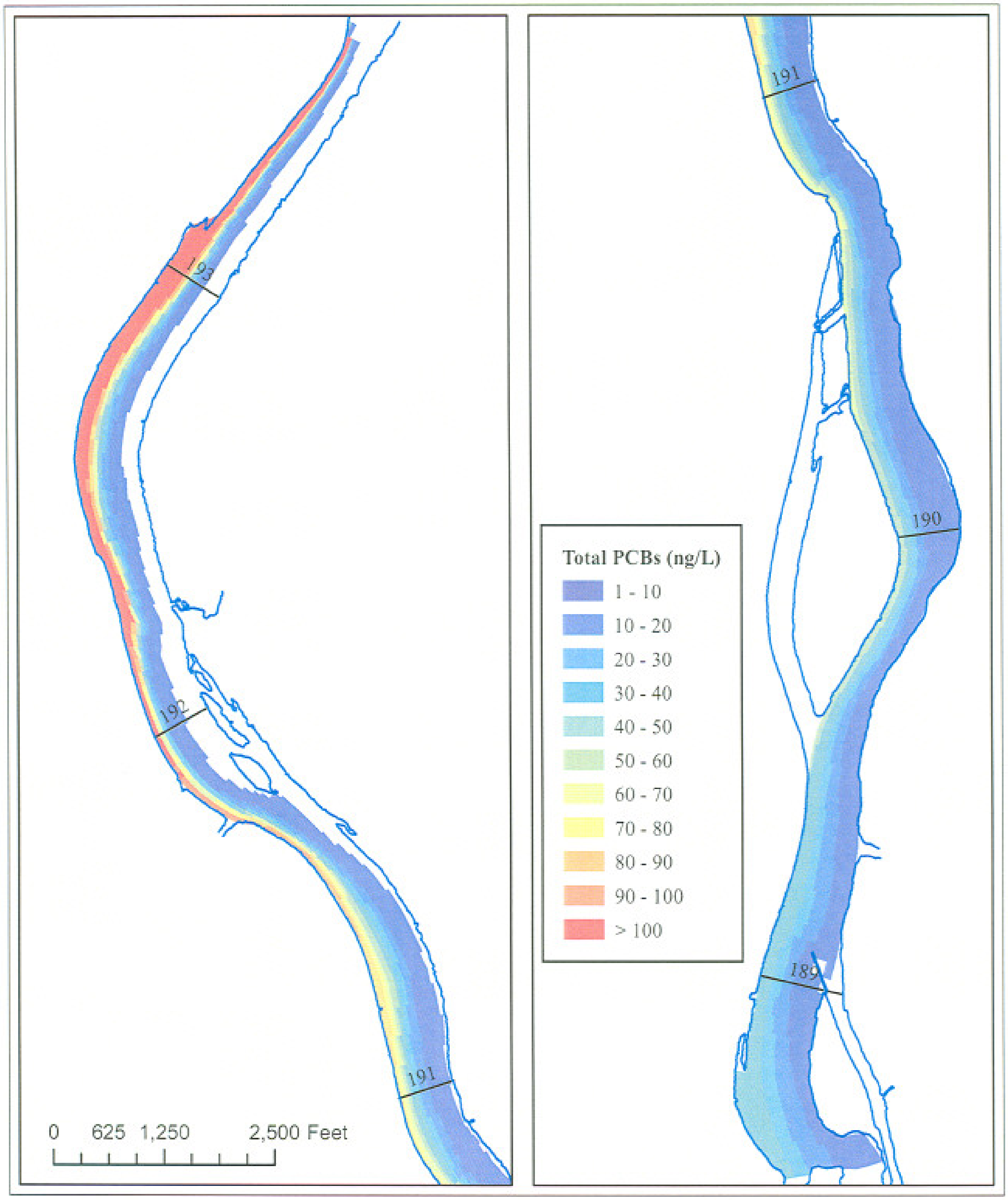

Figure E-7-3. Fully Developed Dredge Resuspension PCB Plume for a Near-Shore Operation.

\\Sam\d_drive\jobs\gendes\analysis\plume_figures\gis\plume_steady_state_bank_release.mxd

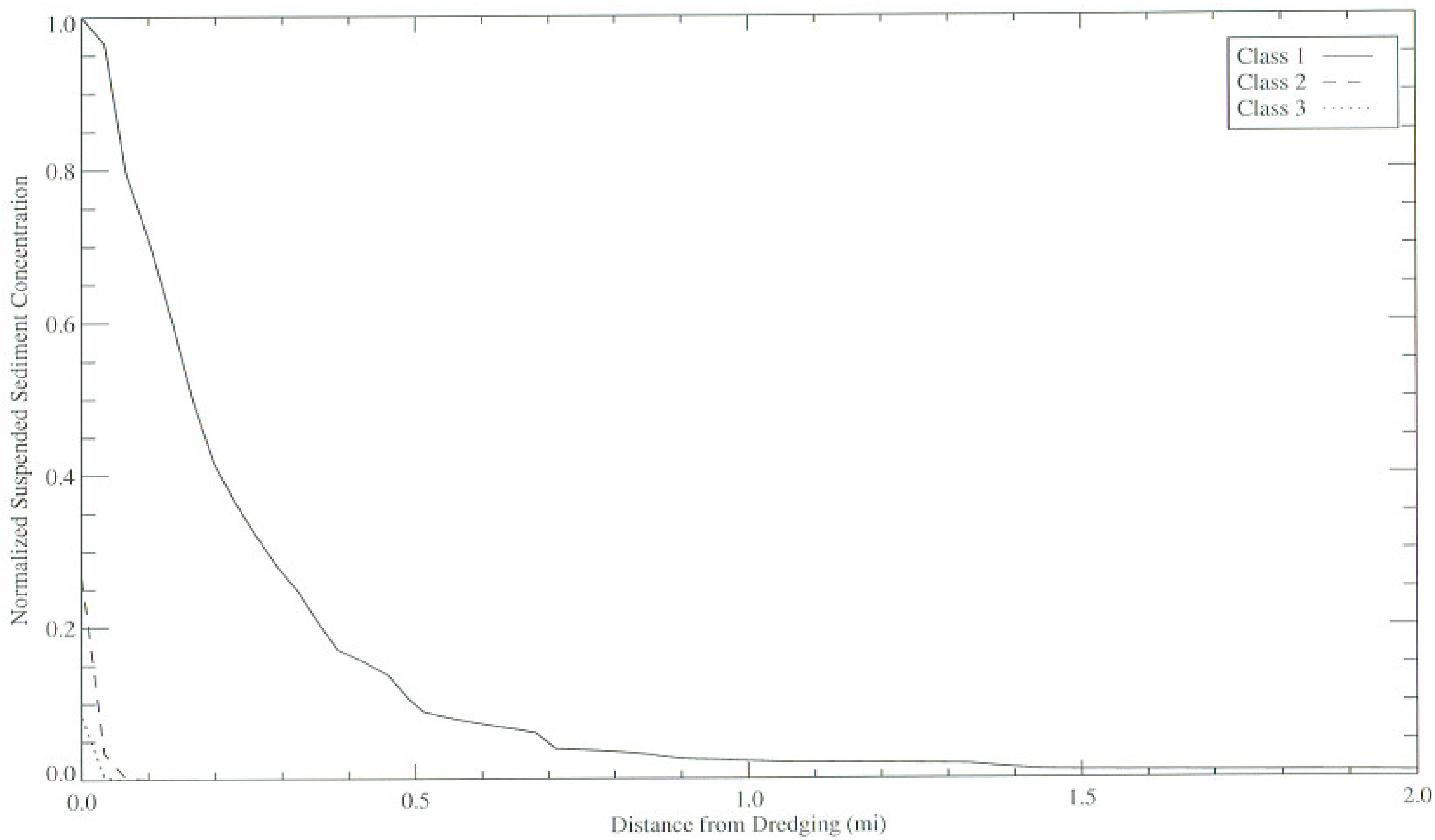

Figure E-7-4. Typical Suspended Sediment Dredge Plume Centerline Concentrations for Near-Shore Release and Median Flow (2,800 cfs)

model runs: doc0508-06a

haz - D:\Harry\GENdes\Report\sed_spatial.pro
Wed Aug 17 15:15:41 2005

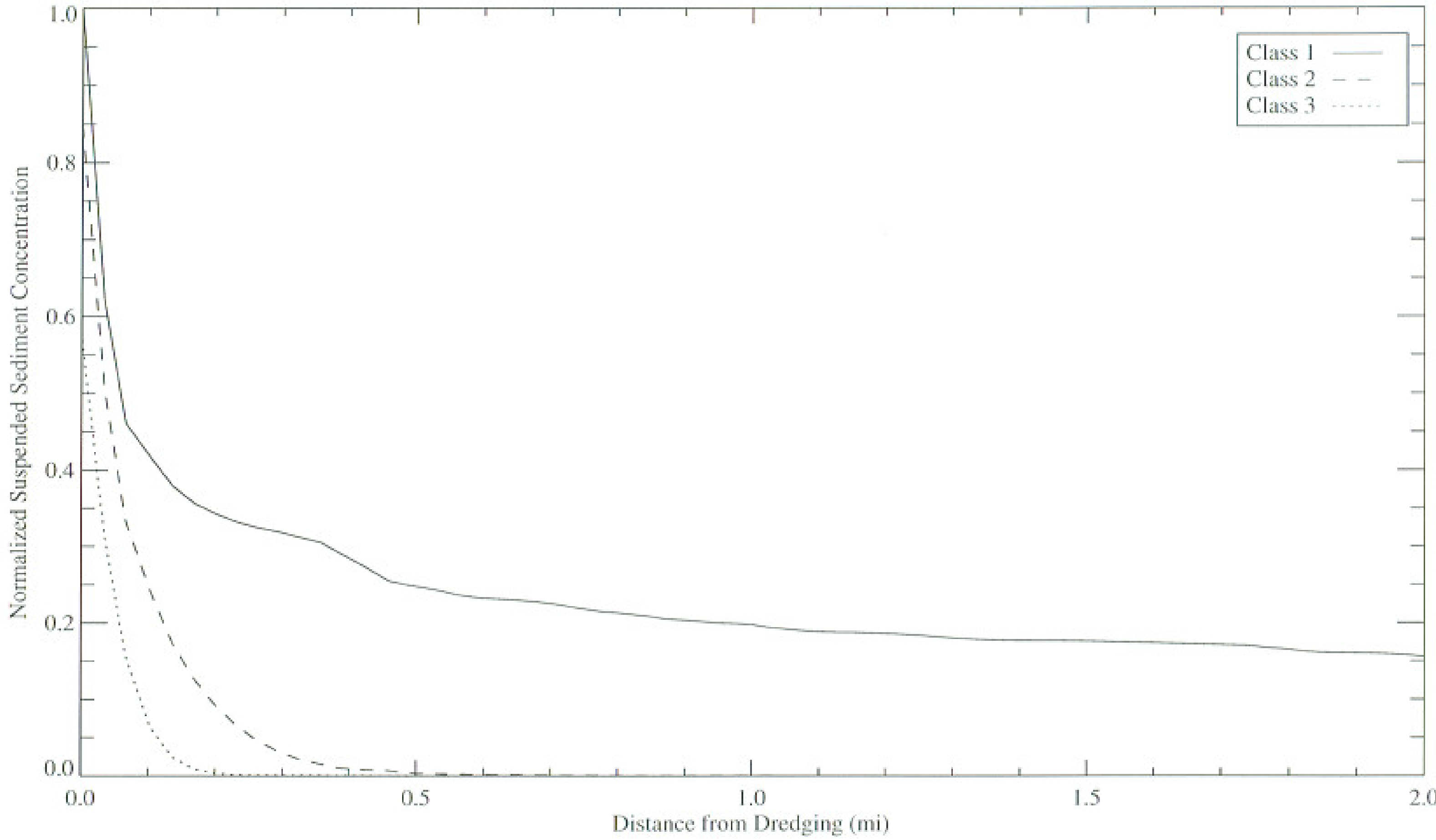

Figure E-7-5. Typical Suspended Sediment Dredge Plume Centerline Concentrations for Mid-Channel Release and Median Flow (2,800 cfs)

model runs: doc0508-05a

haz - D:\Harry\GENdes\Report\sed_spatial.pro
Wed Aug 17 15:15:28 2005

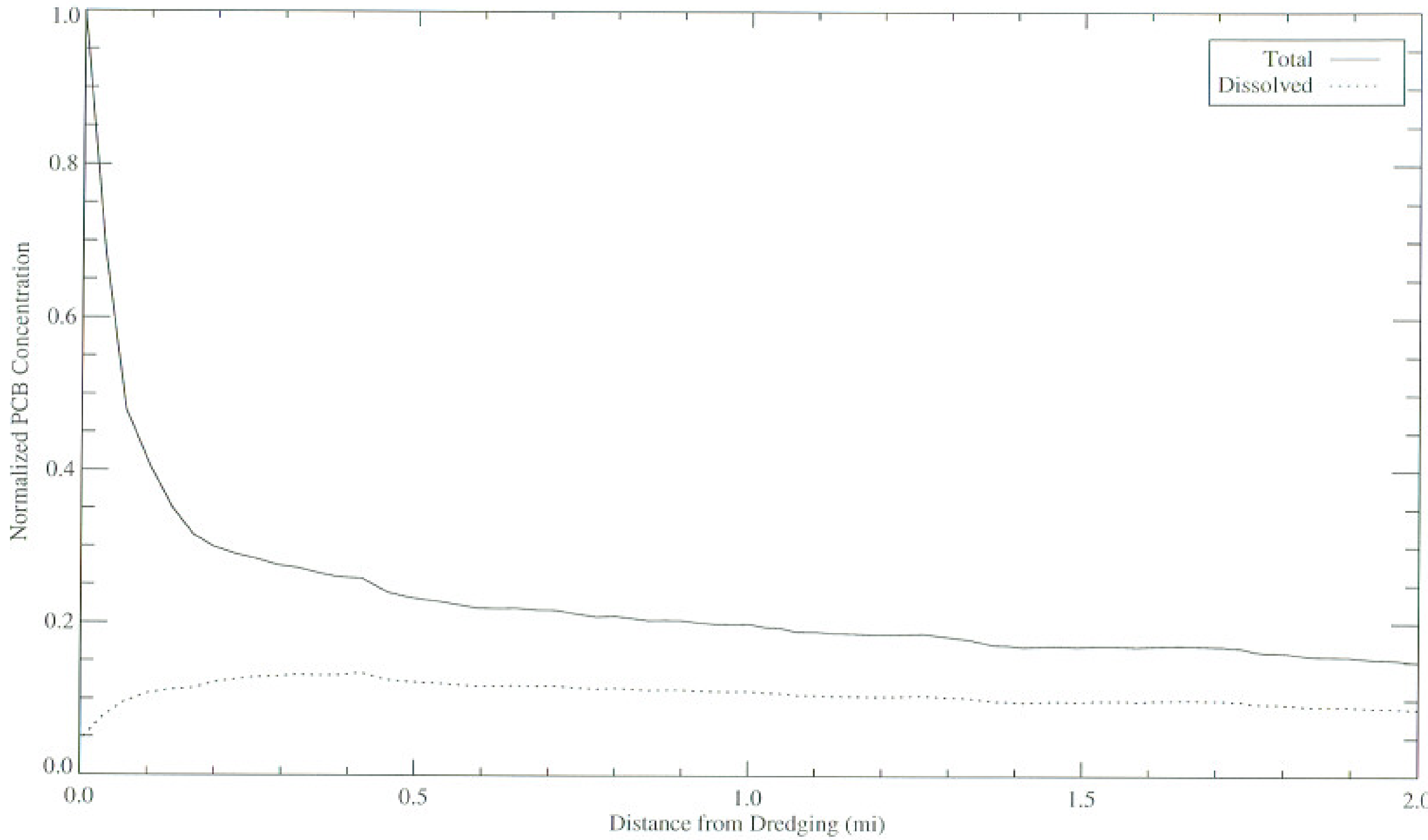

Figure E-7-6. Typical PCB Dredge Plume Centerline Concentrations for Mid-Channel Release and Median Flow (2,800 cfs)

model runs: doc0508-05a

haz - D:\Harry\GENdes\Report\total_diss_pcb_rpt.pro
Wed Aug 17 15:16:26 2005

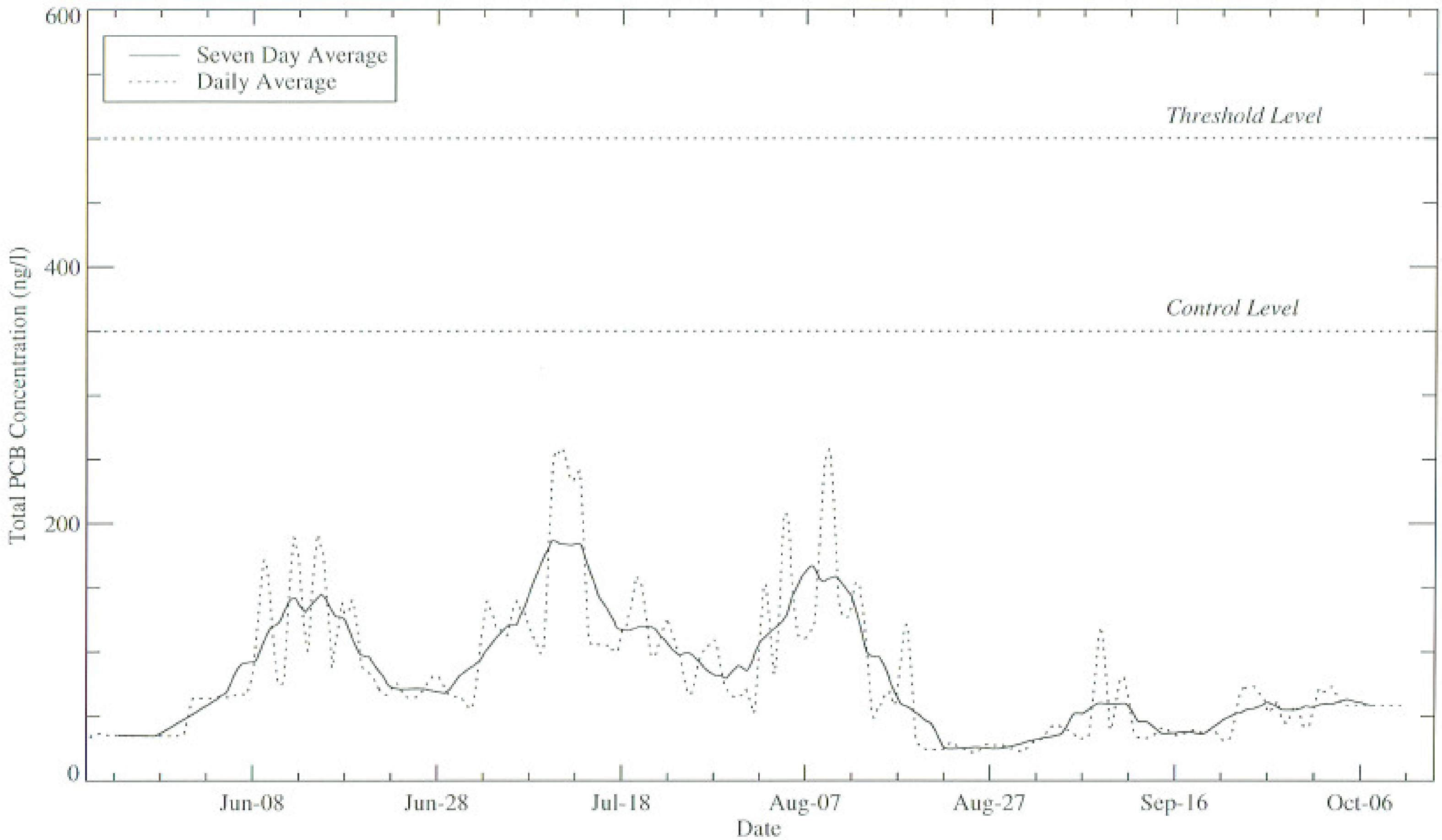

Figure E-7-7. Average TID Total PCB Concentration (including baseline) for Dredging with No Control Structures, 0.35% Loss and Median Flow

Dredge Plan 050805

model run: plan0508-04

haz - D:\Harry\GENdes\Report\tid_avg_pcb_7day.pro
Wed Aug 17 15:19:23 2005

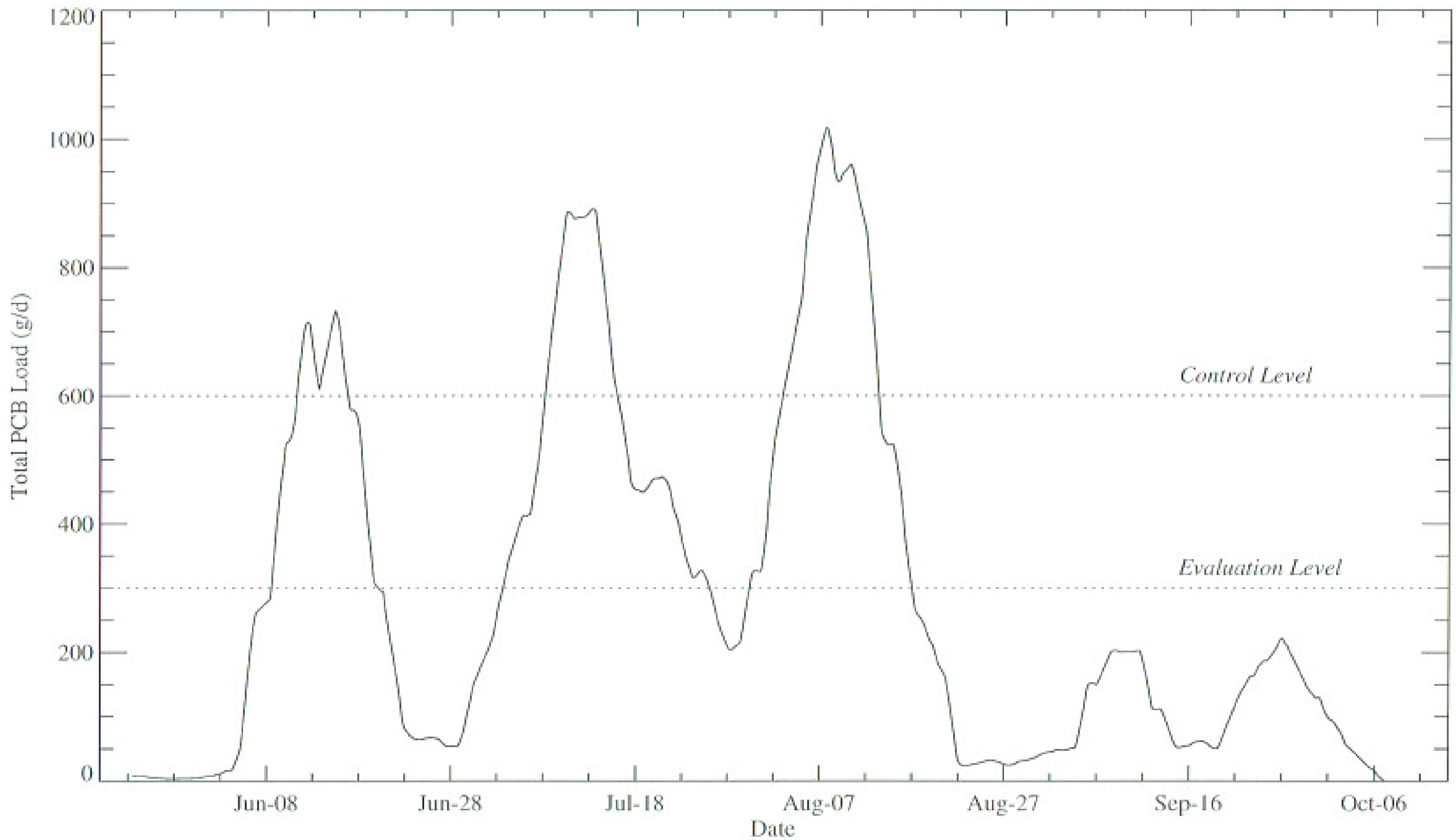

Figure E-7-8. Seven-Day Average TID Total PCB Load Above Baseline for Dredging with No Control Structures, 0.35% Loss and Median Flow

Dredge Plan 050805

model run: plan0508-04

haz - D:\Harry\GENdes\Report\tid_pcb_load_7day.pro
Wed Aug 17 15:17:58 2005

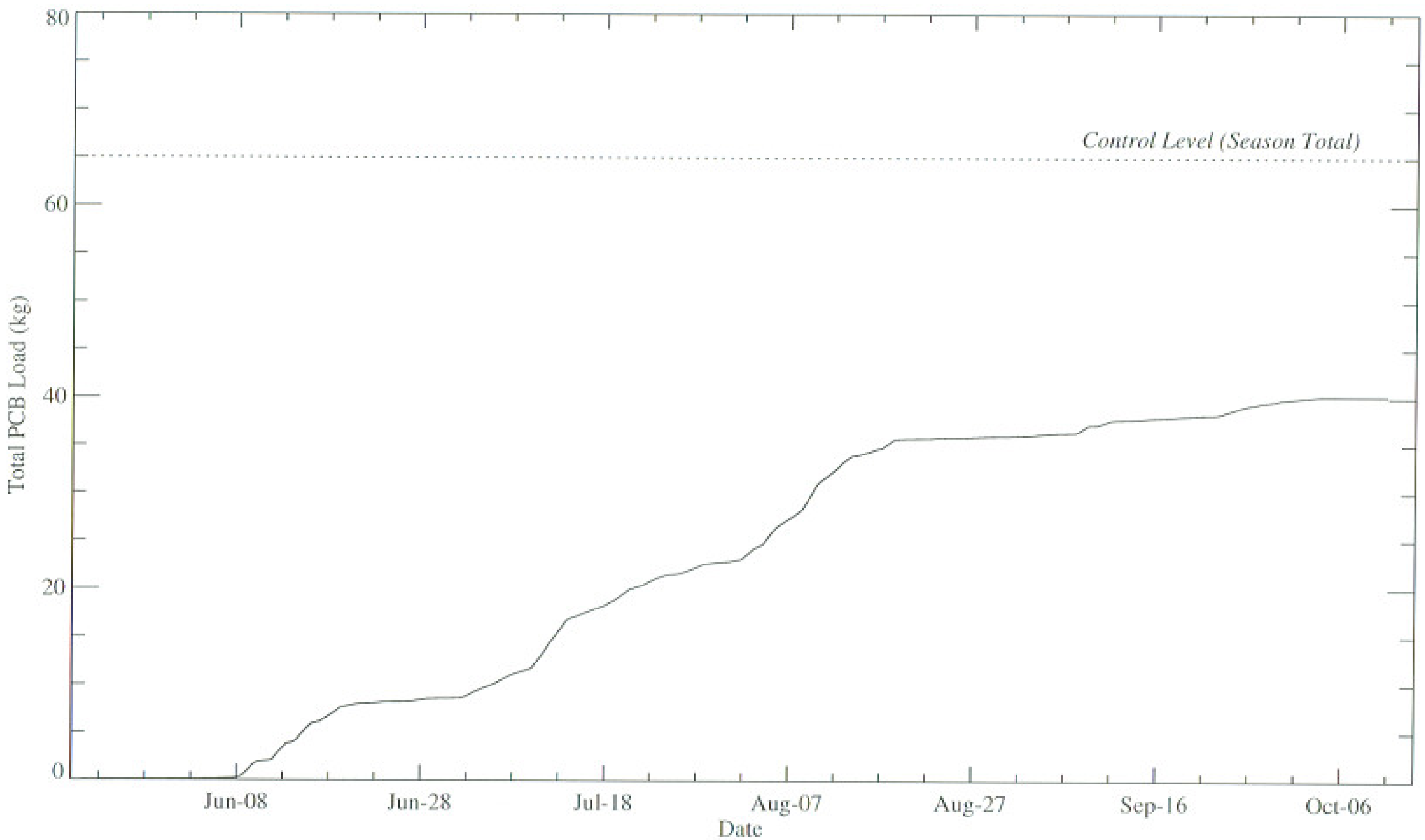

Figure E-7-9. Cumulative TID Total PCB Load Above Baseline for Dredging with No Control Structures, 0.35% Loss and Median Flow

Dredge Plan 050805

model run: plan0508-04

haz - D:\Harry\GENdes\Report\tid_pcb_load_cum.pro
Wed Aug 17 15:17:25 2005

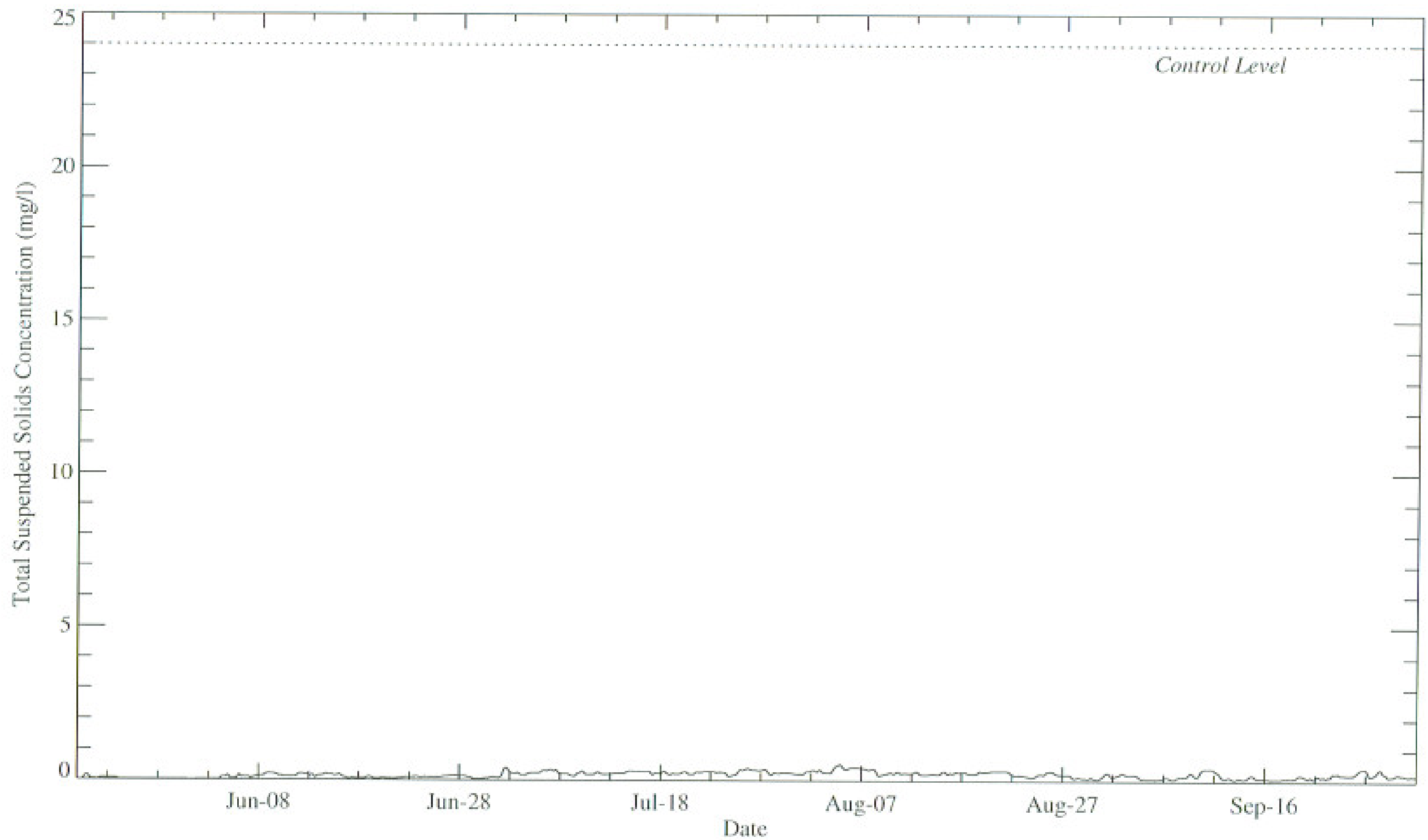

Figure E-7-10. Six Hour Average TID Total TSS Concentration Above Baseline Dredging with No Control Structures, 0.35% Loss and Median Flow

Dredge Plan 050805

model run: plan0508-04

haz - D:\Harry\GENdes\Report\tid_avg_tss_6hour.pro
Wed Aug 17 15:19:49 2005

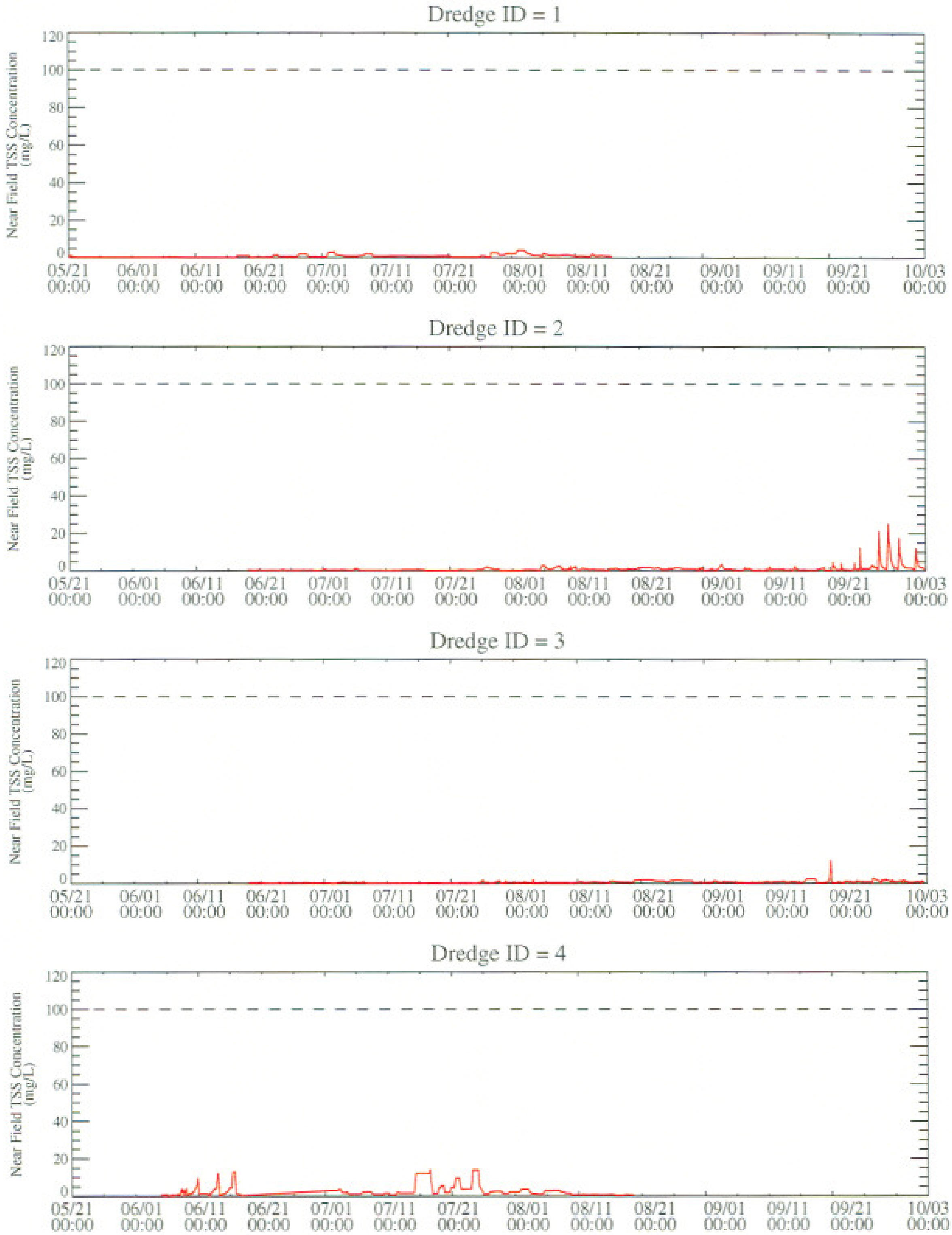

Figure E-7-11. Six-hour average TSS at near field monitoring stations (300 m downstream) with no control structures.

lz - D:\GENdes\Analysis\Model_Outputs\EFDC_Outputs\near_field_tss\get_near_field_tss.pro
Wed Aug 17 21:33:53 2005

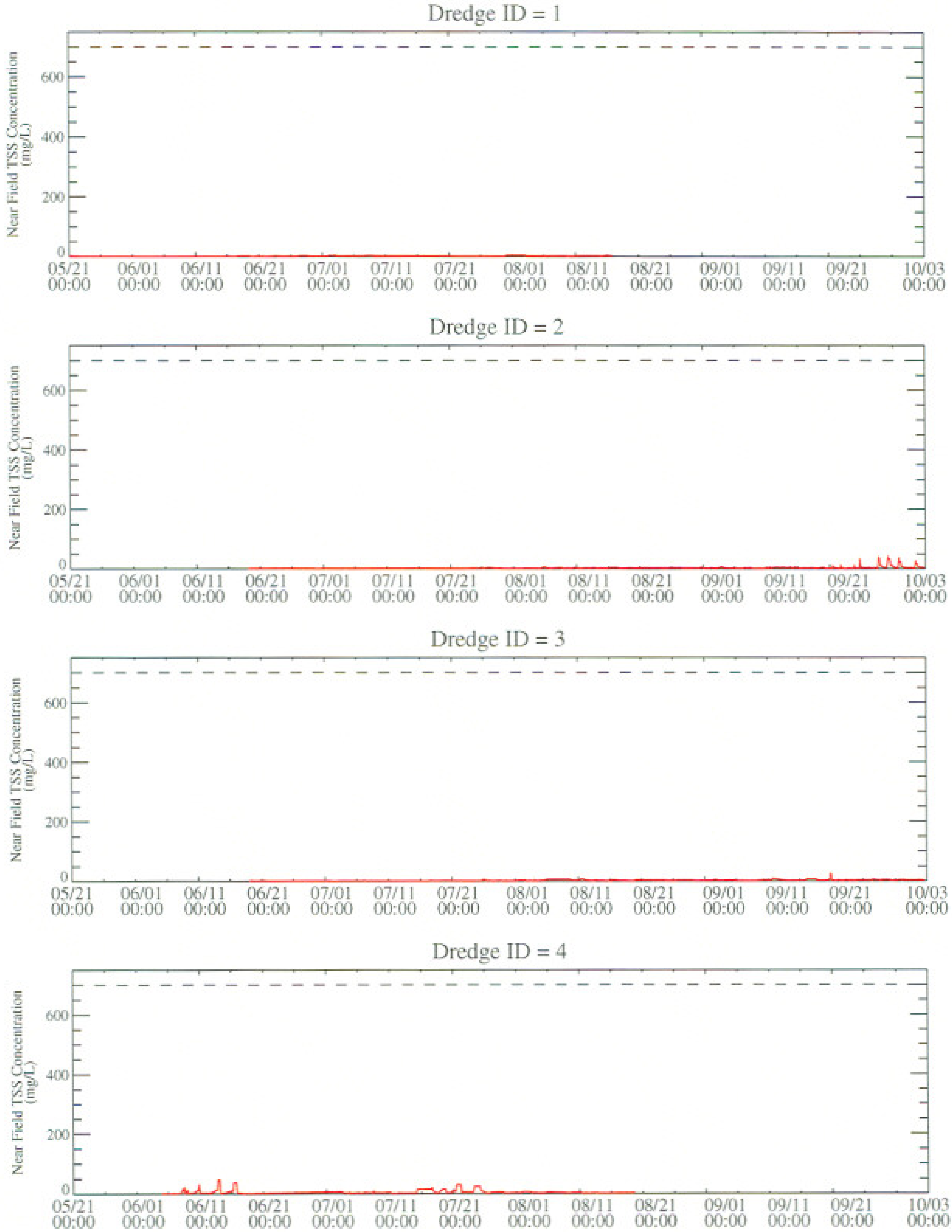

Figure E-7-12. Three-hour average TSS at near field monitoring stations (100 m downstream) with no control structures.

lz - D:\GENdes\Analysis\Model_Outputs\EFDC_Outputs\near_field_tss\get_near_field_tss.pro
Wed Aug 17 21:20:32 2005

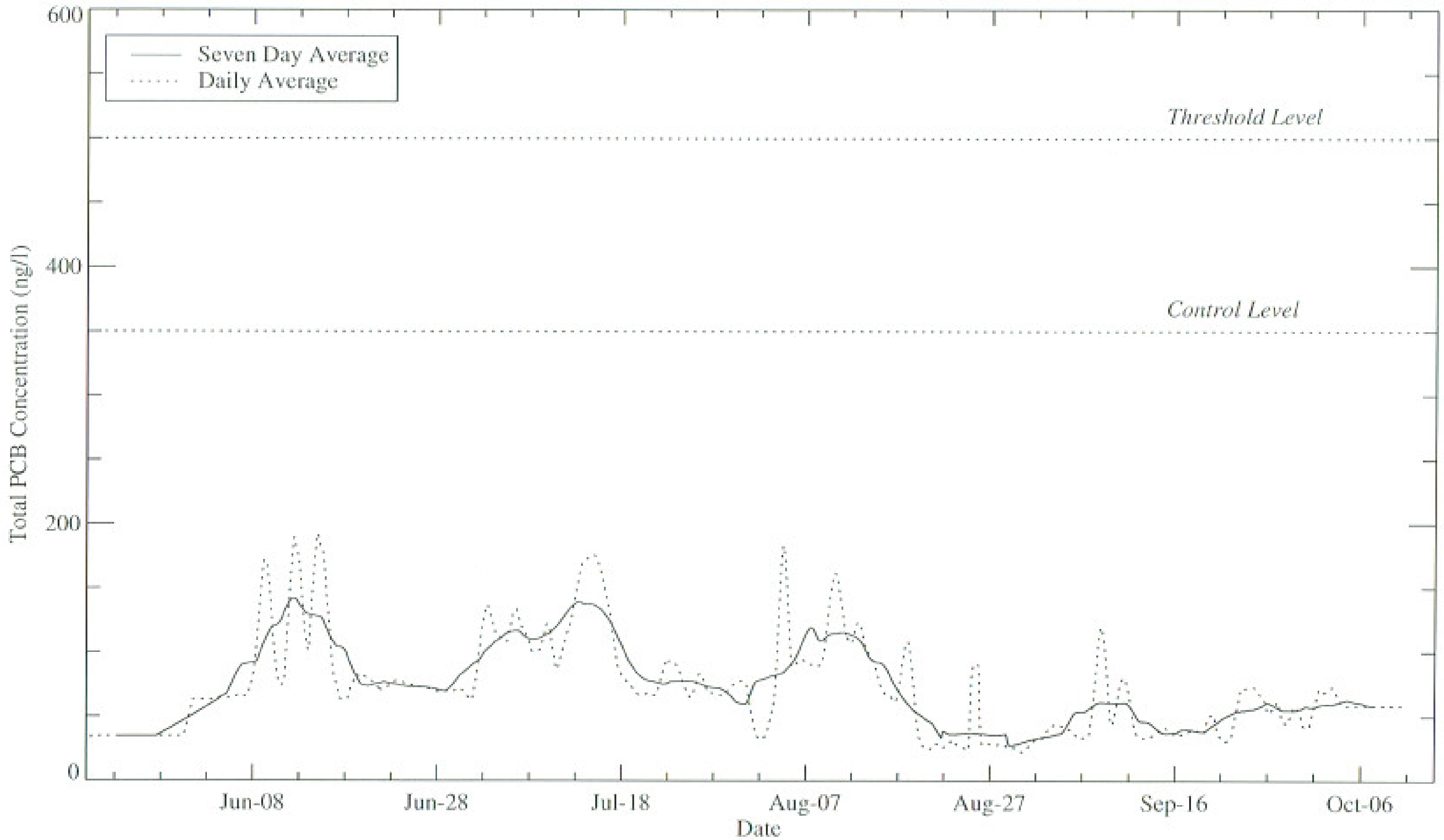

Figure E-7-13. Average TID Total PCB Concentration (including baseline) for Dredging with NTIP and EGIA Control Structures, 0.35% Loss and Median Flow

Dredge Plan 050805

model run: plan0508-05

haz - D:\Harry\GENdes\Report\tid_avg_pcb_7day.pro
Wed Aug 17 15:19:24 2005

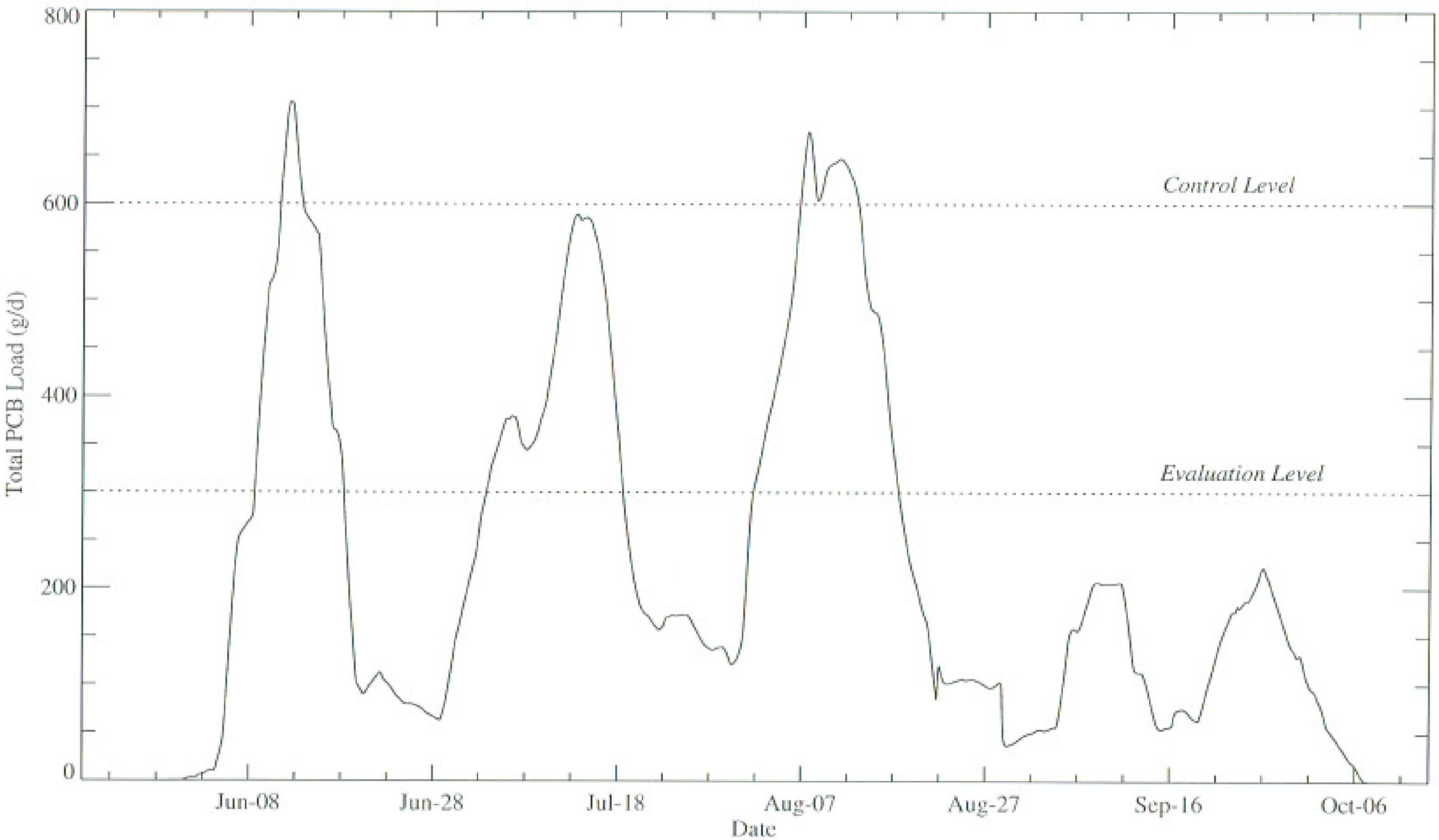

Figure E-7-14. Seven-Day Average TID Total PCB Load Above Baseline for Dredging with NTIP and EGIA Control Structures, 0.35% Loss and Median Flow

Dredge Plan 050805

model run: plan0508-05

haz - D:\Harry\GENdes\Report\tid_pcb_load_7day.pro
Wed Aug 17 15:17:59 2005

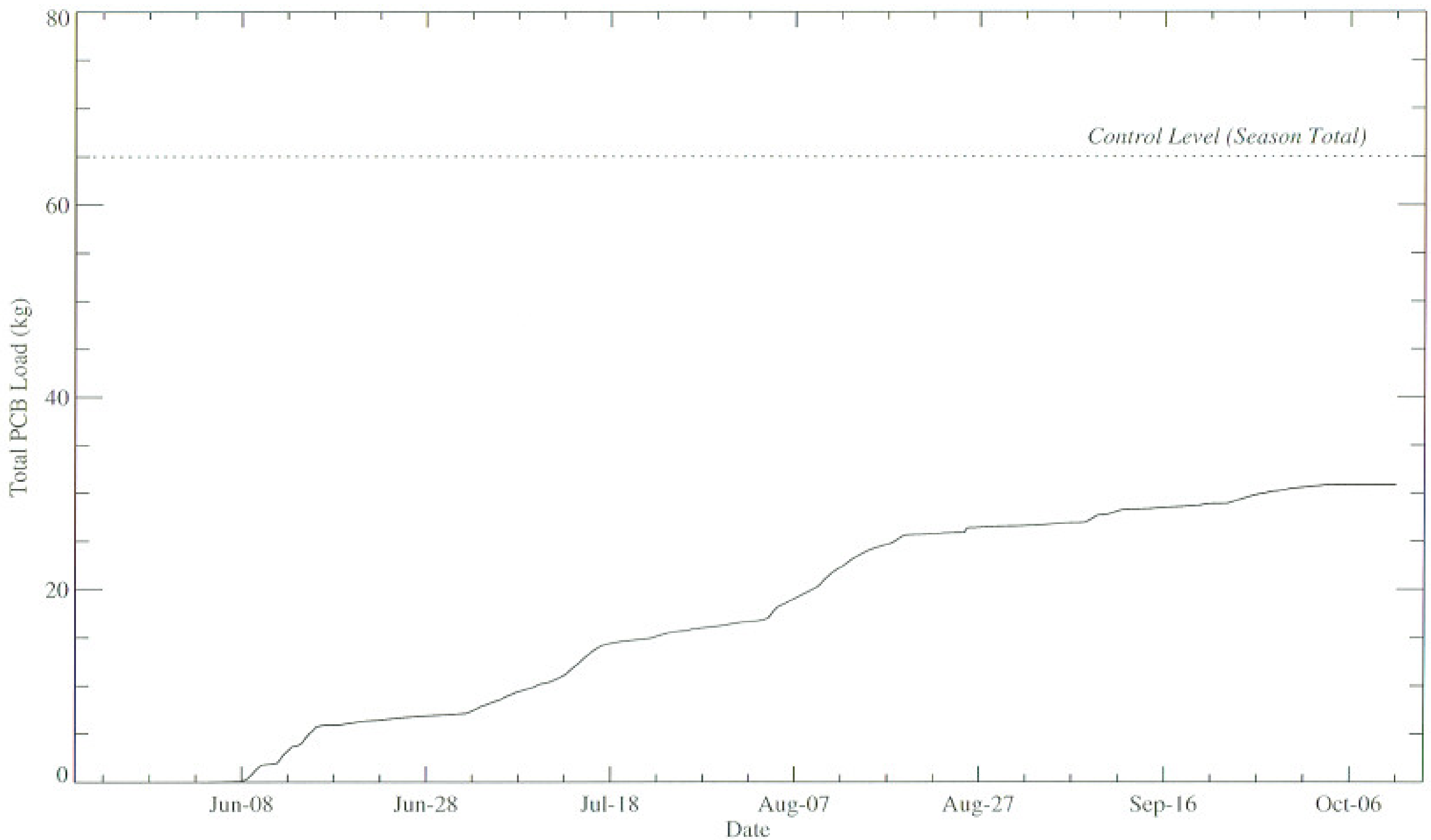

Figure E-7-15. Cumulative TID Total PCB Load Above Baseline for Dredging with NTIP and EGIA Control Structures, 0.35% Loss and Median Flow

Dredge Plan 050805

model run: plan0508-05

haz - D:\Harry\GENdes\Report\tid_pcb_load_cum.pro
Wed Aug 17 15:17:26 2005

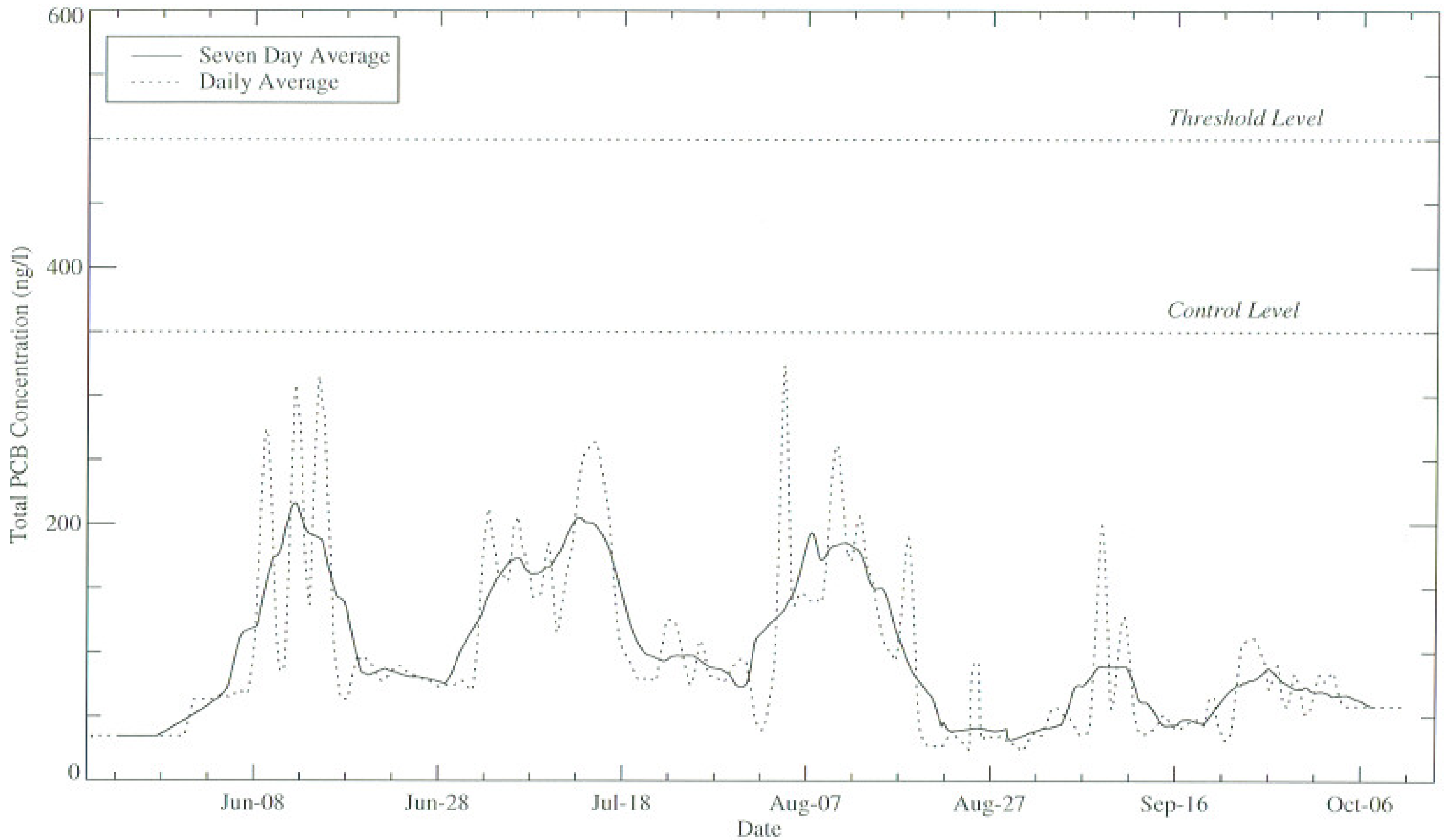

Figure E-7-16. Average TID Total PCB Concentration (including baseline) for Dredging with NTIP and EGIA Control Structures, 0.70% Loss and Median Flow

Dredge Plan 050805

model run: plan0508-06

haz - D:\Harry\GENdes\Report\tid_avg_pcb_7day.pro
Wed Aug 17 15:19:24 2005

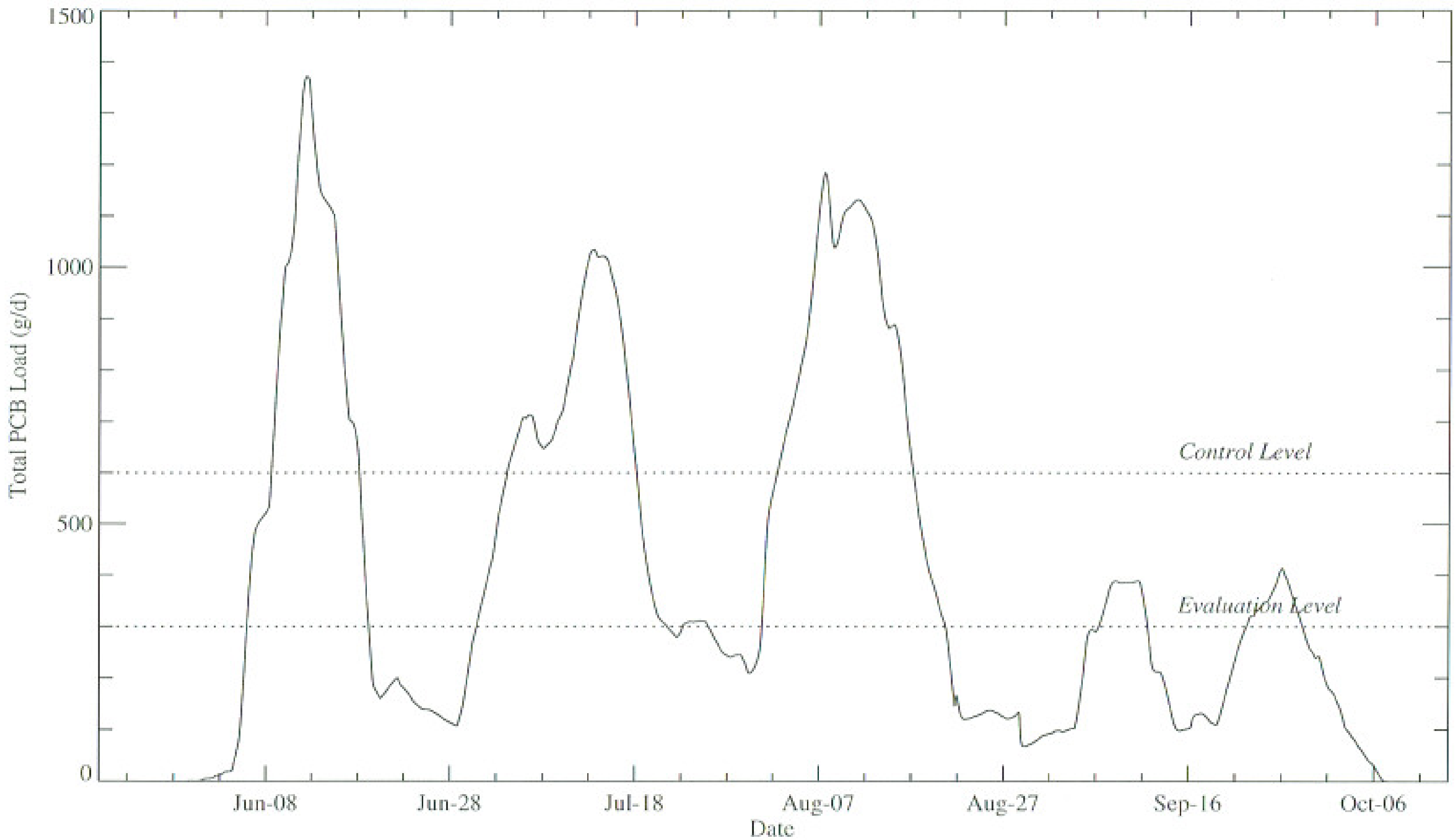

Figure E-7-17. Seven-Day Average TID Total PCB Load Above Baseline for Dredging with NTIP and EGIA Control Structures, 0.70% Loss and Median Flow

Dredge Plan 050805

model run: plan0508-06

haz - D:\Harry\GENdes\Report\tid_pcb_load_7day.pro
Wed Aug 17 15:17:59 2005

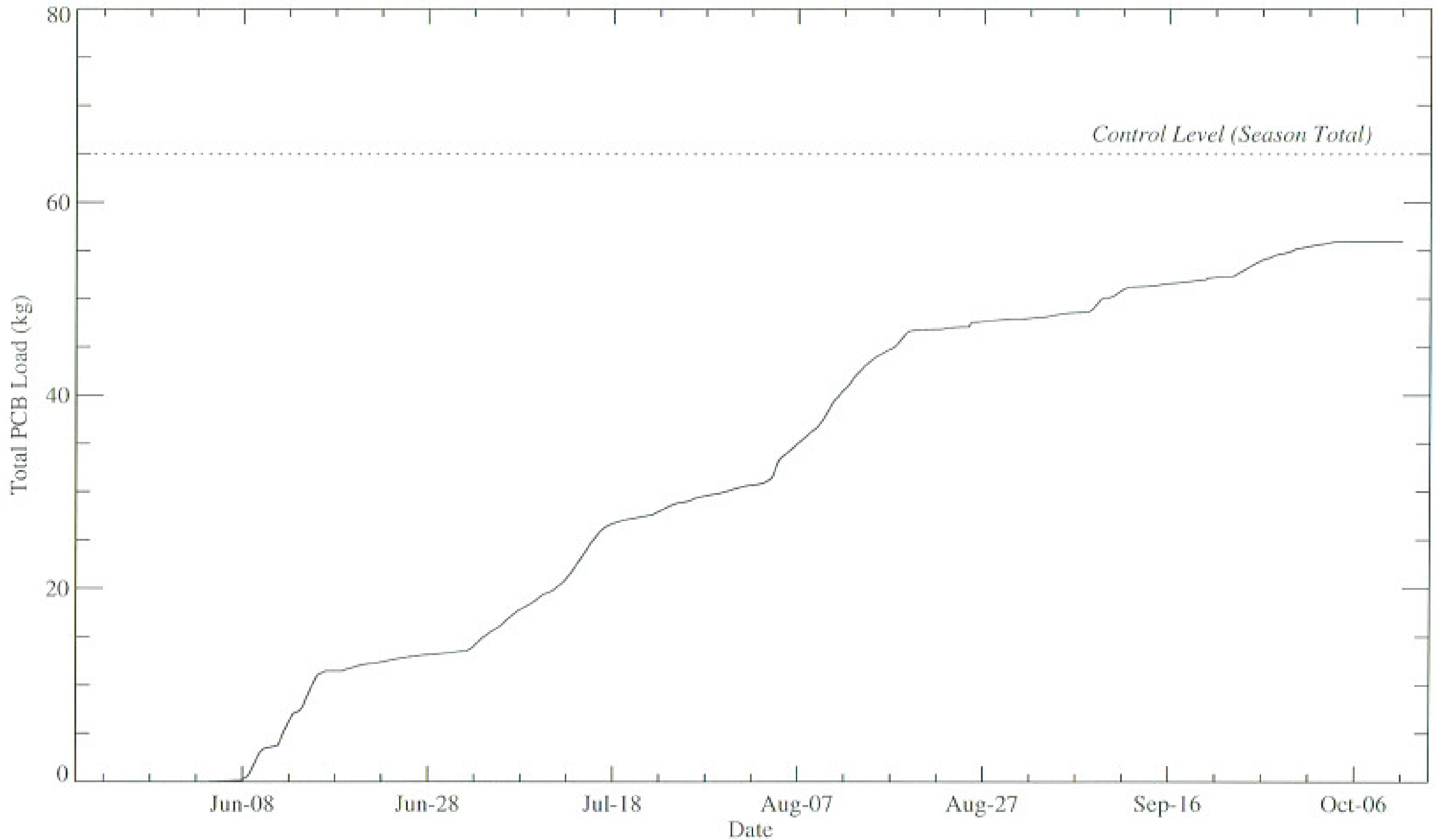

Figure E-7-18. Cumulative TID Total PCB Load Above Baseline for Dredging with NTIP and EGIA Control Structures, 0.70% Loss and Median Flow

Dredge Plan 050805

model run: plan0508-06

haz - D:\Harry\GENdes\Report\tid_pcb_load_cum.pro
Wed Aug 17 15:17:26 2005

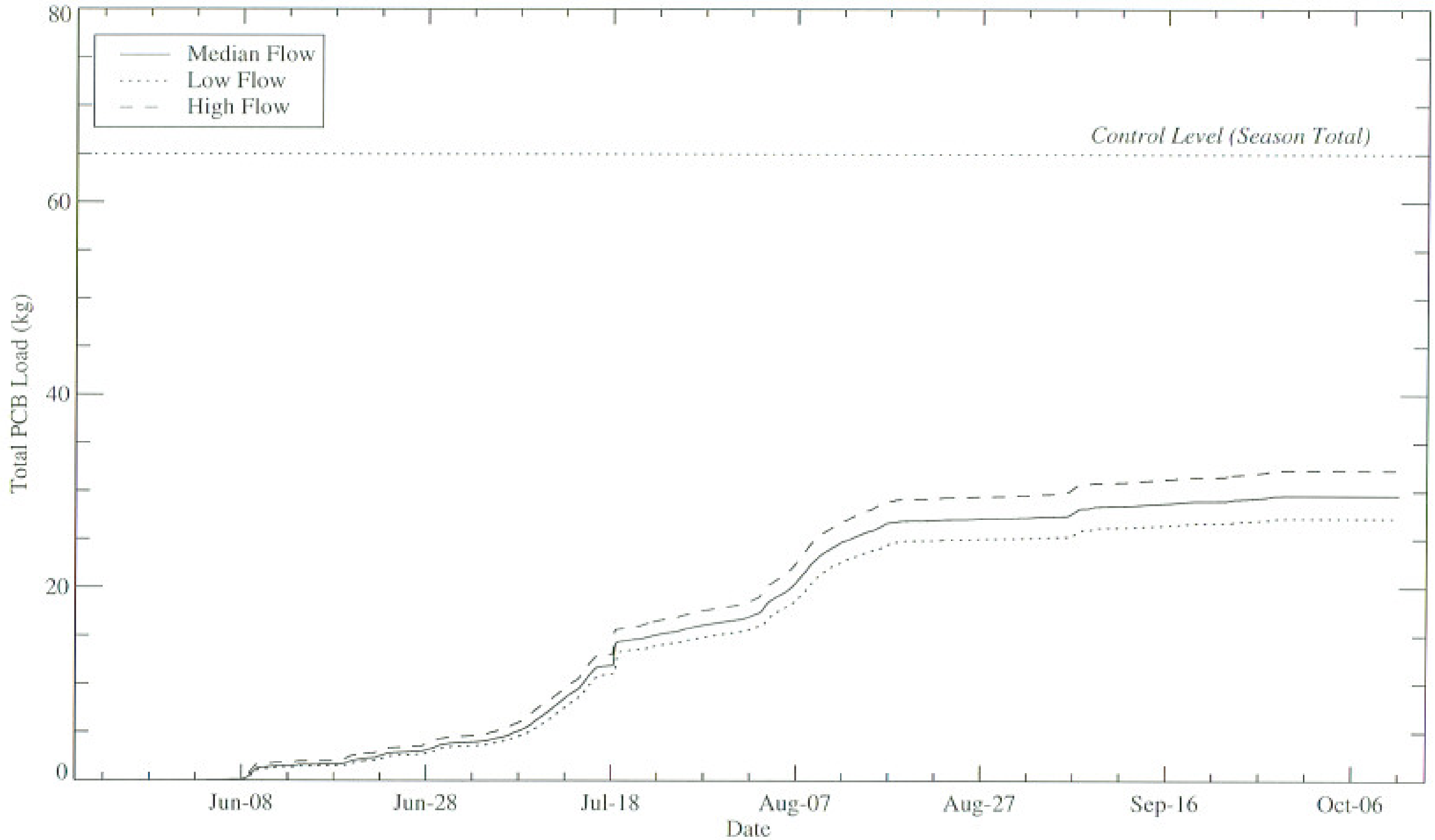

Figure E-7-19. Model Flow Rate Sensitivity of Cumulative TID Total PCB Load Above Baseline for Dredging with NTIP and EGIA Control Structures and 0.35% Loss

Dredge Plan 050701

model run: plan0507-09, plan0507-12, plan0507-11

haz - D:\Harry\GENdes\Report\tid_pcb_load_cum.pro
Wed Aug 17 15:17:27 2005

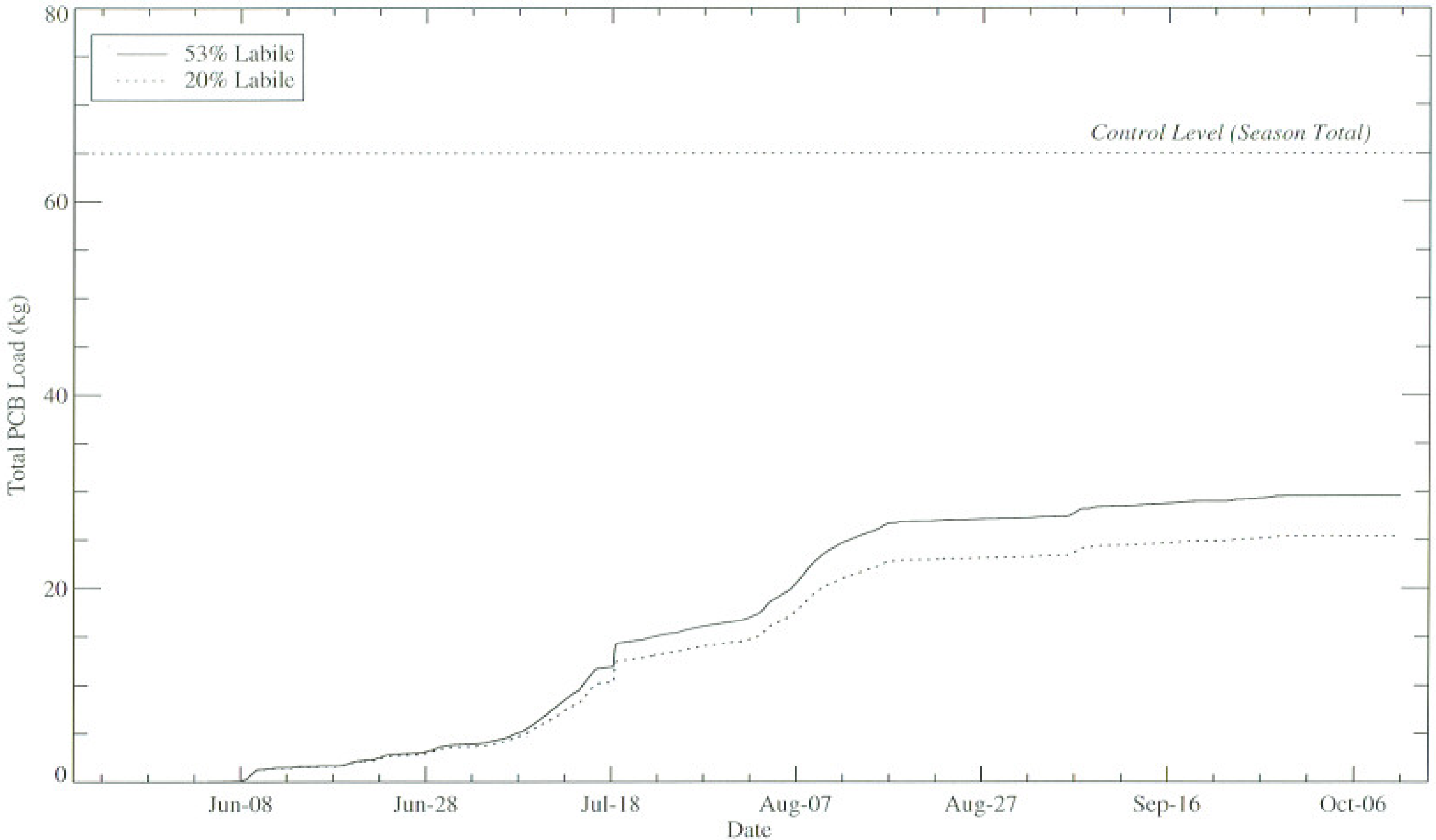

Figure E-7-20. Model Desorption Capacity Sensitivity of Cumulative TID Total PCB Load Above Baseline Dredging with NTIP and EGIA Control Structures, 0.35% Loss and Median Flow

Dredge Plan 050701

model run: plan0507-09, plan0508-02

haz - D:\Harry\GENdes\Report\tid_pcb_load_cum.pro
Thu Aug 18 14:19:17 2005